SEDIMENTOLOGICAL, PETROGRAPHIC AND GEOCHEMICAL CONSTRAINTS ON THE ORIGIN OF EXTENSIVE DOLOMITES OF THE CRETACEOUS SIDI AS SID FORMATION (AIN TOBI MEMBER) IN NW LIBYA

Thesis submitted for the degree of Doctor of Philosophy at the University of Leicester

by:

Mahmoud T. El-Bakai (*BSc, MSc, FGS*)

September, 1996

UMI Number: U085143

UMI

Dissertation Publishing

ProQuest

Dedication

To the memory of my father

Sedimentological, petrographic and geochemical constraints on the origin of extensive dolomites of the Cretaceous Sidi as Sid Formation (Ain Tobi Member) in NW Libya

Mahmoud Taher El-Bakai (Geology Department, Leicester University)

Abstract

The Cretaceous Sidi as Sid Formation outcrops in the Jabal Nafusah Escarpment, northwest Libya. It is composed of two members; the lower Ain Tobi Member and the upper Yifran Member. The Yifran Member consists of marl, dolomitic limestone and gypsum. The Ain Tobi Member is composed entirely of dolomite and in this study is named the "Ain Tobi Dolostone Member". The Sidi as Sid Formation is part of an inner ramp sequence which graded from restricted ramp in the south and southwest into an open to semi-restricted ramp in the northeast. The entire succession is without biostratigraphic markers.

Sedimentological, petrographic, geochemical and isotopic studies have led to the definition of five diagenetic dolomite types within the Ain Tobi dolostones; these reflect more than single diagenetic events which were involved in the formation of these dolomites. Type-1 dolomite is laminated, fine, subhedral, stoichiometric to nearly stoichiometric and poorly ordered. It is characterized by homogeneous luminescence, relatively high Sr and Na contents and low Fe and Mn, positive carbon isotope values and negative oxygen isotopic composition. It is suggested that Type-1 dolomite is formed near-surface by reflux dolomitization. Type-2 dolomite is calcian-rich, poorly to moderately ordered and very fine. It replaces packstone/grainstone facies and shows bright yellow luminescence. Type-2 dolomite is Sr-enriched and Fe, Mn, Na-depleted and possesses a similar isotopic composition as dolomite Type-1. Therefore, it is interpreted as a replacive dolomite formed at the near-surface under the influence of mixed water. Type-3 dolomite is a fine to medium dolomite, interbedded with quartz. It is calcian to nearly stoichiometric and moderately ordered. Type-3 dolomite is characterized by dirty orange luminescent cores and very thin bright luminescent rims, high Fe and Mn, but low Sr and Na contents. It has negative carbon and oxygen isotopic composition and is interpreted as dolomite formed in an intermediate stage probably post-compaction under the influence of mixed marine-meteoric water in shallow burial. Type-4 dolomites are calcian to nearly stoichiometric, well ordered, medium to coarse and have dirty orange luminescent cloudy cores and dull clean rims. Type-4 dolomites possess low trace element contents due to recrystallization from precursor dolomites. Type-4 dolomites have normal marine oxygen and carbon isotopic compositions. The Type-4 dolomites are interpreted as being formed by continuous dolomitization processes involving marine-meteoric pore-water mixing in shallow burial situations. Type-5 dolomite (saddle dolomite) is coarse to very coarse with orange luminescent cloudy cores and dull clean rims. It is calcian-rich, well ordered and posses low Fe, Mn and Sr contents and a relatively high Na concentration. Its isotopic composition is the lightest in oxygen and has a similar carbon composition compared to other dolomite types. Type-5 dolomite is interpreted as being formed at a late stage in deeper burial and elevated temperature environment.

Two types of replacive calcite (dedolomite) are found to replace dolomite in the Ain Tobi sequence. The first, is found close to the unconformity surface. These calcites show replaced cores and thin unreplaced dolomite zones. These dedolomite crystals are characterized by complex luminescent zonation and are interpreted as an early replacement under the influence of marine-meteoric mixing water. The second type is observed in the upper part of the Ain Tobi sequence and is characterized by very coarse or blocky crystals with replaced rims and/or whole dolomite rhombs. This calcite is interpreted as a dolomite replacement formed at a late stage under the influence of freshwater as indicated by very light $\delta^{18}O$ values.

TABLE OF CONTENTS

11. Chapter Eleven (conclusions)

List of Figures

List of Tables

Acknowledgements

CHAPTER ONE

CHAPTER ONE

1. INTRODUCTION

1.1. Nomenclature

Fieldwork for this study was carried out in the region extending between the Libyan-Tunisian border in the west and the Al Khums Coast in the east; and from Al Aziziyah Town at the north to Mizdah Town in the south (Fig.1.1).

Spelling of geologic, geographic and physiographic names in Libya and in North Africa in general varies widely. In this study the names will be spelt following the National Atlas of Libya, which has followed the Official Standard Names Gazetteer of the U.S. Board on Geographic Names.

1.2. Objectives

The Ain Tobi Member of the Sidi as Sid Formation (El Hinnawy and Cheshitev, 1975) forms the subject of the research. The Sidi as Sid Formation was described as a dolomite, limestone and marl succession of Upper Cretaceous (Cenomanian) age (Christie, 1955; Rossi-Ronchetti and Albanesi, 1961; Desio *et al*, 1963). It is exposed in the Jabal Nafusah escarpment south of Tarabulus, Libya.

This study deals with lithofacies field distribution and an in depth petrographic consideration of the Sidi as Sid Formation (Ain Tobi Member) in order to derive a better understanding of its lithologies. The main aims of the project are to elucidate the detailed diagenetic history of the Formation involving petrography and geochemistry, to determine the origin (mechanisms and timing) of dolomite, and the dolomitization processes. This study will also interpret the sedimentary environment of deposition of the Sidi as Sid Formation and will briefly compare it with published information on similar recent environments and related ancient rock sequences. Finally, the Sidi as Sid Formation will be correlated with the equivalent strata in the Sirt Basin and brief attention will be paid to its characteristics as a hydrocarbon reservoir. This study combines field work, laboratory work and literature research. The project was proposed by the author and approved by the Scientific Committee of the Exploration Division in the Petroleum Research Centre, Tarabulus, Libya in 1992.

1.3. Methods of Study

This study was carried out in two stages. The first stage of the project involved data acquisition in Libya from Sept., 1992 through the end of Sept., 1993. This involved measuring 12 sections (Figure 1 and sections 1 to 12) along Jabal Nafusah. Field sections were measured to include all bed details avaliable and were plotted at a scale of 4.8cm: 22m. Considerable attention was paid to lithological variations, sedimentary structures, faunas, textures and weathering profiles. All sections were sampled whenever there were changes in lithology and colour and additionally at a regular basis every 1 to 2 meters. All samples subsequently were cut and polished at the Petroleum Research Centre Laboratories. Photographs were made of field, and laboratory prepared polished samples as necessary for documentation.

Lithological, electrical, and composite borehole logs were also utilised to supplement field site data. They were collected from the General Water Authority of Libya (logs of water wells). Additional logs of oil wells in the Ghadamis Basin and Gabes-Tarabulus-Misratah Basin were obtained from the Petroleum Research Centre, Geological Library.

The second stage of the study involved laboratory work and analysis of the samples. Analytical techniques included; petrographic examination of the polished specimens, and the thin-sections. Thin-sections were stained with alizarin red S and potassium ferricynide, following Dickson (1965) and Friedman (1971) and summarised by Adams *et al*, 1984). X-ray diffraction, cathodoluminescence microscopy, SEM, geochemistry (microprobe and ICP) and isotopes, were also used in the analysis of selective samples (see Appendices One through Four for methodology details).

1.4. <u>Location of the Study Area</u>

The study area is located at the north-western part of Libya (Fig. 1.1), between 10° 30' 00" & 14° 30' 00"E and 31° 30' 00" & 32° 45' 00"N. It lies along the Jabal Nafusah range and extends from the Tunisian Border in the west north-eastwards until the Al Khums Coast (378km). The total area under study is about 51000km^2.
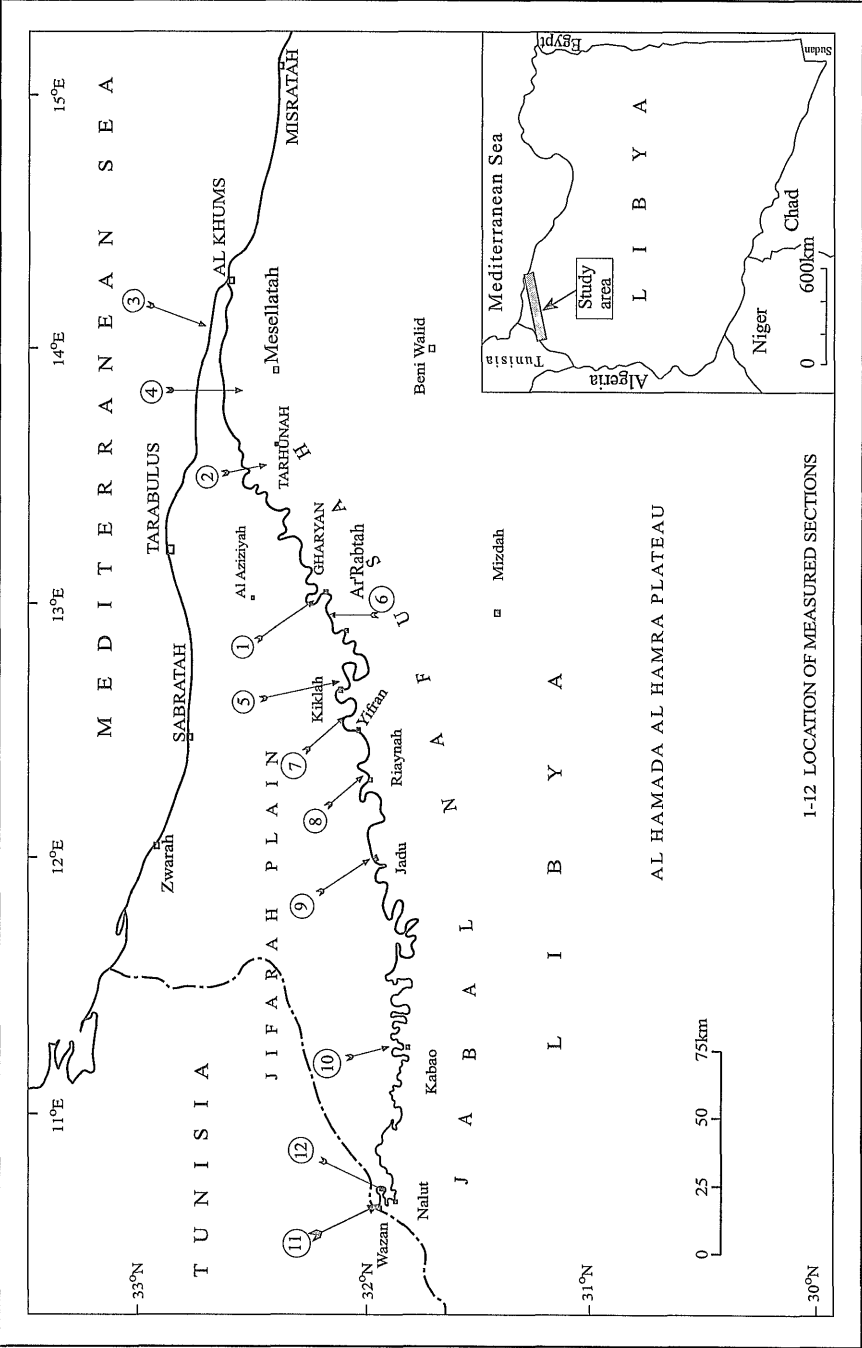
Fig. 1.1 Location map for measured sections 1-12 in northwestern Libya

CHAPTER TWO

CHAPTER TWO

2. GENERAL GEOLOGY

2.1. Introduction

This area of the Mediterranean Sea (Fig. 2.1), is a structural-tectonic unit termed the Pelagian Block by Burollet (1967). It has been a depositional basin at least since Permo-Triassic time (Conant and Goudarzi, 1967; Coqu and Jauzein, 1967; Bishop, 1975; Stephens, 1977b; Burollet *et al*, 1978). The present topographic basin is bounded by Libya, Tunisia, and Sicily on three sides. An abrupt north-south oriented bathymetric drop-off into the Ionian Sea (1000m contour) marks the eastern basin margin (Fig. 2.1). Within the basin, continental shelf areas delimited by the 200m contour are dominant. These shelf areas include the Malta Channel, Medina Bank, Adventure Bank, the Gulf of Hammamet, and the Gulf of Gabes. The principle deep water area is the northwest-southeast trending Pantelleria Rift with a maximum depth of 1698m (Carter *et al*, 1972).

Tunisia can be divided into three gross physiographic regions (Fig. 2.2). The Atlas Mountain System in the northwestern part of the country is the most rugged. Its southwest-northeast topographic trends are governed by the Alpine deformation which formed synclines, anticlines, high-angle faults, and low-angle thrust faults throughout the Atlas Mountains (Burollet, 1967, Burollet and Rouvier, 1971). The eastern Coastal Plain

from Gabes north is a region of plains and low hills. Here, the development of Alpine structures is less evident. The Coastal Plain, however, is influenced by the western edge of the Pelagian Block. Finally, south of Gabes lies the relatively undeformed stable Saharan Platform (Burollet and Rouvier, 1971). Several topographic features are continuous from Tunisia into Libya. Of these, the stable Saharan Platform is the principle one.

The Libyan portion of the Saharan platform is known as the Al Hamra Plateau (Novovic, 1977b) and is flat, gravel covered, and sparsely vegetated. The northern boundary of the plateau is marked by the Jabal Nafusah escarpment. The western boundary is formed by the Al Qarqaf Arch, a breached anticline with a south-facing escarpment that ranges from 0 to 300m in relief.

Jabal Nafusah extends for 350km in a south-west direction in a broad arc from the coast at Al Khums, Libya to the Libyan-Tunisian border where by then it is 130km from the coast. The Jabal continues into Tunisia, turns north, and dies out near Gabes. In Tunisia, Jabal Nafusah is known as the Jifarah Escarpment and trends NNW-SSE. It separates the Jifarah Plain to the east from the Dahar Plateau (Fig. 2.2) to the west (Ben Ismail, 1991). Jabal Nafusah in Libya has a base elevation of approximately 400m and relief of approximately 200-400m. The eastern boundary of the Al Hamada Al Hamra Plateau is the Hun Graben, the westernmost and only surface expression of the Sirt Basin. The last physiographic area of importance is the Jifarah Plain. The Jifarah Plain of Libya and Tunisia is flat and slopes gently towards the sea from Jabal Nafusah. The Jifarah Plain is a sand wave dominated plain extending from Jabal Nafusah as far as the Mediterranean Sea. It is the population centre of Northwest Libya.

2.2. Regional Tectonics

There are two major crustal divisions in Northwest Libya and Tunisia, the African Craton and Pelagian Block (Fig. 2.3). Both divisions are composed of continental crust (Glangeaud, 1962; Ryan *et al,* 1970; Dewey *et al,* 1973). Both units have a northern boundary with the Tyrrenian Sea Plate. This boundary occurs at a transition from continental to oceanic crust some distance north of Sicily (Glangeaud, 1962). The boundary is part of a poorly defined subduction zone extending from northern Tunisia through Sicily, around southern Italy and north through the Apennines (Biju-Duval *et al,* 1977). The African Craton is separated from the Pelagian Block by a series of normal faults along the Tunisian North-South Axis (Burollet, 1977; Burollet *et al,* 1978) and by the east-west trending Jifarah Fault (Al Aziziyah Fault) which lies beneath the middle of the Jifarah Plain (Busson, 1967a, 1970; Goudarzi and Smith, 1977). The eastern boundary of the Pelagian Block is in part fault bounded and in part the result of crustal transition from continental to oceanized continental crust (Burollet *et al,* 1978). This crustal transition occurs along the bathymetric drop-off east of a line between Siracusa, Sicily and Misratah, Libya (Biju-Duval *et al,* 1977). This study thus deals with the northern edge of the African Craton which extends from Morocco in the west to Egypt in the east. It particularly deals with the Libyan and Tunisian parts and southern part of the adjoining Pelagian Block.

2.2.1. African Craton

The African Craton in the Libyan-Tunisian area is divided into two structural provinces (Fig. 2.3). They are the Alpine Zone (Durand-Delga, 1967; Salaj, 1978) and the Saharan Shield (Burollet, 1967) or the Saharan Platform (Salaj, 1978). The Alpine Zone was important during the Jurassic and Cretaceous because it was the transitional area between the broad Saharan Platform to the south and the Tunisian Trough, a Tethyan depocentre, to the north (Burollet, 1967; Durand-Delga, 1967; Bishop, 1975).

The Saharan Platform of the African Craton is relatively undeformed compared to the Alpine Zone. It has been affected by broad Hercynian warping and Mesozoic craton subsidence (Conant and Goudarzi, 1967; Burollet, 1967; Klitzsch, 1968; Van Houten, 1980).

2.2.2. Pelagian Block

The Pelagian Block is dominantly a subsiding feature at least in Post Triassic time. It lies north of the Saharan Platform and east of the North-South Axis of eastern Tunisia (Burollet *et al*, 1978; Pedley and Grasso, 1991). The northern portion of the Pelagian Block in Sicily has been affected by Alpine deformation (Abate *et al*, 1977). The eastern part falls away into the deep Ionian Basin (Pedley and Grasso, 1991). The Sicilian Nappes are thrust sheets composed of Middle-Upper Triassic to Middle Miocene sedimentary rocks which have been thrust south relative to the northern Sicilian Coast. More details on the tectonic evolution of the Mediterranean Sea can be found in (Sylvester, 1968; Carter *et al*, 1972; Pitman and Talwani, 1972; Biju-Duval *et al.,* 1974; Ziegler,1975; Byramjee *et al*, 1975; Grandjacquet and Mascle, 1978; Hammuda and Missallati, 1980; Pitman *et al*, 1981; Finetti, 1982 and Pedley and Grasso, 1991). The Eastern Coastal Plain or Eastern Platform of Tunisia (Fig. 2.3), also part of the Pelagian Block (Salaj, 1978), has been affected by the Alpine deformation, but not as much as the Atlas Mountains (Burollet, 1967; Coque and Jauzein, 1967). North of the Al Aziziyah Fault and east of the North-South Axis (Fig. 2.3) the Pelagian Block is characterised by multiple high-angle normal faults with trends that range from east-west to southeast-northwest (Burollet, 1967). This series of growth faults extends from the southern coast of the Gabes-Tarabulus-Misratah Basin to Malta and Sicily (Stephens, 1977b; Burollet *et al*, 1978; Grandjacquet and Mascle, 1978). The Pantellaria Graben (Grandjacquet and
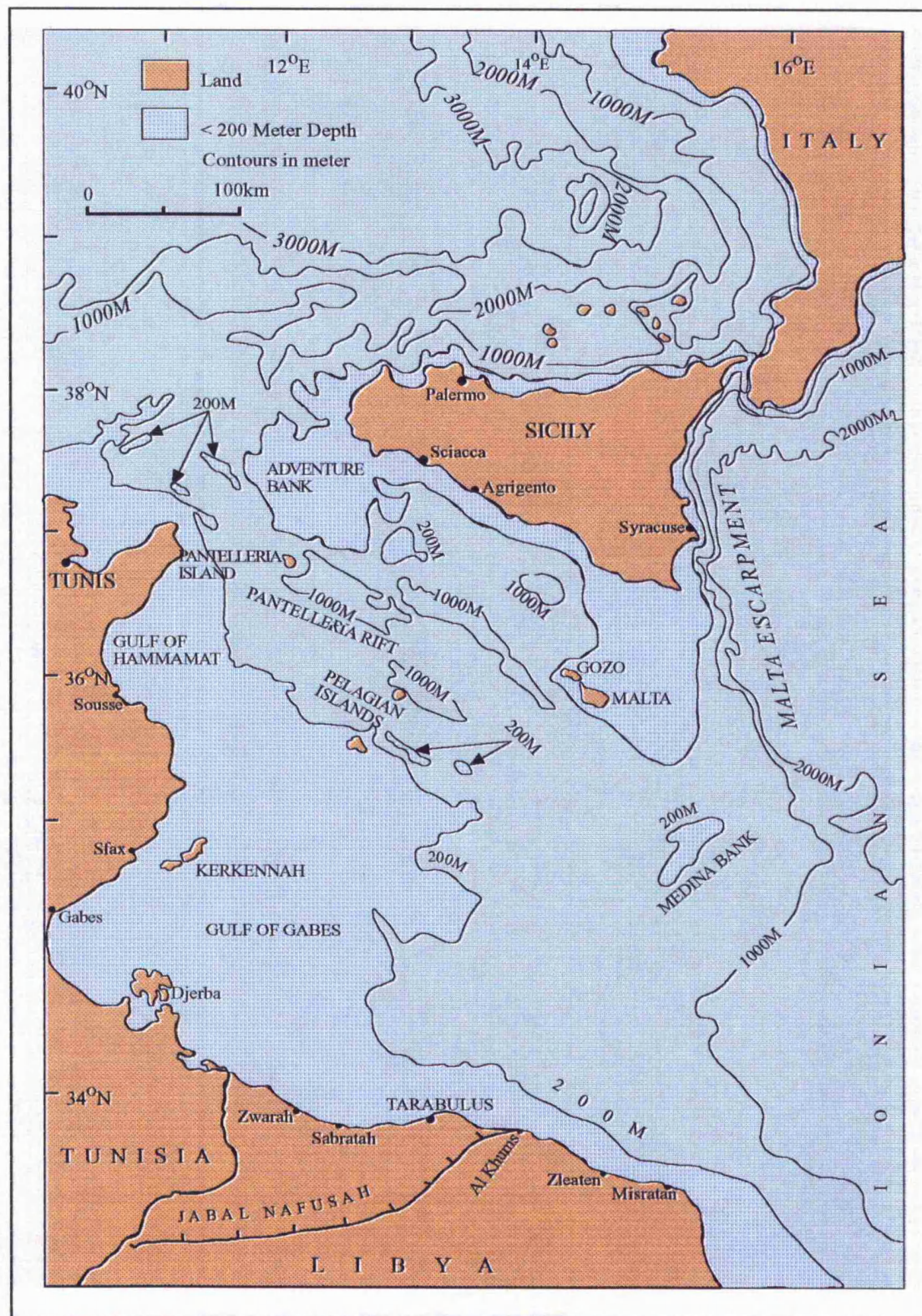
FIG. 2.1 Bathymetric location map (after Carter *et al*, 1972)

Mascle, 1978) is the deepest down-faulted block (Fig. 2.3), and contains offset Miocene sediments (Burollet *et al*, 1978). The faults (based on reflection seismic survey results) are spaced at 5 to 10km intervals (unpublished reports in NOC files). Bishop (1975) cited dislocations up to 1000m in Tunisia. Offshore reflection seismic surveys (Agip Petroleum Company) show similar displacements just north of Tarabulus. Coque and Jauzein (1967) indicate up to 4000m of cumulative displacement in Jurassic sediments from eastern Tunisia into the Gabes-Tarabulus-Misratah Basin. Movement along faults continues as there are historical records of earthquakes in Libya (Campbell, 1968). Little is known about the inception of faulting of the Pelagian Block in the Gabes-Tarabulus-Misratah Basin because wells do not penetrate deeper than the Middle Cretaceous (Etourbi, 1989).

The onshore portion of the Pelagian Block in eastern Tunisia was a stable shelf from the Mesozoic era through the Eocene era (Burollet, 1967; 1969; Burollet *et al*, 1978). It became unstable during Miocene and Pliocene times (Burollet, 1967). Normal faults along the North-South Axis form a series of Recent basins. East of the Recent basins along the coast are a few northeast-southwest trending folds with steeper flanks to the north or northwest. These are caused by Alpine deformation (Burollet, 1967). This area is associated with the N-S Axis and has consistently acted as a zone of positive movement throughout Cretaceous times (Pedley *et al*, 1982). Many structural features of the Pelagian Block influenced the evolution of the Sidi As Sid Formation depositional system. They are discussed below with emphasis on their Mesozoic development.

2.2.2.1. Al Aziziyah Fault

The Al Aziziyah Fault (Figure 2.3) separated the African Shield from the Pelagian Block (Conant and Goudarzi, 1964; 1967; Busson, 1967b; Goudarzi and Smith, 1977).
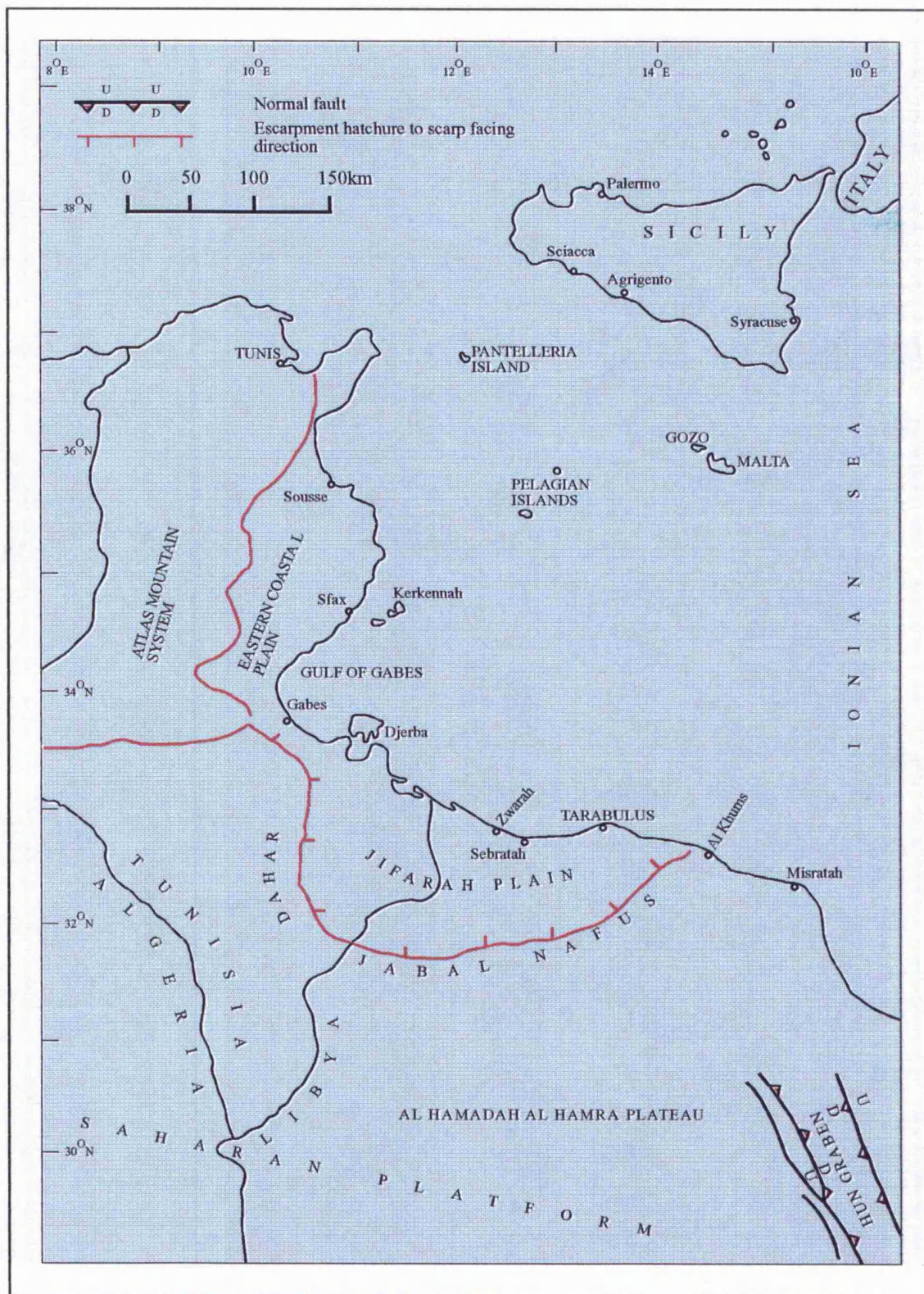
FIG. 2.2 Physiographic regions of northwest Libya, Tunisia, and Aigeria

The Al Aziziyah Fault lies 40 km south of the Tarabulus Coast (Conant and Goudarzi, 1964; 1967; Goudarzi and Smith, 1977). It continues into Tunisia where it lies parallel to the coast (Burollet, 1967; Busson 1967b; 1970; Anketell and Ghellali, 1991). There is no surface expression of the fault on the Jifarah Plain. Evidence for the fault in eastern Tarabulus comes from well log correlation, gravity and magnetic surveys (Conant and Goudarzi, 1967; Hall, 1977). In western Tarabulus the feature is recorded in seismic survey as a series of normal faults (AGOCO Concessions 131 and 132). There are offset to the northwest and splay in the same direction. Normal faulting continues into Tunisia (Burollet, 1967; Busson, 1967b; Burollet and Rouvier, 1971) as far as the vicinity of Gabes.

The Al Aziziyah Fault is at least Permo-Triassic in age (Conant and Goudarzi, 1967; Klitzsch, 1968; Stephens, 1977a). Klitzsch (1968) and Cable (1978) indicate that Carboniferous to Triassic clastics show signs of thickening due to movement of this fault. Several small normal faults, some of which splay from the Jifarah or Al Aziziyah Fault, form small grabens. The thickening of the rock units in the graben indicates that movement along the faults could be as old as Late Silurian (Stephens, 1977a; b). Stephens (1977a) used seismic and borehole information to show thickening of the Late Silurian-Early Carboniferous sequence along the Al Aziziyah Fault at the border between Libya and Tunisia. The Al Aziziyah Fault and faults associated with the western boundary of the Sirt Basin meet near the eastern end of Jabal Nafusah (Fig. 2.4). An east-west segment of the Nafusah escarpment north of Tarhunah and Cussbat is probably fault bounded because it is coincident with the projected surface trace of the Al Aziziyah Fault (Conant and Goudarzi, 1967; Goudarzi and Smith, 1977). Projections of the faults bounding the Hun Graben to the south-southeast intersect this segment of Jabal Nafusah. A single fault on the Al Hamada Al Hamra Plateau just south of Jabal Nafusah is
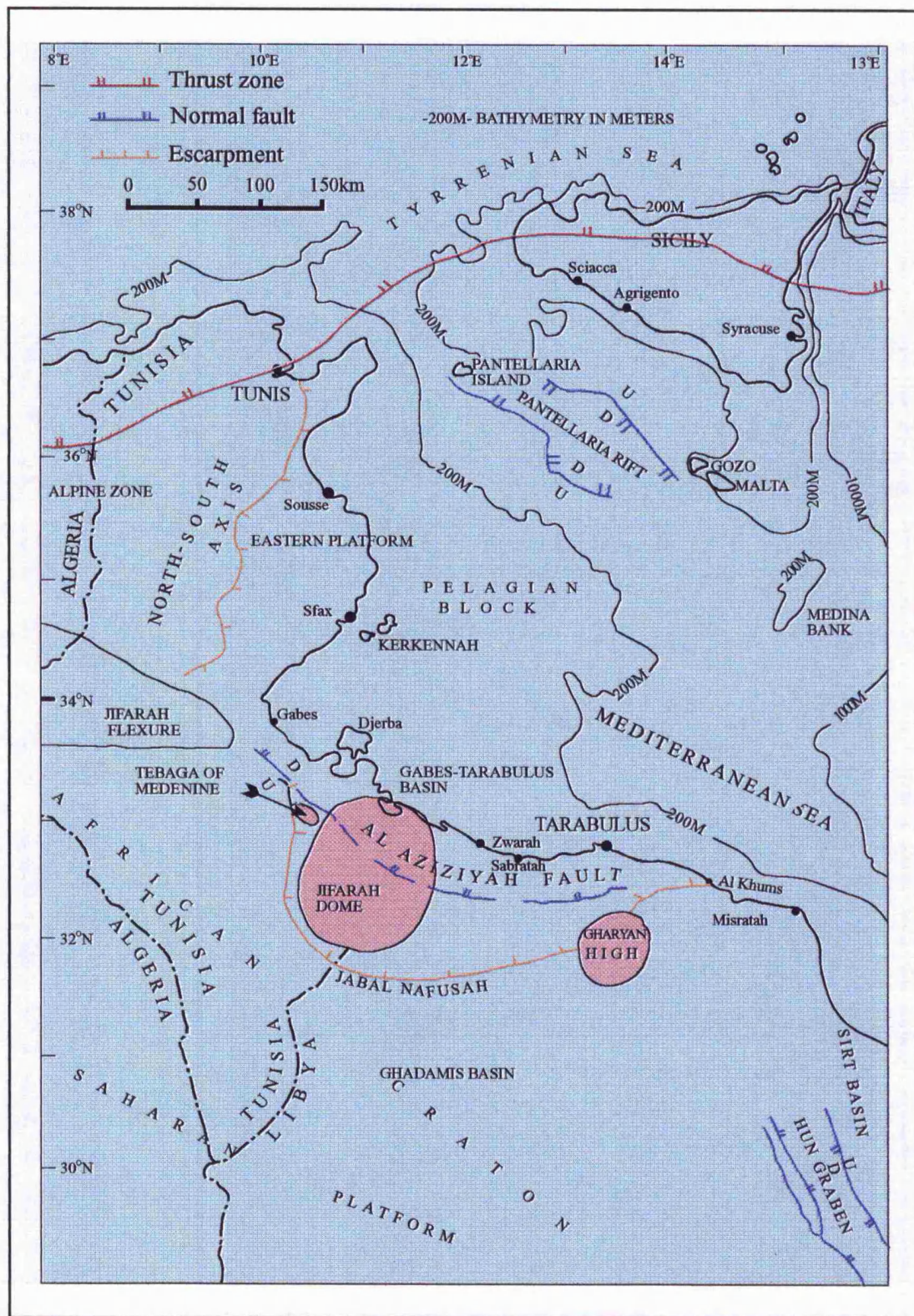
FIG. 2.3   Regional tectonic features northwest Libya, Tunisia and Sicily

coincident with the Hun Graben projections. This single fault terminates against the Al Aziziyah Fault. The intersection of the two fault trends in this area is significant and not unexpected. The intersection makes a major crustal boundary. The Pelagian Block (Continental Crust) lies in the northwest quaradnt; the Ghadamis Basin (Continental-African Craton) lies in the southwest quaradnt; the Sirt Basin (Continental-African Craton) lies in the southeast quaradnt; and the Ionian Sea (Oceanized Continental Crust) lies in the northeast quaradnt.

The western termination of the Al Aziziyah Fault is not clear. West of Gabes in Tunisia (Fig. 2.3) three tectonic features appear to intersect; the Al Aziziyah Fault; the Jifarah Flexure (this is equal to "Accident Sud Tunisien" Castany, 1954); and the North-South Axis. The Jifarah Flexure is a monocline (Burollet *et al*, 1978). It is unclear whether the Jifarah Flexure is caused by an extension of the Al Aziziyah Fault (fault system) or results from another crustal feature.

Like the eastern limb of the Al Aziziyah Fault the western terminus occurs in an area of major crustal change. The Al Aziziyah Fault separates the Saharan Platform (African Craton) from the Pelagian Block. Within and north of the Jifarah Flexure Mesozoic sediments thicken and become more marine (Busson, 1967b; Burollet *et al*, 1978). Because of its northwest-southeast orientation the Jifarah Flexure is thought to be related to the Al Aziziyah Fault (Burollet, 1967; Bishop, 1975). In Algeria and Tunisia the flexure marks the boundary with the African Craton (i.e. between the stable undeformed Saharan Platform and deformed Alpine Zone). Within the North-South Axis are a series of normal faults down stepping to the coast. Jurassic and some Cretaceous rocks are exposed at the surface in the Upthrown Western Block. The North-South Axis separates the Alpine Zone from the Eastern Platform (Burollet, 1967; Bishop, 1975).

2.2.2.2. Gharyan High

The Gharyan Basement High (Fig. 2.3) is known from well logs. The indicated relief

on the Precambrian igneous surface ranges up to 1.5km. Uplift of the basement resulted

in an erosional unconformity. The youngest unit beneath the unconformity that is

affected by the uplift is the Aouinet Ouenine Formation of Late Devonian age. The oldest

unit overlying the unconformity is the Bi'r El Jaja Formation of Late Permian age. The

uplift of the Gharyan Basement High must have occurred between the beginning of

Carboniferous and end of the Middle Permian. Thus the Gharyan High and Jifarah Arch

are similar in age. The relationship between the Gharyan High and the Sirt Basin is that

the Gharyan Basement High occurs at the intersection of two major fault systems. The

southern boundary of the Pelagian Block is the east-west Al Aziziyah Fault. This

intersects the projection of the fault-bounded west margin of the Hun Graben which

makes the western edge of the Sirt Basin. The Al Aziziyah Fault may have been active as

early as Late Silurian (Stephens, 1977a). If the Sirt Basin fault system (NNW-SSE

normal faults) was active earlier than the Cenomanian opening of the Sirt Basin (Conant

and Goudarzi, 1967) then it may have resulted in the formation of the Gharyan Basement

High in conjunction with its intersection with Al Aziziyah Fault. Evidence available based

on palynofossils from the Sirt Basin suggests that the basin formed during Cambro-

Ordovician times and witnessed non-marine and possibly fluvioglacial sedimentation

(Sinha, 1992). There is some evidence also for the reactivation of the Gharyan High at a

time just before initial deposition of the Sidi as Sid Formation (Ain Tobi Member). In the

vicinity of Abu Ghaylan pre-Ain Tobi uplift resulted in an angular unconformity

(Christie, 1955; Desio *et al*, 1963). The Upper Triassic through Early Cretaceous (Al

Aziziyah to Kiklah Formations) section was uplifted, tilted and eroded prior to the

deposition of the Ain Tobi. The Kiklah Formation in this area exhibits coarser facies

(Cable, 1978) indicating that uplift began in the Early Cretaceous. Busson (1967b) has

noted the similarity of the Gharyan Basement High and Tebaga of Medenine in Tunisia

with respect to their Permo-Carboniferous and Early Cretaceous histories.

2.2.2.3. Jabal Tebaga of Medenine

Jabal Tebaga of Medenine and the surrounding area (Fig. 2.3) are important because

their exposures provide a means of interpreting the geological history of the Tunisian

Saharan Platform. Jabal Tebaga is discontinuous east-west ridge that lies west of the City

of Medenine. The name is technically confined to the only exposures of marine Permian

rocks in North Africa (Newell *et al*, 1976). However, references to it also commonly

include Middle Triassic through Cretaceous (Senonian) rocks which crop out in the Jabal

Nafusah in Libya and on the Jifarah Plain in the vicinity of Jabal Tebaga.

The Permian exposures of Jabal Tebaga consist of (bottom to top) interbedded sandy

and/or calcareous shales, carbonate bioherms and laterally equivalent shales, and red

sandstones and shales (Newell *et al*, 1976; Driggs,1977). Despite lateral facies

variations, which are complicated by faulting and diagenesis (dolomitization) the

sequence is interpreted as a shale basin to the north, an east-west trending bioherm or

reef complex along a platform margin, and a carbonate platform to the south (Newell *et

al*, 1976). The platform and platform margin facies prograded north resulting in a

regressive deposit along the passive margin of the Tethyan Sea (Burollet, 1967; Newell

et al, 1976). The extensive thickening of Permo-Carboniferous rocks across the Al

Aziziyah Fault (Fig. 2.6 and 2.7 see Fig. 2.5 for location of the cross-sections) indicates

that this margin may not be so passive.

As a localised topographic high the Jabal Tebaga area had a narrow non-reef

carbonate halo around it (Busson, 1967b). A short distance away from the high, deposits
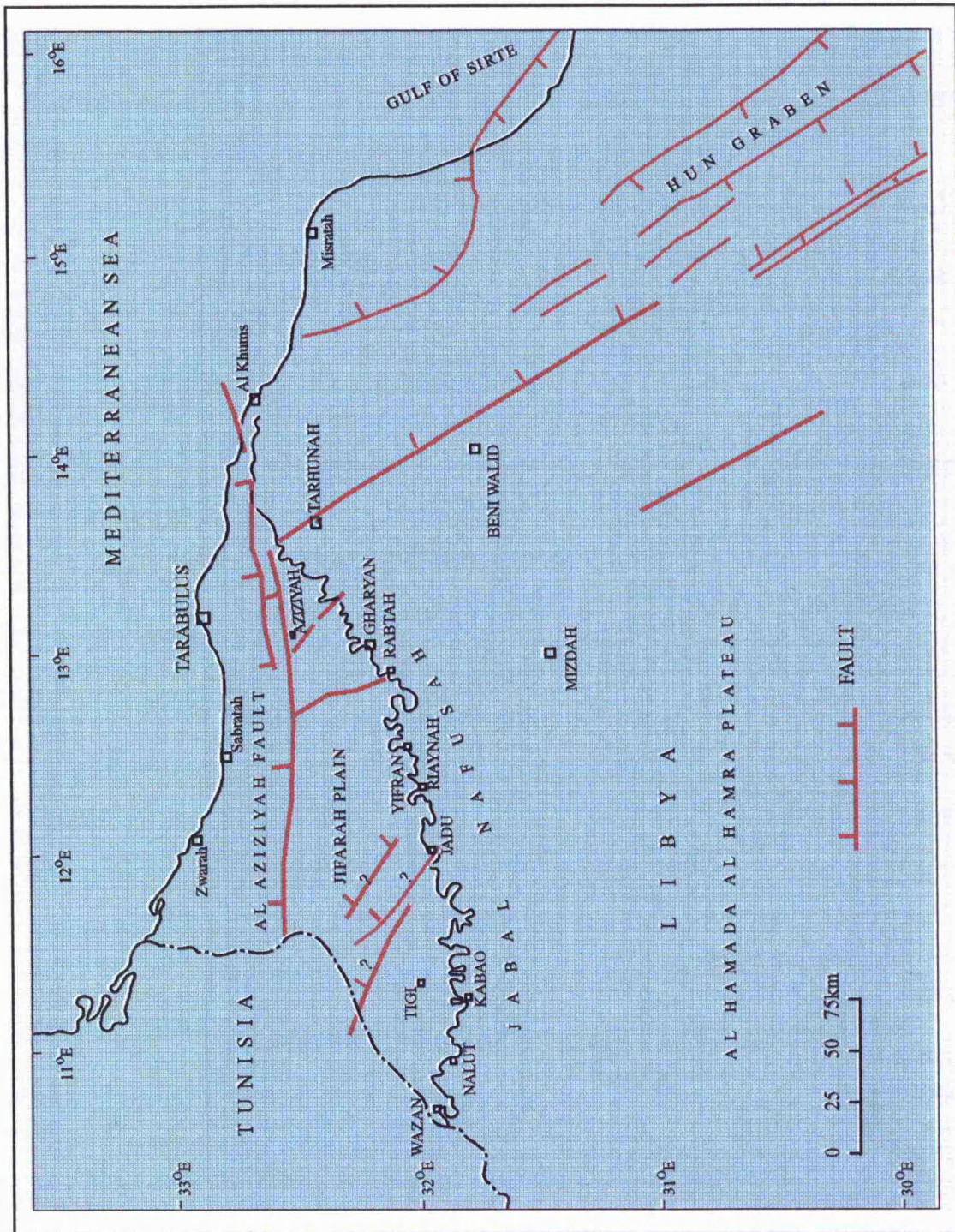
Fig. 2.4. Fault location map, northwestern Libya (after Goudarzi and Smith, 1977)

were laid down which are more characteristic of the Tunisian Saharan Platform and similar to those of Jabal Nafusah. These deposits consisted of continental clastics deposited during the Early and Middle Triassic (red beds in Jabal Tebaga), Late Triassic to Middle Jurassic evaporites and shales, interbedded marine carbonates and non-marine fluvial deltaics deposited from Late Jurassic to the end of the Purbeckian-Wealden, coarse Barremian fluvial deltaics (Kiklah Formation in Libya), graded arenaceous to argillaceous to clean carbonates (Sidi as Sid Formation "Ain Tobi and Yifran Members", and Nalut Formation) deposited from the Aptian through the Turonian, Senonian and Maastrichtian marls and shales with evaporites.

10°E 11°E **A'** 12°E 13°E

Gabes ▫ o Ga-1

Djerba) Gu-1

M E D I T E R R A N E A N   S E A

▫ Medenine

B'
o A1-37

33°N

o Kr-1

o Lg-1

T U N I S I A   J I F A R A H   P L A I N

o A1-131

TARABULUS ▫

o K1-23

o K1-1

o J1-23

o T1-1

o C2-23

N   A   F   U   S   A   H

o M1-23

▫ Gharyan

32°N

Wazan

J   A   B   A   L

Nalut ▫

▫ Yifran

o Q1-23

▫ Jadu

o C1-61

B o A1-61

o N1-23

o G1-23

L I B Y A

31°N

A L   H A M A D A   A L   H A M R A   P L A T E A U

o H1-26

o I1-26

A o N1-90

30°N

▫ Village

o Well location

0   25   50km
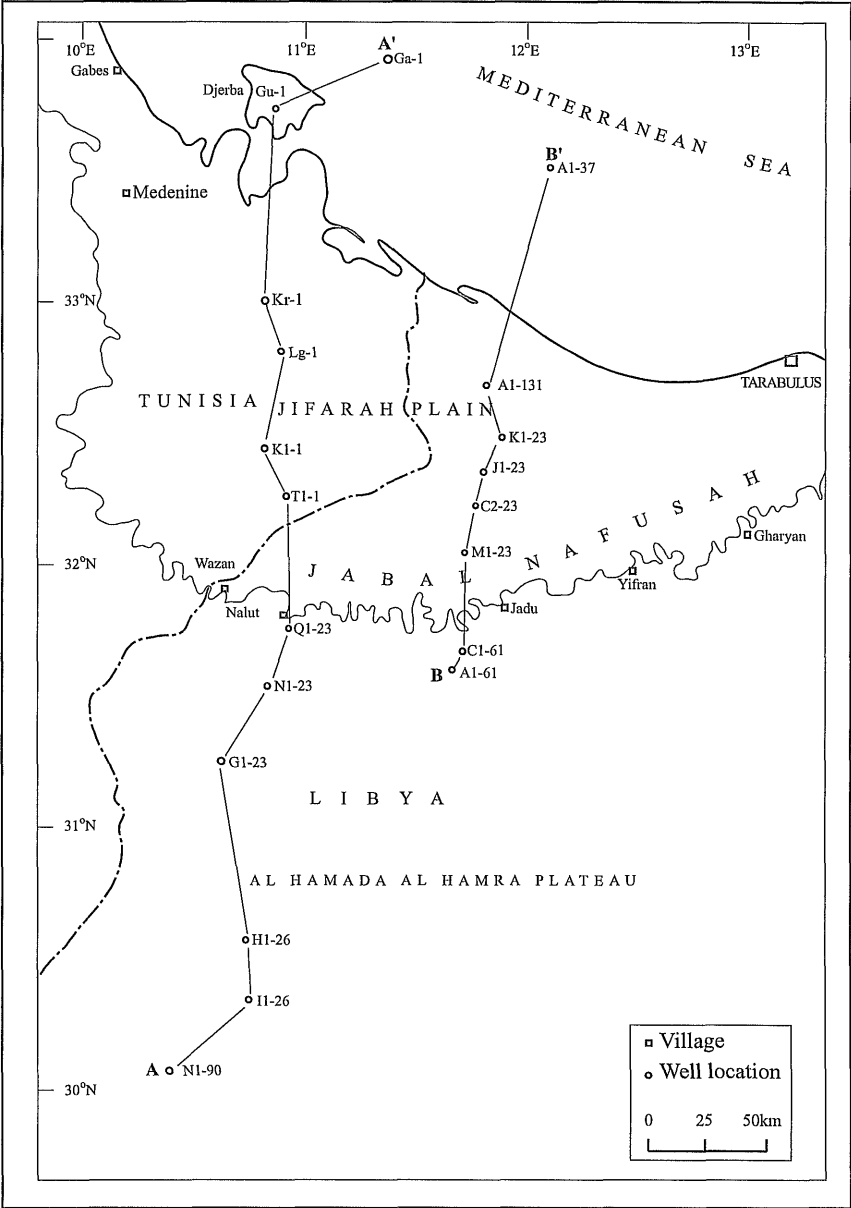
FIG. 2.5   Location map for cross-sections A-A' & B-B'   (after Cable, 1978)

2.2.2.4. <u>Sirt Basin</u>

The Sirt Basin (Fig. 2.8) is one of the important features of northern Libya, and so far

unsurpassed in its petroleum potential by any other Libyan onshore or offshore location.

The onshore area of the basin covers approximately 400,000km². This basin is bordered

on the east by the Daklah Basin in Egypt, the Kufrah Basin in the south, the

Mediterranean Sea to the north, the Cyrenaica Platform and Jabal al Akhdar to the north

and northeast and the Hun Graben to the west (Gumati and Schamel, 1988). Two

hypotheses are available in order to account for the origin of the Sirt Basin. First, the Sirt

has been a permanent "high" or upland relative to other structures e.g. Ghadamis and

Cyrenaica; there was no marine deposition from the Middle Palaeozoic to the Early

Cretaceous times, in the area. During the critical time between Early and Late

Cretaceous, the Sirt Upland disintegrated into a series of horsts and grabens, while the

neighbouring intracratonic basins remained intact (Van Houten, 1983). Second, the Sirt

has been intracratonic subsiding basin comparable to those of Ghadamis, Murzuq,

Cyreniaca and Kufrah has suffered uplift. Active tectonics and the erosion at the Early

Cretaceous was rapid and removed the entire sequence of the Palaeozoic and Early to

Middle Mesozoic, except in some places to the west of the basin. Klitzsch (1981), and

Massa and Delort (1984) do not accept this opinion, as it is considered that erosion of

such magnitude is unlikely to have occurred during that short span of time.

All agree that the Sirt was a permanent tectonic feature represented by a broad

uplifted zone oriented in a northwest-southeast direction, from Silurian until Jurassic

times. Subsidence of the basin was continuous throughout Late Cretaceous and Tertiary

times, reaching a maximum during the Palaeocene and Eocene, when a major
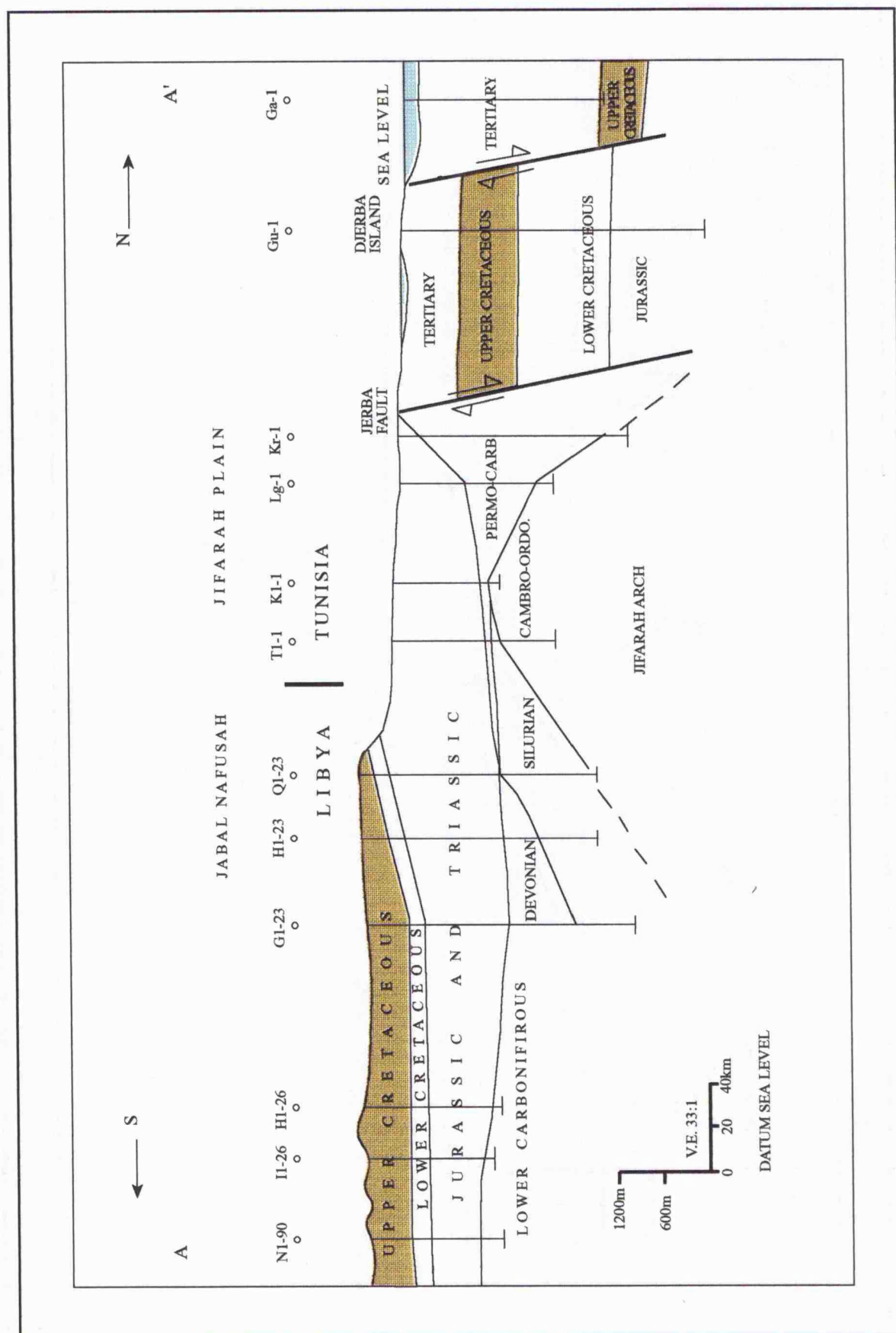
Fig. 2.6 North-south structural-stratigraphic cross section A-A' northwestern Libya and southestern Tunisia

(after Cable, 1978)

reactivation of faults occurred (Gumati and Kanes, 1985). During the period of time from the Cenomanian to the Maastrichtian marine conditions transgressed either over the basement or over the non-marine Pre-Upper Cretaceous clastics (Nubian Sandstone). The sandy transgressive base which began deposition in the Cenomanian and continued into the Maastrichtian, forms a single stratigraphic unit known as the Bahi Formation. The facies variations and thickness in Sirt Basin are controlled by volcanism or subtle basement faults along the edges of platforms. Carbonate facies distribution in particular, because of their sensitivity to any kind of pre-existing topographic high, whether structural or geomorphic may be expected to occur along such sudden break in slope (Wilson,1975). Horst blocks in the Sirt Basin are the focus for large Late Cretaceous and Palaeocene carbonate deposition. In the adjacent grabens shale and marl deposition is more typical. The carbonate platforms built up to sea level and were bordered by reefs associated with patch reefs and tidal-flat and island facies, which often form major oil fields (Wilson, 1985).

2.2.2.5. Jifarah Dome

The Jifarah Dome is centred on the Jifarah Plain between Libya and Tunisia (Fig. 2.3). According to the isopach maps and lithofacies maps by Busson (1970) and Bishop (1975), the Jifarah Dome was also a paleotopographic high from the Late Jurassic to the Turonian. Turonian aged deposits are the youngest in which the Jifarah Dome can be recognised because overlying units have localised areas of deposition or have been eroded.

Busson (1970) presents isopach maps for Tunisia of selected time intervals ranging from Triassic through Eocene in age, and Bishop (1975) constructed isopach maps for Tunisia and adjacent areas of Algeria and Libya of Aptian-Albian and Cenomanian-Turonian. All maps from Upper Jurassic through Turonian aged rocks show the effects

of a palaeotopographic high, the Jifarah Dome. The characteristic gradual to rapid thinning over the structure shown on these maps indicates the Jifarah Dome. Fig. 2.9 is an isopach map of Cenomanian-Turonian aged units combining Busson's (1970) and Bishop's (1975) data for Tunisia and Algeria with data from northwestern Libya. It shows typical thinning onto and possibly over the Jifarah Dome. Relief on the Jifarah Dome probably was not great. Lithofacies maps of Busson (1967b and 1970) show that around the dome shaly siliciclastic shelf units become only slightly more sandy or that carbonate shelf units have lower proportions of fine-grained siliciclastic material. No siliciclastic or carbonate shoreline deposits have been reported in association with the Jifarah Dome. The dominantly siliciclastic lithofacies pattern south of the Dome shifts toward carbonate dominance to the north near the Dome (Busson, 1970; Bishop, 1975). The change is most probably due to the increasing distance from the source area of siliciclastics and proximity of a carbonate platform margin to the north.

2.2.2.6. Igneous Activity

There are two major igneous events in northwest Libya (Fig. 2.10). The first is the emplacement of synorogenic granites in various metamorphic host rocks (Conant and Goudarzi, 1967; Klitzsch, 1968). This is thought to be a Precambrian event (Vail, 1971; 1991), but some intrusives at the floor of the Sirt Basin may be Early Palaeozoic in age (Conant and Goudarzi, 1967). The intrusives may be related to a Pan-African orogeny (Kennedy, 1965). A few of these Precambrian rocks are exposed in the eastern part of the Al Qarqaf Arch south of Jabal as Sawda (Conant and Goudarzi, 1967; Busrewil and Wadsworth, 1980a; Woller and Fediuk, 1980).
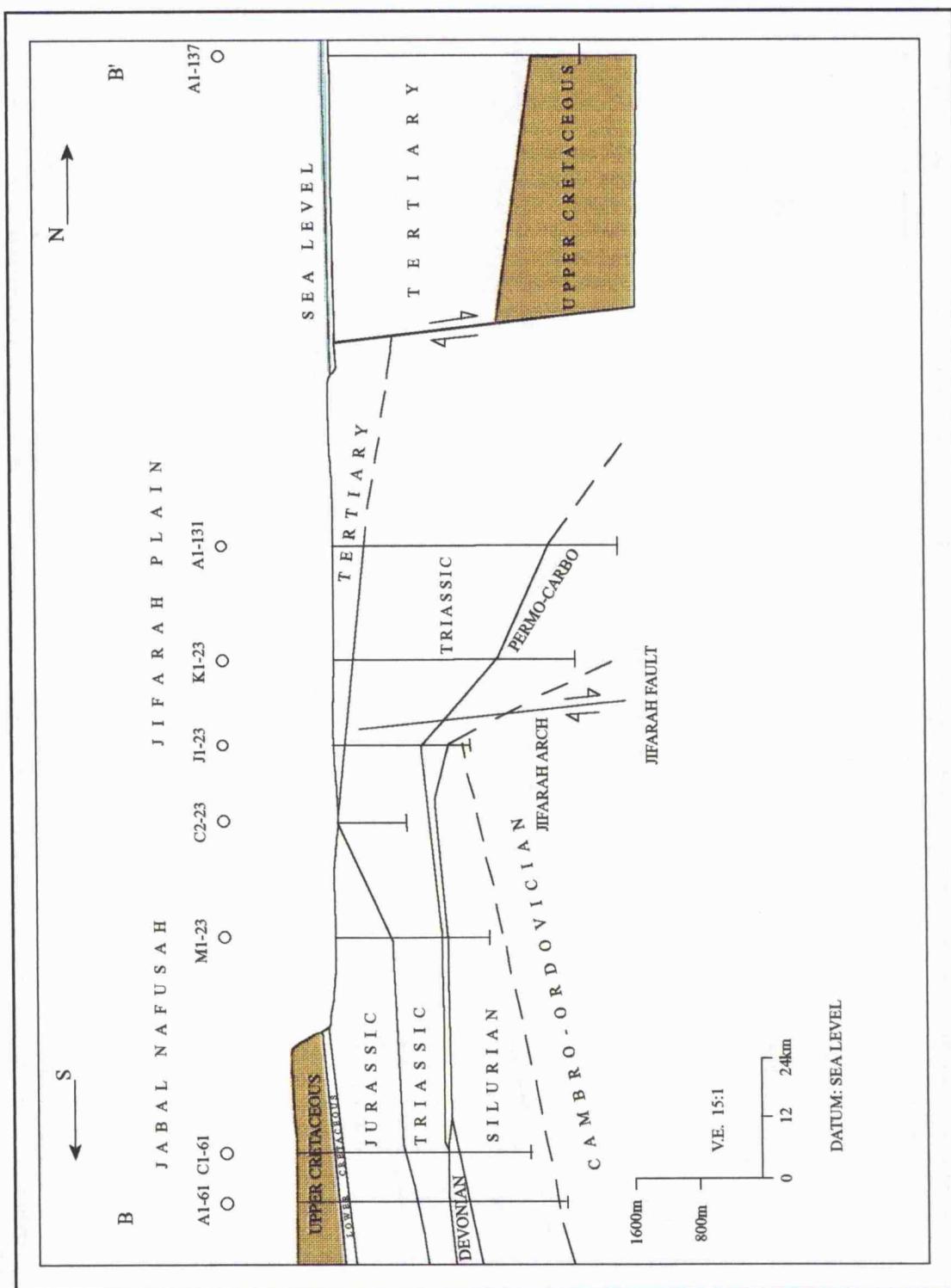
FIG. 2.7. North-south structural-stratigraphic cross section B-B' northwestern Libya

after Cable, 1978

The second period of igneous activity in Northwest Libya occurred in the Cenozoic

(Piccoli, 1971; Busrewil and wadsworth, 1980b). Two compositional groups are present;

basalts-olivine basalts and phonolites-trachytes (Busrewil and wadsworth, 1980a; b;

Bausch and Meduna, 1991). The basalts were emplaced mainly as flood deposits over a

minimum of 900km^2. Flood basalts range from Early Eocene to Palaeocene (Conant and

Goudarzi, 1967; Almond *et al*, 1974; Fatmi *et al*, 1978a; b; Busrewil and Wadsworth,

1980a; b) in age based on radiogenic and stratigraphic dating. Small shield volcanoes lie

on top of flood basalts. They are Middle Miocene to Early Pliocene in age (Almond *et al*,

1974; Busrewil and Wadsworth, 1980a; b). The phonolitic-trachytic complex forms three

localities near Gharyan (Gray, 1971). These bodies cluster at the Eocene-Oligocene

boundary. Gray (1971) found structural-stratigraphic evidence that similar deeply buried

intrusions may have been emplaced in the Late Triassic to Late Cretaceous. Both

compositional groups are similar in their chemistry and expression to other

contemporaneous igneous rocks of the Sahara within Libya and elsewhere. Burollet *et al.*

(1978) suggested that these Tertiary volcanics are related to the founding of the Ionian

Sea. They believe that the rocks are similar to submarine volcanics found along the

escarpment separating the Pelagian Block from the Ionian Sea between Libya and Sicily.

2.2.2.7. Jifarah Plain

The last structural feature of the Pelagian Block which influenced the evolution of the

Sidi as Sid Formation depositional system is the Jifarah Plain which lies at the

intersection of two major structures (Fig. 2.3). The NNW trending Tarabulus-Tibisti

Uplift formed in Caledonian times, and the E-W trending "Jifarah Uplift" formed during

the Hercynian Orogeny (Mikbel, 1977; Goudarzi, 1980; Anketell and Ghellali, 1991).

The Jifarah Plain is flat and appreciably lower than the rest of the area, and its relief does

not exceed 300m (Novovic, 1977b). It is mostly covered by Quaternary deposits. At its
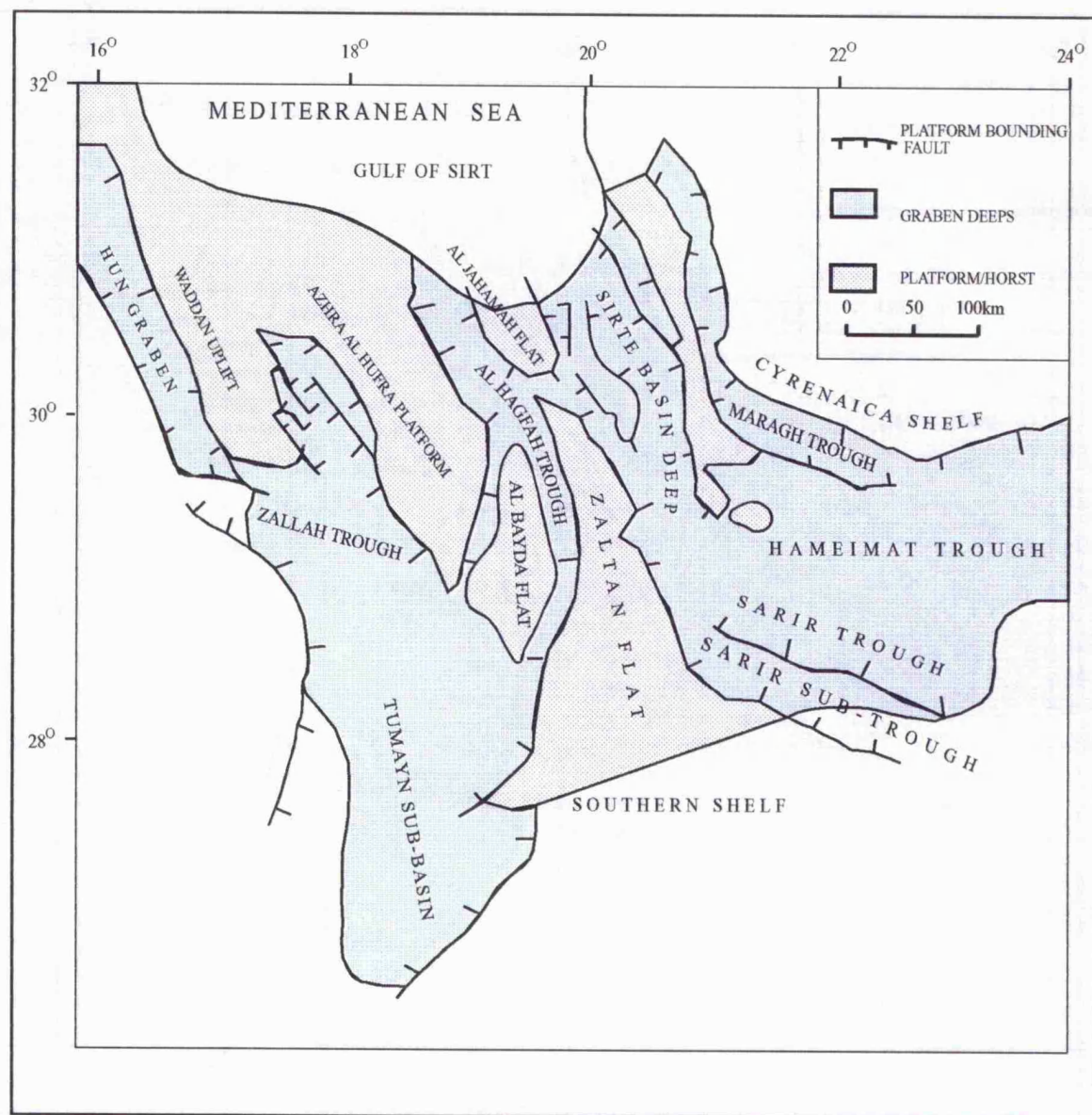
FIG. 2.8   General structural map of Sirt Basin

(after Anketell and Kumati,1991)

rim, near the escarpment, there are few small scattered hills of Mesozoic sediments (Novovic, 1977b).

Deferential movement on the Jifarah Uplift with major downwarp to the north across the "Jifarah Flexure" played an extremely important role in sedimentation of the Tripolitanian region during the Early Mesozoic (Anketell and Ghellali, 1991), and movements on the structure allowed the accumulation of thick sediments of Permian and Triassic deposits to the north (Busson, 1967a; Salaj, 1978). Uplift in southern Jifarah region during the Late Triassic accounts for the unconformity at the base of the Abu Shaybah Formation and the onset of continental conditions of sedimentation at this time (Anketell and Ghellali, 1991).
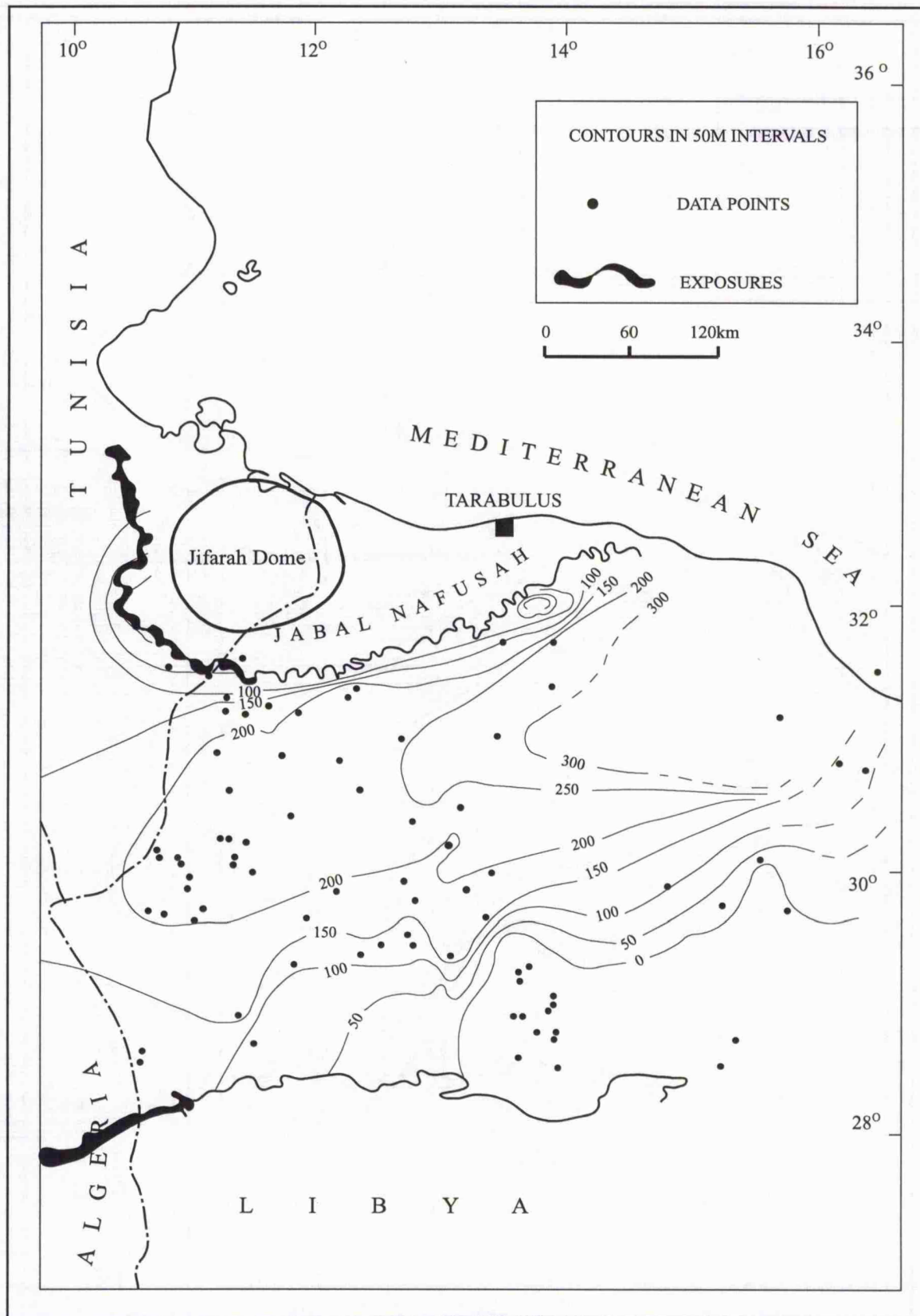
FIG. 2.9 Cenomanian isopach map in northwestern Libya

(Tunisia after Busson, 1970)

2.3. Conclusion

Several topographic features are continuous from Tunisia into Libya. The principle one is the Saharan Platform which has been named the Al Hamada Al Hamra Plateau in Libya. The northern boundary of this plateau is the Jabal Nafusah escarpment which extends from Al Khums coast in the east to the Libyan-Tunisian border in the west.

The two major continental crustal divisions in northwest Libya are the African Craton and the Pelagian Block. Many structural features of the Pelagian Block influenced the evolution of the Cenomanian Sidi as Sid Formation depositional system e.g. Al Aziziyah Fault which separates the African Platform from the Pelagian Block. It is located south of Tarabulus coast and north of the Jabal Nafusah escarpment. The Gharyan High probably occurred between the beginning of Carboniferous and Middle of Permian. Uplift of the basement resulted in an erosional unconformity, and the youngest beneath it is Late Devonian and the oldest overlying it is Late Permian. Jabal Tebaga of Medenine, has the only exposures of marine Permian rocks in North Africa. The deposits away from the high, consist of coarse fluvial deltaics (Kiklah Formation in Libya), graded arenaceous-argillaceous to clean carbonates (Sidi as Sid and Nalut Formations in Libya) deposited from Aptian through Turonian. The fault system of the Sirt Basin was active since the Cambro-Ordovician (Sinha, 1992) which may have resulted in the formation of Gharyan Basement High in conjunction with its intersection with Al Aziziyah Fault.
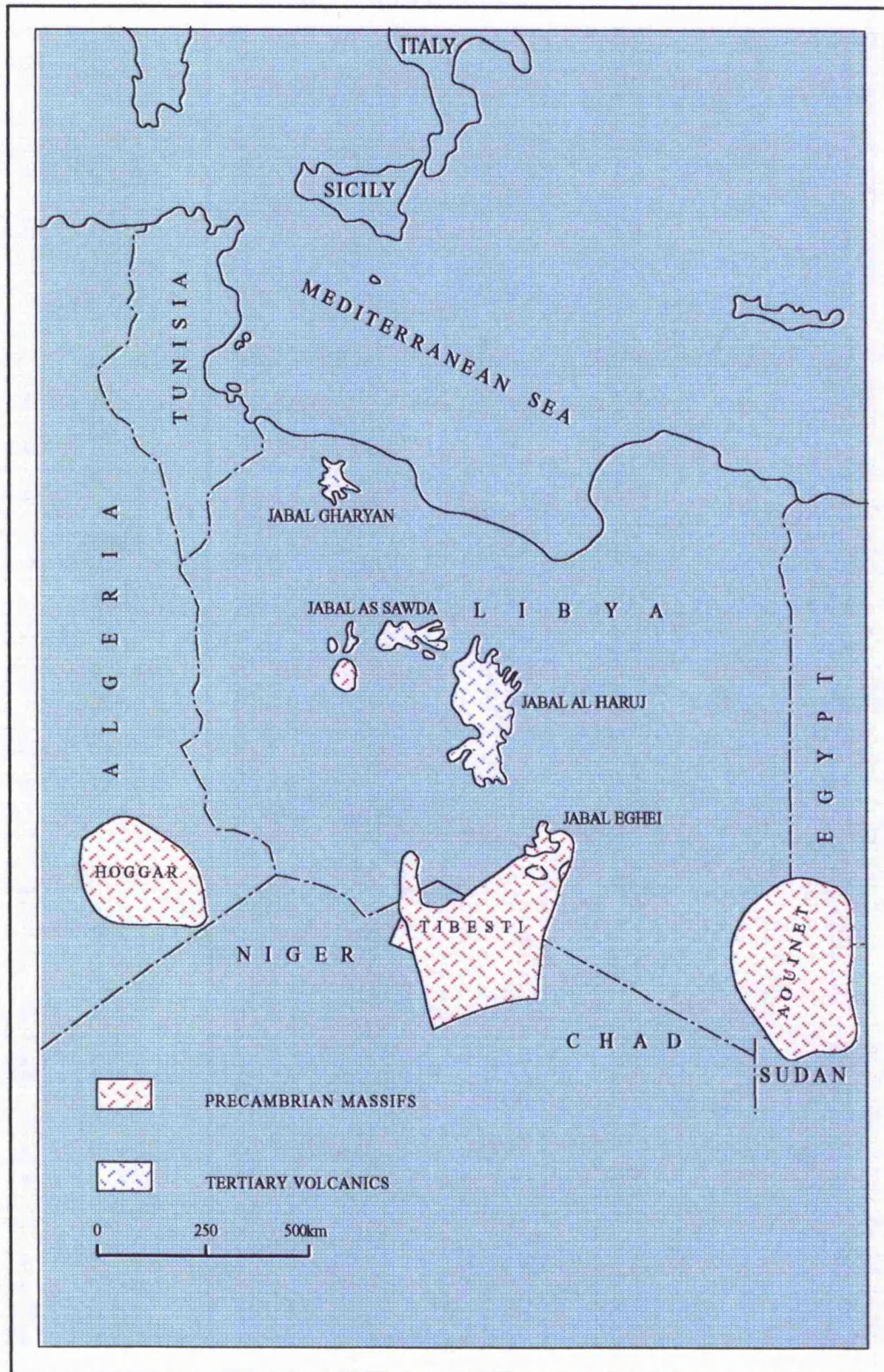
FIG. 2.10. Igneous rocks, Libya

CHAPTER THREE

CHAPTER THREE

3. GENERAL STRATIGRAPHY OF THE CRETACEOUS IN NW LIBYA

3.1. Origin of the formation names

The rocks exposed along the Jabal Nafusah escarpment and adjacent areas from Al Khums to the Tunisian-Libyan border, range in age from Triassic to Recent (Hammuda, 1969). This section deals with the origin of stratigraphic names, lithology and age of the Sidi as Sid Formation and the underlying and overlying strata.

Kiklah Formation was named as "Cabao", "Chameau Mort" and "Giosc" by Burollet (1963b; c), but El Hinnawy and Cheshitev (1975) discarded these names and redefined their Kiklah Formation as a lithostratigraphic unit (Fig. 3.1) unconformably overlying the Takbal Formation and underlying the Sidi as Sid Formation (Ain Tobi and Yifran Members). They dated the Kiklah Formation as "post-Oxfordian-Pre-Cenomanian and most probably of Late Jurassic age".

Christie (1955) described the Ain Tobi and Yifran units as separate formations, but El Hinnawy and Cheshitev (1975) assigned the term Sidi as Sid Formation which includes two members (the Ain Tobi and Yifran members). It is difficult to demarcate these two rock units in many places, therefore they were mapped together by all authors (Banerjee,

1980). The Sidi as Sid Formation incorporates the "Gazzar Dolomite " and its upper

"Scersciara Member" of Desio *et al* (1963). The Sidi as Sid Formation and Nalut

Formation (former Garian Dolomite) were classified under the "Nefusa Group" by

Burollet (1960; 1963a; b) and Barr and Weegar (1972); and as members under the term

"Nefusa Formation of Hamada Group" by Jordi and Lonfat (1963). Lately, Banerjee

(1980) has abolished the term Nefusa Group or Nefusa Formation, and has included the

Sidi as Sid Formation in the Al Hamadah al Hamra Group (Fig. 3.1). Here, in this study

they will be treated as a part of the Nafusah Group.

The name Nalut Limestone was introduced by Zacagna (1919) for strata occurring on

the western part of Jabal Nafusah. This unit was named the Garian Limestone by Christie

(1955) for strata occurring in central Jabal Nafusah. Some authors e.g. Burollet (1960);

Desio *et al* (1963); Hecht *et al* (1964); Hammuda (1969); Barr and Weegar (1972)

continued to use the term "Garian Limestone". However, Burollet (1960); Magnier

(1963); Goudarzi (1970) preferred the term "Garian Dolomite" instead. More recently El

Hinnawy and Cheshitev (1975); Mann (1975a); Novovic (1977a); Antonovic (1977)

reused the original term and named this rock the Nalut Formation (Fig. 3.1).

The term "Qasr Tigrinnah Formation" was first introduced by Christie (1955). Jordi

and Lonfat (1963) lowered its rank to "Tigrinnah Marl Member" of their "Mizdah

Formation". This was followed by many authors e.g. Hecht *et al* (1964); Goudarzi

(1970); Barr and Weegar (1972), whereas, others e.g. Burollet (1960; 1963c); Desio *et*

al (1963); Magnier (1963); Hammuda (1969) continued to treat this unit as a formation.

In recent years El Hinnawy and Cheshitev (1975); Novovic (1977a); Antonovic (1977);

ERA	PERIOD	EPOCH		AGE	STRATIGRAPHIC SEQUENCE IN NW LIBYA		
CENOZOIC	TERTIARY — NEOGENE	MIOCENE	UPPER	TORTONIAN / MESSINIAN	AL KHUM FORMATION	QUWAYRAT AL JIBS MEMBER	
			MIDDLE	SERAVALIAN / LANGHIAN		WADI YUNIS MEMBER	
	TERTIARY — PALAEOGENE	EOCENE	LOWER	YPRESIAN	WADDAN GROUP	BISHIMA FORMATION	RAWAGHAH MEMBER
							WADI ZAKIM MEMBER
							KHAYIR MEMBER
		PALAEOCENE	UPPER	THANETIAN		SHURFAH FORMATION	AMMUR MEMBER
							QALTAH MEMBER
							BU RA'S MEMBER
			M	MONTIAN		ZMAM FORMA.	HAD LIMESTONE MEMBER
			L	DANIAN	AL HAMADA GROUP	AL GHARIYAH FORMATION	UPPER TAR MEMBER
MESOZOIC	CRETACEOUS	UPPER CRETACEOUS	SENONIAN	MAASTRICHTIAN			LOWER TAR MEMBER
							LAWDH ALLAQ MEMBER
				CAMPANIAN		MIZDAH FORMA.	BI'R BU AL GHURAB MEMBER
							THALA MEMBER
				SANTONIAN			MAZUZAH MEMBER
				CONIACIAN	NAFUSAH GROUP	QASR TIGRINNAH FORMATION	
				TURONIAN		NALUT FORMATION	
				CENOMANIAN		SIDI AS SID FORMATION	YIFRAN MARL MEMBER
							AIN TOBI DOLOMITE MEMBER
		LOWER CRETACEOUS		ALBIAN	TIJI GROUP	KIKLAH FORMATION	AR RAJBAN MEMBER
				APTIAN			
				NEOCOMIAN			
	JURASSIC	UPPER		TITHONIAN			
				KIMMERIDGIAN			
				OXFORDIAN			
		MIDDLE		CALLOVIAN			SHAKSHUK MEMBER
				BATHONIAN		TAKBAL FORMATION	
				BAJOCIAN	BI'R AYYAD GROUP	BI'R AL GHANAM FORMATION	ABREGHS MEMBER
							BU EN NIRAN MEMBER
		LOWER		TOARCIAN			BI'R AL GHANAM GYPSUM MEMBER }{ ABU GHAYLAN FORMATION
				PLIENSBACHIAN			
				SINEMURIAN			
				HETTANGIAN			
				RHAETIAN		ABU SHAYBAH FORMATION	
	TRIASSIC	UPPER		NORIAN			
				CARNIAN	AL MAZUL GROUP	AL AZIZIYAH FORMATION	
		LOWER		LADINIAN			
				ANISIAN		KURRUSH FORMATION	

FIG. 3.1 Generalized Cenozoic-Mesozoic stratigraphic sequence in northwest Libya with units covered specifically coloured green.

Zivanovic (1977) treated this rock unit as a separate formation named (Qasr Tigrinnah Formation, Fig. 3.1).

3.2. Stratigraphy and Lithology

Figure 3.1 is a stratigraphic column of the Mesozoic-Cenozoic in northwest Libya. Basement rocks in northwestern Libya are Precambrian in age and are composed principally of granitic intrusives (Conant and Goudarzi, 1967) into metamorphic host rock (Klitzsch, 1968). They outcrop in small areas in the eastern Al Qarqaf Arch which separates the Ghadamis Basin in the north from the Murzuq Basin in the south (El-Rweimi, 1991). The outcrop units in northwestern Libya (Triassic to Late Miocene) (Fig. 3.1). Discussed below are the stratigraphy and lithology of the Cretaceous and underlying and overlying formations in the region.

3.2.1. Jurassic-Lower Cretaceous Rocks

Tiji Group

Kiklah Formation: Desio *et al* (1963); El Hinnawy and Cheshitev (1975) suggested that the whole clastic sequence between the Sidi as Sid Formation at the top and Takbal Formation at the base (Fig. 3.1) belonged to the Kiklah Formation. This formation has previously been stated as being absent from the eastern Jabal, east Wadi Ghan, either due to non-deposition (Christie, 1955) or to later erosion (Desio *et al*, 1963; Burollet, 1963a; Magnier, 1963). Recently, Fatmi and Sbeta (1991) claimed the presence of very thin remnants of the Kiklah Formation below Sidi as Sid Formation in the area around Suq al Ahad in eastern Jabal Nafusah (Fig. 3.2). The formation was also reported by Fatmi *et al* (1978a, b; 1980); Sbeta (1979). El Hinnawy and Cheshitev (1975) divided this formation into three members as follows:

Khashm az Zarzur Member: This member consists of two lithounits; lower lacustrine clays with minor sandstone interbeds and an upper continental cross-bedded sandstone sequence with clay intercalations. The lower shales contain gypsum in the western part. Fresh water fauna, silicified wood and marine fauna occur in these beds indicating various environments - shallow to lagoonal and marine (El-Zouki, 1976; Banerjee, 1980). The lower contact Takbal Formation is well marked by an erosive surface (Banerjee, 1980; Fatmi *et al*, 1980) and the upper contact is transitional with the overlying Shakshuk Member. Novovic (1977b) determined the age of the Khashm az Zarzur Member as Early Bathonian, whereas Fatmi *et al* (1980) ascribed it as Middle to Late Bathonian age.

Shakshuk Member: This member is composed of alternating limestone (dolomitic in places) and clays, with occasional occurrences of sandy beds. The significance of this member lies mainly in its contained marine facies with a marine fauna intercalated within the continental Kiklah facies (El Hinnawy and Cheshitev, 1975).

The lower boundary with the Khashm az Zarzur Member is marked in some areas by a slightly eroded surface and its upper boundary is transitional with the overlying Ar Rajban Member. The Shakshuk Member has been assigned a Late Bathonian-Callovian age by Banerjee (1980); Fatmi *et al* (1980).

Ar Rajban Member: This member exhibits two lithounits as discussed by El Hinnawy and Cheshitev (1975); Antonovic (1977); Novovic (1977b); Banerjee (1980). The lower part consists mostly of clastic rocks dominated by pink to white, light-grey and light-yellow, friable, cross-bedded quartz sandstones. Due to its friability this sandstone is frequent referred to as sand and is fine to coarse-grained and locally conglomeratic. The

upper part composed of sandstone with interval of alternating marly and sandy limestone and sandy clay beds. The friable sandstone contains silicified wood (Novovic, 1977b).

The Ar Rajban Member overlies conformably the Shakshuk Member, and is often overlain by the Ain Tobi Member of the Sidi as Sid Formation (Banerjee, 1980). According to palaeonological data the age of this member is most probably Late Jurassic (Novovic, 1977b; Antonovic, 1977). It is assigned as Upper Jurassic-Lower Cretaceous (Oxfordian to Albian) by Banerjee (1980).

3.2.2. Upper Cretaceous Rocks

Nafusah Group

Sidi as Sid Formation: This formation is the target of this study. According to previous studies (mainly stratigraphic studies), it has been divided into two members; lower Ain Tobi Member and upper Yifran Member (El Hinnawy and Cheshitev, 1975).

Ain Tobi Member: As described by El Hinnawy and Cheshitev (1975); Megerisi and Mamgain (1980a; b), it is composed of greyish limestone and dolomitic limestone with marly intercalations in the lower part and well bedded white to light yellow limestone and dolomitic limestone in the upper part (more details on lithology of this member can be found in Chapter Five). The lower contact with the underlying Kiklah Formation in central and western Jabal Nafusah and with the Abu Shaybah Formation in eastern areas of the Jabal is sharp and unconformable. The upper contact with the Yifran Marl Member is marked by the contact between dolostone and clay-marl succession (Megerisi and Mamgain, 1980a; b). Bivalves and rudists recorded in this member indicate a Cenomanian age (Christie, 1955; Desio *et al*, 1963).

Yifran Member: This member is characterised by a predominantly yellow clay-marl-evaporite sequence forming gentle slopes, between the prominent scarp forming dolostone and dolomitic limestone sequence belonging to both conformably underlying Ain Tobi Member and overlying Nalut Formation (Megerisi and Mamgain, 1980a; b).

Fossils are rare in this member and based on few molluscan fossils collected by Christie (1955); Desio *et al* (1963); Gorhbandt (1966); Mann (1975a) from this member a Cenomanian age is suggested.

Nalut Formation: This formation consists of light grey to cream coloured hard, massive and crystalline dolomitic limestone and dolomite, with common chert bands and concretions in the upper part. As one of the most resistant formations in Jabal Nafusah it forms the upper scarp and plateau surface of Mesellatah, Tarhunah, Gharyan and Nalut areas (Megerisi and Mamgain, 1980a; b).

The Nalut Formation lies conformably between the Qasr Tigrinnah Formation at the top and the Sidi as Sid Formation at the base (El Hinnawy and Cheshitev, 1975). Based on foraminiferal assemblages which have been recorded by Megerisi and Mamgain (1980a, Page 7), a Late Cenomanian-Turonian age is suggested for this formation.

Qasr Tigrinnah Formation: This formation exhibits greenish grey marls, with local development of gypsiferous marl and gypsum in the lower part and alternations of claystone-marl thinly bedded limestone in the middle part. The upper part consists of white porous chalky limestones with marl intercalations (Megerisi and Mamgain, 1980a; b).
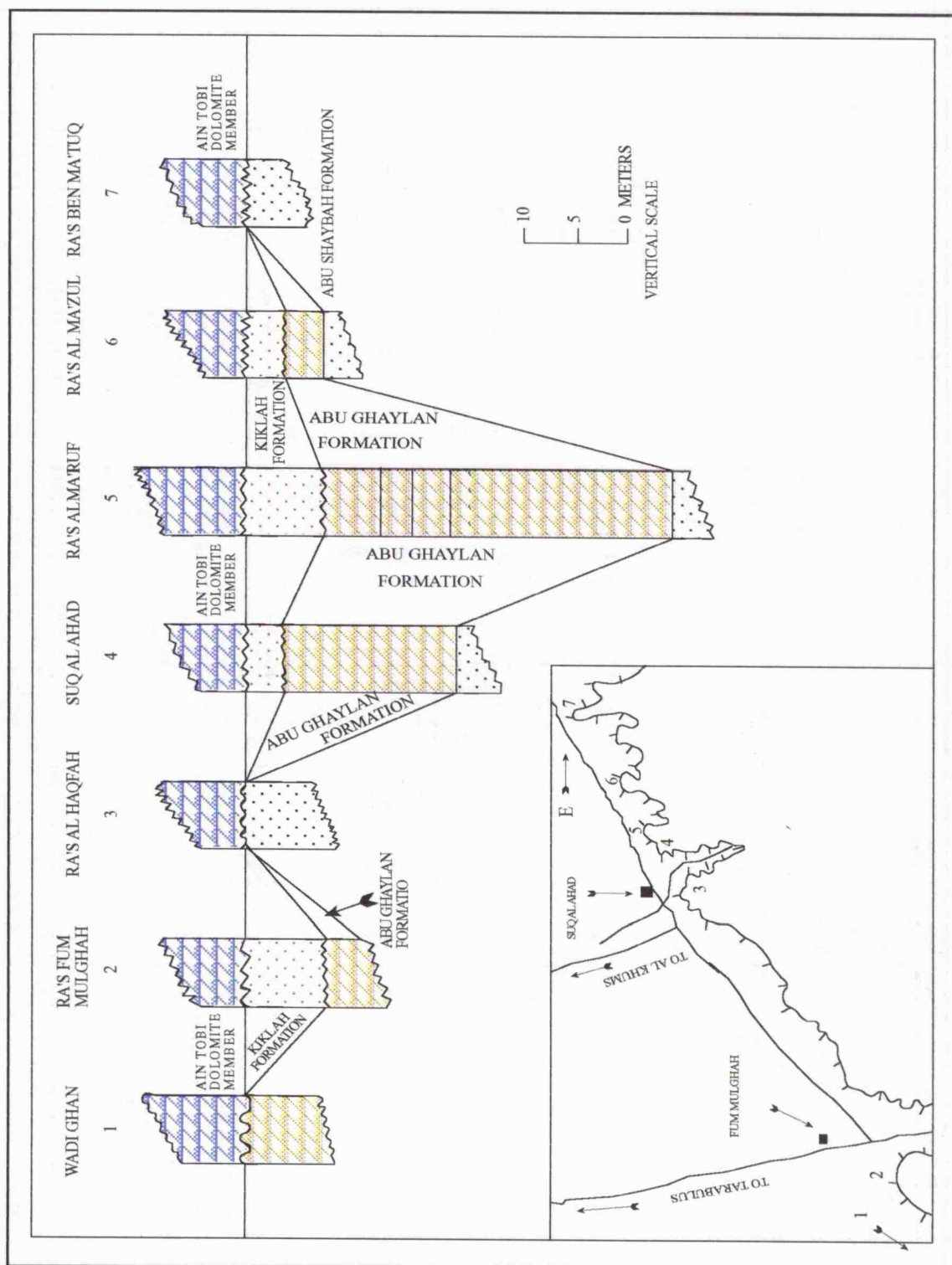
FIG. 3.2 Columnar sections of Kiklah and Abu Ghaylan Formations in eastern Jabal Nafusah

(after Fatmi and Sbeta, 1991)

The formation conformably overlies the Nalut Formation and is overlain by the Mazuzah Member of the Mizdah Formation. The Qasr Tigrinnah Formation is assigned a Late Turonian-Coniacian age by Megerisi and Mamgain (1980a; b). This is based on macrofossils; gastropods, bivalves, echinoids, foraminifera, ostracods and algae.

3.3. Conclusion

The age of the rocks exposed in the northwestern Libya ranges from Triassic to Recent. The nomenclature of northwestern Libya (Jabal Nafusah) varies widely because of the two different schools who worked in the region in the early 1960s. The first Italian group was headed by Desio (1963) and the second French group was headed by Burollet (1963). The work of their teams greatly enhanced the knowledge of the stratigraphy of the area but also resulted in controversies on the nomenclature, boundaries, and ages (Fatmi *et al* 1978a; b; 1980). Recently, during the Second Symposium and the Third Symposium on the Geology of Libya (1980, 1991) and the Geology of the Sedimentary Basins of Libya (First Symposium, the Geology of Sirt Basin 1993) held in Tarabulus, the nomenclature has been revised and the spelling of locality names is now restricted to the same names used in the National Atlas of Libya.

The rocks exposed in the Jabal Nafusah escarpment show a great diversity both laterally and vertically (sandstone, conglomerate, limestone, dolomite, dolostone, marl and evaporites), reflecting frequent environmental shifts from shallow-water marine to continental and back. This, coupled with a lack or paucity of diagnostic fossils and incomplete sequences (unconformities), appears to be the primary reason for all the controversy and confusion in the literature.

CHAPTER FOUR

CHAPTER FOUR

4. AGE AND PALAEOGEOGRAPHY OF THE CENOMANIAN SIDI AS SID FORMATION (AIN TOBI DOLOSTONE MEMBER) IN NORTHWEST LIBYA

4.1.Introduction

This section deals with the Sidi as Sid Formation (Ain Tobi Dolomite Member), a typical Mid-Cretaceous platform carbonate succession of North Africa.

Christie (1955) originally defined what this study calls Ain Tobi Dolomite Member of the Sidi as Sid Formation as the Ain Tobi Limestone. Burollet (1960) retained Christie's name and description, but Desio *et al* (1963) changed the name from limestone to formation. Recently El Hinnawy and Chesitev (1975), used the name Sidi as Sid Formation and they divided it into two members. The lower "Ain Tobi Member", and the upper "Yifran Marl Member".

The dominant rock of the Ain Tobi Member is dolomite. Staining of 200 thin-sections by potassium ferricynide show the completeness of dolomitization. The dolomites contain less than 1% FeO as they did not stain (Sperber *et al*, 1984). X-ray

diffraction analysis of 153 whole rock samples, and is slightly pink stain on some thin

sections indicated only traces of calcium carbonate. Due to these facts, this work re-

designates the Ain Tobi Member as "Ain Tobi Dolostone Member".

The Yifran Marl Member was designated as a formation by Christie (1955) and

Burollet (1960). Desio *et al* (1963) later described the Yifran marl as a member of his

Ain Tobi Formation. In this study the beds are considered as the upper member of the

Sidi as Sid Formation following El Hinnawy and Cheshitev (1975). The Yifran Marl

Member is not a mappable unit from Riaynah eastward up to the Al Khums coast

which reinforces its member status.

4.2. Previous Work

Geological studies of the Sidi as Sid Formation were started by Christie (1955).

Earlier investigations were principally confined to biostratigraphic studies with limited

emphasis on regional stratigraphy, geologic mapping and structure. This limitation

was caused by the absence of subsurface data. During the late 1950's, however,

subsurface data on the Ghadamis Basin and Jifarah Plain became available.

Christie's publication in 1955 includes a brief lithologic description and faunal lists.

Most publications prior to Christie's were written in Italian. Some French and German

authors have also published articles on northwestern Libya. Christie's publication of

the first faunal description of Jabal Nafusah in 1955 included a geologic map of the

Gharyan area. By this time petroleum exploration had begun and extensive subsurface

data become available in Libya. This enabled Burollet (1956) to correlate the Ain Tobi

with part of the Zebbag Formation of Tunisia. Desio *et al* (1963) discussed the

Mesozoic stratigraphy of the Jabal Nafusah from Yifran east to Al Khums. Magnier

(1963) used published and unpublished data to correlate along Jabal Nafusah between southern Tunisia and Libya.

Reports completed since 1963 include completion of a large-scale geologic map of Libya (Conant and Goudarzi, 1964; 1967). Klitzsch (1968; 1971) wrote a summary of Libyan geology with a structural emphasis and more stratigraphic details. Hammuda (1969) wrote a detailed article on the geology of the Jurassic and Lower Cretaceous of the central Jabal Nafusah. Some geologic studies examined specific problems which were published in the First Symposium on the Geology of Libya (Gray, 1971).

The 1: 250,000 scale geologic map by El Hinnawy and Cheshitev (1975) attempted a new representation of the stratigraphic relationships along Jabal Nafusah. Mann, 1975a; b; Zivanovic, 1977; Antonovic, 1977; Novovic, 1977a; b, also produced a 1: 250,000 scale geologic map with explanatory booklets in Al Khums and Misratah; Beni Walid; Mizdah; Djeneien and Nalut areas respectively. Fatmi *et al* (1980) proposed a new nomenclature of the Pre Upper Cretaceous Mesozoic rocks. Megerisi and Mamgain (1980a; b) considered in detail the Upper Cretaceous-Tertiary Formations of northern Libya. Most of these studies were summarised in the Stratigraphic Lexicon of Libya by Banerjee (1980). Many other authors have published articles in the second and third Symposium on the Geology of Libya (1980 and 1991) which was edited by Salem and Busrewil and Salem and others respectively. These articles each considered separate formations of the area.

4.3. Age of the Ain Tobi Dolostone Member

Christie (1955), Rossi-Ronchetti and Albanesi (1961), and Desio *et al* (1963) considered the Ain Tobi Dolomite Member to be Cenomanian (Mid-Cretaceous) in age. Subsequent work by Jordi and Lonfat (1963), Burollet and Manderschied (1965),

and Busson (1967a) have shown that the Ain Tobi sequence could be Late Aptian through Cenomanian.

Christie (1955); Rossi-Ronchetti and Albanesi (1961) and Desio *et al* (1963) derived their age determination by studying an area from Jadu to Messellatah (Fig. 1.1). These studies depended upon the macrofauna present in Jabal Nafusah. Rossi-Ronchetti and Albanesi (1961) presented the most complete macrofauna list. It includes 36 species of bivalves, gastropods, cephalopods, and echinoids. Forms cited by them range in age from Aptian to Maastrichtian. Eleven forms are restricted to the Cenomanian and three to the Turonian. Their conclusion was that the Ain Tobi Dolomite Member is Cenomanian in age.

Desio *et al* (1963) described the "Gezzar Dolomite" in Jabal Nafusah west of the Cussbat. The Gezzar is a calcareous dolomite and dolomitic limestone, crystalline light grey, rosy to light brown and very hard. These Dolomites are yellow, medium to thinly bedded and softer, and are subordinately interbedded. They contain undetermined moulds of microfossils, gastropods, bivalves, and rudists. The upper part of the Gezzar Dolomite consists of dolomitic, slightly marly limestone. This part is named the Scerciara Limestone. The Gezzar-Scerciara couplet unconformably overlies the Abu Shaybah Formation. In the study area the Ain Tobi Dolomite and Gezzar are lithologically similar. No age is given for the Gezzar and it is considered here as a part of the Sidi as Sid Formation (Ain Tobi Dolomite Member) following the recommendations of El Hinnawy and Cheshitev (1975); Mann (1975a).

Due to extensive dolomitization of the Ain Tobi sediments and consequent destruction of most body fossils; it was difficult in this study to identify any index fossils to confirm the age. Clay and marl samples for palaeonological analysis were collected

from Section # 4 (Wadi Jabar, S4-24); Section # 5 (Kiklah, S5-10) and Section # 7

(Taghmah, S7-5 and S7-20). These samples were treated with standard palaeontological

preparation method including HCL and HF; 10 μm screen and $ZnBr_2$ for the separation

of minerals and organic materials. Samples S5-10 and S7-5 were treated with $NaPO_3$ and

no HCL or HF in order to separate siliceous or calcareous microfossils. These treatments

were unsuccessful because the samples were barren. There was some organic material,

black particles and rare pieces of plant tissue in sample S7-5, whereas sample S5-10

yielded several pollengrains (*Quercus* sp, periporate pollen of *composite* family, and

small clusters of reti tricolpate pollengrain). All were recent contaminated and have

greenish/grey colour. Sample S4-24 yielded a possible denocyst but was also

contaminated by modern material.

Because the samples were effectively barren, no age determination or

palaeoenvironmental description could be suggested. The weathering of the rocks was

probably the main factor responsible for the absence of polynomorphs.

4.4 Cenomanian Palaeogeography in Northwestern Libya

The Ain Tobi Member was deposited during a major marine transgression which

began in northwest Libya at the end of the Early Aptian and culminated during the Late

Turonian. This transgression may have begun in the Cenomanian in other parts of Libya

and North Africa.

The Ain Tobi Dolomite Member is a part of a shelf deposit which covers all or part of

Algeria, Tunisia, Libya, Egypt, Niger and Chad (Reyre, 1966). The isopach map (Fig.

2.9) shows that the region of the present Jabal Nafusah in northwest Libya is part of a

wedge of Cenomanian srata which thickens to the south towards the axis of the

Ghadamis Basin. The Jabal Nafusah area lay adjacent to a topographic high or non-

subsident region to the north. Because the axis of the Ghadamis Basin parallels that of the Saharan Atlas Trough to the northwest both presumably were generated by the same tectonic forces. The non-subsiding region to the north may be an extension of the Jifarah Dome in Tunisia.

Based on surface maps (Conant and Goudarzi, 1964; Mann, 1975b), the Misratah area is the westernmost expression of the structural style of the Sirt Basin. The increased Cenomanian thickness may be due to subsidence (Gumati and Kanes, 1985) or the presence of grabens and/or growth faults associated with the opening of the Sirt Basin. Due to poor biostratigraphic data and structural complexity the geology of the area southeast of Misratah can not adequately be integrated (and correlated) with the Sirt Basin or Ghadamis Basin.

The isopach map shows that from the Ghadamis Basin axis south the Cenomanian section thins. East of about 12° 30'E longitude (Fig. 2.9) the Misratah area is abruptly terminated by an erosional unconformity. South of the zero contour (Fig. 2.9), Turonian sediments overlie Pre-Cenomanian deposits, Lower Cretaceous (Kiklah Formation). This unconformity probably is another feature related to the opening of the Sirt Basin. West of 12° 30'E Cenomanian deposits thicken rapidly and the contours tend to be perpendicular or oblique to the Al Qarqaf escarpment. The contours of the thickness map (Fig. 2.9) reflect the generally greater original area of sediment distribution to the south and southwest (Sanders, 1970). Southeast of the Al Qarqaf Arch and west of Jabal al Haruj Upper Cretaceous continental and calcareous marine rocks are exposed (Conant and Goudarzi, 1964). They are part of the Cenomanian seaway of Reyre (1966).

There is a general decrease in carbonate content from northeast to southwest and an increase in siliciclastic content. This reflects generally the gradient between an onshore

clastic source and offshore carbonate production. Possible sources of first cycle siliciclastics in the region are the Precambrian Hoggar Massif in Algeria and the Tibisti Mountains along the Libya-Chad border. Much of the siliciclastic sediment in the Sidi as Sid Formation (Ain Tobi Dolomite Member) of Jabal Nafusah and the underlying Kiklah Formation is of a second or multi-cycle origin. The carbonate material was generated in situ on the Ain Tobi platform.

In the subsurface from northwest Libya into the Sirt Basin there are lithologic and nomenclature changes in the Cenomanian section. The Bahi and Lidam Formations (subsurface) are equivalent to the Sidi as Sid and Nalut Formations (outcrop). The Bahi Formation is a siliciclastic unit composed of interbedded sandstone, siltstone, conglomerate and shale with abundant glauconite pellets in the uppermost part. The lower part is thought to be non-marine, but the glauconitic upper part is apparently marine (Sghair, 1993). It is believed to be a diachronous unit, ranging in age from Cenomanian to Maastrichtian (Butt, 1986; Sghair, 1990; 1993). The Bahi Formation is conformably overlain by the marine Lidam Formation or other younger Upper Cretaceous strata.

The Lidam Formation is dated as Cenomanian in age (Barr and Weegar, 1972). The Lidam Formation is mainly composed of argilaeceous dolomite with common glauconite pellets and quartz grains in the lower portion, oolitic limestone in the middle part, and fine to medium dolomite associated with anhydrite at the upper part (El-Bakai, 1989; 1991). It was deposited in a shallowing upward ramp in the nortwestern part of the Sirt Basin (El-Bakai, 1989; 1992). The Lidam Formation appears to be similar to the Ain Tobi Dolomite Member, but the oolitic facies is totally dolomitized in the Ain Tobi Member.

The Ain Tobi Dolomite Member is part of a transgression sequence that can be found throughout most of North Africa. In North Africa diverse lithologies and facies are associated with the sequence. As in the case of the Ain Tobi Dolomite Member, most of the transgressive units were deposited on a carbonate platform, possibly a carbonate ramp. The dominance of carbonates and presence of evaporites reflects a warm possibly dry Cretaceous climate. The Sidi as Sid transgressive sequence is part of a major worldwide Mid-Cretaceous rise in sea-level.

4.5. Conclusion

Early investigations of the Ain Tobi Dolomite Member were mainly confined to biostratigraphy. However geological studies of the Ain Tobi Dolomite Member were started by Christie (1955). The age of the Ain Tobi Dolomite Member is Mid-Cretaceous (Cenomanian), as pointed out by Christie (1955); Rossi-Ronchetti and Albanesi (1961) and Desio *et al* (1963). There is, however, the possibility that the member could be Late Aptian through to Cenomanian, as mentioned by Jordi and Lonfat (1965) and Busson (1967a). Due to the extensive dolomitization of the original sediments of this member, palaeontological and palaeonological methods were unsuccessful in better defining the age. The Ain Tobi Dolomite Member is a part of a shelf deposit which covers much of North Africa.

The carbonate content, generally decreases from northeast to southwest, with increasing siliciclastic content in the same direction. This may reflect the gradient between an onshore clastic source and offshore carbonate production.

CHAPTER FIVE

CHAPTER FIVE

5. LITHOLOGY AND LITHOFACIES

5.1. Introduction

This section deals with the Ain Tobi Member lithology and the sedimentary structures as observed in the field. The petrography and its relationships with the global sea level changes in the Cretaceous will also be discussed. In this chapter the Ain Tobi Dolostone Member will be divided into lithofacies.

The Ain Tobi Member is a widely distributed rock unit, along the Jabal Nafusah escarpment. It forms the topmost part of this Jabal. This member is developed also in the southern part of the Jabal Nafusah in the Ghadamis Basin as a subsurface unit. Generally, the thickness of the Ain Tobi Dolostone Member increases from southwest to northeast. The entire succession is without biostratigraphic markers. The Ain Tobi Dolostone Member is equivalent to the subsurface Lidam Formation in the Sirt Basin, to the Alalgah Formation in the northwestern Libyan Offshore Basin and to part of the Zebbag Formation in Tunisia.

5.2. Lithology

5.2.1. Western Jabal Nafusah

Five sections have been measured in the area which extends from the Libyan-Tunisian border in the west to Riaynah Village (Fig. 1.1) at Wazan (Section # 11); Nalut (Section # 12); Kabao (Section #10); Jadu (Section # 9) and Riaynah (Section # 8). The thickness

of the Ain Tobi increases from Wazan to Riaynah, but the maximum thickness is developed in the Jadu area (see Section # 9).

Wazan Section

The thickness of the Ain Tobi here is 5m only. The measured section is located on the main road between Wazan Village and Nalut Town, just 2km southeast of the village centre between (31° 53' 00"N and 10° 39' 45"E). The contact between the Ain Tobi Member and the underlying Kiklah Formation is unexposed at this location. The Ain Tobi here is characterized by whitish, well to thinly-bedded, laminated and bioturbated dolomudstone/dolowackestone with marly intercalation. It becomes slightly coarser at the top of the outcrop. Small nodules of gypsum, chert nodules and solution breccias are also developed within these sediments (see Section # 11).

Nalut Section

This section is located immediately below Nalut Town, between 31° 51' 53"N and 10° 59' 31"E. The thickness of Ain Tobi here is 15m. The lower 2m are yellowish, massive, highly bioturbated and porous dolomudstone/dolowackestone commonly containing quartz grains (Fig. 5.1a). The succeding 12m are light-grey, bioturbated and massive, occasionally cross-bedded dolopackstone/dolograinstone. Gypsum, chert nodules and solution breccias consisting of angular clasts commonly occur. Rudists, ooids bivalves and gastropods are also present within this bed. This upper bed probably represents the *Ichthyosarcolites* Band of Christie (1955). Common chert nodules occurred in the topmost part of this section (see Section # 12).

KEY TO SECTIONS 1-12

L I T H O L O G Y
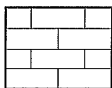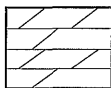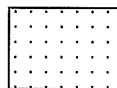
LIMESTONE	DOLOMITE	SANDSTONE	M A R L
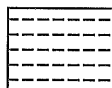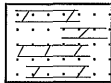
GYPSUM/ ANHYDRITE	DOLOMITIC SANDSTONE	Q U A R T Z G R A I N S
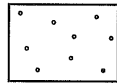
SEDIMENTARY STRUCTURES
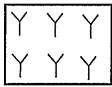
BIOTURBATION	B E D D I N G	WAVY LAMINATION	CROSS-BEDDING
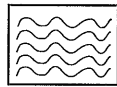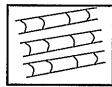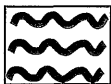
R I P P L E S	ALGAL LAMINAE	INTRACLASTS	CHERT NODULES
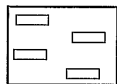
GEOIDS FILLED BY SPARY CALCITE	B I R D S - E Y E	V E R T I C A L FRACTURES	B U R O W S
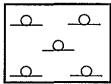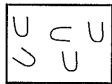
T E X T U R E S
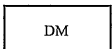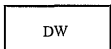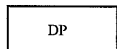
DM	DW	DP	DG
DOLOMUDSTONE	DOLOWACKESTONE	DOLOPACKSTONE	DOLOGRAINSTONE
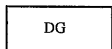
F A U N A
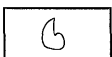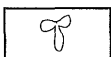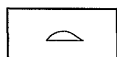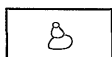
B I V A L V E S	FORAMINIFERA	ECHINODERMS	GASTROPODS

R U D I S T	O O I D S	BRYOZOANS

Stratigraphic column	Sample no.	Scale (m)	Lithology	Sedimentary struc., weathering profile&fauna	Photographs	XRD
Nalut Fm.		15				
↑ Sidi as Sid Fm. (Ain Tobi Member)	S12-4			ᵇY ▽ Y ⊚ ▽ △ Y⊚		o
	S12-3			DP/DG △ ⊚ Y ⊚ △		o
	S12-2			Y ᵠ ⊚ △ Y		o
↓ Kiklah Formation	S12-1	0		Y DM/DW	o	o

Section 12. Immediately below Nalut City (31° 51' 53"N & 10° 59' 31"E).

Stratigraphic column	Sample no.	Scale (m)	Lithology	Sedimentary struc., weathering profile&fauna	Photographs	XRD
Sidi as Sid Fm. (Ain Tobi Mbr.)		5	Top exposure in area	Y ▷ △DM DW Y⊜ △		o o o
	S11-3 S11-2 S11-1	0				

Section 11. Wazan Village on the road between Nalut and Wazan, 2km before the Village center (31° 53' 45"N & 11° 19' 48"E).

<u>Fig 5.1</u> Dolomite lithotypes of the unconformity surface:

a. Photograph of a polished slab (sample No. S12-1), Nalut Section. This is yellowish, bioturbated and porous dolowackestone.

b. Field photograph showing the contact between red sandstone of the Kiklah Formation and the overlying well bedded Ain Tobi Dolomite Member (Jadu Section).

c. Polished slab photograph showing dolomite breccia (dedolomitization) at the unconformity surface, Jadu Section (sample No. S9-1).

d. Polished slab photograph of sample No. S9-2, showing a dolomudstone matrix or dolomite breccia from the unconformity surface, Jadu Section.
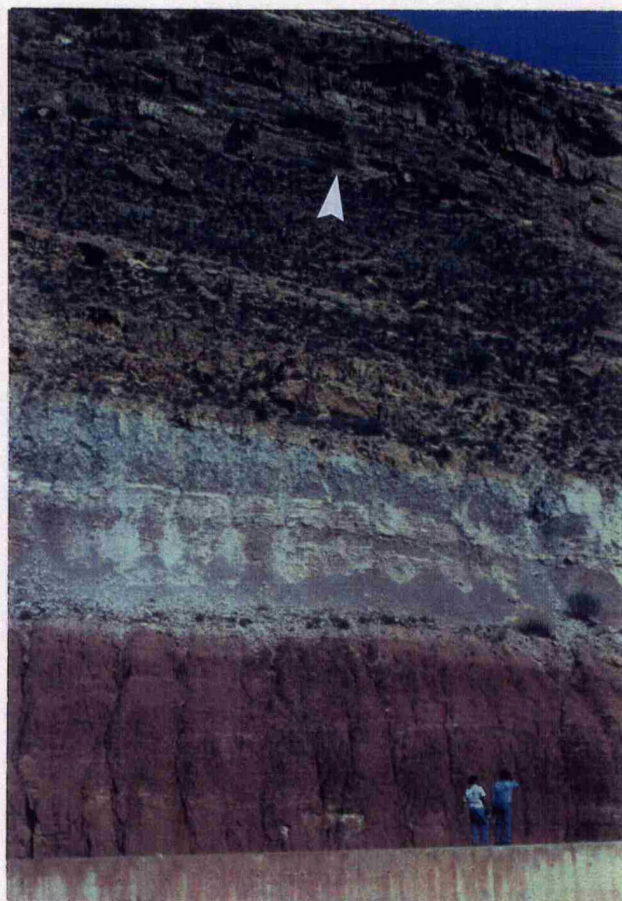
FIG. 5.1

Kabao Section

This section is located at the Kabao Village between 31° 53' 45"N and 11° 19' 48"E. The thickness of Ain Tobi Member in this location is 20m. It is characterized in the lower 6m by light-grey, well thickly bedded and highly bioturbated dolomudstone/dolowackestone, interbedded with gypsum (50cm) and chert nodules. Gypsum nodules are common throughout all this section. Vugs or solution breccias consisting of angular clasts commonly occur within the lower part. Between 6 and 9m above the base of the exposed part of the succession the sediments are composed of light grey, cross-bedded, bioturbated and highly porous dolowackestone/dolopackstone, with intraclasts, chert and gypsum nodules and interlaminated with 20cm of yellow marl. Ooids, gastropods, bivalves and rudists also occur within this interval, which may represent the *Ichthyosarcolites* Band. From this band upwards to the top of exposure the sediments are yellowish, well bedded to bioturbated dolowackestone and dolopackstone. The sediments within this interval are laminated, particularly in the middle part, and discontinuous pinkish laminae occur in the lower part. The topmost part of this interval is highly porous dolowackestone and consists of gypsum, lamination and ripples (see Section # 10).

Jadu Section

The Jadu section was measured on the main road below the Jadu Town, between 31° 57' 20"N and 12° 00' 27"E. The maximum thickness of the Ain Tobi Member in the western part of Jabal Nafusah has been observed in this location. This is due to the higher percentage of coarse clastics in the area. An additional 20m of sandstone and/or dolomitic sandstone, composed of three coarsening-upward sequences (from very fine shaly quartz sandstone and dolomitic sandstone to well sorted coarse quartz sandstone and dolomitic sandstone) are intercalated into the sequence here. The underlying Kiklah

Stratigraphic column	Sample no.	Scale (m)	Lithology	Sedimentary struc., weathering profile & fauna	Photographs	XRD
SIDI AS SID FORMATION (Ain Tobi Member)	S10-6	25	Top exposure in area	DW		o
	S10-5			DW/DP		o
	S10-4					
	S10-3	14		DP		o
	S10-2			DM		o
	S10-1	5		DM/DW		o
Kiklah Formation		0	covered			

Section 10. Kabao Village (31° 53' 45"N & 11° 19' 48"E).
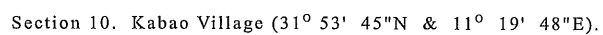
Formation in this area is composed of red-pinkish-grey and yellow cross-bedded, fine to coarse sandstone and siltstone interbedded with red clay. The unconformity surface (Fig. 5.1b) between Kiklah Formation below and Ain Tobi Dolostone Member above is covered by varicoloured conglomerate and silt with red and yellow clay commonly filling the void space (Fig. 5.1c). Gypsum nodules mud-cracks and solution breccias, consisting of angular clasts are also present. The base of Ain Tobi Member is usually marked by an increase in resistance to weathering caused by the carbonate content but is composed generally of coarsening-upward quartz sandstone and dolomitic sandstone (13 m thick). This lithology is pinkish to yellowish-grey, bioturbated (Fig. 5.1d) and thickly-bedded. The succeding 9m of strata are olive-grey to yellowish, well bedded and hard dolomite commonly with quartz sand grains. The thickness (between 22 to 27m, Section # 9) represents the second coarsening-upward quartz sandstone sequence. It is whitish, bioturbated and uncemented. This is followed by 3m of yellowish and whitish-grey, bioturbated dolomite with frequent quartz grains and thin layer (50 cm) of dark-grey or black, very hard and coarse sandstone (Fig. 5.2a) occurred. Thin irregular or wavy laminae and narrow, long and vertical fractures also occur. The successive 7m of strata represent, the third and final coarsening-upward quartz sandstone and dolomitic sandstone sequence within the member. It is yellowish and bioturbated commonly with geodes filled by coarse sparry calcite. The 4m immediately above this are dominated by yellowish-grey, bioturbated, cross-bedded and porous dolopackstone/dolograinstone, commonly with quartz grains. Rudists, gastropods, bivalves and intraclasts also commonly occur. This is succeeded by 4m of light-grey, well to thinly bedded, highly bioturbated and porous dolomitic sandstone, interbedded with yellowish and bioturbated siltstone.

Fig. 5.2 Photographs of representative samples from the Ain Tobi marine deposits in western Jabal Nafusah:

a. Polished slab photograph of sample No. S9-7 from the Jadu Section showing dark grey or black, very hard and coarse sandstone. The thickness of this bed is only 50cm.

b. Outcrop photograph from Jadu Section shows well-bedded lithologies of the Ain Tobi Dolostone Member.

c. Polished slab photograph showing heavy bioturbation, and highly porous dolopackstone at the bottom right corner. Note also intraclasts (arrow), sample (S9-21), Jadu section.

d. Polished slab photograph showing cross-bedding of the oolitic dolopackstone and dolograinstone. Note common mouldic porosity at the top, Jadu Section.
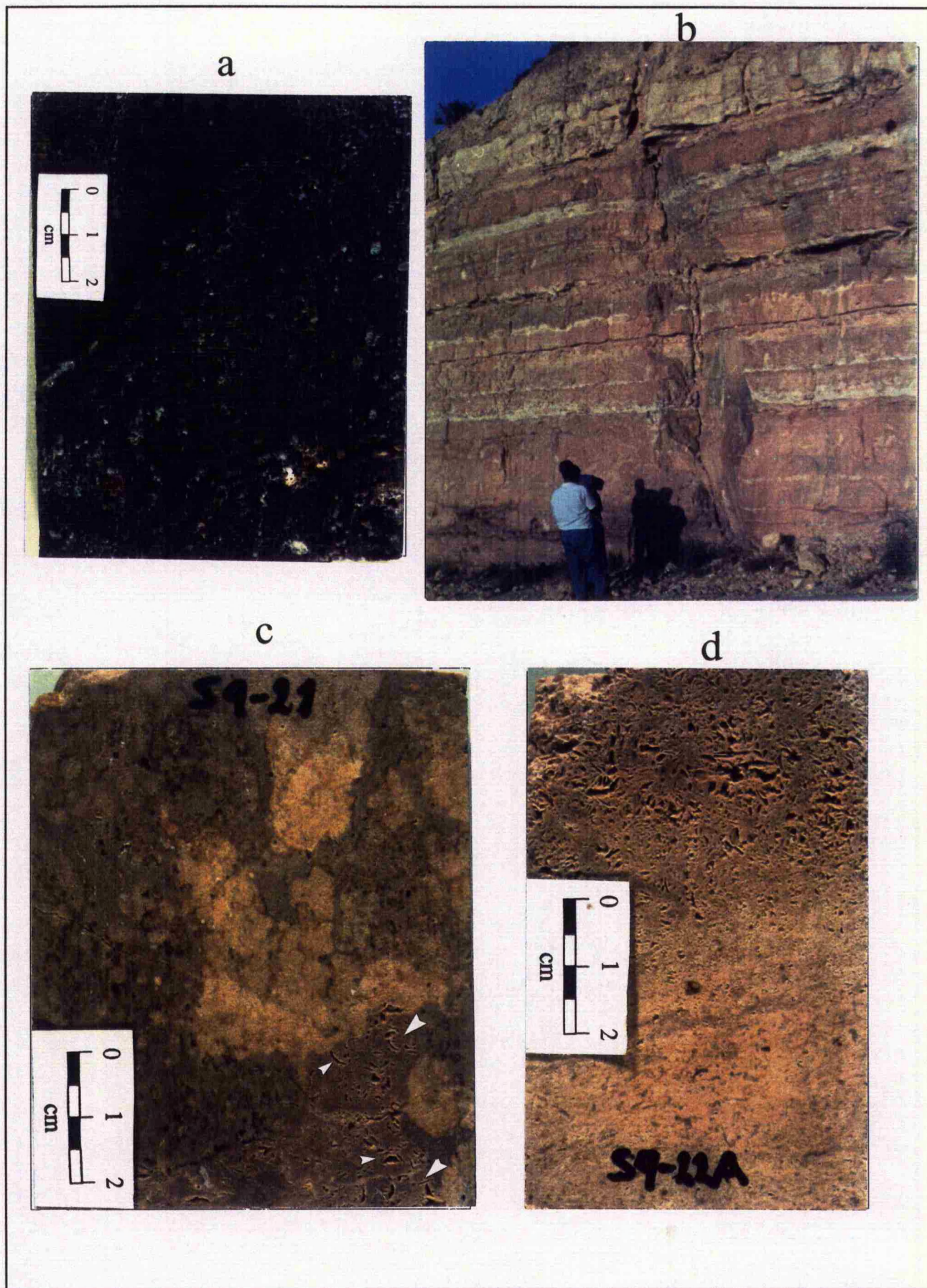
FIG. 5.2

From 47 to 66m may represent the *Ichthyosarcolites* Band of Christie (1955) (Fig.

5.2b, Section # 9). The lower part of the band is composed of yellowish, olive-grey,

thickly-bedded, bioturbated (Fig. 5.2c) and small scale cross-bedded oolitic

dolowackestone and dolopackstone (Fig. 5.2d). Gastropods and bivalves are present.

Geodes filled by spary calcite or gypsum are also common. The upper part of the band is

composed of bioturbated and cross-bedded oolitic dolowackestone/dolopackstone.

Gastropods, bivalves and echinoids are the most common allochems within this interval.

The beds immediately above the band are characterized by whitish and yellow-grey, well

bedded, laminated and highly bioturbated dolomudstone and dolowackestone in the

lower part. These become highly fossiliferous (gastropods, bivalves and echinoids)

dolopackstone, interlaminated with clay and marl (Fig. 5.3a).

The middle part of these beds is composed of yellowish, well-bedded, bioturbated and

porous dolomudstone and dolowackestone with long, and thin fractures filled by spary

calcite. Marl percentage and gypsum nodule percentages increases upwards. The

lithology in the upper part is mainly composed of whitish and light grey, well and thinly

bedded laminated and porous dolopackstone/dolograinstone (Fig. 5.3b) which may

represent the beginning of a new cycle. The topmost 16m are made of light-grey and

yellowish, well thickly bedded, bioturbated and laminated dolowackestone and

dolopackstone. Chert nodules, intraclasts and ripples commonly occur and marl increases

upwards (see Section # 9).

Stratigraphic column	Sample no.	Scale (m)	Lithology	Sedimentary struc., weathering profile&fauna	Photographs	XRD

Section 9. Immediately below the Jadu Town, $31^{O}57'\ 20"N$ & $12^{O}\ 00'\ 27"E$)
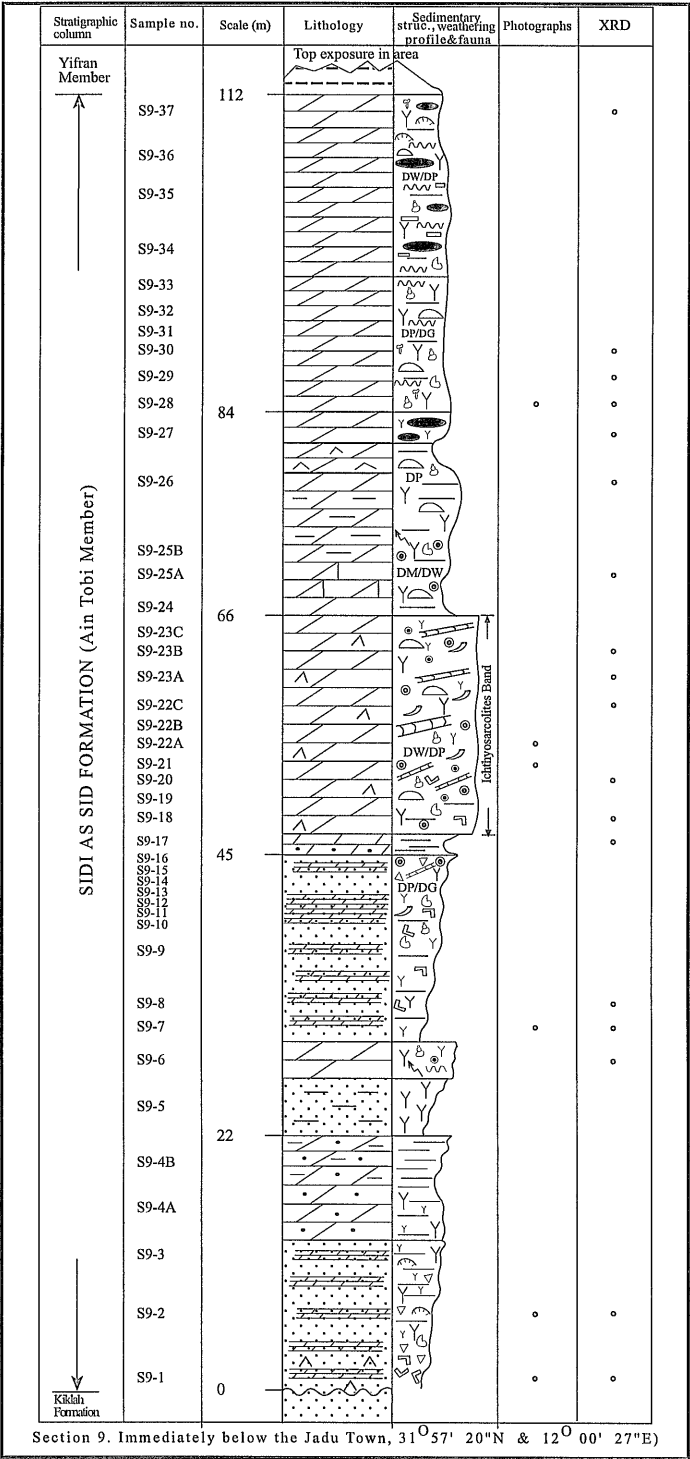
Riaynah Section

This section is measured at the location immediately below Riaynah Village, between

31° 59' 55"N and 12° 19' 54"E. The thickness of Ain Tobi Member in this area is 66m.

Its lower contact with the underlying Kiklah Formation is covered (Eight meters are

hidden) by recent deposits (Fig. 5.3c). The lowest observable 12m are composed of

brownish-yellow, well to thickly bedded (in 1m intervals) and bioturbated dolomudstone

(Fig. 5.3d). Thin and dark laminae (may be microbial laminae) and associated birds-eye

structure commonly occur within this interval. Geodes filled by sparry calcite are also

common. This lithology becomes a light-grey, bioturbated dolopackstone, commonly

with gastropods, bivalves and gypsum nodules in the middle part. The upper part of this

interval exhibits whitish-grey, bioturbated, hard and very thinly laminated

dolowackestone/dolopackstone and dolograinstone, which may represent the beginning

of a new cycle. Rudist shells and gastropods are very common and long, vertical and

horizontal oriented shells are filled by recent soil (Fig. 5.4a and b). This interval has a

sharp contact with the overlying strata. Immediately above that one meter of yellowish to

dark grey, porous, cross-bedded and bioturbated dolowackestone/dolopackstone (Fig.

5.4c) occur. The succeeding 4m (Section # 8) are made of yellowish grey, bioturbated,

soft and cross-bedded dolowackestone/dolopackstone, becoming dolograinstone at the

top. Geodes filled by sparry calcite, and rudists with other indeterminate fossil fragments

are common. This interval may represent the *Ichthyosarcolites* Band and is overlain by

50cm of yellowish, bedded, bioturbated and laminated dolomudstone. The laminae are

pinkish in colour and horizontal burrows also occur (Fig. 5.4d). The lower part of the

beds above the band are composed of whitish, massive, highly porous and soft oolitic

dolowackestone and dolopackstone, becoming dolograinstone in the middle of the

sequence (Fig. 5.5a). The upper part of these beds are characterized by light-grey,

Stratigraphic column	Sample no.	Scale (m)	Lithology	Sedimentary struc., weathering profile & fauna	Photographs	XRD
			Top exposure in area			
Yifran Mbr.	S8-20	66				o
	S8-19			YO	o	
				DM/DW		
	S8-18			Y		
		50.5		YoY		
	S8-17			DMDW		
	S8-16			Y		
	S8-15				o	o
	S8-14					o
	S8-13			DG		o
	S8-12			DW/DP		
	S8-11			Y		
	S8-10	31			o	o
	S8-9 S8-8 S8-7 S8-6			DP/DG	o	o
	S8-5 S8-4					o
	S8-3				o	
	S8-2			DWDP		
	S8-1			DP	o	o
		8	covered	DM		
Kiklah Formation		0				

SIDI AS SID FORMATION (Ain Tobi Member)

Section 8. Riaynah village, 32° 06' 23"N & 12° 32' 51"E)

<u>Fig. 5.3</u>: Dolomite lithotypes in the western Jabal Nafusah escarpment:

a. Field photograph showing the thickly-bedded structure of the Ain Tobi Member interbedded with 50cm thick of olive grey clay at the bottom of the photo (arrow). Jadu Section.

b. Polished slab photograph of sample S9-28, from Jadu Section showing highly porous and laminated dolopackstone/dolograinstone.

c. Outcrop photograph showing the contact (covers) between the Kiklah Formation below and well bedded Ain Tobi Dolostone Member above. Riaynah Section.

d. Polished slab photograph of sample S8-1 from the lower part of the Ain Tobi Dolostone Member at the Riaynah Section showing bioturbated and well preserved sedimentary laminae in a totally dolomitized brownish mudstone.
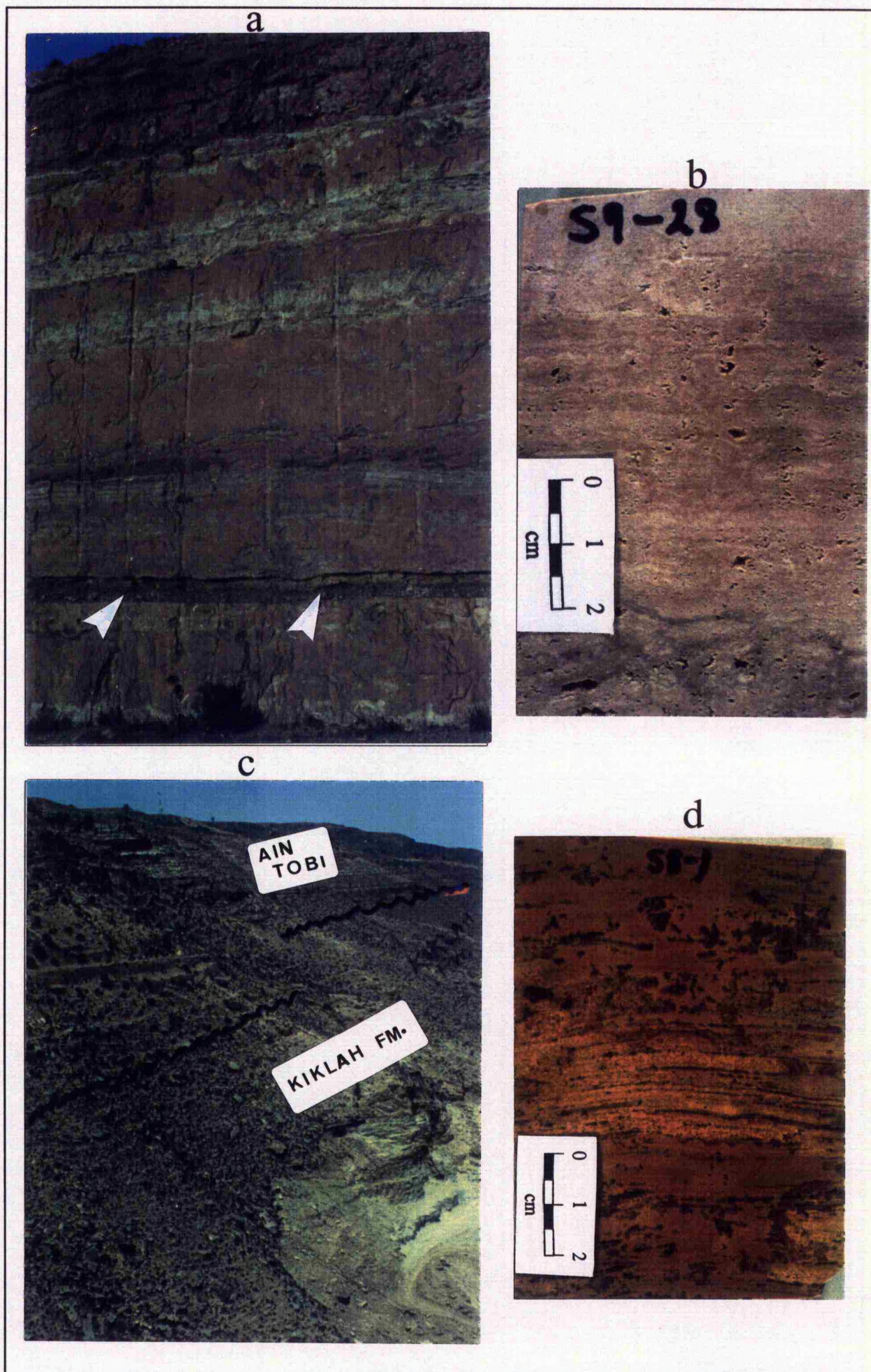
FIG. 5.3

well to thinly-bedded, laminated and bioturbated dolomudstone/dolowackestone.

Gastropod shells, bivalves, ripples and gypsum nodules are observed within this interval.

Marl content increases upward commonly with birds-eye structure in the middle part

(Fig. 5.5b). The Ain Tobi Dolostone Member in this area is overlain with gradational

contact by yellow, well bedded and soft marls of the Yifran Marl Member (see section #

8).

5.2.2. Central Jabal Nafusah (West Wadi Ghan)

This area extends from Wadi Ghan in the east to Yifran Village in the west. Four

sections have been measured within this area; at Abu Ghaylan (Section # 1), at Ar'Rabtah

(Section # 6), at Kiklah (Section # 5) and at Yifran area (Section # 7).

Abu Ghaylan Section

The thickness of the Ain Tobi Dolostone Member in this area is 77m. The measured

section is located at the intersection of the motorway between Tarabulus and Gharyan

cities, and Jabal Nafusah between 32° 15' 53" North and 13° 01' 10" East (Fig. 1.1).

The Ain Tobi Dolostone Member here is unconformably underlain by reddish to dark

brown, fine to silty and bioturbated dolomitic sandstone of the Kiklah Formation (Middle

Jurassic to Lower Cretaceous). The unconformity between the Kiklah Formation below

and the Ain Tobi above is angular (Fig. 5.5c) and its surface (transition zone) is

composed of 2m of yellowish, well bedded conglomerate and

dolomudstone/dolowackestone, full of horizontal burrows. A fining upward sandstone is

associated with this lithology. The lower 17m (Section # 1) are characterized by thickly-

bedded yellow, highly bioturbated dolowackestone/dolopackstone, with some high-spire

macrogastropod shells (Fig. 5.5d), intraclasts, bivalves and foraminifera and scattered

fine to coarse quartz grains. In the middle of this interval

Stratigraphic column	Sample no.	Scale(m)	Lithology	Sedimentary struc., weathering profile&fauna	Photographs	XRD

Top exposure in area

77

59

S1-16

S1-15

S1-14

S1-13

40

S1-12

S1-11

S1-10

22

S1-9

S1-8
S1-7
S1-6
S1-5
S1-4
S1-3
S1-2
S1-1
S1-0

0

SIDI AS SID FORMATION (Ain Tobi Member)

Kiklah Formation

Ichthyosarcolites Band

DM/DW

DP/DG

DP/DG

DW/DP

DW

Section 1. Abu Ghaylan (intersection of Tarabulus-Gharyan motorway and Jabal Nafusah (32° 15' 53"N & 13° 01' 10"E).

Fig. 5.4 Dolomite lithotypes of the Ain Tobi Member in the Riaynah area:

a. Polished slab photograph of sample No. S8-3 showing well preserved laminae in a completely dolomitized packstone with common vertical and horizontal oriented shells (arrows) filled by recent sediments (probably rudist shells).

b. Field photograph showing the *Ichthyosarcolites* Band in the Riaynah Section. Note the rudist shells.

c. Polished slab photograph of sample No. S8-7 showing yellowish, dark-grey, bioturbated dolowackestone/dolopackstone.

d. Polished slab photograph of sample No. S8-11 showing leisegang rings produced diagenetically.
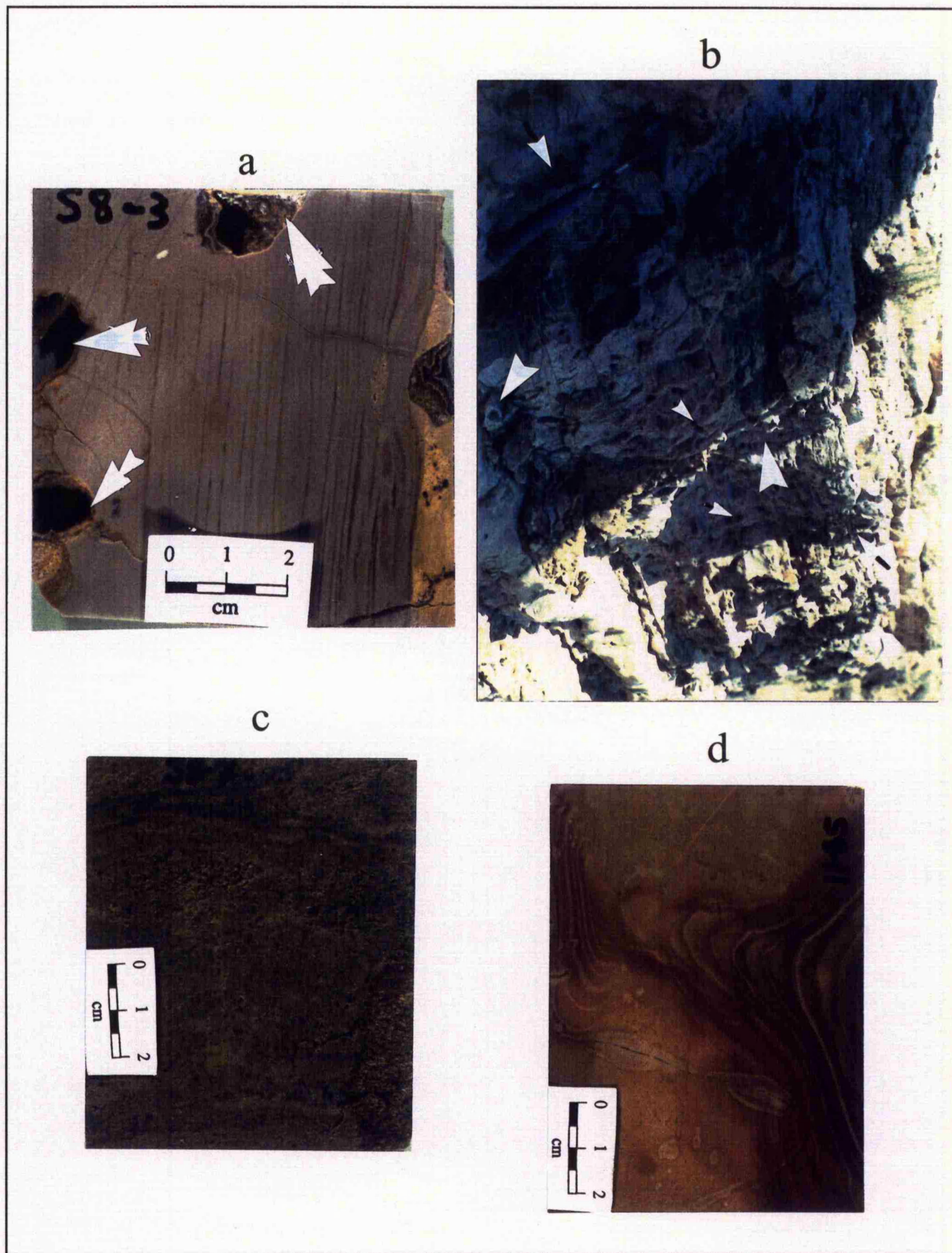
FIG. 5.4

lithologies are dominated by whitish, highly bioturbated dolomudstone commonly with

birds-eye structure (fig. 5.6a) and large bivalve boring (Fig. 5.6b). These are succeeded

by 2m of yellow, highly porous and bioturbated dolomudstone to dolowackestone which

are overlain by 50cm of carbonate conglomerate or coarse dolomite (probably an

erosional surface or end of cycle, Fig. 5.6c). The upper beds of this interval are

dominated by whitish grey, well laminated (irregular or wavy laminae)

dolomudstone/dolowackestone (Fig. 5.6d and Fig. 5.7a). The alternation of laminae is

between dolomite commonly with quartz grains of more porous, and succeeding bed of

pure dolomite with less porosity. The 5m immediately above this (Section # 1) are

composed of yellowish and reddish thickly-bedded, highly bioturbated and small scale

cross-bedded oolitic dolopackstone/dolograinstone (Fig. 5.7b), commonly with

gastropods, intraclasts, chert nodules and breccias. These oolitic dolograinstones may

represent reefooidal development prior to dolomitization. These are succeeded by 18 m

of grey and brownish, highly bioturbated and thickly-bedded

dolopackstone/dolograinstone dominated by dolomitized rudist shells, moulds (Fig.

5.7c), and intraclasts. This may represent the *Ichthyosarcolites* Band of Christie (1955).

Beds overlying the band are grey, thinly bedded, and bioturbated dolowackestone,

becoming laminated marly dolomudstone/dolowackestone in the top. They contain

gastropods, echinoderms, chert nodules and bivalve moulds (Fig. 5.7d).

Ar'Rabtah Section

This section is located on the main road between Ar'Rabtah Village in the north-east

and Abu Zayan Village in the south-west between 32° 08' 05" North and 12° 51' 49"

East. The thickness of Ain Tobi Member in this location is 69m and is

<u>Fig. 5.5</u>: Outcrops (Abu Ghaylan sectoin) and hand specimens (from western part of the study area) of fossiliferous dolostone:

a. Polished slab photograph of dolopackstone/dolograinstone (sample S8-15) from the Riaynah Section showing coarse gastropod shells (g) and fossil moulds (arrow) with common large calcite crystals (white area).

b. Polished slab photograph of sample No. S8-19 from the Riaynah Section showing brownish colour, typical porosity and birds-eye structure occurring within totally dolomitized wackestone.

c. Field photograph showing the angular unconformity between the Kiklah Formation below and the Ain Tobi Dolostone Member above in the Abu Ghaylan area. People in front of photo provide scale.

d. Outcrop view in the Abu Ghaylan area showing macrofosils (high spire gastropod moulds, arrow).
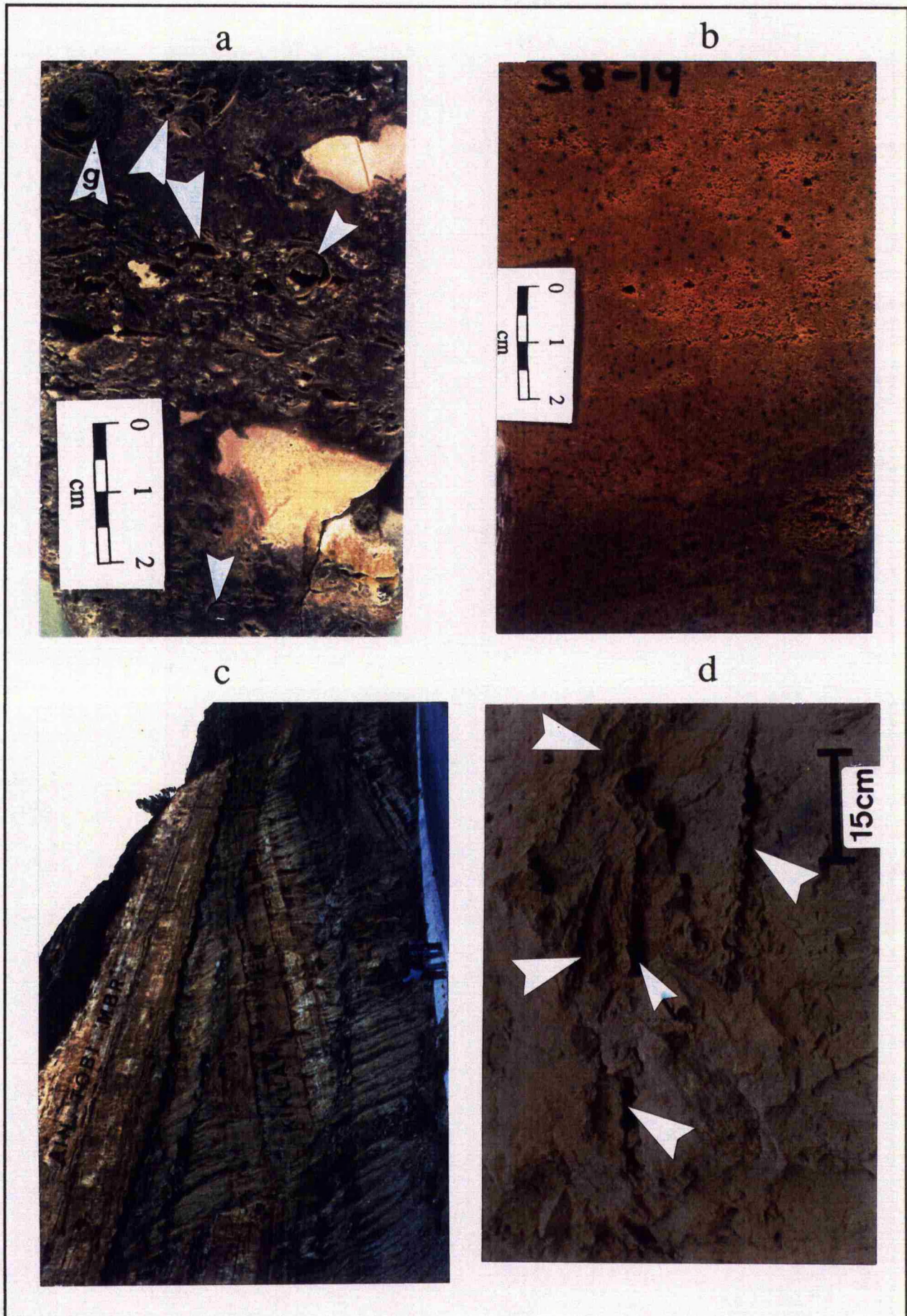
Fig. 5.5

unconformably underlain by the Kiklah Formation. The lower part of the Ain Tobi Member is characterized by yellowish, massive, fine to coarse, bioturbated and poorly sorted dolomitic sandstone. This becomes highly bioturbated (Fig. 5.8a) and well-bedded dolomudstones/dolowackestones commonly with gastropods, bivalves, ostracods and gypsum nodules also occur. The 6m immediately overlying these are composed of yellowish, bioturbated, thinly-bedded and porous dolowackestones/dolopackestones with ripples. This interval is succeeded by 13m of whitish to tan, thickly-bedded, highly bioturbated dolopackstones/dolograinstones commonly with shell debris, gastropods and?corals. The fossil fragments are probably rudist shells (Fig. 5.8c). The top 7m of this interval are dominated by small scale-cross-stratified dolograinstones containing ooids. This entire interval may represent the *Ichthyosarcolites* Band of Christie (1955). The 36m immediately above the band (Section # 6) are dominated by yellowish, thinly-bedded, laminated and bioturbated dolowackestones/dolopackstones interbedded with 2 to 3m thick marl beds. The top 2m of the Ain Tobi Member in this section exhibit yellowish, thinly-bedded and bioturbated dolomudstones with rare bivalves and solution breccias. This makes a sharp contact with the overlying Maastrichtian Qasar Tigrinnah Formation (Section # 6).

Kiklah Section

The section is measured in the side of the main road below the Kiklah Village between $32°$ $03'$ $28''$ North and $12°$ $42'$ $54''$ East. The thickness of the Ain Tobi Dolostone Member in this area is 65m and it is underlain by the Kiklah Formation. The lower 20m are dominated by light grey, bioturbated (Fig. 5.8d), thickly-bedded and slightly laminated dolomudstones/dolowackestones commonly with gastropods and bivalves. The succeeding 10m are characterized by yellowish, well-bedded and highly bioturbated dolopackstone commonly with moulds, rudists, gastropods and fossil fragments (Fig.

Stratigraphic column	Sample no.	Scale(m)	Lithology	Sedimentary struc.,weathering profile&fauna	Photographs	XRD
		77	Top exposure in area	Y Y Y		
	S6-16					o
	S6-15			DM Y		o
	S6-14	64		Y Y Y Y bY b Y Y		
	S6-13			DW Y b Y o b Y Y		o
	S6-12	46		DM Y b DW/DP Y b Y		o
	S6-11			Y		o
	S6-10			b Y DWDP Y Y b		
	S6-9	30		o b Y o Y	o	o
	S6-8			DP/DG b	o	o
	S6-7			b Y b o Y Y b		
	S6-6	16		DM Y		o
	S6-5			Y b	o	o
	S6-4			DW/DP b Y Y		o
	S6-3			Y Y b		o
	S6-2B			Y b Y		
	S6-2A			DM/DW Y	o	o
	S6-1B			Y		
	S6-1A	0		b Y		o

Qasar Tigrinnah Fm.

SIDI AS SID FORMATION (Ain Tobi Member)

Ichthyosarcolites Band

Kiklah Formation

Section 6.Ar'Rabtah areal (32° 08' 05"N & 12° 51' 49"E).

Fig. 5.6 Outcrop and hand specimen photographs of mottled and laminated dolostone of Ain Tobi Member at central Jabal Nafusah:

a. Polished slab photograph of sample (S1-4) at Abu Ghaylan section showing possibly storm deposits (arrow).

b. Field view showing bioturbated dolomudstone with long bivalve boring (centre).

c. Outcrop photograph from Abu Ghaylan section showing coarse or conglomeratic dolomite (centre of photo marked by hammer) which probably represents an erosional surface, between thickly-bedded units below and thinly-bedded ones above.

d. Polished slab photograph of sample (S1-8) at Abu Ghaylan area showing well preserved laminae in a completely dolomitized mudstone. Dolomite and quartz laminae (1) and pure dolomite laminae (2).
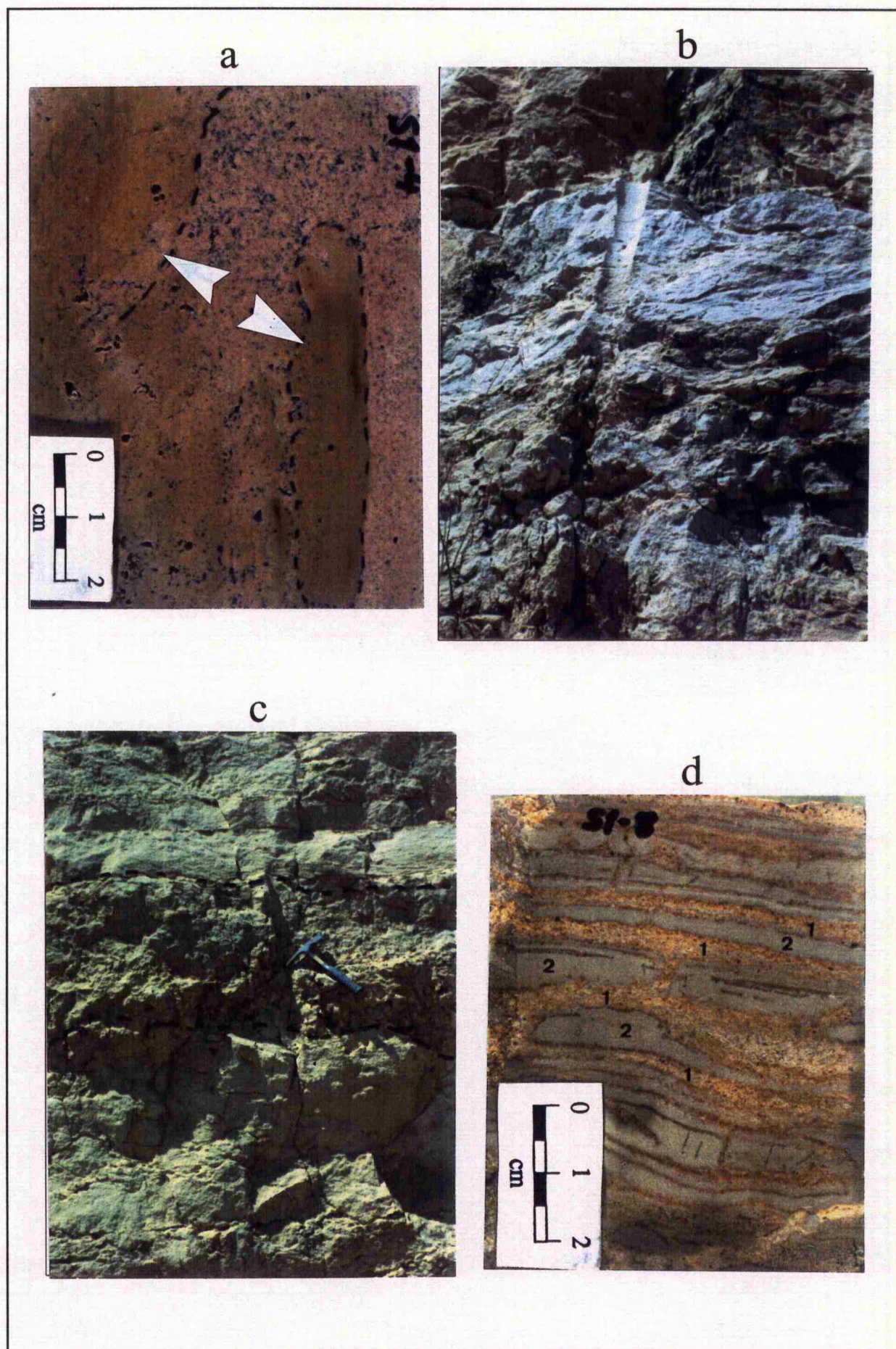
Fig. 5.6

5.9a). They become bioturbated and there are cross-bedded dolowackestones at the top. This interval may represent the *Ichthyosarcolites* Band. The 19m immediately above this are dominated by yellowish grey, thinly-bedded, laminated and highly bioturbated and soft dolomudstones/dolowackestones, with sandstone levels, breccias and possibly birds-eye structure. The top 15m interval is characterized by light-grey, thinly-bedded, laminated and bioturbated dolomudstones with chert nodules and geodes filled by spary calcite (Section # 5). This is a sharp contact with the overlying Nalut Formation, the latter forming the top of the escarpment in this area.

Taghmah Section

This section is located in the Yifran area by the side of the main road below Taghmah village between 32° 06' 23" North and 12° 32' 51" East (Fig. 1.1). The thickness of the Ain Tobi Dolostone Member in this area is 62m. Here, Ain Tobi Member is unconformably underlain by the Kiklah Formation (Shakshuk Member) which is dominated by reddish clay, fossiliferous limestone (dolomitic in places) and siltstone. The lower part of the Ain Tobi is characterized by light-grey and yellowish, thickly-bedded highly fossiliferous (Fig. 5.9b) and bioturbated dolomudstone/dolopackstone commonly with fossil moulds (bivalves and gastropods), intraclasts, chert nodules and quartz grains. It is well bedded and laminated at the middle of this interval and is overlain by 50cm of olive bioturbated siltstone and clay. The upper beds of this interval are dominated by yellowish-grey, laminated, well-bedded, bioturbated and porous dolowackestone/dolopackstone. Bivalves, quartz grains, intraclasts, chert nodules, ripples, breccia and burrows (Fig. 5.9c) are present. The succeeding 17m represents the *Ichthayosarcolites* band (Christie, 1955) which is dominated at its base by light-grey, bioturbated, highly porous (moulds), and cross-bedded coarse oolitic dolopackstone/dolograinstone (Fig. 5.9d and Fig.5.10a). In the middle and top

Stratigraphic column	Sample no.	Scale(m)	Lithology	Sedimentary struc., weathering profile&fauna	Photographs	XRD
Nalut Formation		65	Top exposure in area			
	S5-10			DM		o
	S5-9	49		DW		o
	S5-8					
	S5-7			DM/DW		o
	S5-6					o
	S5-5			DW		
	S5-4	20		DP	o	o
	S5-3				o	o
	S5-2			DMDW		
	S5-1					o
Kiklah Formation		0				

(Stratigraphic column labeled: SIDI AS SID FORMATION (Ain Tobi Member); Ichthyosarcolites Band)

Section 5. Kiklah area (32° 03' 28"N & 12° 42' 54"E).

<u>Fig. 5.7</u> Sedimentary structures within the Ain Tobi Dolostone Member in the Abu Ghaylan area:

a. Field view of the Abu Ghaylan section showing well laminated interval.

b. Outcrop photograph at Abu Ghaylan section showing small-scale cross-bedded oolitic dolopackstone/dolograinstone.

c. Polished slab photograph showing dolomitized rudist shells (arrow) and moulds.

d. Outcrop view showing occurrences of the mouldic porosity (bivalve moulds) within the Ain Tobi Dolostone Member in the Abu Ghaylan area.
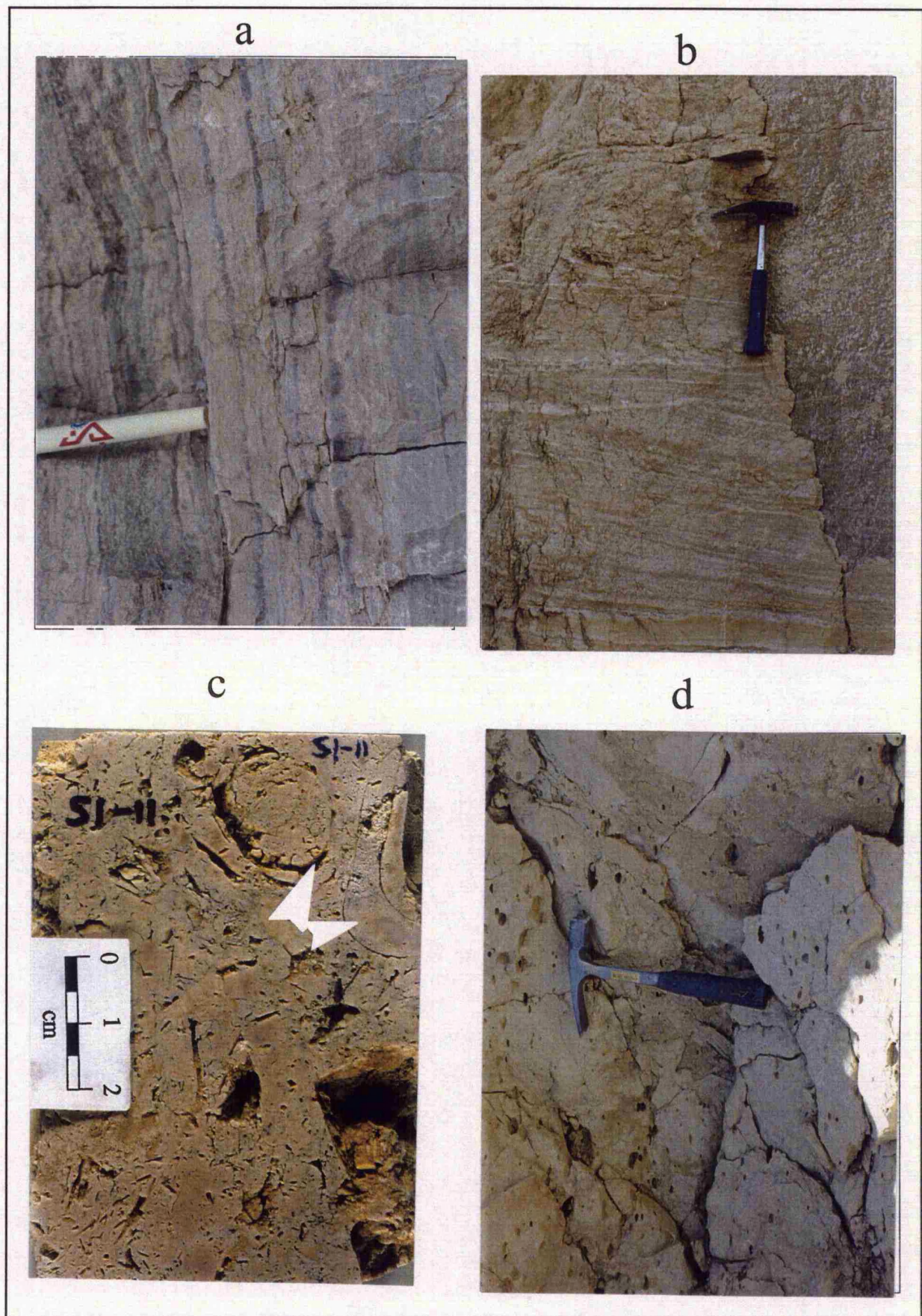
Fig. 5.7

of the lithological unit is light grey, laminated (Fig. 5.10b), bioturbated and small-scale

cross-bedded dolopackstone, commonly with dolomitized rudist shells, fossil fragments

and ooids. Common chert nodules becoming massive chert at the top. The beds above

the band are yellowish, thinly-bedded and bioturbated dolowackestone/dolopackstone,

locally with small-scale cross-bedding oolitic dolograinstone (fig. 5.10c) at the lower part

of this interval. The top of this interval is light-grey, thinly-bedded, laminated and

bioturbated dolowackestone/dolopackstone (Fig. 5.10d) with indeterminate fossil

fragments, moulds and ripples. This makes the top of escarpment in the area (see section

7).

5.2.3. Eastern Jabal Nafusah (East Wadi Ghan)

This area is located between Wadi Ghan in the west and Al Khums Coast in the east.

Three sections are measured within this area, at Ras Fam Mulghah (Tarhunah area), at

Wadi Jabbar (between Qasr Khiar and Mesellatah) and at the mouth of Wadi Ghanimah

on the Mediterranean Coast.

Ras Fam Mulghah Section

This section is situated about 1km east of the main road between Tarabulus and

Tarhunah (32° 15' 53"N and 13° 01' 10"E) and locally is called Ras Fam Mulghah. The

Ain Tobi Dolostone Member in this area previously was thought to be unconformably

underlain by the Abu Shaybah Formation (Upper Triassic- Lower Jurassic). Recently,

Fatmi and Sbeta (1991) claimed that Ain Tobi is unconformably underlain by remnants of

the Kiklah Formation which is very thin in this location. This has also been confirmed in

this study. The total thickness of Ain Tobi Member in this section is 84m and makes the

top of the escarpment.

Stratigraphic column	Sample no.	Scale(m)	Lithology	Sedimentary struc., weathering profile&fauna	Photographs	XRD
			Top exposure in area			
	S7-26	59.5		Y Y		o
	S7-25			Y ~~ Y	o	o
	S7-24			Y	o	o
	S7-23			DWDP Y	o	o
	S7-22 S7-21			Y		o o
	S7-20			Y Y		o
	S7-19	33		DW/DP Y		o
	S7-18				o	o
	S7-17					o
	S7-16			DP Y	o	o
	S7-15			Y		o
	S7-14					o
	S7-13				o	o
	S7-12 S7-11	16		Y DP/DG	o o	o o
	S7-10 S7-9			Y	o	o o
	S7-8			DW/DP		o
	S7-7			Y		
	S7-6			U	o	o
	S7-5			U Y		o
	S7-4			~~ Y		o
	S7-3			Y		o
	S7-2			DM/DP	o	o
	S7-1	0		Y		o

SIDI AS SID FORMATION (Ain Tobi Member)

Abu Shaybah Formation

Ichthyosarcolites Band

Section 7. Taghmah Yifran area, 32° 06' 23"N & 12° 32' 51"E)

<u>Fig. 5.8</u> Dolomite lithotypes of the Ain Tobi Member at central Jabal Nafusah escarpment:

a. Polished slab photograph of highly bioturbated dolomudstone/dolowackestone from Ar'Rabtah section. Note possibly dolomite breccia, where the light clasts (L) are sharply separated from yellow dolomite matrix (Y), sample (S6-2A).

b. Polished slab photograph of bioturbated, porous dolopackstone. Note mouldic porosity and fossil shells (e.g. gastropod, arrow), Ar'Rabtah section, sample (S6-5).

c. Polished slab photograph of heavily bioturbated dolopackstone/dolograinstone. Note the abundant porosity.

d. Polished slab photograph of bioturbated dolomudstone/dolowackestone from Kiklah section, sample (S5-3). Note rounded and infilled burows with Fe leaching of the immediately surrounding dolomite matrix (arrow) with softer sediments within them.
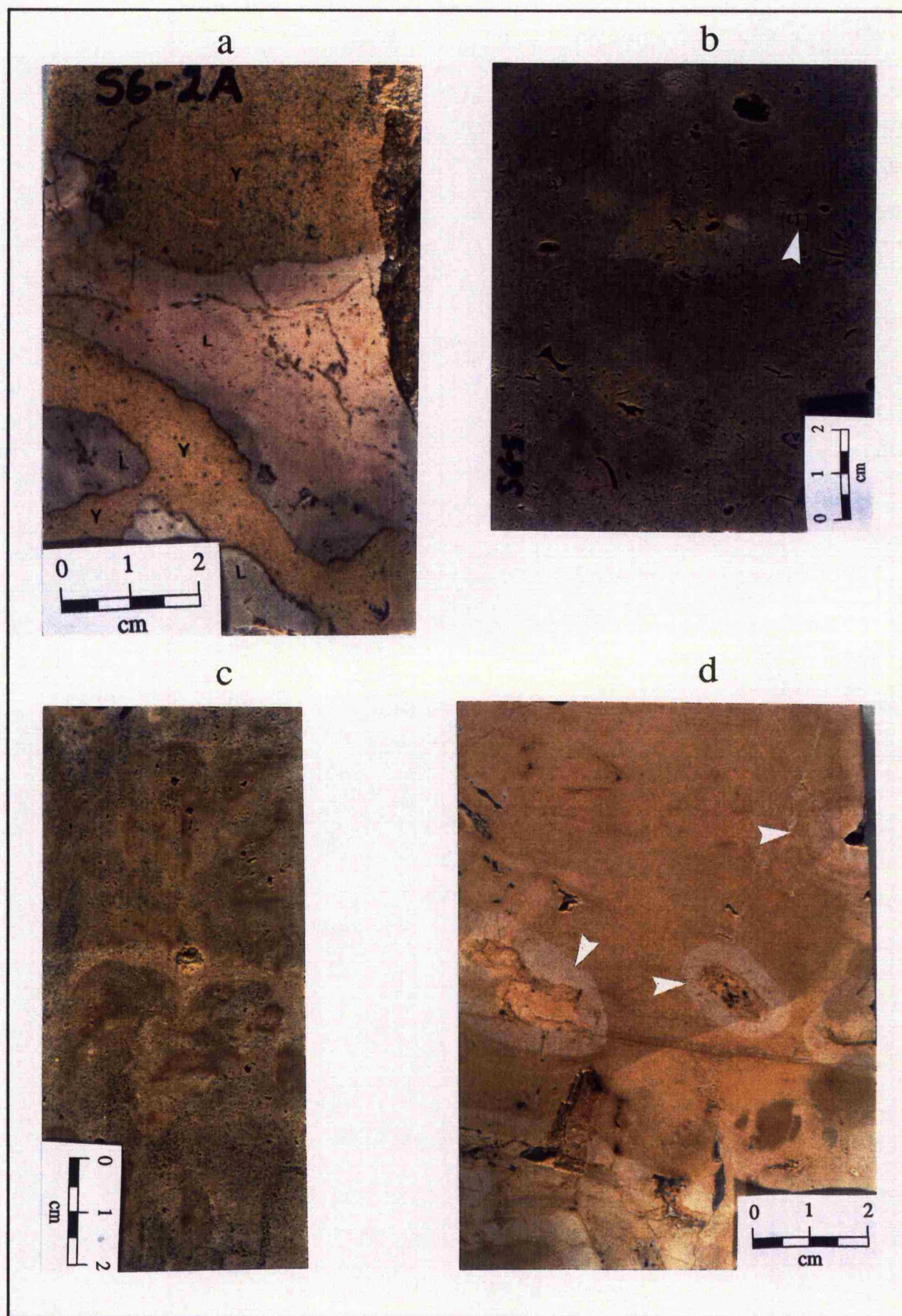
Fig 5.8

The lower 14m of Ain Tobi in this location are characterized by yellowish, well laminated (Fig. 5.11a and b) marly strata with large scale cross-bedded oolitic dolopackstone and dolograinstone. Ripple marks and bivalves are common and chert nodules and breccia are present. These beds become massive marly dolomudstone in the middle of the section, with quartz grains becoming common. The top of this interval is mainly composed of small-scale cross-bedding and coarse oolitic and bioclastic dolograinstone (Fig. 5.11c). This interval between 6 and 14m represents a first cycle of oolitic dolograinstone (Section # 2) which is succeeded by 2m of yellowish, massive, bioturbated strata. Hard karstic dolomudstone, with reworked sediments and birds-eye structure and interbedded clays mark the end of cycle and beginning of new cycle. This surface has a sharp contact with the lower unit (Fig. 5.11d).

The interval between 16 and 42m in this section represents the second cycle of oolitc dolograinstone and exhibits three lithologies; the lower 10m (Section # 2) are composed of light-grey, bioturbated, laminated, thickly-bedded and cross-bedded oolitic dolowackestone/dolopackstone. Bivalves, intraclasts, chert nodules, breccia and birds-eye structure (Fig. 5.12a) are present. This is followed by 6m of light-grey, thickly-bedded, laminated and highly bioturbated cross-bedded oolitic dolomudstone/dolowackestone with birds-eye structure. The top 10m of this cycle are characterized by light-grey, thickly-bedded. well laminated and cross-bedded oolitic dolograinstone commonly with bivalves, gastropods, intraclasts and birds-eye structure and stromatolitic laminae within the middle part of the unit (Fig. 5.12b and c). The succeeding 10m (Section # 2) represents the *Ichthyosarcolites* band (Figs 5.12d and 13a) of Christie (1955). It is composed of a light-grey, massive and bioturbated dolopackstone/dolograinstone, commonly with rudist, gastropods, and bivalves (Fig.

<u>Fig. 5.9</u> Dolomite lithotypes from Ain Tobi Dolostone Member:

a. Polished slab photograph of bioturbated dolopackstone from the Kiklah section, sample (S5-4). Note completely dolomitized fossil fragments with shells, probably rudists, and common unidentified fragments.

b. Polished slab photograph of bioturbated, grey and highly fossiliferous dolopackstone with mouldic porosity. Sample (S7-2), Taghmah section.

c. Polished slab photograph of sample (S7-11), Taghmah section. Note well preserved lamination in a completely dolomitized mudstone. Some laminae are disturbed by burrows.

d. Polished slab photograph of sample (S7-12), Taghmah section. It shows coarse, bioturbated and highly porous oolitic dolopackstone/dolograinstone.
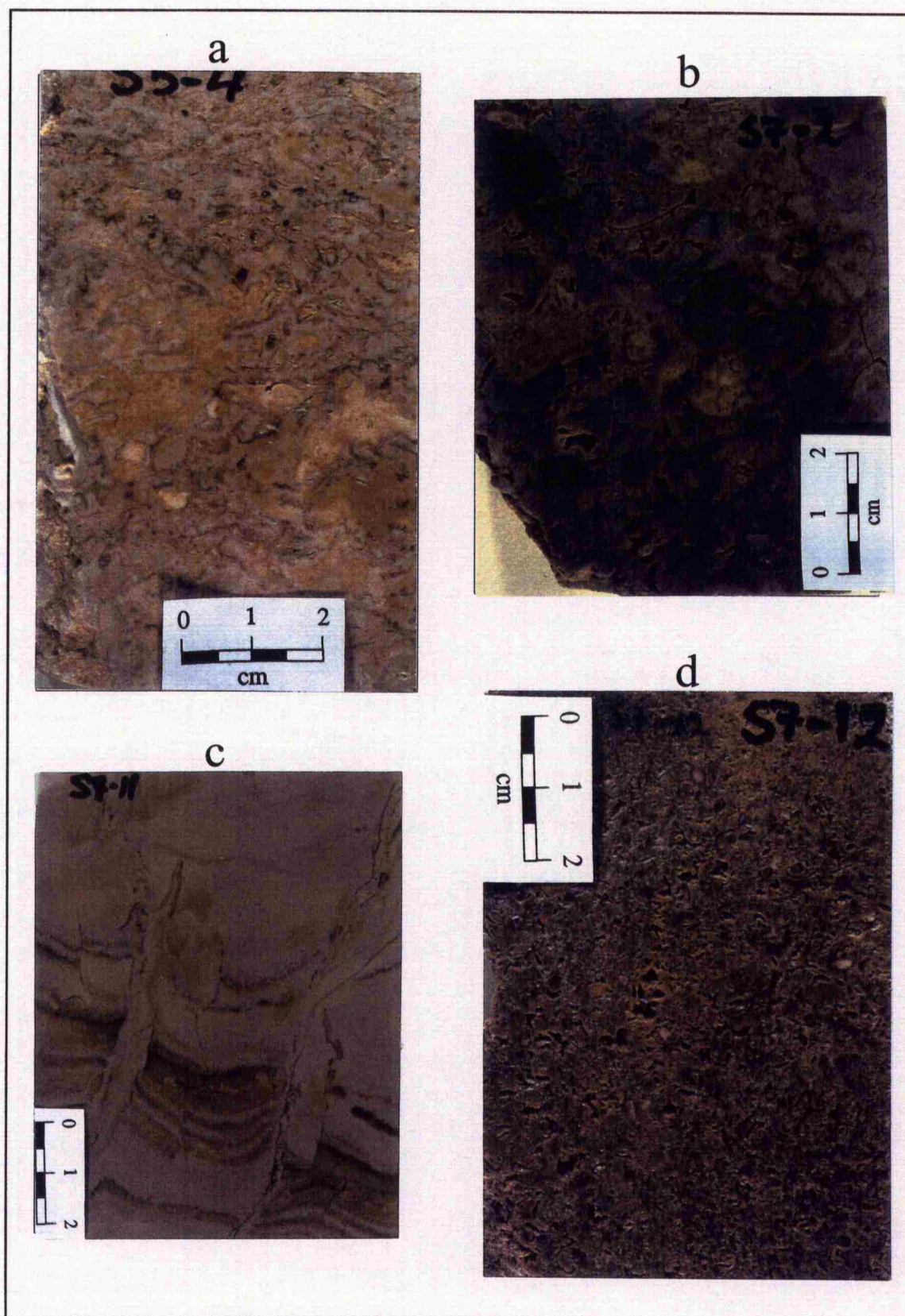
Fig. 5.9

5.13b). Pink and greenish-grey dolowackestone (30cm) occurs in the top of the band (Fig. 5.13c). This top bed may be associated with an erosional surface.

The lithology of the 16m immediately above this are characterized by whitish-grey to tan, thinly-bedded and cross-bedded, highly porous oolitic dolograinstones (Fig.5.13d and Fig. 5.14a).), commonly with bivalves, foraminifera, gastropods and echinoderms. The succeeding 7m exhibit yellowish-grey, bioturbated and cross-bedded dolowackestone/dolopackstone. Bivalves, gastropods, foraminifera and breccia are present. The top 10m are composed of light-grey, hard and massive dolomudstone/dolowackestone commonly with bivalves, foraminifera, echinoderms and chert nodules but an absence of evaporite minerals (see section # 2).

Wadi Jabbar Section

This section was measured at the quarry between 32° 39' 18"N and 13° 56' 17"E about half way along the main road between Qasr Khiar in the north and Mesellatah in the south. The section is known locally as Wadi Jabbar Quarry. The thickness of the Ain Tobi Dolostone Member in this area is 88m. The lower 8m in this location are covered by recent sediments. Above this, the lithology of the Ain Tobi Member, between 8 and 22.5m (Section # 4), is characterized by light-grey, highly bioturbated and highly porous dolomudstone (particularly at the top). It has a sharp contact with the overlying unit. The succeeding 4m are composed of yellowish and light-grey, mottled, laminated (Fig. 5.14b), well bedded and porous (Fig. 5.14c) dolomudstone with ripple lamination at the top. These are followed by 1.5m of yellowish-grey, slightly bioturbated, hard, bedded dolomudstone (Section # 4). The 5m immediately above this exhibit yellowish to tan, highly bioturbated and highly porous, well to thickly-bedded dolomudstone commonly with bivalves, gastropods and ripple lamination. The lithology immediately

Section 2. Ras Fam Mulghah (Tarhunahu), (32° 27' 29"N & 13° 23' 25"E).
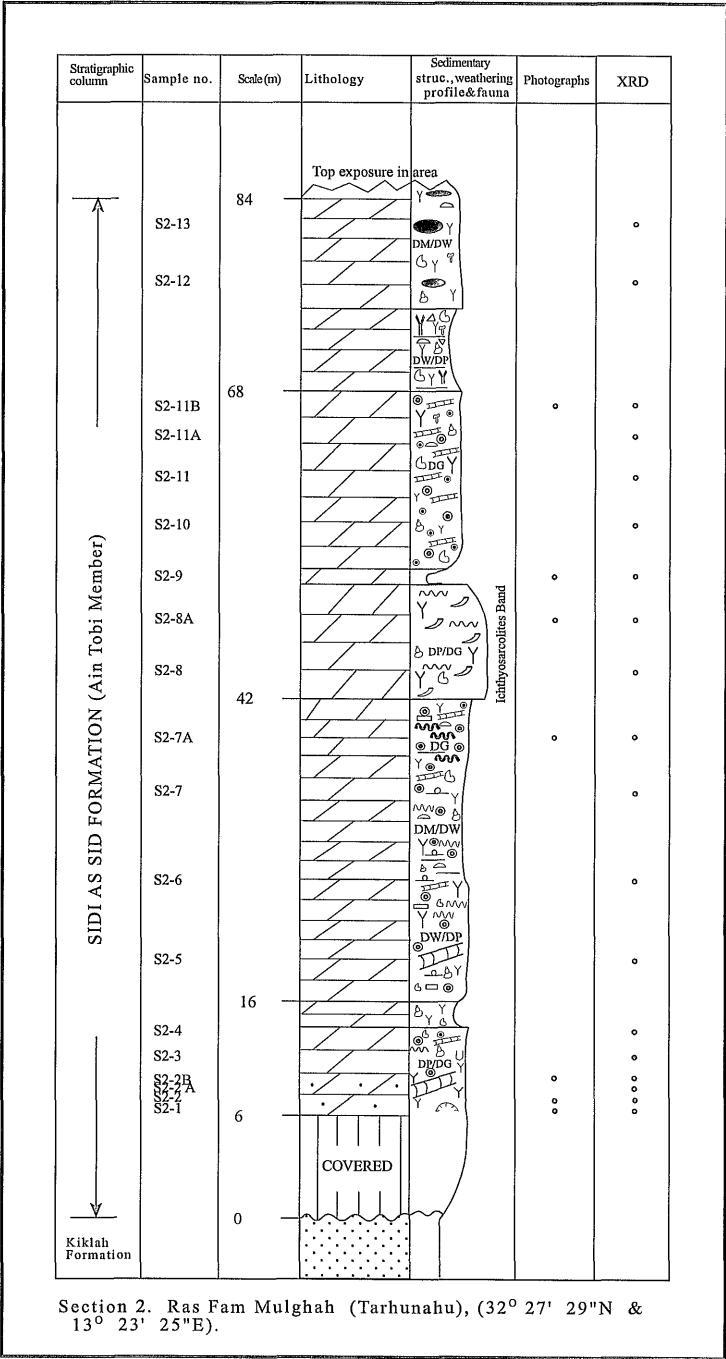
Fig. 5.10 Outcrop and hand specimen photographs of laminated and mottled dolostones in the Yifran Area, Taghmah section:

a. Polished slab photograph of fine cross-bedded oolitic dolograinstone, sample (S7-13).

b. Polished slab photograph of bioturbated and laminated dolopackstone. Note well preserved laminae in a totally dolomitized packstone. Sample (S7-18), Taghmah section.

c. Polished slab photograph of mottled oolitic dolopackstone with extensive porosity. Sample (S7-23), Taghmah section.

d. Polished slab photograph of laminated dolowackestone. Note excellent preservation of lamination and birds-eye (arrow) structure. Sample (S7-25), Taghmah section.
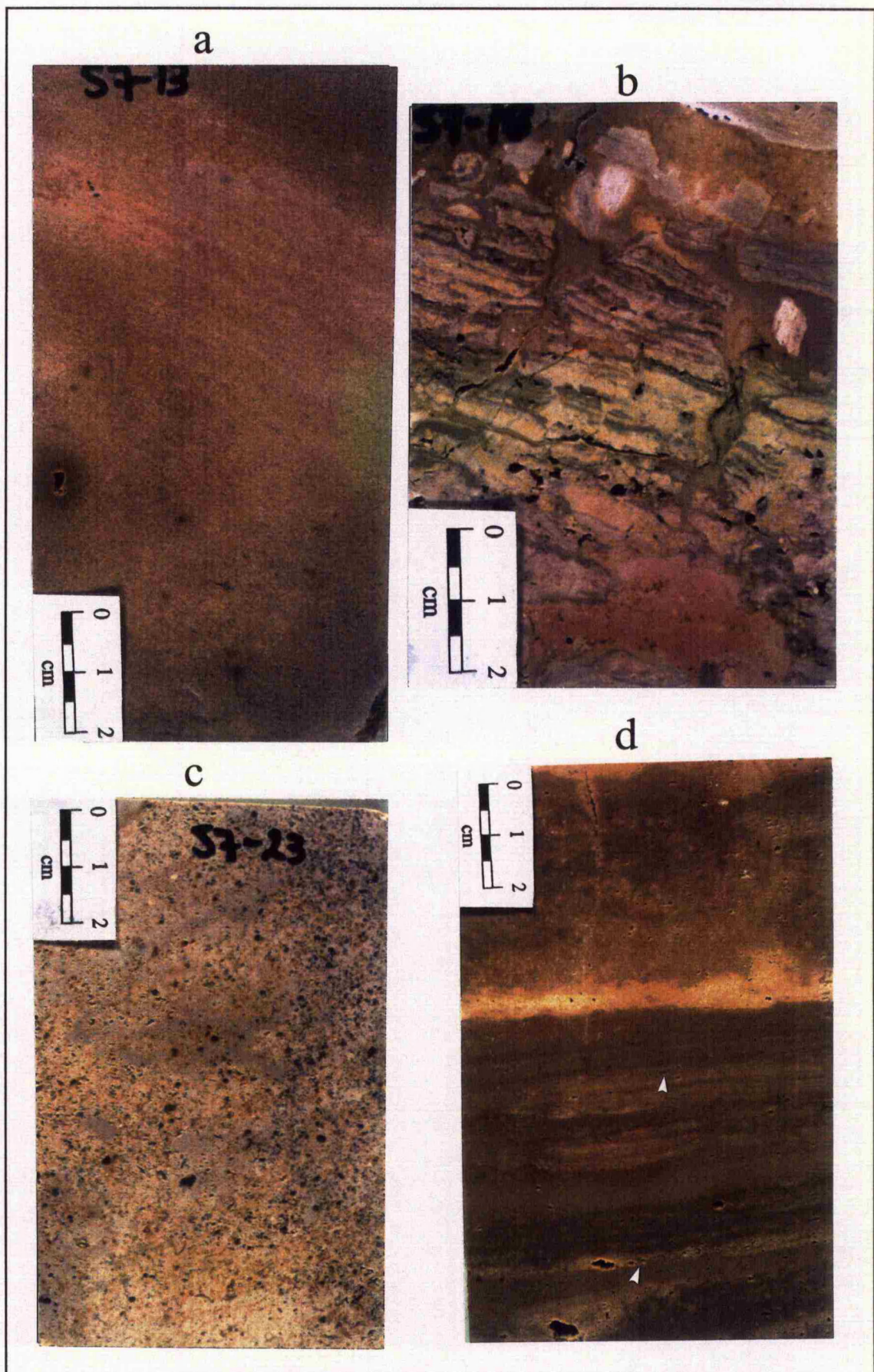
Fig. 5.10

below the _Ichthyosarcolites_ band (between 33 and 39m) is composed of light-grey, bioturbated, massive or thickly-bedded and highly porous dolowackestone, commonly with bivalves, echinoderms, gastropods and geodes filled by rosy and white calcite.

The thickness of the _Ichthyosarcolites_ Band of Christie (1955) in this section is 12m and is characterized by yellowish and light-grey, thickly-bedded, highly bioturbated (Fig. 5.14d) and porous dolowackestone/dolopackstone. This fossiliferous horizon contains large rudist moulds, bivalves, echinoderms, foraminifera and ooids. The geodes are filled by calcite (Fig. 5.15a). The 7m immediately above the band are light-grey, massive and coarse dolomudstone. The top 25m of the Ain Tobi Member in this section are composed of grey to tan (become brownish at the top), thinly-bedded (Fig. 5.15b) and bioturbated (Fig. 5.15c) dolomudstone commonly with bivalves, gastropods and fossil moulds (Fig.5.15d). Chert nodules and breccias are present. This makes the top of escarpment in this area (see section # 4).

Al Khums Section

This section is located on the Mediterranean Coast (3km west of the Al Khums Town) and in the mouth of Wadi Ghanimah (Fig. 5.16a), between 32° 43' 03"N and 14° 04' 48"E. The lower boundary of the Sidi as Sid Formation (Ain Tobi Dolostone Member) is not exposed (Fig. 5.16b). Thickness of the Ain Tobi Dolostone Member is not known because strata exposed here, is only 28m, whereas the rest is below the sea level (Fig. 5.16b). The Ain Tobi sediments in this location are overlain by 8m of white chalky and fossiliferous limestone and dolomitic limestone of the Al Khums Formation (Miocene). The lower 2m of the exposed strata of the Ain Tobi Member in this section are composed of yellowish-grey, well-bedded, medium to coarse dolostone. The successive 24m are dominated by grey, bioturbated coarse to very coarse dolostone with

Section 4. Wadi Jabbar (on the main Road between Qasr Khiar and Mesellatah, 32° 39' 18"N & 13° 56' 17"E)
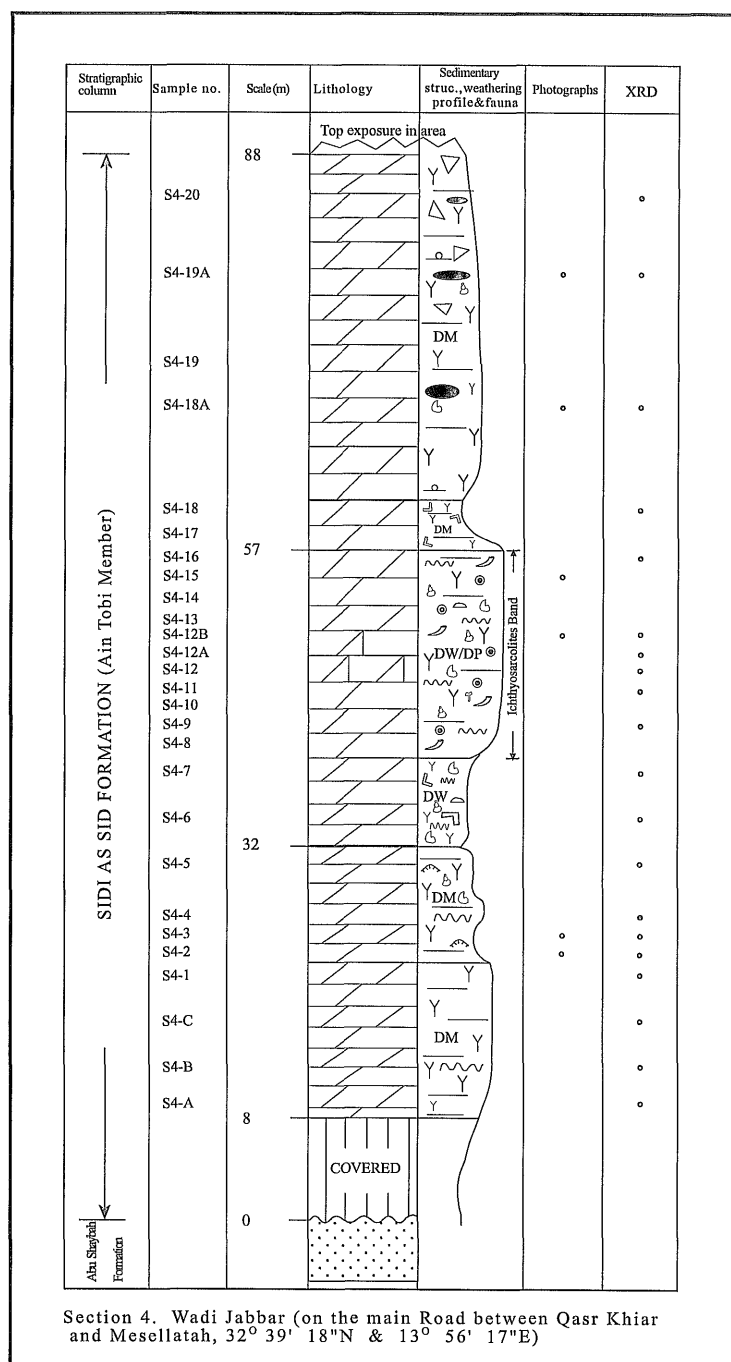
<u>Fig. 5.11</u>   Hand specimen and outcrop photographs of sedimentary structure characterized the Ain Tobi Dolostone Member in the Tarhunah area:

a. Polished slab photograph showing well preserved lamination within small-scale cross bedded oolitic dolograinstone. Sample (S2-1), Fam Mulghah section.

b. Outcrop photograph showing the contact surface between the Kiklah Formation and the Ain Tobi Member.

c. Polished slab photograph of coarse, cross-bedded oolitic dolograinstone. Sample (S2-2), Fam Mulghah section.

d. Outcrop photograph showing the sharp contact (arrow) between two cycles within the Ain Tobi Dolostone Member at Tarhunah.
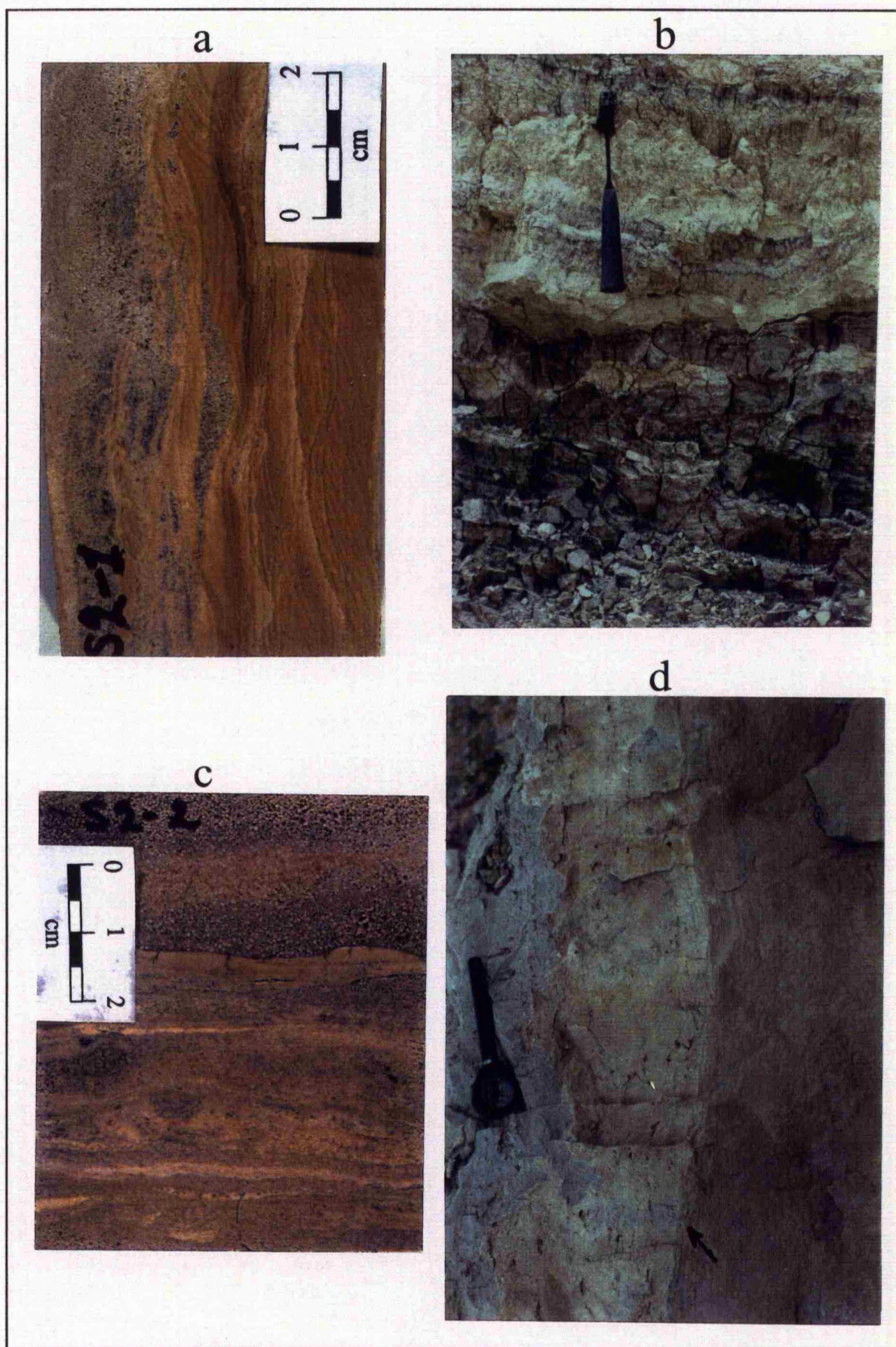
Fig. 5.11

pearly lustre and commonly with intercrystalline porosity (Fig. 5.16c and d). The top 2m

are composed of yellowish, well bedded and fine dolostone, very common with porosity

created by weathering by wind and sea water action (see section # 3).

5.3. *Ichthyosarcolites* Band

The *Ichttyosarcolites* Band is a marker bed across the whole Jabal Nafusah. It is

consistently present at each locality at the lower and/or middle of the Ain Tobi

Dolostone Member. The band was recognized and defined by Christie (1955) in eastern

Jabal Nafusah because of leached moulds of the rudist *Ichthyosarcolites* sp. commonly

found at its top. Rudists have been destroyed probably by diagenesis at the western Jabal

Nafusah, but the band can still be recognized due to its prominent position, thickness and

relatively resistance to weathering comparing with the other beds (Fig. 5.4a and b).

The *Ichthyosarcolites* Band is an unusually thick unit compared to other bedded

intervals in the Ain Tobi. It ranges from 3 to 18m in thickness although it is sometimes

difficult to locate the base (specially at the western Jabal Nafusah) due to the diagenetic

alteration. The band is composed of dolomite, chert and some quartz sand. Generally, the

band is cross-bedded in the central and eastern Jabal Nafusah areas and appears to be

uniformly bioturbated at the western area of Jabal Nafusah. In addition to rudists (Fig.

5.12d and 5.13a), which give the band its name, other bivalves, gastropods, echinoids,

bryozoans and foraminifera occur mainly as moulds. Ooids are also present.

The *Ichthyosarcolites* Band makes a gross change from the dominance of thicker

bioturbated beds below to thinner beds above. Beds below the band are more resistant to

weathering than those above. The upper beds are often soft and powdery while

underlying beds tend to be crystalline. This is due to differences in depositional lithology

across the band. Sediments above the band contain more argillaceous material and

STRATIGRAPHIC COLUMN	SAMPLE NO.	SCALE (METER)	LITHOLOGY	SEDIMRNTARY STRUCTURE, WEATHERING PROFILE & FAUNA	PHOTOGRAPHS	X R D
			Top exposure in area			
		36				
	S3-6				o	o
		27				
	S3-5			DW		o
	S3-4			DW	o	o
	S3-3			DW		o
	S3-2			DW	o	o
	S3-1	Sea Level				o

Al Khums Fm. (Miocene)

Sidi as Sid Fm. (Ain Tobi Mbr.)

SECTION 3. Wadi Ghanimah Mouth (Al Khums Coast, 32° 43' 03"N AND 14° 04' 48"E)
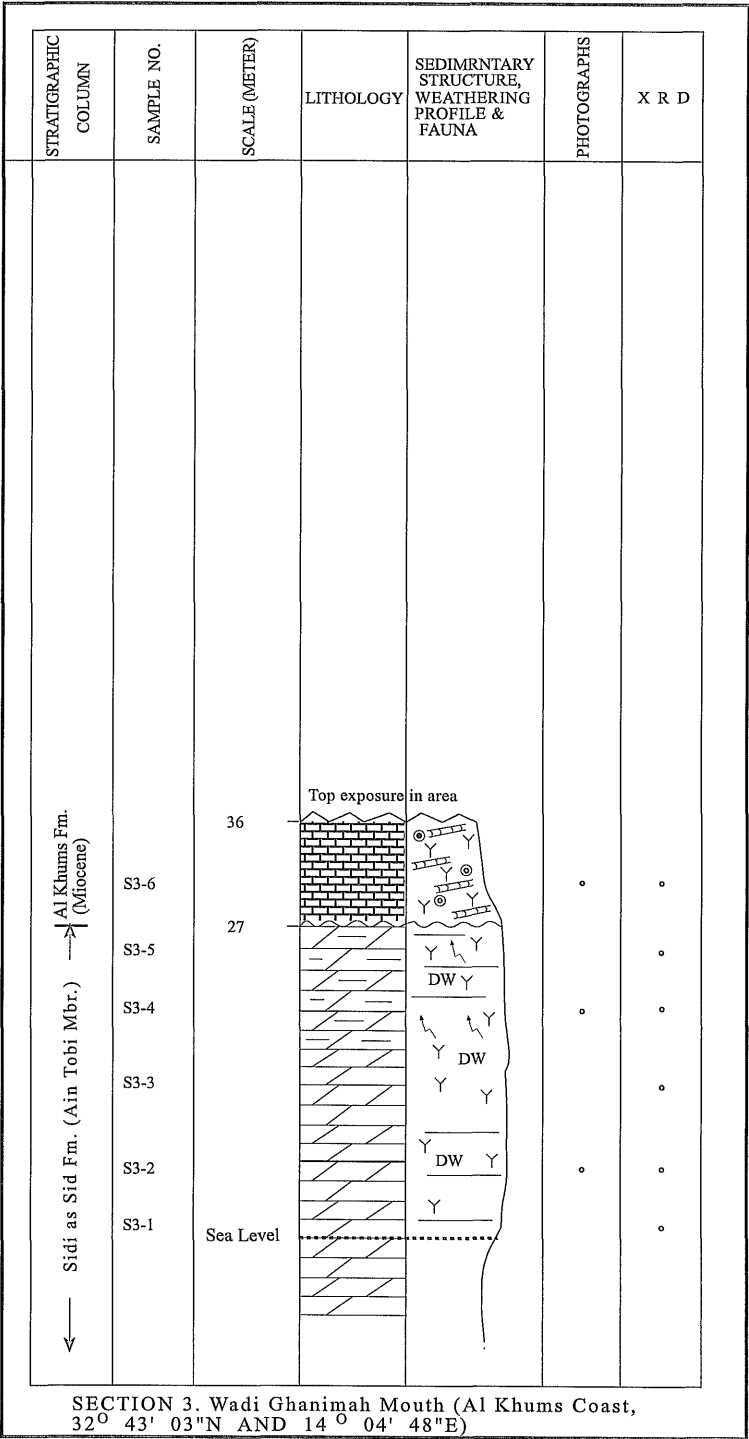
<u>Fig. 5.12</u> Sedimentary structure of the Ain Tobi Member at Tarhunah area:

a. Field photograph showing laminated (microbial laminae), oolitic dolopackstone and birds-eye structure, Fam Mulghah section.

b. Outcrop photograph showing well preserved stromatolitic lamination in a completely dolomitized mudstone/wackestone. Note birds-eye structure, Fam Mulghah section.

c. Polished slab photograph of excellent preservation of stromatolites and burrows in a totally dolomitized mudstone at Fam Mulghah section, sample (S2-7A).

d. Field photograph showing the dolomitized rudist shells occurring within the *Ichthyosarcolites* Band at the Fam Mulghah section.
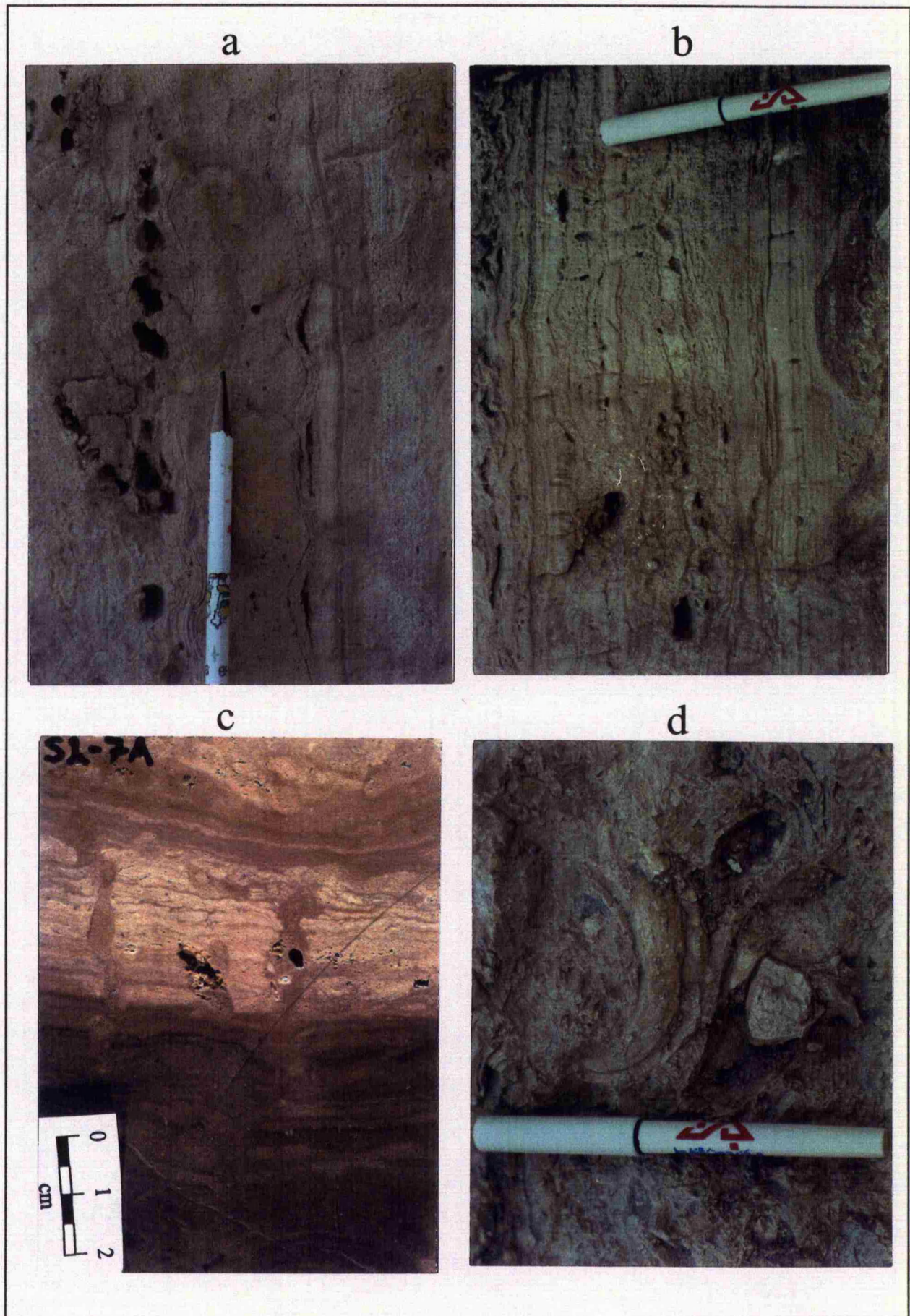
Fig. 5.12

gypsum than those below it, thus, this part of the Ain Tobi Member has the steepest weathering profiles found in the section. The *Ichthyosarcolites* Band may be the result of a facies change in response to a change in sea level. The change in bedding thickness, dominated types of sedimentary structures, and lithology are probably due to a shift from deposition in tens of metres to less than that. The coincidence of the band and sea level fluctuation is only suggested here because the microfauna does not provide the necessary biostratigraphic detail.

In the eastern part of the escarpment the *Ichthyosarcolites* Band is characterized by a distinctive fauna including rudist bivalves. In the west it is represented by dolomite.

5.4. Sedimentary Structures

Three types of sedimentary structures are characteristic of the Ain Tobi Dolostone Member. These are bioturbation, lamination and cross-bedding. These structures are the most abundant and widespread. Other sedimentary structures or bodies occur rarely in the Ain Tobi Member. These include solution breccias, mud cracks, ripples, birds-eye and channels.

Bioturbation: Bioturbation structures are the most common form of structures found in units of the Ain Tobi of Jabal Nafusah. The *Ichthyosarcolites* Band is bioturbated throughout Jabal Nafusah in NW Libya where diagenesis has had a less obscuring effect on primary fabric. Bioturbated units can be found above and below any of the other sedimentary units.

Generally, dolomitization has obscured most of the primary depositional textures of the bioturbated beds. Most of the grains have either been leached and left as mouldic porosity or they have been replaced. The precursor matrix material was probably limestone because of the random orientation of dolomite crystal axes and the uniform

<u>Fig. 5.13</u> Textures of Ain Tobi Member in the Fam Mulgha section:

a. Outcrop photograph showing general view of the *Ichthyosarcolites* Band in the Fam Mulghah section. Note rudist shells (arrow), Tarhunah area, Ras Fam Mulghah section.

b. Polished slab photograph showing mottled dolowackestone/dolopackstone from the rudist biohermal horizon at Fam Mulghah section.

c. Polished slab photograph of sample S2-9 above the *Ichthyosarcolites* Band. This dolomite breccia bed may represent an erosional surface. Fam Mulghah section.

d. Polished slab photograph from the oolitic dolograinstone, showing small-scale cross-bedding.
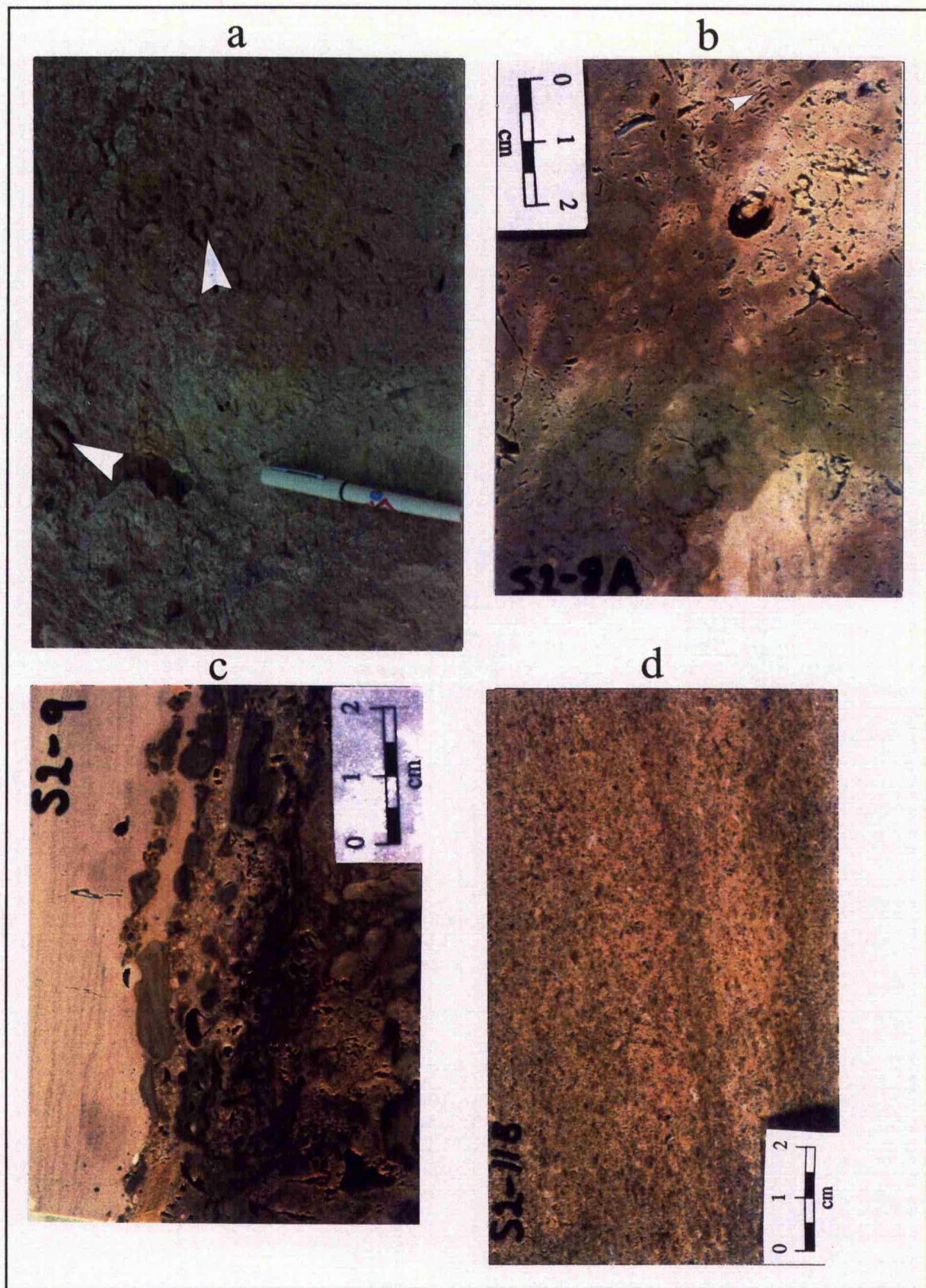
Fig. 5.13

crystal size (Evamy, 1967). Intercrystalline and leached mouldic porosity averages between 10-20% (estimates from thin sections). If each of the leached mouldic pores is assumed to be precursor grain, bioturbated units were wackestones, packstones and possibly grainstones. The original bioturbated sediments of the Ain Tobi Member were probably bioturbated by the combined activity of crustaceans worms, echinoderms and molluscs.

Interpretation: Deposition of the Ain Tobi sediments probably has occurred on an open marine platform with alternating periods of storm reworking and bioturbation. Storm generated currents rather than tidal currents are thought to be principally responsible for disturbing sediments over the Ain Tobi platform. Storm activity is indicated by cross-bedded carbonate sand units up to 4m thick in and above the *Ichthyosarcolites* Band..

Tidal currents are thought to play a minor roll in the Ain Tobi deposition because of the absence of extensive channel development, absence of levees and limited development of distinctly intertidal or supratidal environments.

Lamination: Laminated units are found principally in the dolomudstone units, but may be present in dolowackestones and dolopackstones. The laminated units are generally less than 1m thick, but may range up to 2m in thickness. They may extend laterally for kilometres although the laminated units are difficult to trace because of differences in weathering. These laminae are flat to slightly undulatory with fenestrae and smooth, flat without fenestrae. Fenestrae range up to about 1cm and they are irregularly shaped with tendency to be spherical. Individual laminae extend for a few metres. Laminae in the flat laminated non-fenestral mudstone are smooth and flat to slightly

undulatory. Individual laminae extend laterally from 1 to 30m. Narrow vertical burrows

(Fig. 5.9c) may extend down for 5 to 6cm. The burrows do not branch.

Interpretation: The flat to undulatory laminated units with fenestrae are most easily

recognizable as microbial stromatolites. The fenestrae, fine lamination, flat to undulatory

surfaces are the criteria used to identify them as stromatolites. Most of the fenestral and

non-fenestral units are flat, therefore could have originated in several environments.

Laminated units of the Ain Tobi are attributed to the trapping and binding of microbial

mats. The inferred location of microbial mat development is in some type of lagoonal

setting in the intertidal zone.

The thickness of the flat laminae, the lack of fenestrae and probably the aridity of the

climate of the Ain Tobi sedimentary environment (judging from Cretaceous

palaeotemperature curves of Savin, 1977 and the presence of gypsum in Yifran Marl

Member of Jabal Nafusah and Ghadamis Basin) indicate that Ain Tobi laminated units

were probably deposited in an intertidal environment.

Cross-bedding: The cross-bedding units of the Ain Tobi Member increase in

thickness towards the northeast. The dominant types of cross-bedded units are dune or

tabular which mainly occurred in Ras Fam Mulghah and Taghmah sections. Trough

cross-bedding occurs at the Abu Ghaylan section. The thick cross-bedded unit at Ras

Fam Mulghah is composed of dolograinstones. The grains which form these carbonate

sands include ooids, peloids, foraminifera, quartz grains and fragments of gastropods,

bivalves and echinoids. Cross-bedded carbonate sands are the only units that commonly

contained recognizable ooids. These units are the only ones in which grains can be

identified because dolomitization was fabric retentive and the exterior forms of the grains

are preserved (non-mimetic replacement).

Interpretation: The generation of ooid grains and grainstone sand bodies in Recent carbonate environments occurs in shallow agitated waters, less than 2m deep (Milliman, 1974). Hine (1977) suggested that ooids were generated through interaction of tidal currents and storm-generated waves. Tidal currents are primarily responsible for ooid generation while storm currents distribute them. The cross-bedded units of the Ain Tobi were generated by tidal current and storm wave activity. Because ooids make up a significant proportion of the grains in these units, some tidal activity is indicated. These cross-bedded units represent the highest energy environment of the Ain Tobi Member and probably are shoal deposits.

Other sedimentary structures: Dolomudstone units, which occur in the top of most of the measured sections consist of gypsum nodules and/or thin layers of gypsum. Dissolution of some of these evaporite minerals and the subsequent collapse of interbedded or overlying material result in solution breccias. In the Ain Tobi Member true solution breccias are rare. This type of feature occurs commonly on sabkhas (Wilson, 1975). In this case precipitation and dissolution of the gypsum may have occurred during a brief period of exposure, despite the fact that there is little real evidence of subaerial exposure in the Ain Tobi. Distinct mudcracks are found only in the Tarhunah area (Ras Fam Mulghah section), the Wadi Jabbar section and the Abu Ghaylan section. The lack of horizontal surface may have hindered the recognition of mudcracks and makes positive identification of vertical cross sections through possible mudcracks difficult. The mudcracks generally are uncommon, and suggests that subaerial exposure was rare during the deposition of the Ain Tobi Member.

5.5. Petrography

Field observation and lab work indicate that all sediments within the Ain Tobi Member have been completely dolomitized (details of the petrography of dolomite are

Fig. 5.14 Outcrop and hand specimen photographs of mottled and bedded dolostones:

a. Field photograph from the sand body lobe showing small-scale cross-bedding at the top of the Fam Mulghah section (people in the front of photo provide scale).

b. Polished slab photograph showing thin brownish laminae. Sample (S4-2), Wadi Jabar section.

c. Polished slab photograph showing highly porous and mottled dolomudstone/dolowackestone at Wadi Jabar section.

d. Outcrop photograph showing large bioturbation structures (burrows) within the *Ichthyosarcolites* Band (arrow) at Wadi Jabar section.
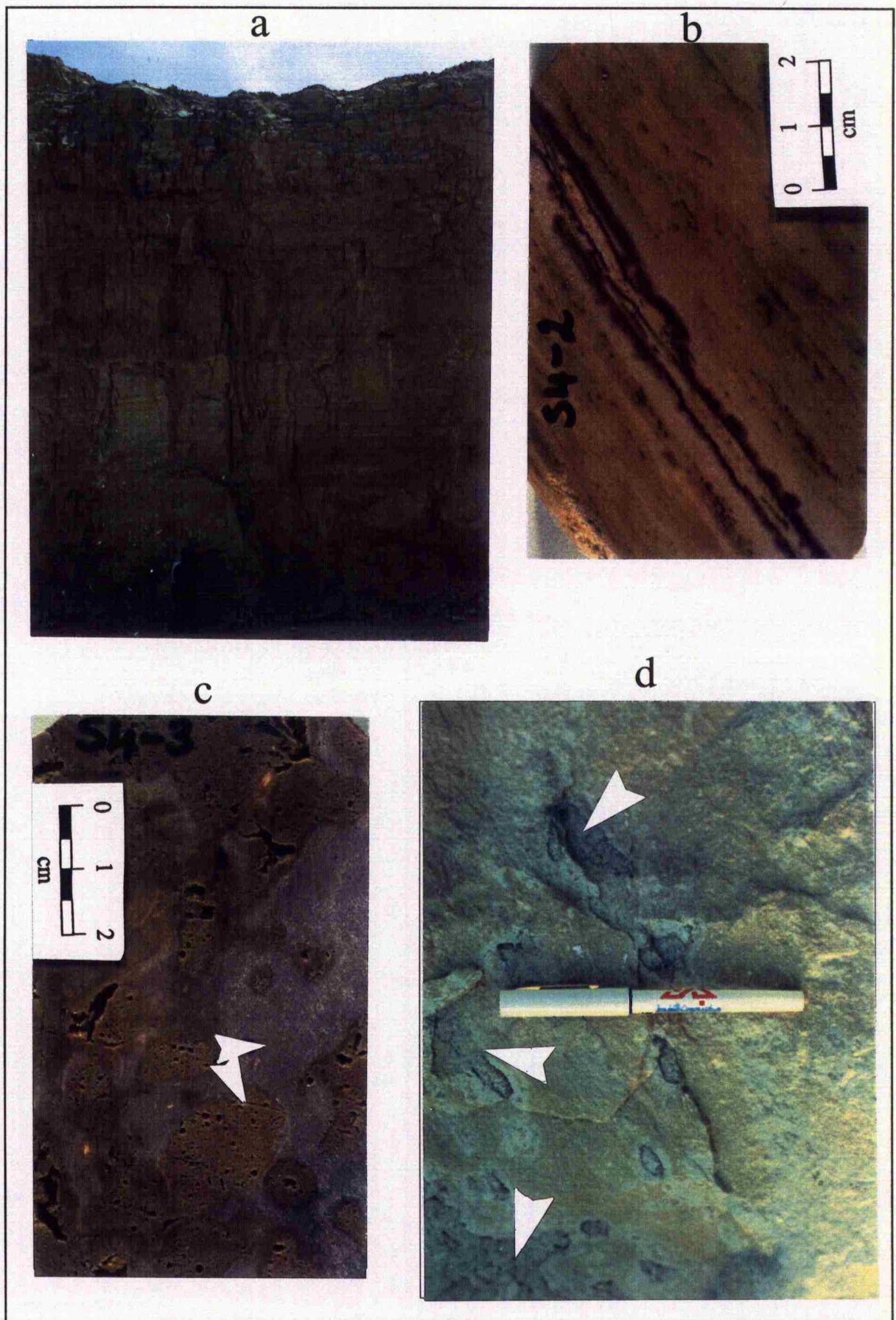
Fig. 5.14

discussed in another section). Only traces of calcite were recorded during XRD analysis of 154 samples. The petrographic study of more than 200 thin-sections shows that rare large and blocky calcite crystals do occur as non-ferroan equant cement within vugs or moulds. Crystal size decreases away from the centre of the pores (Fig. 5.17a) and a very fine to medium dolomite fabric, mainly xenotopic crystals, has replaced the original sediments (see Chapter Seven). The precursor sediments can be recognized in some cases, particularly in the shoals where ooids still can be seen. These grains have been non-mimetically replaced by dolomite (see Chapter Seven). In the *Ichthyosarcolites* Band the microfauna are dissolved out leaving moulds. Very few micritic grains, echinoderm fragments and foraminifera tests survived dolomitization (Fig. 5.17b), whereas transverse sections of gastropods are dissolved out and their outlines replaced by coarse, probably late dolomite crystals. Quartz grains are very common within the lower part of the member specially below the *Ichthyosarcolites* Band. Its percentage decreases upward, whereas gypsum increases upward particularly in the western part of the study area. The sandstone intervals mainly occur in the western part of the study area, particularly at Jadu area. In thin section samples taken from these intervals are characterized by quartz sandstones. Quartz grains are medium to coarse (300-1000μm in diameter), well to subrounded, unicrystalline and moderately sorted (Fig. 5.17c). They are cemented by quartz overgrowth (Fig. 5.17d) and sometimes are fractured and float in dolomite matrix. Dolomite associated with quartz sometimes replaced them at their margins.

5.6. Yifran Marl Member

The Ain Tobi Dolostone Member is overlain by the Yifran Marl (upper member of the Sidi as Sid Formation). It consists of yellow soft marls, marly limestone and dolomites and calcareous shales with uncommon interbeds of bedded gypsum, gypsiferous shales

<u>Fig. 5.15</u> Dolomite lithotypes of Ain Tobi Dolostone Member at eastern Jabal Nafusah escarpment:

a. Polished slab photograph of sample S4-12B from Wadi Jabar section showing geode filled by late calcite (white).

b. Field photograph illustrating tabular bedding which is the dominant sedimentary structure within Ain Tobi Dolostone Member.

c. Polished slab photograph showing yellowish, heavily mottled dolomudstone at Wadi Jabar section.

d. Polished slab photograph showing typical porosity in the top part of the Wadi Jabar section.
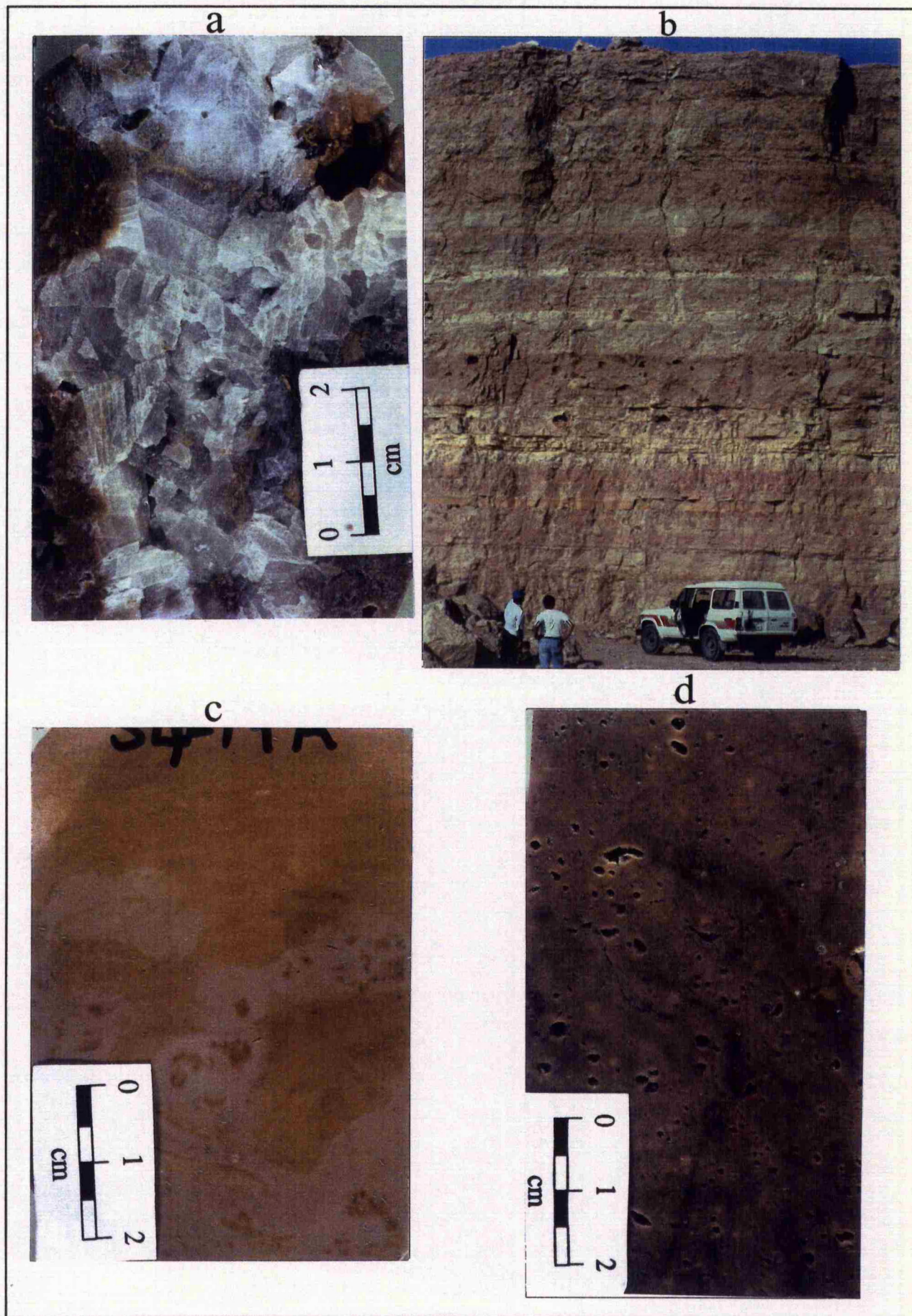
Fig. 5.15

and oolitic limestone. Marls with bedded gypsum predominate sections west of Yifran whereas to the east the thickness decreases and dolomitic limestone predominate. Recrystallization makes identification of textures difficult, mudstones, wackestones, and wackestones/packstones occurred with occasional oolitic grainstone.

Parallel lamination is the most common sedimentary structure and the sparse fauna generally consists of molluscs. Bioturbation is commonly encountered throughout the member. The lithology of Yifran Marl Member is interpreted as a restricted inner-ramp in the western and south of Jabal Nafusah, and as an open to semi-restricted ramp in the eastern Jabal Nafusah (see Chapter Six).

5.7. Lithofacies of the Ain Tobi Member (Summary and Interpretation)

The Ain Tobi Member is an arenaceous to argillaceous dolostone. It is thickest in the northeast and thins gradually to the southwest direction to only 5m thick at Wazan Village. The dolomitized limestone or dolostone contains a varying proportion of clay and poorly sorted, subangular to subrounded quartz sand, particularly at the Jadu area. Cross-bedded units are common in the northeast sequences particularly at the Abu Ghaylan and Fam Mulghah areas.

Summary: According to the field observations and petrographic studies of samples from twelve measured sections, Ain Tobi sediments can be summurized as follows:

1. Cross-bedded oolitic dolograinstones and dolopackstones. The scale of cross-bedding locally decreases upward and may show erosional relief at the basal surfaces. Channel geometry is suggested in some areas by the lateral changes into marls (Lithotype 1).

2. Coarse-grained, shelly bioclastic and bioturbated dolowackestones and dolopackstones, interbedded with oolitic dolopackstone. This lithotype contains rudists,

gastropods, echinoderm fragments and ooids. These contain subhorizontal fractures and fossil animal burrows (Lithotype 2).

3. Bedded dolomudstones and dolopackstones with rare wavy laminations and bioturbation. This facies is generally interbedded with bioturbated dolowackestones and oolitic dolograinstones (Lithotype 3).

4. Laminated, thinly-bedded dolomudstones and dolowackestones with microbial laminae, birds-eye structure and gypsum. Bioturbation is extensive. These sediments include bivalves, gastropods and intraclasts (Lithotype 4).

5. Bedded and bioturbated dolomudstone/dolopackstone with solution breccias consisting of angular clasts, commonly silicified in a dolomitized matrix (Lithotype 5).

Interpretation: Lithotype 1 represents deposits of highest energy found in the Ain Tobi Dolostone Member. The diverse fauna and distribution in Lithotype 2 indicate an origin as biostorms. Both lithotypes 1 and 2 represent shoal deposits. Lithotypes 3 and 4 probably represent a zone of sediment between shoal and lagoon. The dolowackestone may represent interior lagoon, while dolopackstone and oolitic dolograinstone beds are mostly shoal-derived carbonate sand or tidal channels. Lithotype 5 represent deposits of a shallow-marine environments which probably were isolated from open-marine environments and were more saline than normal seawater.

Generally, lithologies of the Ain Tobi Dolostone Member are interpreted as a shallow-shelf or ramp carbonate deposit. These represent shoaling-upward cycles deposited during regressive phases (see Chapter Six).

5.8. The Sidi as Sid Formation and Sea-Level Changes

Eustatic sea level curves may help in recognizing and predicting the presence and areal distribution of unconformities and diagenetic events. The curves may be especially useful in petroleum exploration because of their predictive capabilities as unconformities and diagenetic alteration may directly affect hydrocarbon accumulation. For this reason a comparison is made between the Middle Cretaceous Jabal Nafusah sequence and eustatic sea-level curves.

The age determinations within the Nafusah sequence are not accurate enough to allow a confident comparison with the available sea level curves. Unfortunately, no sea level curves expressly concerned with Libya are available. If the age of the Ain Tobi Dolomite Member is considered to be Aptian-Albian then, the ages of the Cretaceous units overlying the Ain Tobi must be Cenomanian. Attempts to put relative magnitudes on the transgressive-regressive cycles by some authors, and bearing in mind the simplified detail in which eustatic curves have been published, the Ain Tobi sequence is best matched to the Arabian Gulf curve of Harris *et al.*, 1984 (Fig. 5.18). The Harris curve is favoured because in it the Middle Cenomanian transgression is subordinate to that of the Early Aptian.

The relative magnitudes of the transgressive cycles appear to be reflected in the rock units of the Jabal Nafusah sequence. Northwestern Libya and Arabia were part of the same crustal plate through the Cretaceous (Smith and Briden, 1977). Thus their response to the sea level changes may have been linked. The Harris *et al.* (1984) curve infers a rise in sea level which began at the end of the Early Aptian. The lower part of the Ain Tobi Member is considered to correspond to this transgression. The basal contact of the Ain Tobi Dolomite Member with the Kiklah Formation does not exhibit

<u>Fig. 5.16</u> Outcrop and hand specimen photographs of saddle or baroque dolomite from the eastern part of the study area:

a. Field view of well-bedded Ain Tobi Dolostone Member sampled near the mouth of Wadi Ghanimah, Al Khums area.

b. Outcrop photograph shows general view of out-cropping part and bedding of the Ain Tobi Dolostone Member in the Al Khums area, Mediterranean Coast. The Ain Tobi Member (A) here is overlain by Miocene Al Khums Formation (K).

c. Polished slab photograph showing the very coarse yellowish saddle dolomite seen around the Al Khums coast. Note the abundant porosity.

d. Polished slab photograph. Note the very coarse black or grey saddle dolomite which has a pearly lustrus appearance.
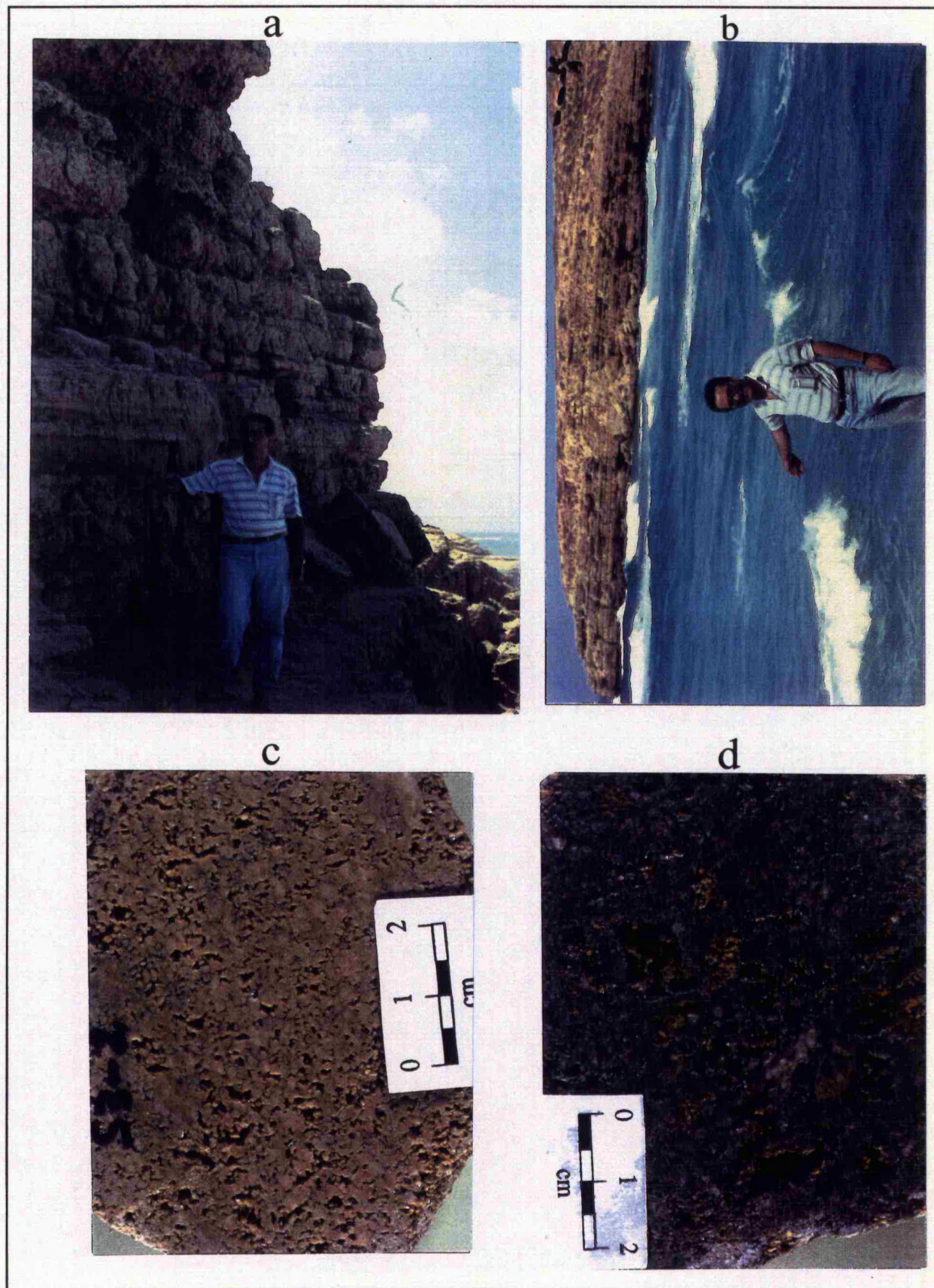
Fig. 5.16

much evidence of weathering, exposure or erosion. The start of the transgression is most strongly shown by an abrupt regional facies change from siliciclastic (Kiklah Formation) to carbonate deposition (Ain Tobi Dolomite Member). This is identical to the Nahr Umr-Mauddud boundary in Southern Arabian Gulf described by Burchette (1993). The lack of evidence of exposure may indicate a relatively short period of time between the end of siliciclastic and the start of carbonate deposition. If so, this would favour an Aptian age for the lower part of the Ain Tobi Dolomite Member.

The *Ichthyosarcolites* Band of Christie (1955) is an especially thick bed within the Ain Tobi which is commonly capped by moulds of the rudist bivalve *Ichthyosarcolites*. The band probably represents some kind of brief depositional hiatus. The Harris curve show a minor sea level fluctuation of the Albian-Cenomanian boundary which may correspond to the *Ichthyosarcolites* Band.

The Ain Tobi is dominated by subtidal carbonate sands. This may represent a disequilibrium basin fill at a time when sea level was rising faster than the topographic basin could be filled by sedimentation. The Yifran Marl Member, which grades up from the lower part of the Ain Tobi, contains a greater amount of lime mud, shales and evaporites of possible lagoonal origin. These may indicate that basin filling through progradation had caught up to the rising sea level. The lag in basin filling is a response to the rate of change in sea level as indicated by the shape of the sea level curve for this interval; hence, a rapid initial rise and then a gradual decline to a constant rate. The *Ichthyosarcolites* Band may represent a complicating factor in that it may represent an unconformity. The units above and below the band would be due to deposition during two separate and distinct sea-level cycles and not one continuous cycle. Whether or not the *Ichthyosarcolites* Band represents an unconformity, the Ain Tobi Dolostone

Fig. 5.17 Petrographic photographs of Ain Tobi sediments:.

a- Photomicrograph from sample S6-16 at top of Ar'Rabtah section (contact between Sidi As Sid and Qasr Tigrinnah Formations) showing the equant calcite cement within a mould. Note the crystals size increasing towards pore centre, and very fine dolomite crystals within the pore. XN.

b. survived Photomicrograph from sample S8-9 at the Riaynah section showing tests of foraminifera which have survived dolomitization (fabric retentive texture). This sample probably represents a packstone/grainstone facies before dolomitization. PPL.

c. Photomicrograph of sample S9-7 from the Jadu area showing quartz grains associated with the sandstone intervals. These grains are mainly rounded, unicrystalline and cemented by quartz overgrowths. PPL.

d. Cross-polarized view of the same sample as 'c'.

a

b

c

d
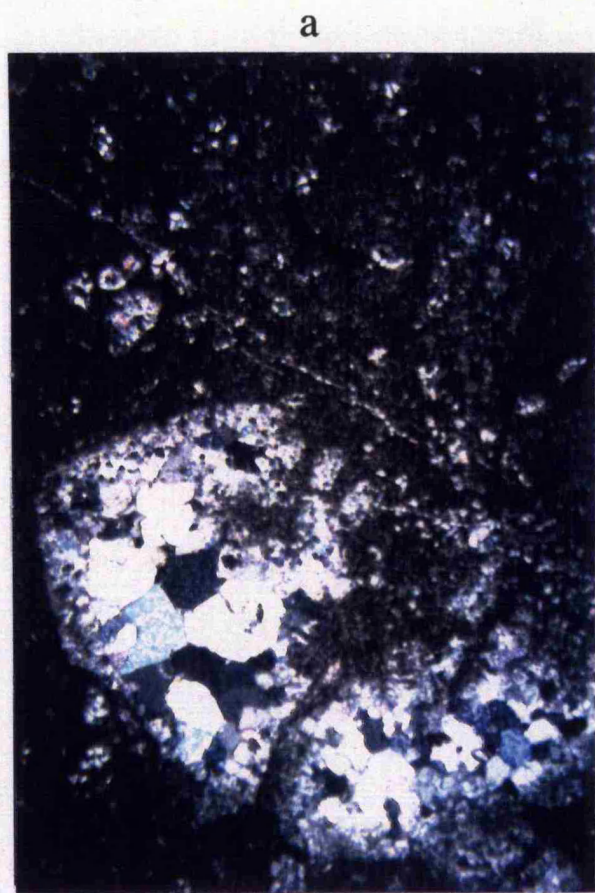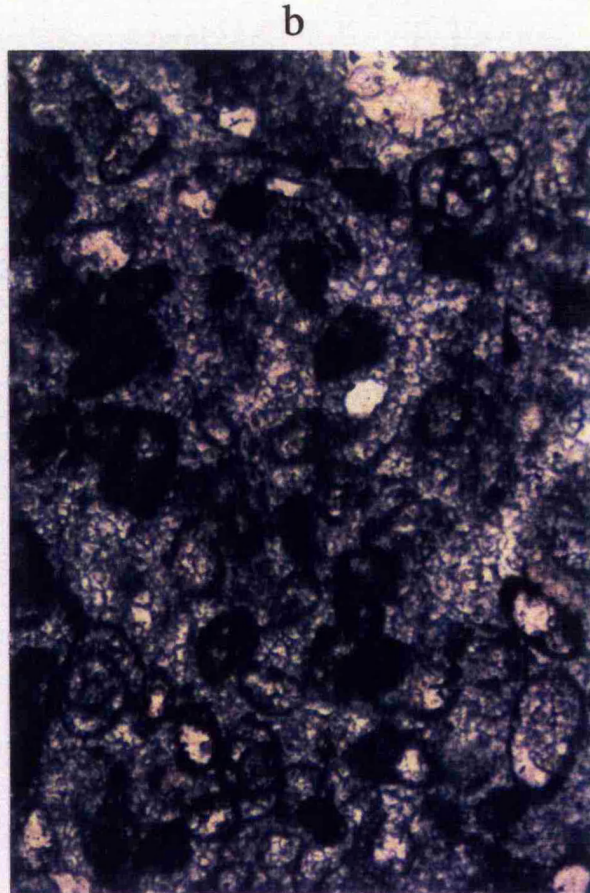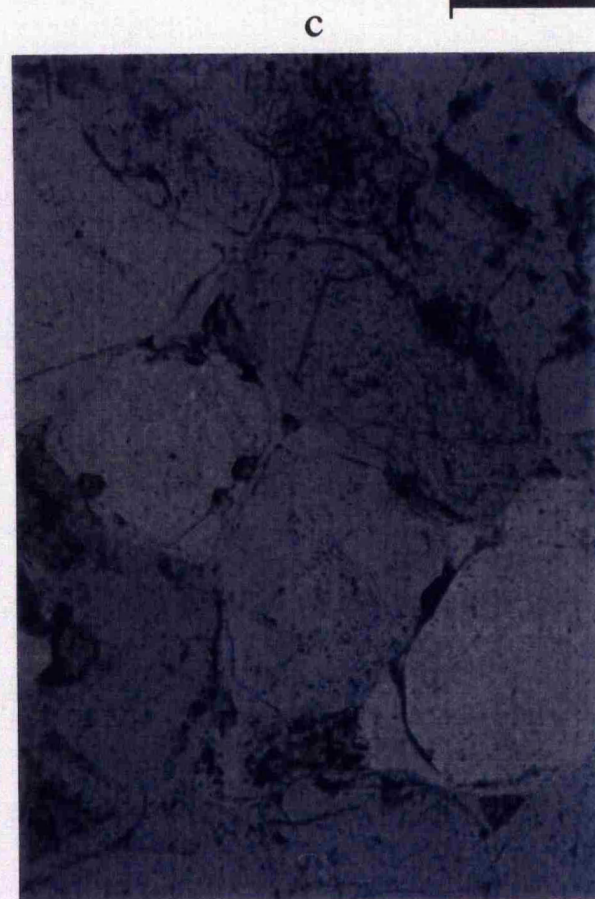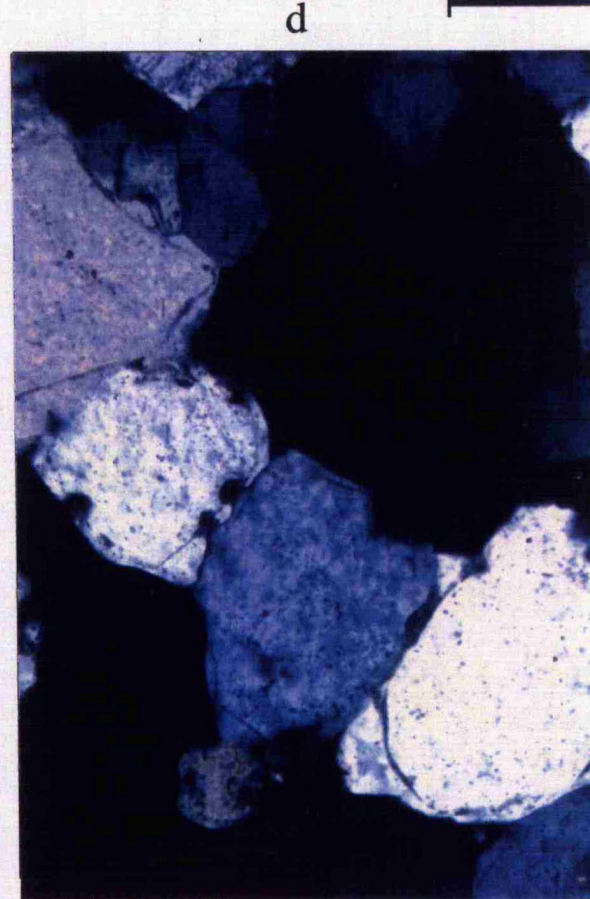
200μm

200μm

200μm

200μm

Fig. 5.17

Member as a unit was deposited during a major sea level rise. Its shallowing upward

character is comparable to that which would be expected from the Harris *et al* (1984) sea

level curve.

The Nalut Formation (Turonian) is a medium to coarsely crystalline dolomite that

originated as a platform deposit. The Nalut Formation overlies the Yifran Marl Member

of the Sidi as Sid Formation without obvious erosion of the contact. In the subsurface

the dominant marls and evaporites of the Yifran may be interbedded with the dolomite of

the Nalut. The Nalut Formation appears to have been deposited in water possibly deeper

than that in which the Yifran Marl was deposited. This change may correspond to an

inferred drop and subsequent rise of sea level in the Early Turonian, as shown on the

Harris curve.

The Qasr Tigrinnah Formation (Turonian) overlies the Nalut Formation and is in turn

overlain by Mizdah Formation of Al Hamadah Group (Santonian). The ages of these

units imply that the Qasr Tigrinnah could represent the cap of the Aptian-Turonian

transgressive cycle of the Harris curve and that the Mizdah represents the initial deposit

of the following cycle. The Middle Cretaceous sequence of Jabal Nafusah appears to be

most closely approximated by an eustatic curve constructed by Harris *et al*, 1984 (Fig.

5.18) for the eastern Arabian Peninsula (see also Harris *et al*, 1980).

5.9. Conclusion

The Ain Tobi Dolostone Member is a widely distributed rock unit, along the Jabal

Nafusah escarpment. Its thickness increases from southwest towards the northeast. The

only exception is thickening in the Jadu area caused by the high percentage of the quartz

sandstone. The Ain Tobi Dolostone Member is mainly composed of light grey, well

bedded, highly bioturbated and very fine to coarse dolostones, with minor amount of calcite.

The coarse to very coarse crystalline dolomites (saddle dolomite) have only been observed in the eastern Jabal Nafusah. Sandstone is very common in the lower part but it decreases upwards. The highest percentage of sandstone occurred in the Jadu area. Gypsum and chert occur commonly in the upper part as nodules and/or thin beds. These occur mainly at the western part of the Jabal Nafusah. Solution breccias, consisting of angular clasts, occur at the top of most measured sections in the western part of the study area. Marl percentage increases upwards, particularly in the western Jabal Nafusah area.

The *Ichthyosarcolites* Band occurred at the middle part of the Ain Tobi Member. It is well defined at the eastern Jabal Nafusah because of its dolomitized and leached moulds of rudist shells. In western areas of the Jabal rudists have been destroyed, probably during silicification, but still can be recognized due to their resistance to weathering. The Band is thicker and less dolomitized at the eastern end of Jabal Nafusah (i.e. east of Wadi Ghan). It may represents a minor disconformity. It makes a distinctive marker bed throughout Jabal Nafusah.

Three types of sedimentary structures are most abundant and widespread within the Ain Tobi Dolostone Member; they are bioturbation, lamination and cross-bedding. Other sedimentary structures occur rarely in the Ain Tobi but include solution breccias, mud cracks, ripples, birds-eye and channels. The units affected by bioturbation probably were developed in an open marine platforms with alternating periods of storm reworking and bioturbation. The aridity of the climate during Ain Tobi deposion, the thickness of the

laminations and occurrences of the gypsum in the Yifran Member may indicate that the laminated units of the Ain Tobi were deposited in an intertidal environment.

Five lithotypes are identified on bases of field observation and petrography. They are lithotype 1, cross-bedded dolograinstones and dolopackstones; lithotype 2, bioturbated dolowackestones and dolopackstones; lithotype 3, bedded dolomudstones; lithotype 4 laminated dolomudstones and lithotype 5, solution breccias. The Yifran Marl Member which succeeded Ain Tobi Member is mainly composed of marl, marly limestone, dolomite and bedded gypsum. The bioturbated and parallel laminae with sparse fauna and gypsum may be indicative of restricted platform deposits.

The Ain Tobi Dolostone Member is a unit that was deposited during a major sea level rise. Its shallowing upward character is comparable to that of the Arabian Peninsula sea level curve prepared by Harris *et al* (1984).
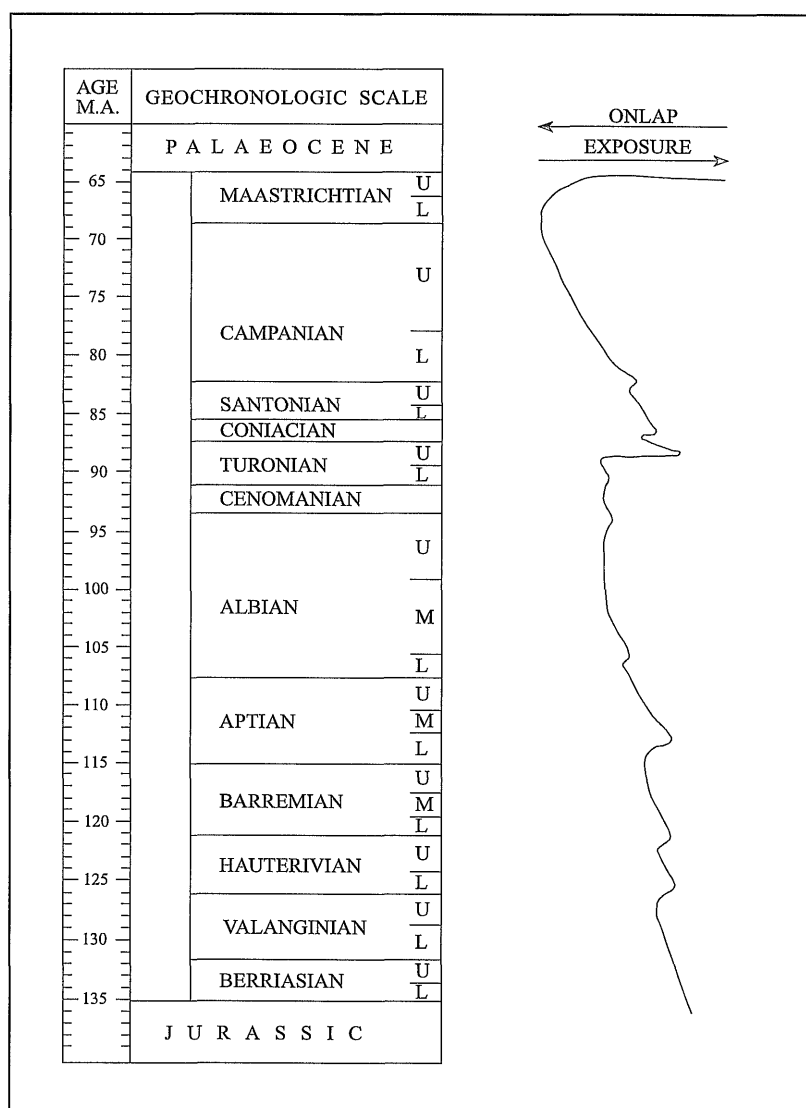
FIG. 5.18 Cretaceous sea level curve of the Middle East

(after Harris *et al*, 1984)

CHAPTER SIX

6. ENVIRONMENT OF DEPOSITION

6.1. Introduction

A sedimentary model is proposed for the Sidi as Sid Formation which includes the Ain Tobi Dolostone Member and Yifran Marl Member (El Hinnawy and Cheshitev, 1975) in the Jabal Nafusah escarpment and Ghadamis Basin to the south. In this section the term facies is avoided because the depositional environments could be defined on the basis of sedimentary structures and because dolomitization has obliterated most of the criteria used to define microfacies based on textures and grain types. The environments of the Ain Tobi and Yifran Members of the Sidi as Sid Formation are probably ramp deposits (Fig. 6.1) according to Ahr, 1973; Buxton and Pedley, 1989; Elrick and Read, 1991; Burchette and Wright, 1992.

The Cenomanian depositional environments found on the Jabal Nafusah escarpment and Ghadamis Basin are part of an inner ramp sequence which ranged from open to semi-restricted ramp and restricted or lagoon ramp. In this study the open to semi-restricted and restricted ramps will be discussed, because they occur in the exposures of

the Sidi as Sid Formation and in the subsurface Ghadamis Basin where well logs are available. In the offshore Gabes-Tarabulus-Misratah Basin most drilled wells did not penetrate deeper than the Maastrichtian and in Tunisia the data are not available. Published data on the Gabes-Tarabulus-Misratah Basin and Tunisia areas and data gathered during this study from outcrop and subsurface Ghadamis Basin will be used in order to propose a model for the Upper Cretaceous in northwestern Libya.

6.2. Inner Ramp

6.2.1. Restricted or lagoon Ramp

The restricted ramp environment is represented by the Yifran Marl Member of the Sidi as Sid Formation in the subsurface Ghadamis Basin, southern Nafusah uplift and in Jabal Nafusah. The Yifran Member is composed of approximately 70m of marls, marly limestone, dolomites and calcareous shales interbeds of bedded gypsum in western Jabal Nafusah and dominated by limestone in eastern part of the study area. In the subsurface (Ghadamis Basin) it consists of 150m of interbedded dolomite, shale and evaporites. In both Jabal Nafusah and the Ghadamis Basin it overlies open to semi-restricted dolostones of the Ain Tobi Member and is overlain by the Nalut Formation. Units associated with the restricted ramp occurred commonly above the *Ichthyosarcolites* Band close to the contact between Ain Tobi and Yifran Marl.

The rare fauna present in the Yifran Marl suggest deposition in a shallow-marine, neritic environment (Fig. 6.1) with restricted lagoonal conditions (intertidal and supratidal with no tidal channels) in the western part of the basin (Megerisi and Mamgain, 1980a, b). A lagoon palaeoenvironment is suggested because it could impound water whose evaporation would result in evaporite deposition indicated by the solution breccias in the Ain Tobi Dolostone Member (lithotype-5) and in actual evaporite layers

in the Yifran Marl Member. Upward-shoaling is suggested for the Yifran Member but it is different from Ain Tobi (discussed below) in that the cycles here are thinner, contain higher proportion of micrite and greater amount of evaporite beds.

6.2.2. Open to Semi-Restricted Ramp

The open to semi-restricted ramp environment is represented by the Ain Tobi Dolostone Member of the Sidi as Sid Formation in the Jabal Nafusah escarpment and in the subsurface Ghadamis Basin where it can be traced on completion logs. In the Ghadamis Basin the open to semi-restricted ramp consists of dolomite which overlies Early Cretaceous siliciclastics of the Kiklah Formation and underlies lagoonal rocks of the Yifran Marl Member. The Ain Tobi Member thins to the south as the Yifran Marl thickens. In the Jabal Nafusah escarpment the open to semi-restricted ramp consists of dolostones, sandy dolomite, chert and quartz sandstone. It is composed mainly of bioturbated bedded carbonate units, with cross-bedded oolitic dolograinstones and laminated dolomudstones (see discussion in Chapter Five). The bioturbated units especially those containing rudists such as the *Ichthyosarcolites* Band and cross-bedded sands are more abundant towards the north of the Nafusah escarpment. The carbonate muds and associated evaporites are more abundant south of the escarpment and at the top of the escarpment (Yifran Marl Member) towards the restricted or lagoon ramp.

The vertical change from dolowackestones/dolopackstones through dolomudstones and dolowackestones to thinly bedded dolomudstones probably represent cycles of shoaling-upward deposited (Fig. 6.3) during regressive phases. The lower part of each cycle is composed of interbedded, bioturbated dolowackestones/dolopackstones and bedded dolomudstones (lithotype-2 and 3). The upper part consists of thinly bedded dolomudstones with gypsum nodules, microbial lamination and solution breccias

(lithotype-4 and 5). Each cycle was initiated by a rapid rise in sea level, conditions suggested by the sharp contact between the intertidal lithotype-4 and the overlying carbonate lithotype-2 (Fig. 5.11d) at Tarhunah and in the Abu Ghaylan area. Gradual shallowing as a result of sedimentation created extensive tidal flats and evaporitic sabkhas in which lithotype-3 and 4 were deposited. The bedded dolomudstones and dolopackstones of lithotype-3 were deposited in a low intertidal zone, and the microbial laminae of lithotype-4 were deposited in a higher intertidal zone.

Evaporites formed at the top of the cycles in the sabkha type environment were probably extensive at the time of deposition. However, subsequent leaching, during subaerial exposure, removed many of the evaporite layers, now represented by solution breccias (lithotype-5). These are best developed in the thinner sequences of the western outcrops (Wazan and Nalut, Section # 12 and # 11), which show rather restricted marine aspect (Fig. 6.1). Cycles involving lithotype-1 (large-scale cross-bedded dolograinstones and dolopackstones) are well developed in the northeast sequence at Tarhunah area (Section # 2). This cycle is interpreted as a tidal-channel deposit. Deposition occurred during progradation of broad shoals or lateral migration of tidal channels.

Based on the subsurface data it is thought that the lithotypes of the Sidi as Sid Formation (Ain Tobi and Yifran members) regressive megasequence conditions could be more evaporitic south of Jabal Nafusah, with better development of sabkha sequences.
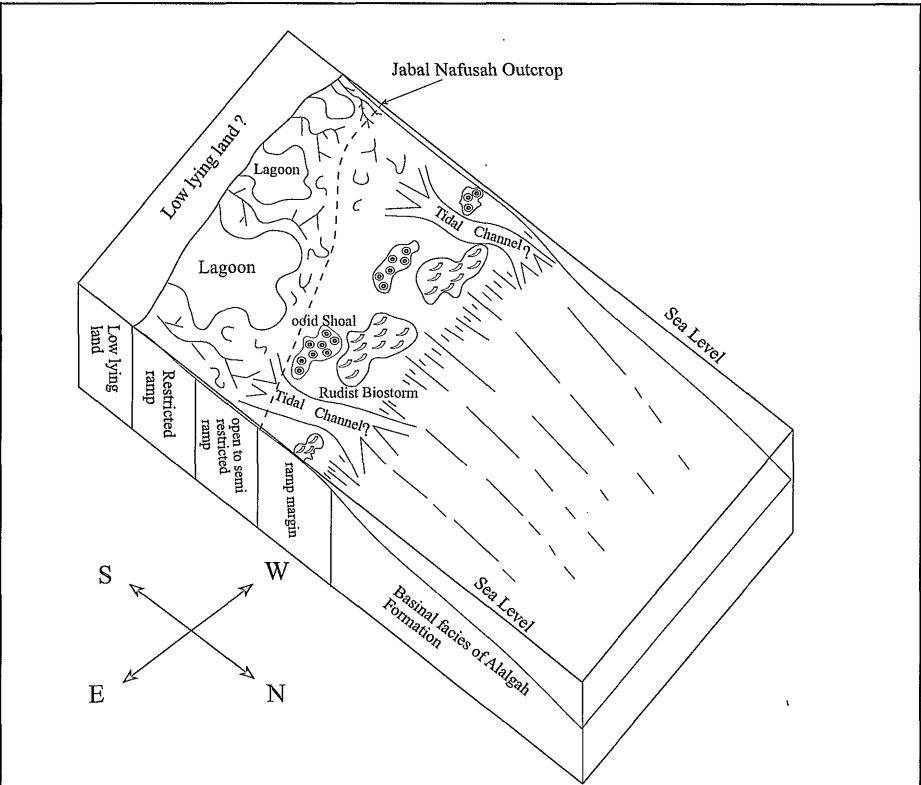
Fig. 6.1 Idealized block diagram of proposed Cenomanian sedimentary environment
in NW libya.
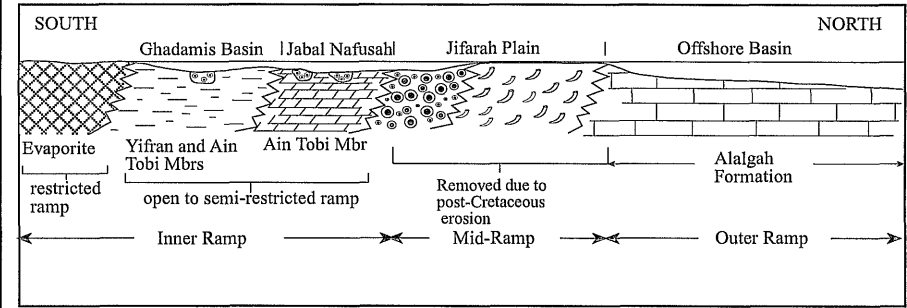
Fig. 6.2. Postulated changes in Cenomanian lithofacies in onshore and offshore NW Libya.

6.3. <u>Mid-Ramp or Ramp Margin</u>

Stratigraphic sequences in wells drilled on the Jifarah Plain north of Jabal Nafusah indicate that post-Cretaceous erosion has removed the Ain Tobi and the remainder of the Cenomanian in at least part of that area. The open to semi-restricted ramp environment probably graded northwards into mid-ramp or ramp margin environments. The margin is thought to occupy a narrow band in the subsurface that parallels the present coastline.

The presence of ramp margin is inferred on the basis of Cenomanian rudist debris in the Ain Tobi Member of the Jabal Nafusah, from oyster debris found at a point southeast of Tarabulus in Jabal Nafusah where its orientation changes from north-south to east-west, and from oyster packstones and grainstones of the Zebbag Formation in Tunisia (Pedley *et al*, 1982). This depositional environment probably also contains cross-bedded carbonate bodies and bioturbated units such as those found in the Ain Tobi Member in the Nafusah Escarpment. The presence of the *Ichthyosarcolites* Band as a series of buildups and the absence of a visible shelf-slope break on seismic lines implies that this is a ramp margin. The extensive post-Cretaceous erosion which removed the Cretaceous deposits along the coast may have resulted in obliteration of any ramp margin that was present.

6.4. <u>Outer Ramp</u>

The Gabes-Tarabulus-Misratah Basin lies to the north of the ramp margin (Fig. 6.2). The Cenomanian strata in this basin is represented by the Alalgah Formation (Hammuda *et al*, 1985). The outer ramp environment is only known from the description of completion logs which reached the Cretaceous in offshore Libya (e.g. K1-137, H1-137, L1-137 and J1-NC35A wells)

Cenomanian sediments of the Alalgah Formation consist of laminated dolomitic marls containing miliolid and pelagic foraminifera and rudist material. The miliolids and rudists are thought to be derived from higher up the slope near the crest of the uplift. The pelagic foraminifera represent normal sediment accumulation for this environment.

Because of the paucity of the Upper Cretaceous subsurface data, and absence of surface data in the northwestern Libyan offshore region, elaboration upon the basinal and slope environments is not possible.

Solution breccia

Transgressive surface
Mudstones with anhydrite nodules and microbial

Bioturbated dolomudstones and dolowackestones

Wackestones-packstones with cross-bedding and restricted fauna

Packstones/grainstones with large scale cross-stratification grading upward into small scale cross-lamination

Transgressive surface
Microbial

Progradational lagoon/sabkha

SHOALING-UPWARD CYCLE

Tidal channel

Algal lamination
Echinoderms
Gastropods
Bivalves
Foraminifera
Anhydrite
Intraclasts

5 meter approx.

Fig. 6.3 Idealized shoaling-upward cycle in Sidi as Sid Formation, Jabal Nafusah, Libya.

6.5. Conclusion

The Sidi as Sid Formation (Ain Tobi Dolostone Member and Yifran Marl Member) in northwest Libya may represent a part of a large carbonate platform located in North Africa. Alternatively it fits the middle and inner parts of a ramp model.

The inner ramp or shallow lagoon deposits are represented at outcrop by the Yifran Marl and the upper part of Ain Tobi Member in the western part of Jabal Nafusah and subsurface in Ghadamis Basin south of Nafusah escarpment. The inner ramp is indicated by the presence of solution brecias in Ain Tobi Member and actual evaporite layers and rare fauna within the Yifran Marl Member.

The open to semi-restricted ramp is represented by the Ain Tobi Member in Jabal Nafusah and in subsurface Ghadamis Basin. It is composed of laminated and bioturbated dolopackstones through dolomudstones and dolograinstones. The later become more abundant in the northeastern (east of Wadi Ghan) of the study area.

The mid-ramp or ramp margin is thought to be deposited parallel to the present coast line which was removed by the post-Cretaceous erosion. The outer ramp deposits are represented by the subsurface Ain Tobi equivalent (Alalgah Formation) in the offshore Gabes-Tarabulus-Misratah Basin. These sediments are composed mainly of laminated dolomitic marls, and pelagic foraminifera, the contained rudist and miliolid faunas are thought to be derived from the ramp margin by means of gravity transport mechanisms.

CHAPTER SEVEN

CHAPTER SEVEN

7. PETROGRAPHY AND GEOCHEMISTRY OF REGIONALLY EXTENSIVE DOLOMITES (RESULTS)

7.1. Introduction

This Chapter deals with the major textural and compositional features of a shallow to deep burial-dolomite sequence that occurs within Upper Cretaceous (Cenomanian, probably Late Aptian through Cenomanian) shallow-water carbonates of northwestern Libya.

Dolomite is very common in the geological record. Most geologists agree that dolomite is a replacive mineral. However, some authors (e.g. Shinn, 1973; Wade, 1989) pointed out that dolomite may be precipitated as a primary mineral. Shinn found that dolomitization in brines beneath porous quartz and sabkhas in the Persian Gulf was primary. Wade mentioned that the near-surface dolomite of the Salt Basin is authigenic. Land (1973; 1985), documented that dolomite can form by primary precipitation, both as pore-filling cement and as lithified sediments. Longman (1980) concluded that some ancient dolomites lack definitive evidence for a secondary origin and may, therefore, be primary.

Dolomite and dolomitization studies focused on developing general models of dolomitization mechanisms (see Chapter 8) e.g. Adams and Rhodes (1960) who

developed the "seepage refluxion" model. Hanshaw *et al* (1971) suggested the "mixing zone dolomites" were supported by Land (1973); Land *et al* (1975) and Badiozamani (1973). Badiozamani (1973) used the term "Dorag" for this model. Dolomitization may result from water circulation near the mixing zone (Muchez and Viaene, 1994). The other accepted models for dolomitization are that of burial compaction (Mattes and Mountjoy, 1980), evaporative (sabkha) dolomitization (Patterson and Kinsman, 1982), normal seawater dolomitization (Land, 1985; 1991), and lagoon dolomitization (Von der Borch *et al*, 1975).

A major problem in the study of ancient dolomites is to explain the great thickness and areal extent of massive dolomite in the stratigraphic record (e.g. Ain Tobi dolomite) compared with scarcity of dolomite in recent marine environments. Recent research using different techniques (petrography and geochemistry) has produced a considerable range of ideas regarding the origin and mechanisms of dolomitization (e.g. Friedman and Sanders, 1967; Zenger and Dunham, 1980; M'Rabet, 1981; Morrow, 1982a; 1982b; Tucker, 1983; Shukla and Friedman, 1983; Land, 1983; 1985; 1986; Machel and Mountjoy, 1986; Hardie, 1987; Lee and Friedman, 1987; Shukla, 1988; Holail *et al*, 1988; Moore *et al*, 1988; Ruppel and Cander *et al*, 1988; Amthor and Friedman, 1992 and many others). These different ideas reflect the real differences between dolomite types, and the presence of a variety of dolomite types in nature. A single process or mechanism of dolomitization does not exist (Amthor and Friedman, 1992).

The dolomites of the Sidi as Sid Formation (Ain Tobi Dolostone Member) are an example of bedded dolostones (the term dolostone is used for sedimentary beds or units that consist of more than 90% dolomite, Machel and Mountjoy, 1987), which have a complex diagenetic history. Ain Tobi dolostone is well and thinly bedded and has an

angular unconformable contact with the underlying Kiklah Formation and gradational

contact with the overlying Yifran Marl Member (Fig. 7.1a) which is difficult to

distinguish at places. These ancient complex bedded dolomites may have formed by early

and late diagenetic dolomitization and recrystallization (Gregg and Sibley, 1984; Zenger

and Dunham, 1988; Qing and Mountjoy, 1989; Gao, 1990; Gregg and Shelton, 1990).

The calcitization of dolomite (dedolomitization) has also occurred within the Ain Tobi

sediments and is often interpreted as an early diagenetic process (Magaritz and Kafri,

1981) occurring near-surface or during burial (Chafetz, 1972; Budai *et al*, 1984; Holail

et al, 1988).

7.2. Petrography

Two diagenetic dolomites are recognized in the Ain Tobi Dolostone Member. They

are early dolomites and late dolomites. Early dolomite is differentiated from late dolomite

by its characteristics as replacive in origin and makes up the bulk (> 90%) of the studied

sections, whilst the late dolomite consists of saddle dolomite (replacive and cement). All

dolomites of the Ain Tobi Member are nonferroan and probably contain less than 1%

FeO (see section 7.3.3) as they did not stain upon immersion in alizarin red S and

potassium ferricyanide (Sperber, *et al*, 1984). The terms produced by Friedman (1965)

and classification of Sibley and Gregg (1987) will be used throught this section.

7.2.1. Hand specimen petrography

Five different dolomite types are identified within the Ain Tobi Dolostone Member

(discussed below). Type-1 dolomite is yellowish-grey, porous and laminated mainly

replacing wackestone/packstone. The laminae are usually pinkish in colour. This type of

dolomite is rarely associated with ripples, birds-eye, gypsum nodules, breccias and quartz

Type-1 dolomite. Early replacive, dirty, non-ferroan, unimodal and nonplanar-a crystalline. It has homogeneous dully orange to orange luminescent pattern. Scale bar equal 100μm. "P" is pore space.

Type-2 dolomite. It is mimetically and/or nonmimetically replaced packstone/grainstone and its crystals are unimodal, nonplanar-a. They show orange, bright yellow and red luminescence. Scale bar equal 100μm. "P" is pore space.

Type-3 dolomite. Unimodal, nonferroan and nonplanar-a post-compaction dolomite crystals associated with quartz grains (Q). It shows dull cores and orange luminescent rims. Scale bar equal 100μm.

Type-4 dolomite. Early to intermediate replacive, nonferroan polymodal and planar-s crystalline. Crystals show orange luminescent cloudy cores and dull or nonluminescent rims. Scale bar equal 200 μm. "P" is pore space.

Type-5 dolomite. Polymodal, planar-s and saddle dolomite with cloudy cores and clean rims, being replaced origin micrite sediments and/or precursor idiotopic unimodal early dolomite crystalline. This type exhibits orange luminescent cloudy cores, nonluminescent clean overgrowths and bright-yellow cleavage lines. Scale bar equal 1mm.

Dedolomite. polymodal, planar-s zoned dolomite crystalline with their cores are mainly dissolved out and usually replaced by calcite (c) with optical continuity with calcite between dolomite crystals. Calcite also replaced zones between dissolved cores (p) and rims. Calcite zones and cores show dully luminescent whereas dolomite zones show bright orange luminescent pattern. Scale bar equal 200 μm.

Fig. 7.1. **a)**. Field sketch showing relationship of Ain Tobi Dolostone Member to underlying and overlying strata at Abu Ghaylan area (not to scale). **b)**. The five dolomite types and dedolomite textures observed in the Ain Tobi Dolostone Member of Jabal Nafusah escarpment NW Libya.

grains particularly in the western part of the study area. Type-2 dolomite is very fine, whitish-grey, cross-bedded, slightly porous and calcareous mainly replaces packstone and grainstone facies. Type-3 dolomite is also laminated tan to grey and calcareous. It is interbedded with medium quartz sandstone. Type-4 dolomite is light-grey to yellowish, slightly porous and calcareous, having replaced highly fossiliferous sediments. It occurred at various stratigraphic positions of almost all measured sections. Type-5 dolomite is grey, coarse to very coarse and porous with pearly luster appearance, replacing calcarenitic packstone lithofacies. This type is restricted to the eastern part of the study area.

7.2.2. Transmitted light and Cathodoluminescence microscopy

According to the crystal shape and size distribution five different types of dolomite (Fig. 7.1b) recognized in the studied sections (see Chapter 5 for description and locations of sections). These differences may reflect the variation of origin, mechanisms, chemistry and may be the timing of dolomitization. Some individual samples of these sections are composed of more than one type of dolomite.

Type-1 dolomite

It is pervasively non-ferroan dolomite, generally consists of unimodal or very fine to fine (10-50μm), closely packed nonplanar-a (Sibley and Gregg, 1987) or xenotopic (anhedral) dolomite crystals (Fig. 7.2a). These dolomite crystals have totally replaced the precursor sediments which probably were lime mudstones and wackestones. It exhibits undulose extinction but lack of characteristics as saddle dolomite. The cores of some crystals are selectively dissolved out leaving intracrystalline pores (Fig. 7.8a). The texture is mainly xenomorphic. Type-1 dolomite is characterized by homogenous dull to orange luminescence pattern at zones succeeded disolved cores and yellow rims (Fig.

7.5d). Type-1 dolomite is the most common type in the Ain Tobi Dolostone Member and occurred at all locations.

Type-2 dolomite

The crystals of this type of dolomite are made up of unimodal or very fine (4-15μm), closely packed nonplanar-a or xenotopic dolomite fabric (Fig. 7.3c). The crystals are usually dirty or cloudy and mainly mimetically and/or nonmimetically replaced skeletal and non-skeletal allochems (Fig. 7.3d & 7.4a). Original fabrics are commonly preserved where they have been replaced by this type of dolomite. Type-2 dolomite exhibits alternation of orange luminescence (inner and middle concentric layers of the ooids) and bright yellow luminescence (Fig. 7.6d). The crystals outlined the intraparticle and interparticle pores and ooids show red or dark brown luminescence. Mouldic, interparticle and vuggy porosities are commonly occurred within this xenomorphic mosaic dolomite, which has been found in the lower and middle intervals of most measured sections.

Type-3 dolomite

Type-3 dolomite is unimodal or fine to medium (average 100μm), nonplanar-a and planar-s crystalline. This type is mainly associated with quartz grains (Fig. 7.2b) and occurs at the bottom of most measured sections. Rare echinoderm fragments that have survived dolomitization are present. Quartz grains associated with this dolomite are subrounded, medium to coarse and unicrystalline. They are usually coarser than dolomite crystals and are sometimes fractured due to compaction (Fig. 7.2c). Dolomite crystals replace margins of some quartz grains and occur at fractures within them (Fig. 7.6a). Type-3 dolomite is mainly characterized by orange luminescent rims and a dully luminescent pattern at cores (Fig. 7.6a).

Fig. 7.2   Petrography of the Ain Tobi Dolostone Member in western Jabal Nafusah,

Libya:

a. Photomicrograph from sample No. S1-8 showing Type-1 dolomite crystal fabric, which has unimodal nonplanar-a tight interlocking or sucrosic texture. (ppl).

b. Photomicrograph from sample No. S9-2, showing dolomite Type-3 which is associated with quartz and it is mainly xenotopic or nonplanar-a and tight interlocking texture. Note also that in this dolomite type partially replaces margins of quartz grains (arrow). (ppl).

c. Photomicrograph from sample No. S9-17. It shows dolomite Type-3 associated with quartz grains, which are fractured (arrow) due to compaction and dolomite crystals formed along the fractures which indicate that this type of dolomite was formed post-compaction, see also Fig. 7.6a. (ppl).

d. Photomicrograph taken from sample No. S1-7 showing Type-4 dolomite which exhibits cloudy cores and clean rims. (ppl).

a

b

c

d

100μm

200μm

1000μm

200μm
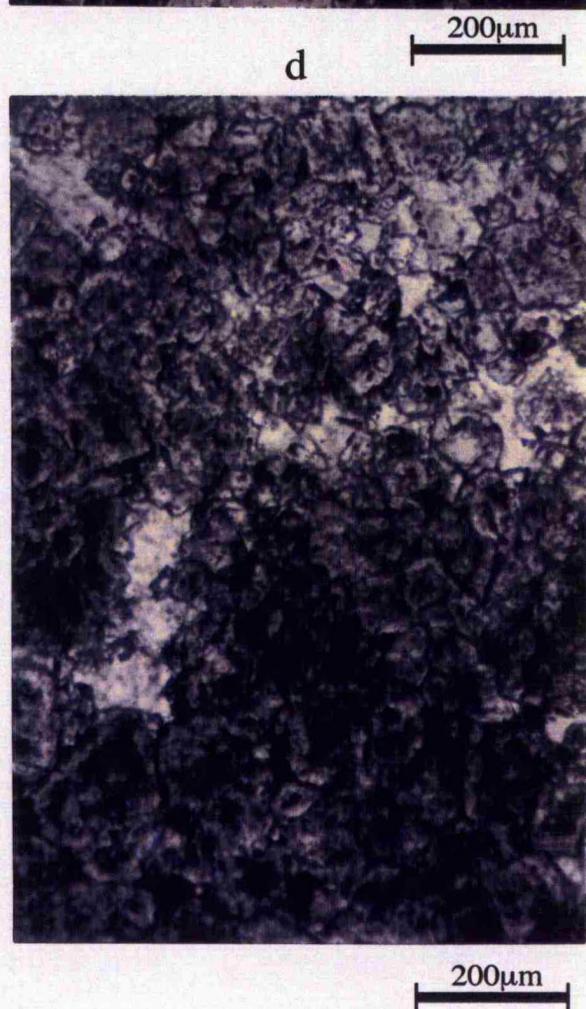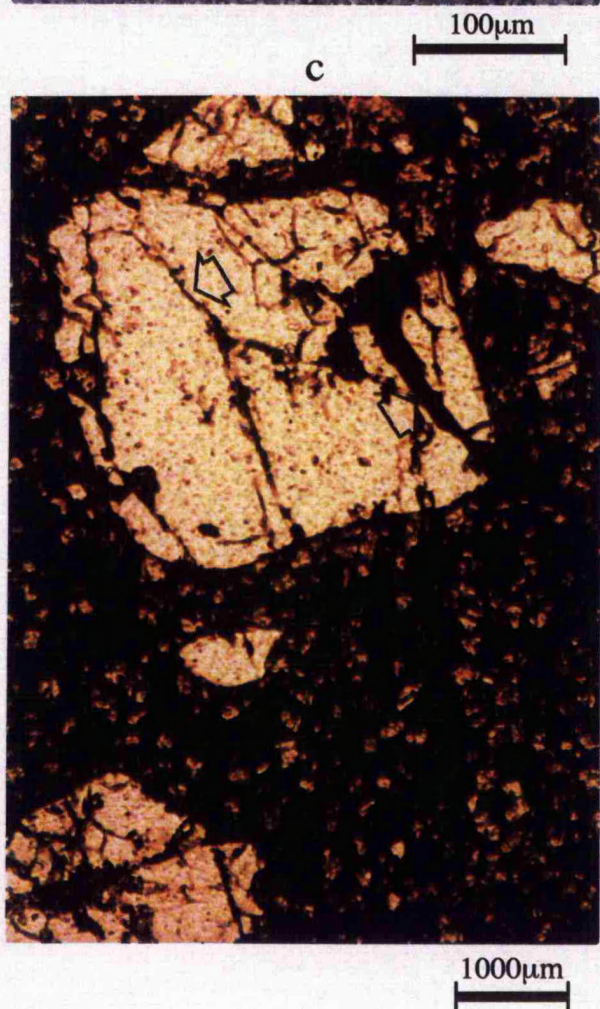
Fig. 7.2

Type-4 dolomite

It is polymodal or medium to coarse (100-300μm), nonplanar-s or hypidiotopic and non-ferroan dolomite (Fig. 7.2d). The crystals are cloudy (inclusion rich) at the cores with cleaner rims. In some cases crystals of Type-4 dolomite are isolated, planar-e (Fig. 7.3a) being replaced matrix and/or ghosts.

Type-4 dolomite has totally replaced the original sediments which probably were bioclastic wackestone/packstone. Some crystals show replacement of precursor fine and nonplanar-a (Type-1) dolomite crystals, whereas others have their cores partially or completely dissolved out due to continued dissolution, leaving irregular voids indicating dedolomitization. In some instances dissolution has proceeded to the point where almost the whole crystal has been completely dissolved out, leaving rhombic moulds. The texture of Type-4 dolomite is generally idiomorphic to hypidiomorphic. Intercrystalline is the most common types of porosity associated with this dolomite type (Fig. 7.3b). Mouldic and vuggy porosities are not common and have been observed in various stratigraphic intervals. Cathodoluminescence microscopy shows that the cores are mainly orange luminescent due to many inclusions, whereas clean rims exhibit dully orange luminescence (Fig. 7.6b).

The intercrystalline and vuggy porosities associated with this type of dolomite are sometimes filled by non-ferroan calcite cement which selectively replaced rims of some dolomite crystals (Fig. 7.6c).

Type-5 dolomite

This type of dolomite occurs in the eastern Jabal Nafusah and rarely in the western area and has been observed in Al Khums and Wadi Jabbar areas (Sections # 3 and # 4). Type-5 dolomite is composed of coarse to very coarse or polymodal (500μm-2mm),

planar-s baroque or saddle crystals (Fig.7.4b). These replacive crystals have curved faces or boundaries and cleavage planes. They show extremely undulose extinction (Fig. 7.4c). It occurs as a replacive mineral and/or as a cement. The crystals are characterized by dully orange luminescent (clear overgrowth or rims), orange luminescent (euhedral inclusion-rich and dark cores) and very thin bright yellow luminescent cleavage planes (Fig. 7.4b). Rims and cores have an irregular dissolution contacts between them (Fig. 7.7a).

Dedolomitization

The term dedolomitization was first proposed by Von Morlot (1848) to describe a possible mechanism by which the mineral calcite replaces the mineral dolomite.

Evidence for dedolomitization has been observed under the microscope and by XRD analysis of whole rock of the Ain Tobi dolomite sediments. Presence of euhedral or idiomorphic dolomite crystals with their cores leached out leaving intracrystalline pores (Fig. 7.4d) and sometimes the whole rhomb dissolved out leaving euhedral mouldic pores indicates dedolomitization. The dissolved cores of some crystals are filled or replaced by calcite (Fig. 7.5a). This occurs mainly in the lower part of the sequence. Some other rhombohedral crystals are replaced by large non-ferroan, and late calcite crystals. These calcite crystals occur as an overgrowth in optical continuity with dolomite substrates. In some cases the dolomite rhombs are corroded or rounded crystals (Fig. 7.5a), whereas elsewhere in the upper part of the sequence some dolomite crystals float in coarser calcite crystals with irregular contacts between them (Fig. 7.5b) indicating dedolomitization. Dolomite crystals which have been partially dissolved and replaced by calcite show complex zonation under cathodoluminescent microscopy (Fig. 7.7c & d). Calcite at cores and at outer zone of dolomite crystal have dully luminescent pattern whereas unreplaced dolomite zones between them has bright orange luminescent (Fig.

<u>Fig. 7.3</u> Pervasive dolostone fabrics:

a. Photomicrograph of sample No. S9-27 from Jadu Section showing isolated crystals of Type-4 dolomite. Note the crystal shapes are planar-e and are isolated or loose interlocking. (ppl).

b. Photomicrograph of sample No. S6-16 from Kiklah Section. It shows planar-e or idiotopic crystal shape of Type-4 crystalline dolomite with very common intercrystalline porosity (p). (ppl).

c. Photomicrograph showing Type-2 crystalline dolomite which is very fine or unimodal and nonplanar-a being replacing oolitic grainstone. Brown area is porosity, sample No. S2-2. (ppl).

d. Photomicrograph from sample S2-1, showing Type-2 dolomite being mimetically replaced oolitic grainstone facies. Note common interparticle porosity (1) and intraparticle (2) porosity. (ppl).

a

b

c

d
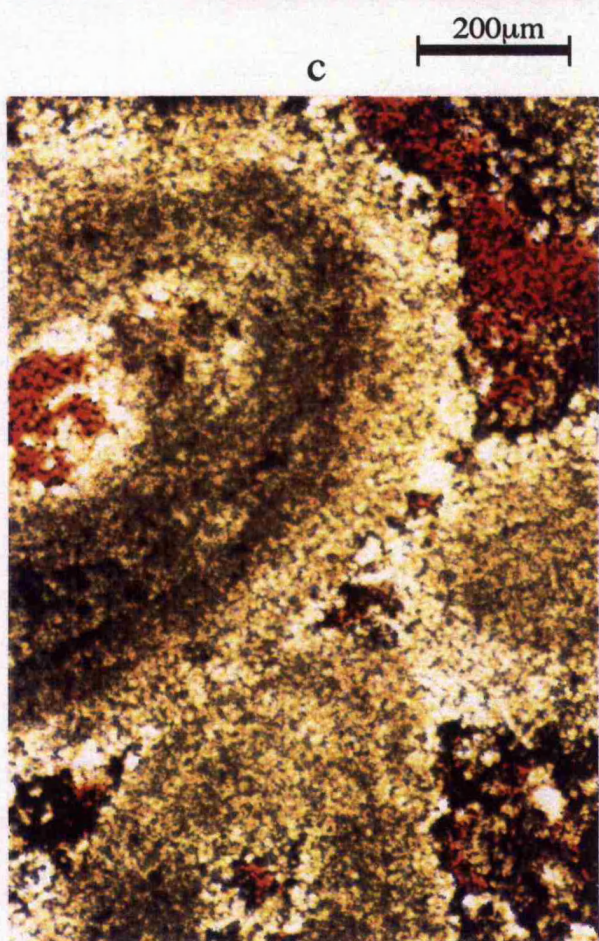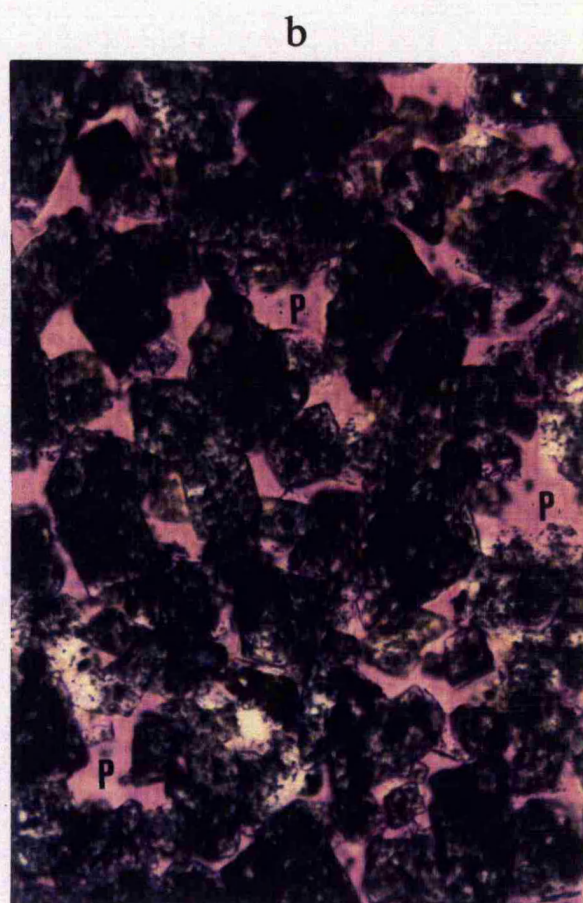
Fig. 7.3

<u>Fig. 7.4</u> dolomitized grain-supported fabrics of the Ain Tobi Member:

a. Photomicrograph of sample No. S2-2 from Ras Fam Mulghah Section showing unimodal, nonplanar-a, pre-compaction dolomite Type-2 nonmimetically replacing ooids and fossil fragments. Note interparticle porosity (p) lined by dark brown material. (ppl).

b. Photomicrograph of sample No. S3-3 from Al Khums Section showing polymodal (coarse to very coarse), planar-s saddle dolomite with cloudy cores and clean rims. Note also intercrystalline porosity (p). (ppl).

c. Same view as in (b), but XN.

d. Thin-section photomicrograph showing polymodal, idiotopic or euhedral saddle dolomite from Al Khums section (sample S3-4). Note that saddle dolomite replaced earlier metastable and very fine dolomite crystals (arrow) which partially dissolved out leaving intracrystalline porosity (p). Common intercrystalline porosity (o). (ppl).

a

b

c

d
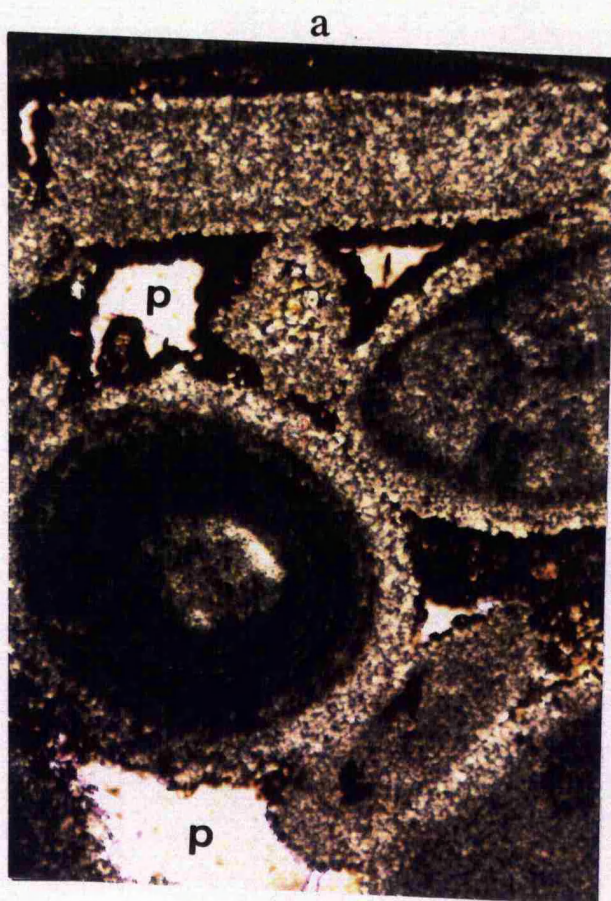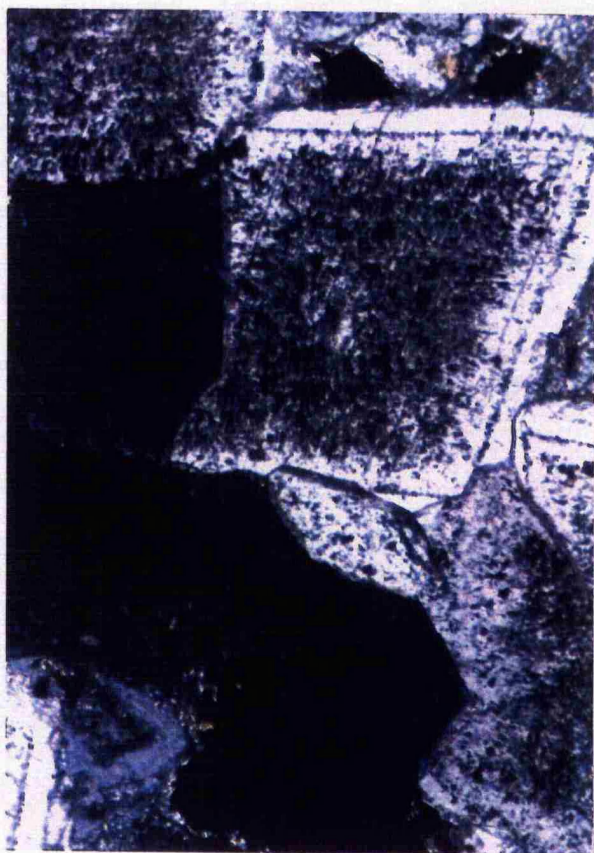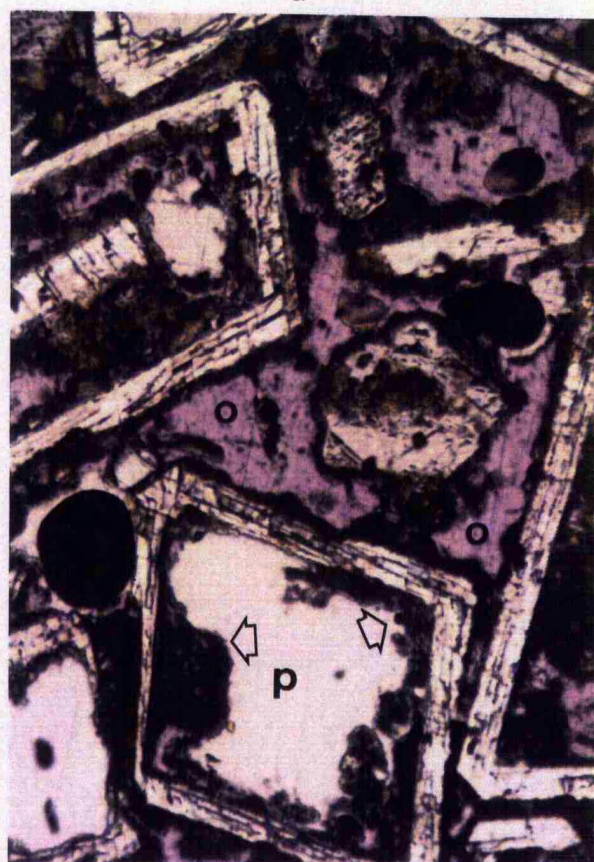
200μm

200μm

200μm

200μm

Fig. 7.4

Fig. 7.5   Petrography of dedolomitization and cathodoluminescence of the Ain Tobi

dolomites:

a. Thin-section photomicrograph from sample S9-1 at Jadu Section showing the contact (arrow) between very coarse and slightly ferroan calcite (c) and corroded dolomite crystals (d). Note that cores of some dolomite crystals are replaced by calcite. (ppl).

b. Photomicrograph from sample S1-10 at Abu Ghaylan section, showing dedolomitization. The dolomite crystals are floating in a much coarser calcite crystals (c). Some dolomite crystals have their cores replaced by calcite and others are totally replaced by calcite but still recognizable (arrow). (ppl).

c. Photomicrograph of fine and sucrosic texture of Type-1 dolomite crystalline. Cores of some crystals are dissolved out. Sample S2-1 at Ras Fam Mulghah section. (ppl).

d. Luminescence microscopy of same sample at (c) showing the homogeneous orange luminescence pattern of Type-1 dolomite with very thin bright yellow outer zones. Black area is intracrystalline pores.
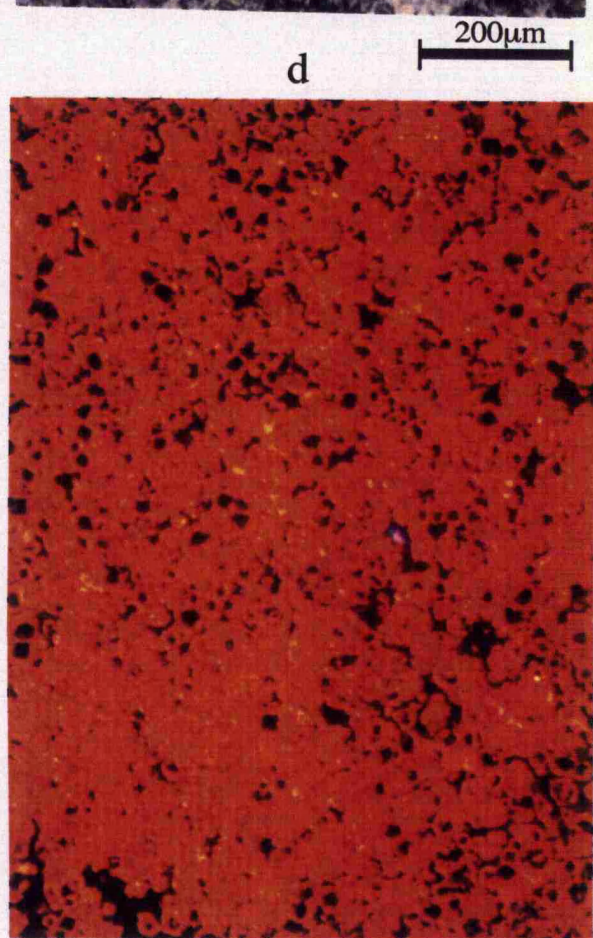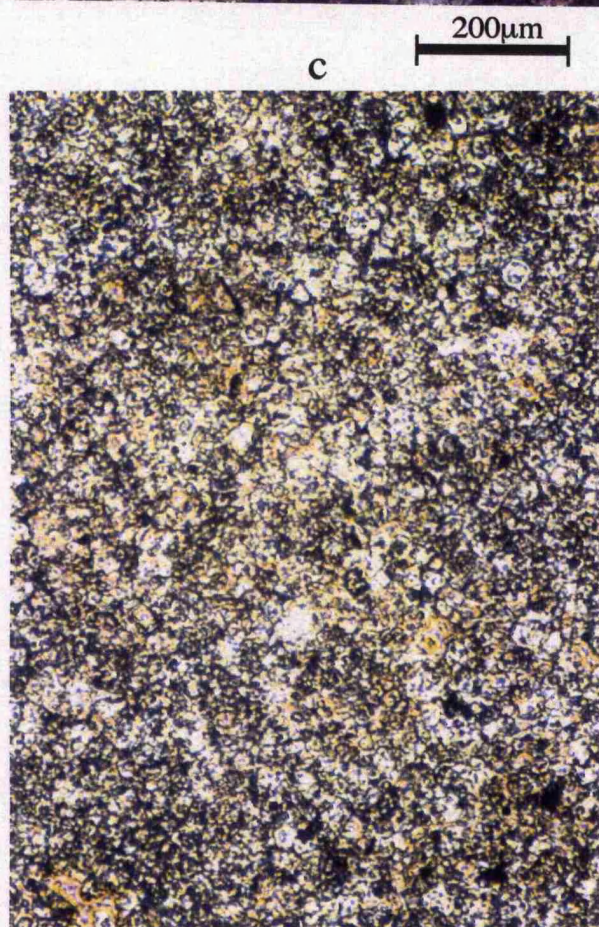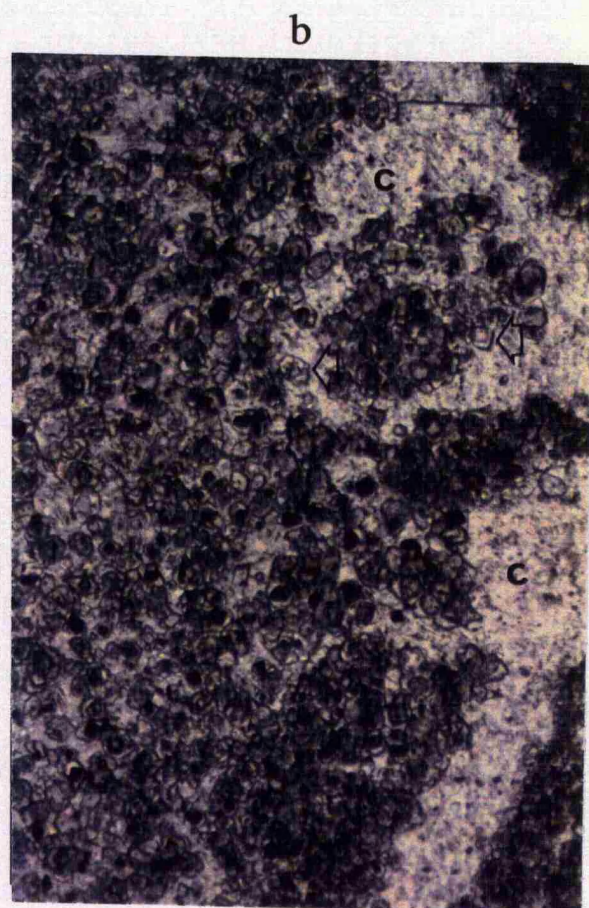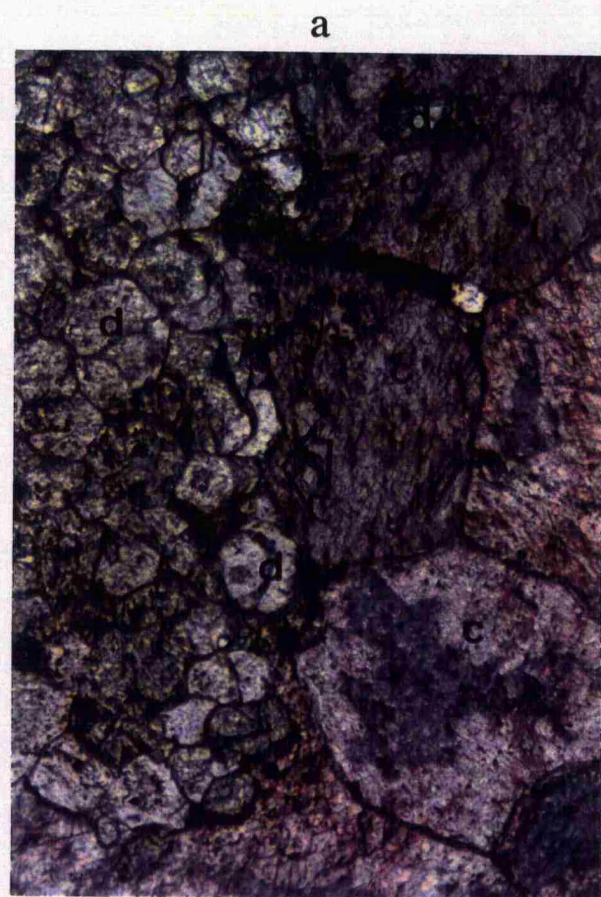
Fig. 7.5

<u>Fig. 7.6</u>. Cathodoluminescence microscopy of the Ain Tobi dolomites:

a. Luminescence microscopy of sample S9-17 shown in (Fig. 7.2c). Note that Type-3 dolomite which is associated with quartz has dully luminescent cores and bright rims, whereas quartz grains (Q) show dark blue or black colour.

b. Luminescence microscopy of sample S8-7 at Riaynah area showing Type-4 dolomite. The cloudy cores show orange luminescent pattern (c) and clean rims have dully orange luminescent.

c. Thin-section photomicrograph from sample S4-12B at Wadi Jabar section showing cloudy rhomb and clear outer zone (arrow) within very coarse poikilotopic and nonferroan calcite (c).

d. Luminescence microscopy of sample S2-2 shown in (Fig. 7.3c). Note that very fine dolomite replacing concentric structure of ooids have bright yellow luminescence (Y), whereas dolomite within intraparticle porosity or lining interparticle pores have red luminescence (arrow). The red luminescence appearance probably indicate that these crystals are formed later as a cement.
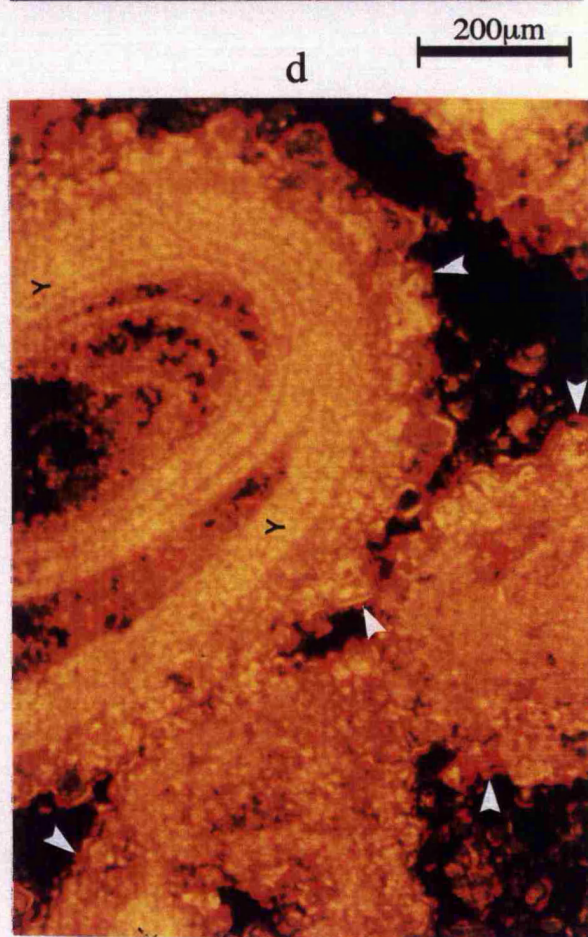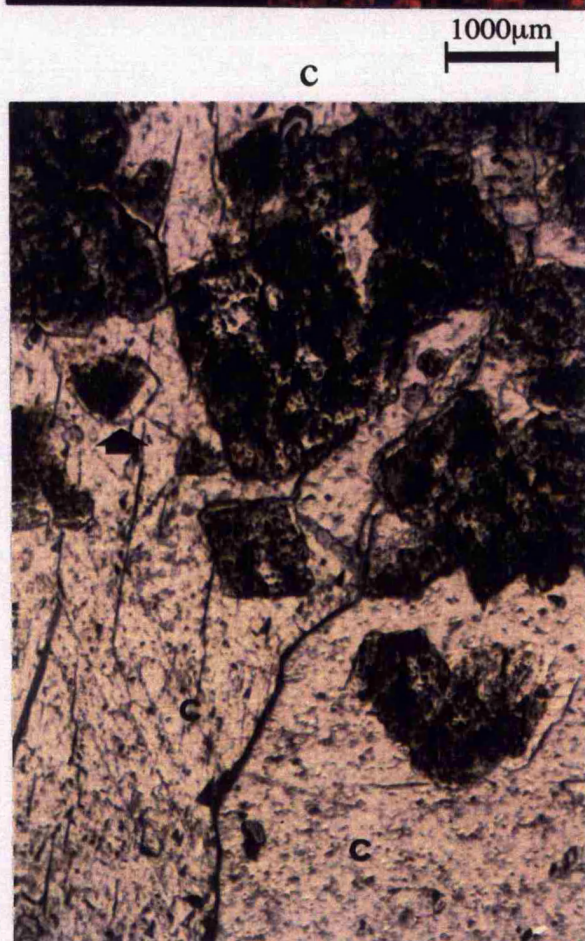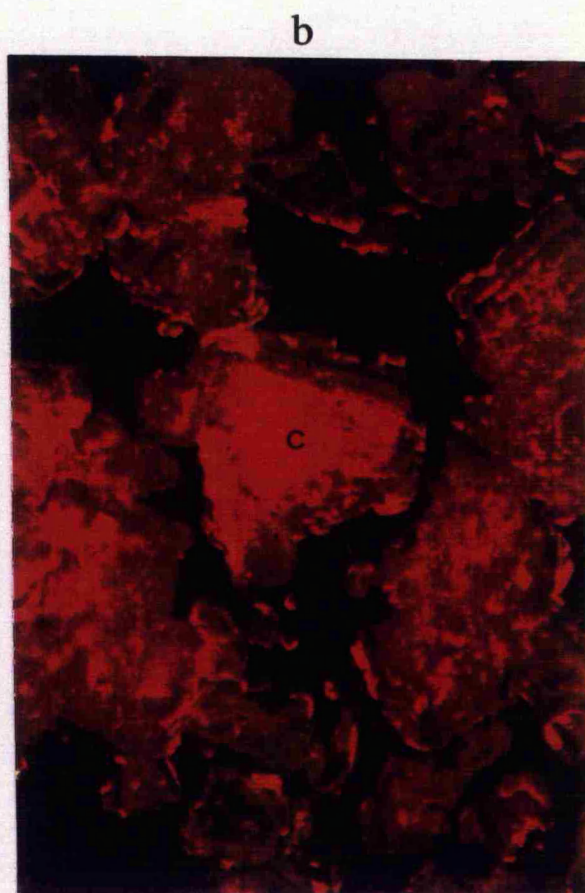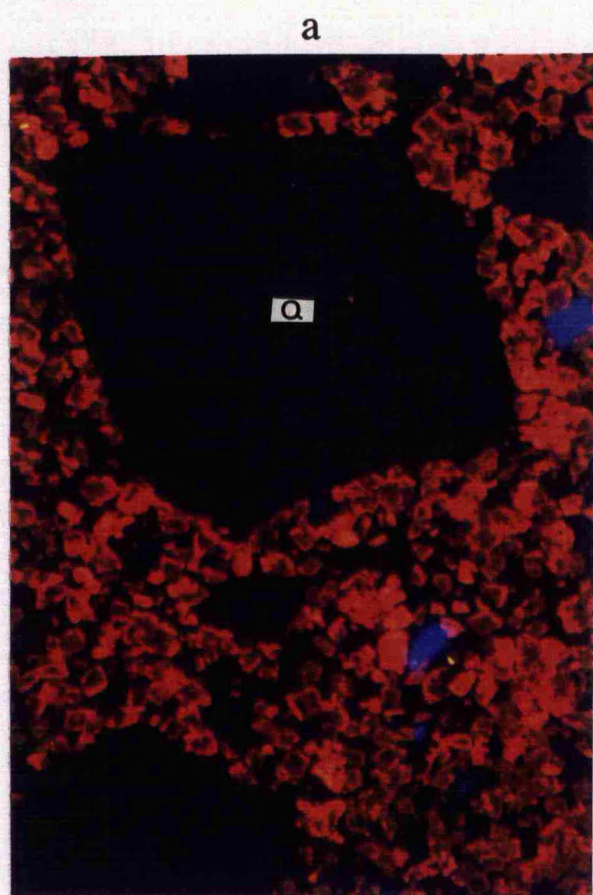
Fig. 7.6

7.7d). The coarse calcite replaces margins and/or cores of the dolomite rhombs shows no

luminescence.

7.2.3. Scanning Electron Microscopy (SEM)

SEM was performed on polished and carbon coated thin sections. Type-1 dolomite

appears as loose crystals with common intercrystalline porosity and the cores of the

crystals are selectively dissolved out leaving intracrystalline porosity (Fig. 7.8a). Crystals

of this type are planar-s or subhedral mosaics on SEM scale. These characteristics have

been observed mainly in samples taken from the central and western area of Jabal

Nafusah escarpment. Samples taken from this type of dolomite in the eastern area of the

escarpment seem as loose or isolated crystals on SEM scale, anhedral to subhedral and

unaffected by dissolution (Fig. 7.8b) being replaced matrix, with low porosity. Dolomite

Type-2, which has mimetically replaced allochems particularly ooids, appears as very fine

on SEM scale, but crystals occurred as cement filling interparticle porosity and lined

ooids are fine, nonplanar or anhedral to subhedral mosaic (Fig. 7.9a). Common

interparticle pores and rare mouldic and intraparticle pores also occur (Fig. 7.9b). Type-3

dolomite crystals are subhedral on SEM scale and have irregular contacts with quartz

grains and/or replacing them. Type-4 dolomite appears as tight interlocking, low

intercrystalline porosity, anhedral to subhedral mosaics on SEM scale and no visible

effect of dissolution on crystals (Fig. 7.8c), but the other petrographic crystals of this

type are isolated and euhedral with very common intercrystalline porosity. Some crystals

have selectively dissolved at thin zones separating cores from rims (Fig. 7.8d). Type-5

dolomite crystalline fabric appears as very coarse or polymodal and planar-s. Smaller and

planar-e crystals (probably of Type-4 dolomite) also occurred and their cores are

<u>Fig. 7.7.</u>   Luminescence microscopy of saddle dolomites and dedolomitization of the

Ain Tobi Member:

a.Thin-section photomicrograph of Type-5 saddle dolomite crystalline. It shows cloudy cores (h) and clean rims (R). (ppl).

b. Luminescence microscopy of sample shown in (a). Note that cloudy cores have brighter luminescence than clean rims whereas cleavage lines show bright yellow luminescent pattern (arrow).

c. thin-section photomicrograph of sample S10-2 at Kabao section showing dedolomitization and dissolution. Note that cores of some crystals are selectively dissolved out leaving intracrystalline pores (p) and some of them are replaced by calcite (c) in later stage. (ppl).

d. Luminescence microscopy of sample shown in (c). Note the complex zonation of the dedolomitization where dolomite zones show bright luminescent and calcite zones show dully luminescence and pores are black.
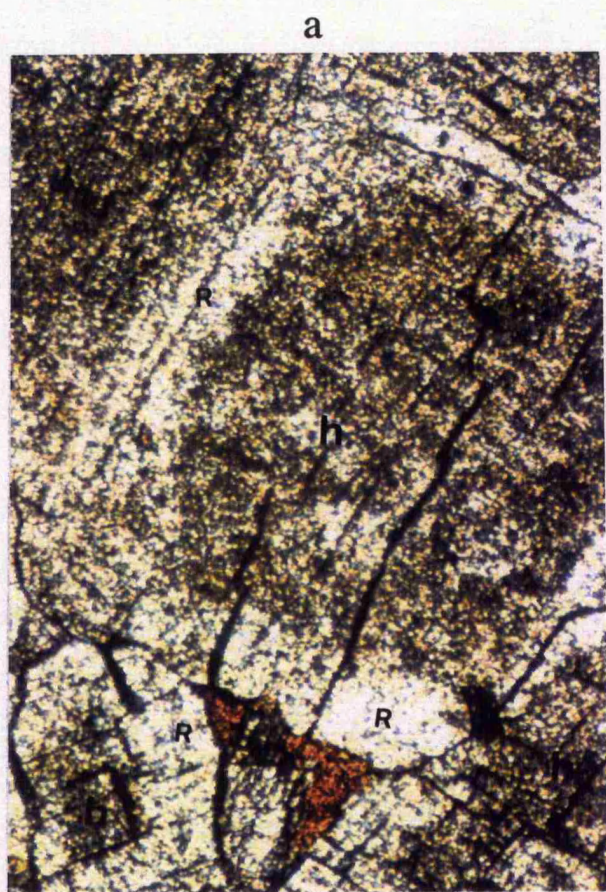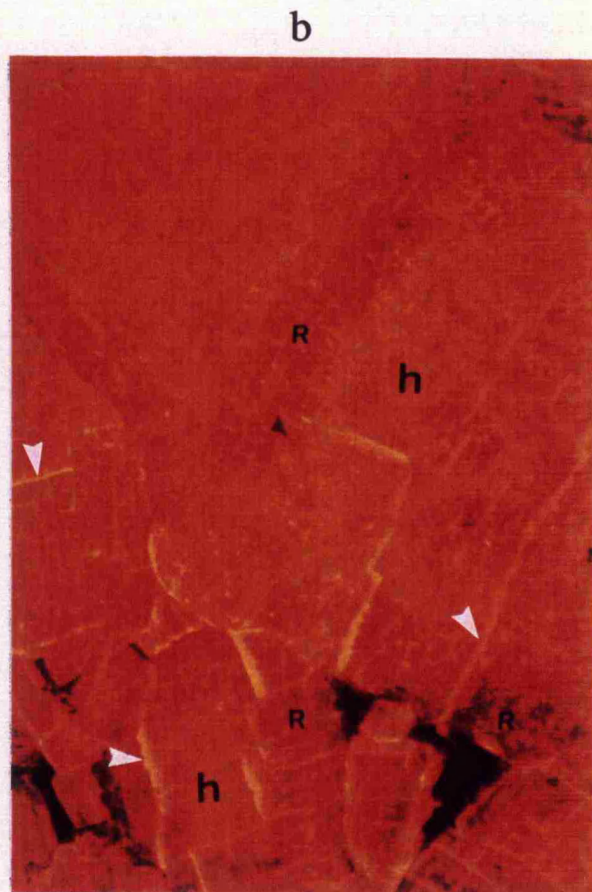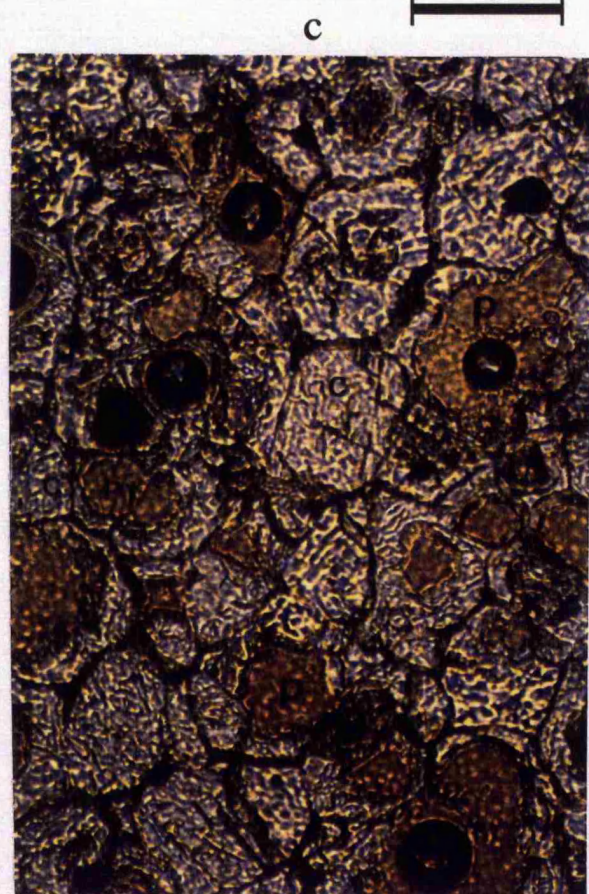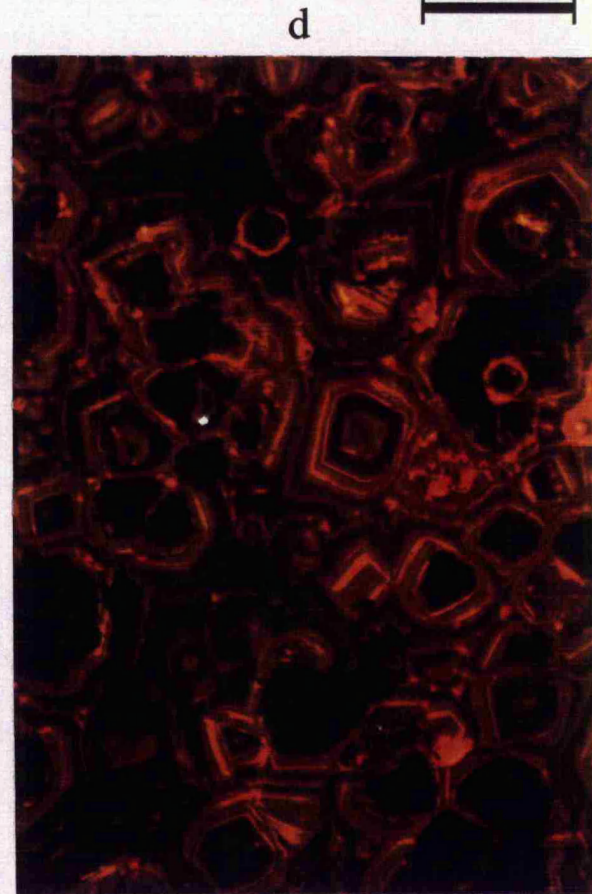
Fig. 7.7

partially dissolved out and partially or completely replaced by Type-5 dolomite (Fig. 7.9c). Intercrystalline and intracrystalline porosities are not common.

Dedolomitization

Fine and euhedral or idiotopic dolomite crystals float in a very coarse calcite crystals with irregular contacts between them (Fig. 7.9d) indicating replacement of dolomite by calcite in late stage.

7.2.4. Distribution of dolomite

Type-1 and Type-4 dolomites occurred in all sections in different stratigraphic positions. Type-1 dolomite mainly replaces laminated mudstone and wackestone facies. Type-2 dolomite has been found mainly at the middle parts of measured sections in the western and central parts of the study area within the *Ichthyosarcolites* band or replacing packstone and grainstone facies. It has replaced the oolitic grainstone intervals in the lower and middle parts of the measured sections at the eastern part of Jabal Nafusah (east Wadi Ghan). Type-3 dolomite has been found at all locations, commonly at the lower parts associated with sandstone. Finally, Type-5 dolomite is restricted to the eastern part of the study area at the top of measured sections in Fam Mulghah, Wadi Jabbar and Al Khums area and rarely at Abu Ghaylan and Riaynah areas. Dedolomitization or the replacement of the dolomite by calcite crystals has been observed at various stratigraphic positions. It has been found mainly at the bottom of section # 9 and section #10, close to the unconformity between Kiklah Formation below and Ain Tobi Member above, and occurred also at top of sections # 2, # 4, # 7, # 8 and # 9.

Fig. 7.8. Scanning electron microscopy of the Ain Tobi dolomite types:

a. Scanning electron microscopy of Type-1 dolomite showing the euhedral to subhedral appearance of crystals. Note cores of most crystals are mainly dissolved. This dolomite is very common in the western area of Jabal Nafusah. Sample S1-2, Abu Ghaylan area.

b. Scanning electron photomicrograph of Type-1 dolomite in eastern part of Jabal Nafusah, showing subhedral crystals (c) slightly affected by dissolution. Sample S4-2, Wadi Jabar section.

c. Scanning electron image of Type-4 dolomite. Note cloudy cores (c1) are unaffected by dissolution. (c2) is the clean rims of Type-4 crystalline which probably represent overgrowth. Common intercrystalline porosity associated with this dolomite crystalline. Sample S9-29, Jadu section.

d. Scanning electron photomicrograph of the second petrographic crystals of Type-4 dolomite. They are planar-e or euhedral and isolated crystals (D) with very common intercrystalline porosity. Note dissolved zones separated cores from outer rims. sample S9-27, Jadu section.

a

b

86μm

43μm

c

d
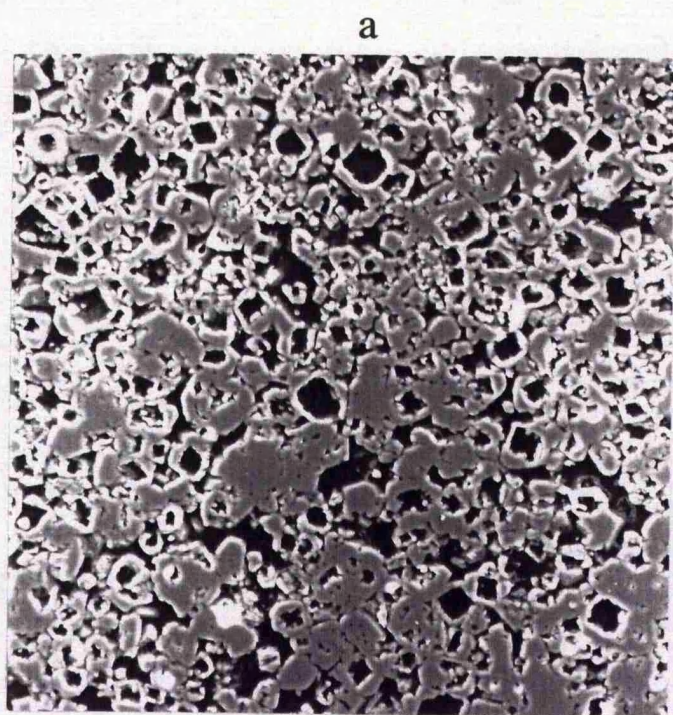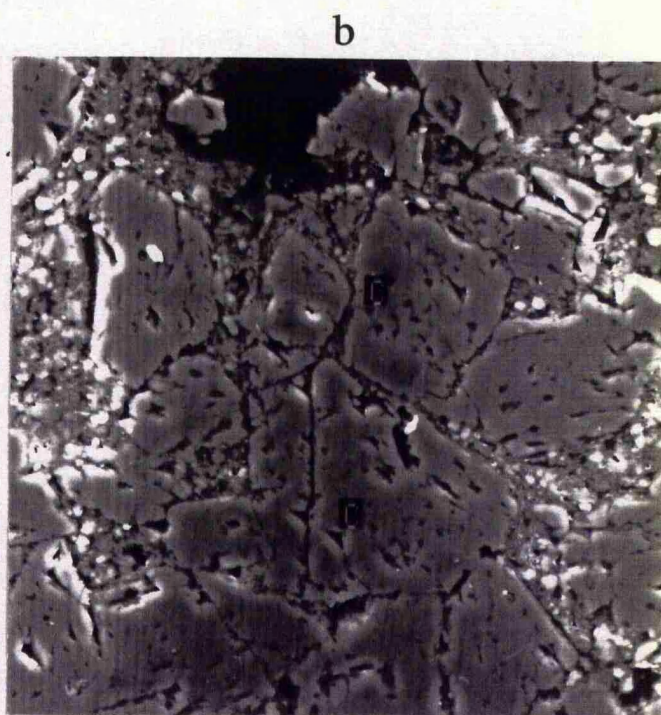
75μm
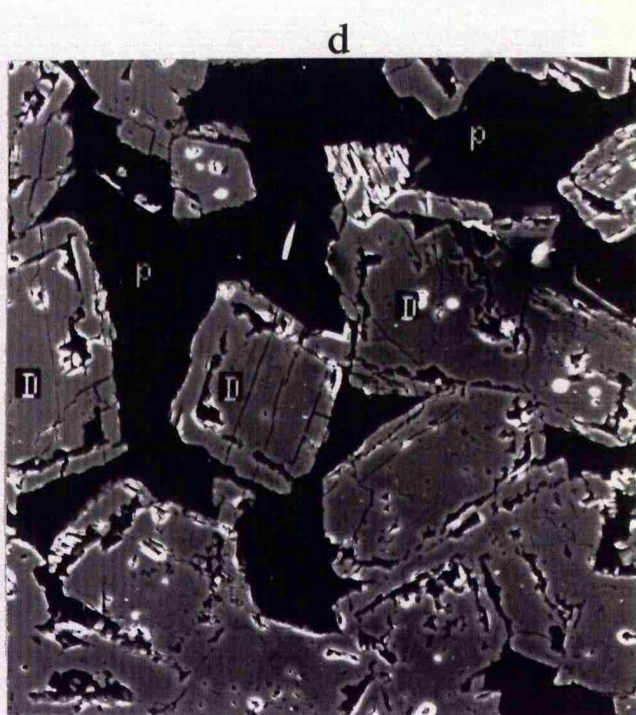
86μm

Fig. 7.8

<u>Fig. 7.9.</u>   Scanning electron microscopy of the Ain Tobi dolomites and dedolomitization:

a. Backscattered electron image of Type-2 dolomite which are nonmimetically replacing ooids (O) and later dolomite cement (DC) lining ooids and intraparticle porosity (p1) and interparticle porosity (p2). Sample S2-2, Ras Fam Mulghah section, Tarhunah area.

b. Same as (a) showing Type-2 dolomite crystalline mimetically replaced oolitic grainstone facies. Common interparticle porosity (p) and absence of intraparticle porosity. Sample S2-1, Ras Fam Mulghah section.

c. Scanning electron photomicrograph of Type-5 saddle dolomite (T6) being partially and/or totally replaced precursor earlier and euhedral dolomite crystalline (T1), which have been partially to completely dissolved. Sample S3-4, Al Khums section on the Mediterranean Coast.

d. Scanning electron photomicrograph of dedolomitization showing euhedral dolomite crystals (D) floating in a coarser calcite (C). Note irregular contacts between dolomite and calcite indicating dedolomitization. Sample S4-12B, Wadi Jabar section.
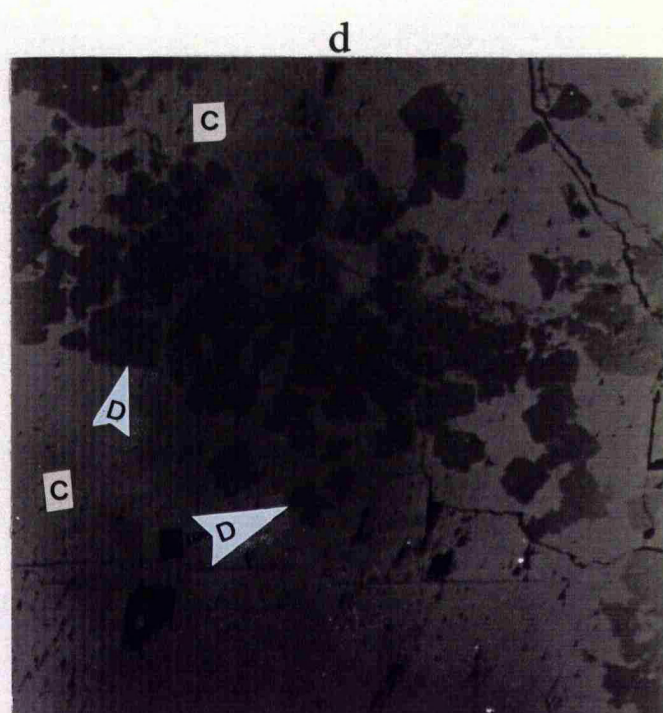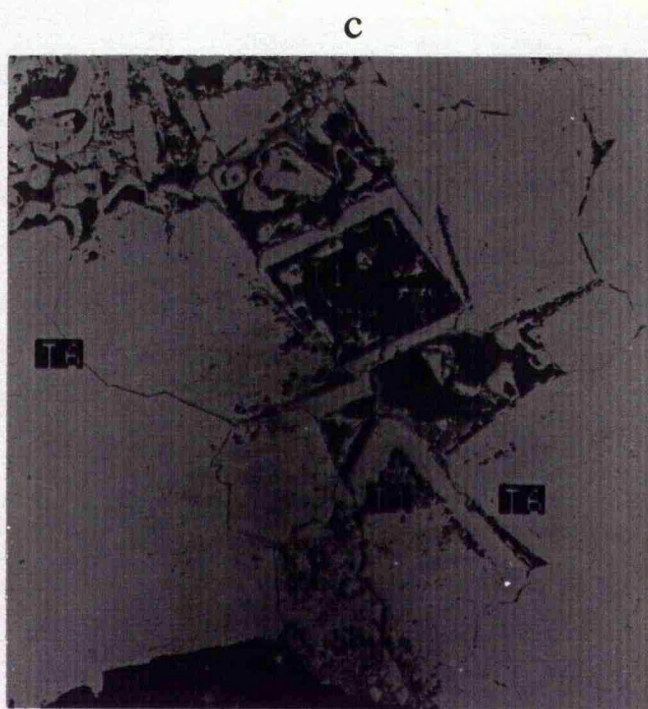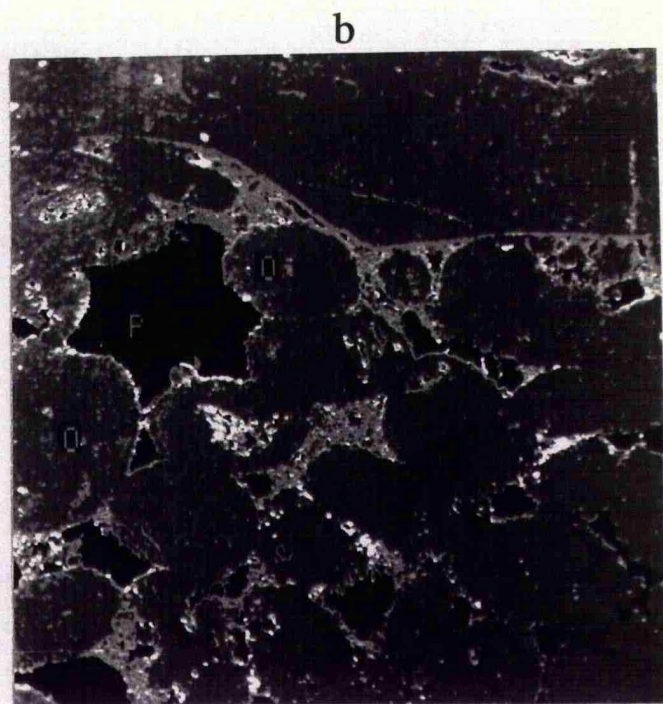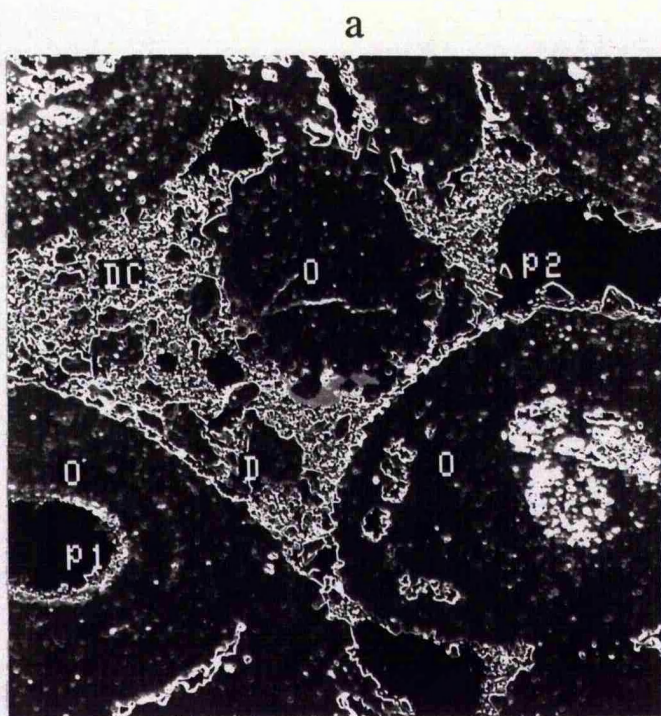
Fig. 7.9

7.3. Geochemistry

7.3.1. Introduction

Recently it has been shown that the geochemistry of dolomites, including their major and trace element concentrations and isotopic composition, is an essential complement to geologic and petrographic studies (Veizer, 1983). In this section, several geochemical approaches are used to provide constraints on mechanism and origin of extensive dolomitization.

Most diagenetic carbonates represent the alteration products of sedimentary phases that were originally crystallized from seawater. Over the past two decades, studies of modern seawater and sediment samples as well as ancient fossils permit the estimation of the trace element and stable isotopic composition of equilibrium marine carbonates for a given time (e.g. M'Rabet, 1981; Veizer, 1983; DePaolo and Ingram, 1985).

7.3.2. Stoichiometry and Crystal order

As discussed by Hardy and Tucker (1988); Tucker and Wright (1990), many if not most, natural dolomites are non-stoichiometric, i.e. they do not have the ideal molar ratio of $CaCO_3/MgCO_3$ of 50/50. Stoichiometry of the Ain Tobi dolomite is determined by XRD analysis of whole rock powder of 153 samples. The $CaCO_3$ content was calculated using Lumsden's (1979) equation "mole % $CaCO_3$ = Md + B"; where M is (333.33), B is (-911.99) and d is the observed d-spacing (Å) (see Appendix 1 for precision of the XRD). This technique is also used in order to give more information on the ordering of the dolomite crystals by dividing the intensity of peak (015) over peak (110). The greater the ratio of the highest of the ordering peak 015 to diffraction peak 110, the higher the degree of order (Tucker and Wright, 1990). XRD data can be useful to distinguish between different types of dolomite (Fig. 7.10a) explained above within one carbonate

formation, but with some overlap (Hardy and Tucker, 1988), by plotting relationships between the ordering ratio versus the mole % $CaCO_3$ for all recognized types of dolomite from the Ain Tobi dolomites outcropped in Jabal Nafusah escarpment presented in (Fig. 7.10a). Dolomite types have different degrees of order and Ca/Mg ratios. Five types of dolomite can be recognized based on stoichiometry and ordering ratio. Type-1, Type-2 and Type-3 dolomites are poorly to moderately ordered. Type-2 dolomite is calcian to calcian-rich whereas Type-1 dolomite is stoichiometric to calcian and Type-3 dolomite is nearly stiochiometric to calcian. Type-4 and Type-5 dolomites are well ordered but Type-5 is more calcian and better ordered than Type-4 dolomite. Also it can be used along with trace elements and stable isotopes to discriminate early from late dolomites (Frisia, 1994). In fact, most ancient dolomites studied (e.g. Cretaceous dolomite of Ain Tobi dolomites, this study; Cretaceous dolomites of Meloussi, Bouhedma and Kebar formations of central Tunisia, M'Rabet, 1981 and Cretaceous dolomites of El Heiz and El Hefhuf formations in Egypt, Holail *et al*, 1988) are calcian (except Type-1 of this study, Table 7.1) and characterized by well ordered to disordered cation (Reeder, 1983). They are therefore unstable and have a recrystallization potential that increases with increasing burial temperature (Hardie, 1987). This can be applied to the most of the Ain Tobi dolomites as will be discussed below.

From the data gathered from XRD analysis (Table 7.2), the Ain Tobi dolomite types seem to be mainly non-stoichiometric with an exception of Type-1, and moderately to well ordered. The mole% $CaCO_3$ of fine crystalline (Type-1) dolomite ranges ($Ca_{0.50}Mg_{0.50}CO_3$ to $Ca_{0.52}Mg_{0.49}CO_3$, average mole% $CaCO_3$ 51), and its ordering ratio ranges from (0.61 to 0.79, average 0.70). Very fine dolomite (Type-2) shows a wide compositional range from calcian to calcian-rich ($Ca_{0.52}Mg_{0.48}CO_3$ to
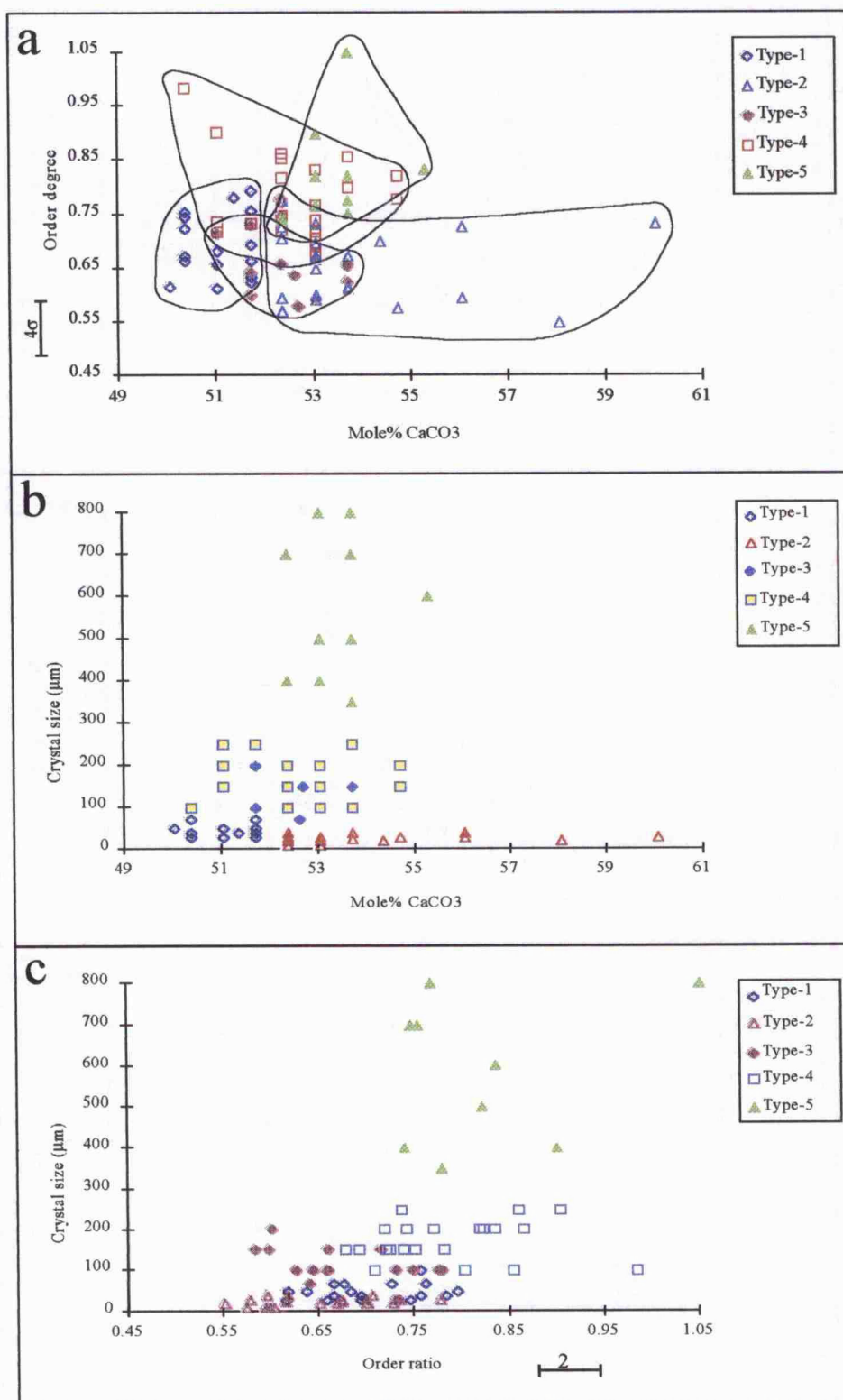
Fig. 7.10. Ain Tobi dolomites composition. a: recognition of dolomite types using mole% $CaCO_3$ vs order degree, b: cross plot showing relationship between crystal size (determined by microscope) and mole% $CaCO_3$, and c: relationship between crystal size and ordering ratio.

$Ca_{0.60}Mg_{0.40}CO_3$, average mole% $CaCO_3$ 53.65), and its ordering ratio ranges from (0.57 to 0.78, with an average of 0.67). Fine to medium crystalline dolomite associated with quartz grains (Type-3) shows a wide compositional range from near stoichiometry to calcian ($Ca_{0.51}Mg_{0.49}CO_3$ to $Ca_{0.58}Mg_{0.42}CO_3$, average mole% $CaCO_3$ 53.76) and poorly to moderately ordered (average 0.64). Medium to coarse crystalline dolomite (Type-4) shows a compositional range from stoichiometry to calcian-rich ($Ca_{0.50}Mg_{0.50}CO_3$ to $Ca_{0.55}Mg_{0.45}CO_3$, average mole% $CaCO_3$ 52.59) and well ordered (0.68 to 0.98, with an average of 0.78). The coarse to very coarse white or baroque dolomite crystalline (Type-5) is nonstoichiometric ($Ca_{0.52}Mg_{0.48}CO_3$ to $Ca_{0.55}Mg_{0.45}CO_3$, average mole% $CaCO_3$ 53.36) and well ordered (average 0.82).

Cross-plots of mole % $CaCO_3$ versus crystal size illustrate no covariance (Fig. 7.10b). All types of dolomite are nonstoichiometric except Type-1, but coarse to very coarse saddle dolomite crystalline (Type-5) is more calcian than all fine to coarse replacive dolomites (Types-1, 3 and 4), except Type-2 dolomite (Fig. 7.10b). Fine to coarse dolomite fabric types (Types-1, -3 and -4) have more variability than other types. The fine to very fine replacive dolomites (Type-1 and Type-2) show weak covariance between crystal size and cation ordering (Fig. 10c), whereas medium to coarse dolomite crystals (Type-4) and very coarse saddle dolomite (Type-5) show slightly better relations between cation order and crystal size, i.e. cation order increases with increasing crystal size.

All Ain Tobi dolomite types are mainly calcian and better ordered in western part of the study area than they are in the eastern part.

Table 7.1 Mole % $CaCO_3$ and degree of ordering of Cretaceous Ain Tobi dolomites and other

Cretaceous dolomites from Egypt and Tunisia reported in the literature:

Locality	Formation (age)	Dolomite petrography	Mole% $CaCO_3$	Ordering	Reference
Tunisia	Meloussi Fm. (L. Cretac.).	Fine to medium ferroan dolomite crystalline.	50-54	disordered	M'Rabet (1981)
	Bouhedma Fm. (L. Cretac.).	Very fine, anhedral and non-ferroan crystalline.	50-53	well ordered	
	Orbata Fm. (L. Cretac.).	Fine to very coarse, anhedral to subhedral and ferroan crystalline.	51-56	disordered	
	Kebar Fm. (L. Cretac.).	Non-ferroan replacive dolomite crystalline.	54-56	disordered	
Libya	Ain Tobi Mbr. (M. Cretac.)	Type-1 dolomite: fine, nonplanar-a and non-ferroan crystalline.	50-51.67 (51.00)	moderetaly ordered	This study
		Type-2 dolomite: very fine, nonplanar-a, nonferroan replacive crystalline	52.33-60.00 (53.65)	disordered	
		Type-3 dolomite: fine to medium, nonplanar-a, nonferroan crystalline and associated with quartz grains.	51.00-53.67 (53.76)	moderately ordered	
		Type-4 dolomite: fine to medium, planar-s and nonferroan crystalline.	50.33-54.67 (52.59)	well ordered	
		Type-5 dolomite: very coarse, planar-s, nonferroan and replacive saddle crystalline.	52.33-55.25 (53.36)	well ordered	
Egypt	El Heiz Fm. (M. Cretac.).	Medium, idiotopic and ferroan dolomite crystalline.	51-57.9	well ordered.	Holail *et al*, 1988
	El Hefhuf Fm. (U. Cretac.).	Mediun to coarse, idiotopic to hypidiotopic and nonferroan dolomite crystalline	51-52.5	well ordered.	

Table 7.2 XRD data for the Ain Tobi dolomites in NW Libya

Sample No.	Dolomite type-	Mole% CaCO$_3$	Order degree
S2-4	**Type-1**	51.0	0.61
S2-6		51. 7	0.62
S2-7A		51.7	0.66
S2-8A		51.7	0.69
S2-13		51.0	0.68
S8-16		50.3	0.73
S8-17		50.3	0.75
S8-18		50.3	0.75
S8-20		51.7	0.79
S9-22C		51.7	0.69
S9-23A		50.3	0.66
S9-23B		51.3	0.78
S9-25B		50.3	0.74
S9-26		51.0	0.66
S9-28		50.0	0.62
S9-30		50.3	0.67
S9-36		51.7	0.64
S9-37		51.7	0.76
Average		*51.0*	*0.70*
S1-4	**Type-2**	53.0	0.73
S1-8		53.0	0.70
S1-10		53.7	0.61
S1-12		53.7	0.62
S1-13		54.3	0.70
S2-2A		56.0	0.60
S2-2B		53.7	0.67
S2-9		52.3	0.60
S2-11B		52.3	0.73
S7-16		53.0	0.67
S7-18		53.0	0.67
S7-20		53.0	0.70
S7-22		53.0	0.59
S7-24		53.0	0.65
S7-26		53.0	0.60
S8-5		52.3	0.78
S8-13		52.3	0.57
S8-14		56.0	0.73
S8-15		60.0	0.73
S11-1		52.3	0.71
Average		*53.7*	*0.67*
S1-2	**Type-3**	53.7	0.62
S2-1		54.7	0.58
S2-2		58.0	0.55
S4-A		52.3	0.77
S4-C		51.7	0.64
S4-1		53.7	0.66
S4-19A		52.3	0.66
S7-1		53.0	0.60

Table 7.2 cont.

Sample No.	Dolomite type-	Mole% CaCO$_3$	Order degree
S7-4		52.3	0.78
S8-1		52.7	0.58
S8-11		53.7	0.66
S9-4B		51.0	0.71
S9-8		51.7	0.60
S9-6		52.6	0.64
S9-9		51.7	0.73
S9-20		52.3	0.75
Average		*53.8*	*0.64*
S1-0	__Type-4__	53.7	0.86
S1-1		54.7	0.78
S1-5		52.3	0.82
S1-15		52.3	0.86
S2-11		51.0	0.90
S4-3		52.3	0.75
S4-4		53.0	0.77
S4-5		53.0.	0.83
S4-9		53.0	0.69
S4-11		53.0	0.74
S4-12		52.3	0.72
S4-20		51.7	0.73
S7-6		53.0	0.71
S7-8		53.0	0.68
S7-12		53.0	0.72
S7-14		53.7	0.80
S9-11		50.3	0.98
S9-27		52.3	0.85
S9-29		54.7	0.82
S9-32		51.0	0.72
S9-34		51.0	0.74
Average		*52.6*	*0.78*
S3-1	__Type-5__	53.7	0.78
S3-2		53.7	0.75
S3-3		52.3	0.75
S3-4		53.7	1.05
S4-6		53.0	0.77
S4-7		52.3	0.74
S4-16		53.0	0.90
S4-18		53.0	0.82
S7-10		53.7	0.82
S8-7		55.3	0.83
Average		*53.4*	*0.82*

7.3.3. Major elements (Microprobe analysis)

An electron microprobe (n=300) JEOL JXA-8600s (see Appendix 3 for details of the method and precision used for microprobe analysis) was performed on polished and carbon coated thin-sections to analyse and compare the chemical composition of the different dolomite textures. It is worth noting that the total is generally low (Table 7.3) in the dolomite crystals. This is probably because of the following:

1). Differences in sections polishing between standard and specimen.

2). The size of dolomite crystals is smaller than the beam diameter used in the analysis (15µm) specially dolomites Type-1 and Type-2.

3). Possibility of interstitial clays and/or other alumina-silicates specially in dolomite Type-3.

The homogeneous orange luminescent dolomite Type-1 is nonstoichiometric and contains on average 53.40 mole % $CaCO_3$ and 41.36 mole % $MgCO_3$ (Table 7.3) with a range of 50.95 - 55.05 mole % $CaCO_3$ and 39.41 - 43.55 mole % $MgCO_3$. This percentage is higher than that determined by XRD (average 51 mole % $CaCO_3$). Notably there are slight compositional differences between the zones surrounding dissolved cores and rims of the crystals of this type; usually rims tend to be less calcian (average 52.12) than cores (average 54.68, Table 7.3). Dolomite Type-1 is generally iron-poor (mole % $FeCO_3$, average 0.35). Mole % $FeCO_3$ is slightly lower at cores (average 0.17) than it is at rims (average 0.52). This type of dolomite has low mole % $MnCO_3$ and $SrCO_3$ (average 0.021 and 0.041 respectively) and no obvious difference between cores and rims.

Dolomite Type-2 is generally calcian-rich, with a range of 51.71 - 54.54 mole % $CaCO_3$ (average 53.41 mole % $CaCO_3$) the same as determined by XRD. Notably the

dolomite replacing concentric layers of ooids which show bright yellow luminescence pattern are more calcian than dolomite replaced the rest of the same ooid which show orange luminescent. The same holds for $MgCO_3$ (average 39.83). Type-2 dolomite is generally iron-poor (mole % $FeCO_3$ average is 0.30), but relatively more than Type-4 and less than Type-3 and Type-5 dolomites. It generally has high mole% $MnCO_3$ compared to other types of Ain Tobi (average being 0.11). This may be the reason for the bright luminescent appearances (will be discussed later). Mole % $SrCO_3$ is low within Type-2 dolomite (average is 0.04).

Type-3 dolomite is less calcian than Type-1 dolomite as determined by microprobe. The crystals of this type contain, on average 50 mole % $CaCO_3$, with a range of 44 - 55 mole % $CaCO_3$ (Table 7.3). Clearly the crystals' interior and exterior of this type are different in terms of composition. Mole % $CaCO_3$ decreases outward. Cores are calcian having an average of 54.6 mole % $CaCO_3$, whereas rims are nearly stoichiometric (average 45.3 mole % $CaCO_3$). Mole % $MgCO_3$ is nearly same as Type-1 dolomite (average 40.94). Type-3 dolomite is relatively enriched in Fe as determined by microprobe compared with other dolomite types of the Ain Tobi. Mole % $FeCO_3$ ranges from 0.23 to 3.53 with an average 1.45, higher than dolomite typically formed from normal marine to evaporitic marine environments (Ruppel and Cander, 1988). Rims of crystals of Type-3 dolomite have high mole % $FeCO_3$ (average 2.4), in contrast to cores of the same crystals have relatively low mole % $FeCO_3$ (average 0.48). Mole % $MnCO_3$ is low within Type-3 dolomite crystalline (average 0.08), but interior of crystals have slightly lower mole % $MnCO_3$ than rims. This dolomite type is depleted in strontium (mole% $SrCO_3$ 0.04).

Type-4 dolomite is calcian-rich (Mole % $CaCO_3$ average 53.56), slightly higher than XRD results (52.59). Clean rims are less calcian (average 52.3) than that cloudy cores
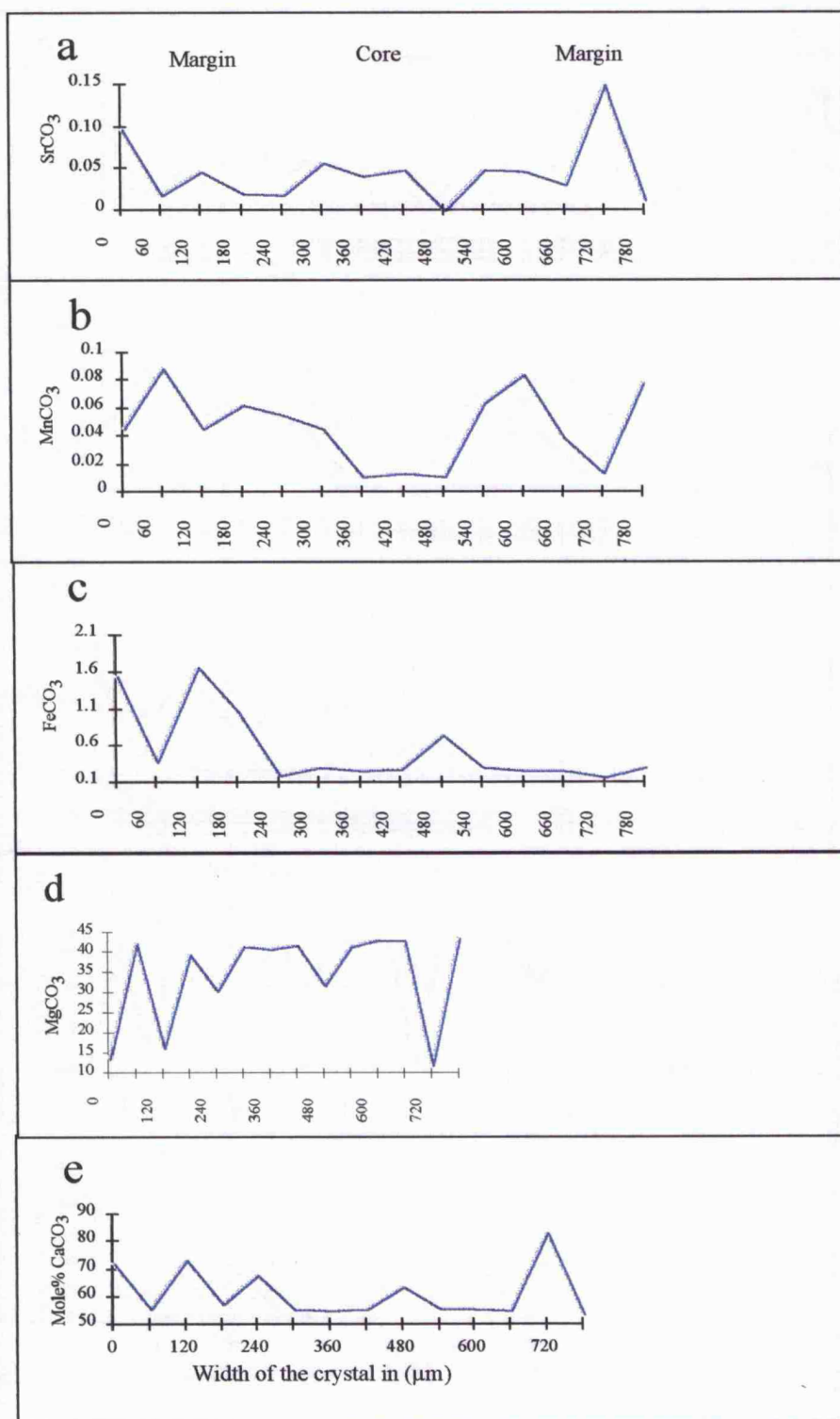
Fig. 7.11. Microprobe data for single saddle dolomite crystal (Sample S3-3).

(average 55). Type-4 dolomite has nearly the same mole % $MgCO_3$ as Type-1 and Type-3 dolomites (average 40.55). It is the poorest in terms of iron content among the Ain Tobi dolomites. Mole % $FeCO_3$ is 0.03 in average and tends to be slightly higher at rims (average 0.04) than at cores (average 0.02, Table 7.3). Type-4 dolomite is generally depleted in $MnCO_3$ (average 0.05) and no obvious difference between cores and rims (average 0.07 and 0.02 respectively). It has low Mole % $SrCO_3$ (average 0.04).

Type-5 dolomite (saddle dolomite) is characterized by calcian-rich (mole % $CaCO_3$ average is 61.52). The clean rims are more calcian than cloudy cores (Fig. 7.11e). Mole % $MgCO_3$ is low within crystals of Type-5 dolomite compared to other types (average being 34.3), and the maximum was at centre of crystals (Fig. 7.11d). Type-5 dolomite is generally iron-poor, mainly less than 1% weight (mole % $FeCO_3$ average 0.55), but cloudy cores are relatively iron-rich compared to clean rims (Fig. 7.11c). This coarse saddle dolomite is generally depleted in $MnCO_3$ (average 0.05), but it is slightly lower at cloudy cores than clean rims (Fig. 7.11b). Type-5 dolomite has low mole % $SrCO_3$ (average 0.05, Table 7.3) and mainly no difference between rims and cores (Fig 7.11a).

Dedolomite crystals show complex zonation under cathodoluminescence. Dull appearances zones are selectively replaced by calcite, whereas, bright appearance zones are composed of pure dolomite as indicated by probe analysis. Dully luminescent zones are calcian-rich, whereas bright zones are less calcian. Notably mole % $CaCO_3$ within these crystals decreases outward. Generally, dedolomitized crystals are calcian-rich (average 57.53 mole % $CaCO_3$). Mole % $MgCO_3$ is low compared to all types of dolomite (average 34.53) but similar to Type-5 dolomite. The crystals are Fe and Mn-poor; they contain, on average 0.03 mole % $FeCO_3$ and 0.04 mole % $MnCO_3$, with a

range of 0.01-0.07 mole % $FeCO_3$ and 0.01-0.05 mole % $MnCO_3$. Generally, dedolomitization is depleted in Sr (Table 7.3).

Coarse replacive calcite (S4-12B) of the Ain Tobi is generally Mn and Sr-poor and is relatively Fe-rich compared to dolomite.

Table 7.3. Microprobe data (Mole%) for the Ain Tobi dolomite types (R: rim; C: core; xl: crystal):

Sample no.	Type-	Core/Rim	CaCO$_3$	MgCO$_3$	FeCO$_3$	MnCO$_3$	SrCO$_3$	Fe/Mn
S4-2	Type-1	R	50.95	40.89	0.79	0.016	0.048	49.21
		C	54.31	43.55	0.132	0.01	0.051	13.73
		R	53.29	39.41	0.247	0.011	0.03	21.95
		C	55.05	41.57	0.211	0.045	0.033	4.7
		Average	*53.4*	*41.36*	*0.345*	*0.021*	*0.041*	*22.4*
S2-2	Type-2	R of ooid (1)	53.82	43.78	0.281	0.134	0.063	2.11
		between conc.layers (2)	53.54	42.97	0.235	0.007	0.031	36.66
		concentric layer (3)	54.54	43.82	0.274	0.122	0.044	2.28
		between conc.layer &C.(4)	52.71	42.82	0.224	0.1	0.023	2.25
		dol. lining intra. pore (5)	54.25	43.7	0.321	0.084	0	3.84
		dol. within intra. pore (6)	51.71	42.07	0.377	0.063	0.044	6.03
		ooid rim (1)	53.61	36.38	0.335	0.076	0.021	4.44
		ooid rim (2)	53.37	35.73	0.626	0.228	0.039	2.76
		concentric layer (3)	52.61	35.59	0.234	0.113	0.09	2.08
		core of ooid (4)	53.65	36.85	0.376	0.154	0.04	2.46
		concentric layer (5)	53.02	36.62	0.185	0.13	0.061	1.44
		rim of ooid (6)	54.14	37.59	0.142	0.092	0.03	1.55
		Average	*53.41*	*39.83*	*0.301*	*0.109*	*0.041*	*5.66*
S1-2	**Type-3**	C	54.75	45.49	0.229	0.063	0.046	3.7
		R	47.58	40.05	2.608	0.107	0.003	24.58
		C	55.21	44.52	0.411	0.047	0.05	8.82
		R	44.73	36.19	1.145	0.023	0.009	50.21
		C	53.91	43.28	0.787	0.089	0.087	8.92
		R	43.57	36.08	3.532	0.126	0.038	28.27
		Average	*50*	*40.94*	*1.452*	*0.076*	*0.039*	*20.75*
S9-27	Type-4	R	55.98	42	0.053	0.026	0.024	2.07
		C	55.88	41.94	0.003	0.057	0.033	0.057
		R	50.66	39.74	0.042	0.034	0.038	1.24
		C	53.93	40.48	0.024	0.099	0.048	0.247
		R	50.18	38.51	0.024	0.013	0.016	1.88
		C	54.75	40.64	0.019	0.039	0.05	0.502
		Average	*53.56*	*40.55*	*0.028*	*0.045*	*0.035*	*0.99*
S3-4	Type-5	outer R of xl. (1)	72.2	13.66	1.55	0.045	0.098	34.4
		R of same xl. (2)	55.43	42.17	0.371	0.089	0.019	4.2
		R of same xl. (3)	73.09	16.46	1.67	0.045	0.047	37.09
		before cleavage plane (4)	57.27	39.45	1.06	0.062	0.02	17.42
		cleavage plane (5)	68.07	30.31	0.198	0.055	0.0185	3.63
		after cleavage plane (6)	55.64	41.56	0.3	0.045	0.057	6.78
		C of same xl. (7)	54.73	40.87	0.271	0.11	0.04	2.48
		C of same xl. (8)	55.29	41.9	0.292	0.013	0.048	22.72
		Cleavage plane (9)	63.63	31.73	0.745	0.011	0.001	66.28
		after C of same xl (10)	55.32	41.36	0.313	0.063	0.048	4.99
		away from C. towards R.(11)	55.75	43.13	0.263	0.084	0.046	3.15
		R of same xl (12)	55.16	43.05	0.263	0.0389	0.031	6.82
		cleavage plane (13)	83.23	11.88	0.173	0.013	0.151	13.43
		R of xl close to pore (1)	56.48	42.67	0.189	0.062	0.043	3.09
		Average	*61.52*	*34.3*	*0.547*	*0.053*	*0.048*	*16.18*
S10-2	**Dedolo.**	R of xl (1)	57.08	35.46	0.015	0.06	0.031	0.244

Sample no.	Type-	Core/Rim	CaCO₃	MgCO₃	FeCO₃	MnCO₃	SrCO₃	Fe/Mn
		R of xl (2)	58.45	33.87	0.016	0.032	0.085	0.502
		R of xl (3)	57.74	34.23	0.021	0.07	0.017	0.304
		C of same xl (4)	57.87	34.17	0.011	0.015	0.058	0.781
		C of same xl (5)	57.55	33.68	0.065	0.005	0.026	13.39
		C of same xl (6)	57.55	34.96	0.05	0.058	0.038	0.865
		R of same xl (7)	56.5	35.35	0.037	0.021	0.0328	1.78
		Average	*57.53*	*34.53*	*0.031*	*0.037*	*0.041*	*2.55*
S4-12B	Calcite	Replacive calc. xl	100.16	0.352	0.023	0.047	0.006	0.485
		coarse calc. xl (1)	100.2	0.639	0.01	0.049	0.024	0.201
		coarse calc. xl (2)	100.3	0.202	0.048	0.047	0.011	1.04
		coarse calc. xl (3)	100.5	0.163	0.023	0.047	0.046	0.485
		coarse calc. xl (4)	100.6	0.121	0.055	0.01	0.047	5.69
		calcite replaced dol. xl. (1)	83.3	15.01	0.277	0.076	0.019	3.68
		C. of dol xl lined by calc (2)	55.34	36.73	0.455	0.071	0.004	6.44
		R of same xl (3)	55.97	36.27	0.476	0.015	0.083	32.92
		Average	*87.05*	*11.19*	*0.171*	*0.045*	*0.03*	*6.37*
S6-16	Cement	Coarse. equ. calc..cemt. (1)	99.79	0.35	0.106	0.016	0.037	6.63
		Coarse. equ. calc..cemt.(2)	100.02	0.341	0.171	0.06	0.073	2.88
		Fine equ. calc. cemt. (3)	97.51	0.275	0.082	0.011	0.006	7.32
		Fine equ. calc. cemt.(4)	93.62	0.611	0.39	0.047	0.016	8.38
		Fine equ. calc. cemt.(1)	97.29	0.37	0.168	0.016	0.064	10.44
		Coarse. equ. calc..cemt.(2)	98.7	0.409	0.184	0.044.	0.031	4.24
		Coarse. equ. calc..cemt.(3)	98.07	0.491	0.223	0.063	0.003	3.55
		Coarse. equ. calc..cemt.(4)	98.92	0.132	0.01	0.016	0.016	0.6
		Coarse. equ. calc..cemt.(5)	97.98	0.366	0.134	0.049	0.02	2.78
		Fine equ. calc. cemt (6)	96.29	0.332	0.5	0.03	0.011	16.39
		Average	*97.82*	*0.368*	*0.197*	*0.035*	*0.0277*	*6.32*

7.3.4. Trace elements (ICP)

Trace elements concentration within the different dolomite types of the Ain Tobi

Dolostone Member are determined by Inductively Coupled Plasma Mass Spectrometry

model 8200 (See Appendix 2 for details of the method and precision used for ICP

analysis).

Strontium: Strontium has received more attention in recent years than any other trace

element in order to use it in the interpretation of the dolomite mechanism and diagenetic

environment (Land, 1980, 1985; M'Rabet, 1981; Veizer, 1983 and others).

The strontium concentration of the Ain Tobi dolomite types is generally low with

some differences (discussed below) between the very fine (assumed early) and very

coarse fabric (assumed late) dolomites (Table 7.4a). Table 7.4b reports trace element

concentrations in the Ain Tobi dolomite types (this study) and in other dolomites

reported in the literature.

The Sr concentration of Type-1 dolomite of the Ain Tobi Dolostone Member ranges

from 94 ppm to 138 ppm, with an average of 110 ppm. The average Sr concentration in

Type-1 in the western part of the study area is (111 ppm), slightly higher than it is in the

eastern area (108 ppm). Type-2 which replaced packstones and grainstones has the

highest Sr concentration in the Ain Tobi dolomite types. Sr concentration in this type

ranges from 91 ppm to 245 ppm with an average of 123 ppm. Type-2 has higher Sr

concentration in the western part (average 126 ppm) than in the eastern part (average

118 ppm). Type-3 has quite low Sr concentration compared to Type-1 dolomite. Sr

concentration ranges from 55 ppm to 110 ppm, with an average of 87 ppm. The average

Sr concentration in the western part of the study area is 80 ppm and in the eastern part is

70 ppm. Type-4 dolomite has Sr contents range from 63 ppm to 106 ppm with an

Table 7.4a. Trace element concentrations of dolomit types of the Ain Tobi Dolostone Member in NW

Libya as determined by ICP.

Sample No.	Dolomite Type-	Fe (ppm)	Mn (ppm)	Na (ppm)	Sr (ppm)
S2-4	**Type-1**	4135	433	390	138
S2-6		1503	116	270	94
S2-7A		1203	126	290	96
S2-8A		1261	183	300	103
S2-13		1086	174	290	108
S8-16		4226	274	466	96
S8-17		3545	415	460	98
S8-18		5243	179	550	103
S8-20		20871	362	BDL	106
S9-22C		5797	296	BDL	136
S9-23A		7620	326	470	119
S9-23B		3875	320	BDL	115
S9-25B		4698	380	953	125
S9-26		12012	567	207	117
S9-28		293	35	1375	106
S9-30		204	66	BDL	101
S9-36		4631	50	157	110
S9-37		427	32	34	114
Average		*4591*	*241*	*444*	*110*
S1-4	**Type-2**	1745	295	270	105
S1-8		4967	279	BDL	105
S1-10		2169	200	390	102
S1-12		8126	333	34	91
S1-13		6671	336	530	133
S2-2A		2399	163	9	96
S2-2B		4460	790	390	100
S2-9		4195	167	525	245
S2-11B		1129	187	280	101
S7-16		3483	302	60	100
S7-18		3349	342	330	109
S7-20		10774	169	254	118
S7-22		4869	161	264	174
S7-24		9310	367	20	124
S7-26		3553	366	16	131
S8-5		3473	187	BDL	108
S8-13		4555	204	454	194
S8-14		3698	231	32	110
S8-15		3820	282	94	109
S11-1		707	54	619	106
Average		*4373*	*271*	*254*	*123*
S1-2	**Type-3**	3629	325	209	81
S2-1		11207	766	BDL	108
S2-2		3957	687	270	110
S4-A		3319	99	370	61
S4-C		5568	104	340	73
S4-1		2989	109	420	68
S4-19A		3828	122	560	69
S7-1		4080	545	20	84

Table 7.4a cont.

Sample No.	Dolomite Type-	Fe (ppm)	Mn (ppm)	Na (ppm)	Sr (ppm)
S7-4		9587	572	574	80
S8-1		24223	1749	777	92
S8-11		6572	274	265	93
S9-4B		4935	976	10	63
S9-8		8228	741	120	55
S9-6		4020	981	85	107
S9-9		10738	1433	BDL	68
S9-20		5735	254	237	80
Average		*6913*	*606*	*295*	*87*
S1-0	**Type-4**	8296	352	334	106
S1-1		13194	349	192	102
S1-5		5458	259	554	103
S1-15		5859	255	270	104
S2-11		1360	188	190	106
S4-3		618	98	310	76
S4-4		2924	145	BDL	63
S4-5		1695	101	290	66
S4-9		4974	143	380	81
S4-11		8702	138	400	82
S4-12		2852	102	340	81
S4-20		2697	80	74	88
S7-6		6492	435	330	84
S7-8		7483	474	100	88
S7-12		4160	197	340	86
S7-14		4284	217	10	76
S9-11		2508	198	258	70
S9-27		181	33	25	70
S9-29		223	59	BDL	99
S9-32		186	77	320	97
S9-34		565	149	BDL	93
Average		*4034*	*193*	*262*	*87*
S3-1	**Type-5**	2586	473	820	93
S3-2		1426	293	BDL	80
S3-3		1165	227	95	81
S3-4		4224	357	32	77
S4-6		474	72	460	67
S4-7		1280	79	360	75
S4-16		914	60	350	92
S4-18		1625	64	330	81
S7-10		4636	341	30	83
S8-7		3287	242	1222	85
Average		*2161.7*	*220.8*	*411*	*81.4*

average of 87 ppm lower than Type-1 and Type-2 but similar to Type-3. This type has a

lower Sr concentration in the western part of Jabal Nafusah escarpment (average 85

ppm) than in the eastern part (average 88 ppm). Saddle dolomite (Type-5) has a very low

Sr concentration compared to other types (lowest among the Ain Tobi dolomites) and

ranges from 67 ppm to 93 ppm having an average of 81 ppm. The above results reflect

the fact that Sr content decreases with increasing crystal size (M'Rabet, 1981) (Fig.

7.12a). Sr contents in Type-5 indicate averages of 84 and 81 ppm in western and eastern

parts of the study area respectively.

Notably the Sr concentration in the Ain Tobi dolomites is relatively higher in western

and central Jabal Nafusah escarpment than it is in the eastern part of the escarpment.

Sodium: Sodium concentration in diagenetic phases are used in order to obtain more

information about the salinity of the diagentic fluids during precipitation and accordingly

the mechanism(s) responsible for dolomitization (Land, 1980; M'Rabet, 1981;

Humphrey, 1988; Shukla; 1988).

Sodium in the Ain Tobi dolostones is generally low. Na concentration is relatively

high in the Type-1 dolomite compared to the other dolomite types of the Ain Tobi.

Sodium concentration in this type ranges from 34 to 1375 ppm with an average of 444

ppm (Table 7.4a). In the western area Na concentration is considerably higher (519 ppm)

than it is in the eastern area (206 ppm). Type-2 dolomite has a relatively low Na

concentration compared to Types-1, and 5. Its concentration ranges from 9 to 619 ppm,

the average being 254 ppm. Na concentration in this type in the western part is 214 ppm

average and is 300 ppm in the eastern area. Na concentration within Type-3 dolomite

ranges from 10-777 ppm with an average being 295 ppm. There is slight difference in Na

concentration within Type-3 in western part of the study area (261 ppm) and in the

eastern part (380 ppm). Na concentration in Type-4 dolomite is low. It ranges from 10

ppm to 554 ppm with an average of 262 ppm, but it is slightly lower in the western part

(198 ppm) than in the eastern part of the study area (303 ppm). The Na concentration in

Type-5 dolomite is 411 ppm average and ranges from 30 to 1222 ppm. This is relatively

high sodium concentration within the Ain Tobi dolostones as compared to types -2, -3,

and -4, but similar to dolomite Type-1. In the western part of the escarpment Na

concentration in Type-5 is higher (626 ppm) than it is at eastern part (average 350 ppm).

Na concentration seems to be relatively higher in the saddle dolomite (Type-5) than it

does in the other types except Type-1, and has no correlation with crystal size (Fig.

7.12b). Sodium content in Ain Tobi dolomites becomes higher towards the south-west

part and in the eastern end of the study area. Na values in the western part of Jabal

Nafusah escarpment are 395, 489, 181 and 309 ppm in sections #9, #8, #7 and #1

respectively. In the eastern part of the escarpment Na concentrations are 291, 316 and

357 ppm in sections #2, #3 and #4 respectively.

Manganese: Mn contents in Type-1 dolomite of the Ain Tobi dolostones are low,

ranging from 32 to 567 ppm (Table 7.4a), having an average of 241 ppm. Type-2 ranges

from 54 to 790 ppm, having an average of 271 ppm. Type-3 dolomite is widely variable

and is relatively Mn-rich compared to other dolomite types. Mn concentration in Type-3

ranges from 99 to 1749 ppm with an average of 606 ppm. The Mn concentration in

Type-4 dolomite is low, ranging from 33 to 474 ppm with an average of 193 ppm. It is

Mn-poor compared to Type-3 dolomite. Manganese content in Type-5 dolomite is

relatively low compared to Type-3, but similar to Type-1. It ranges from 60 to 473 ppm,

with an average of 221 ppm.

Table 7.4b Correlation of trace elements concentrations in the Ain Tobi dolomites (this study)

and various other dolomites reported in the literature:

Locality & reference(s)	Formation (age) & dolomite type(s)	Sr (ppm)	Na (ppm)	Mn (ppm)	Fe (ppm)
Egypt	El Heiz Formation				-
Holail *et al* (1988)	(Cenomanian dolom.)	120	650	1900	
	El Hefhuf Formation				-
	(Campanian dolom.)	103	425	720	
U.S.A.	Smackover Fm.				
Moore *et al* (1988)	(U. Jurassic)				
	Evaporatic dolomite	261-490	512-990	89-172	416-1200
	Early coarse dol.	42-69	117-185	42-137	51-114
	Early fine dolomite	40-89	129-212	59-710	58-2663
	Late zoned replacive				
	dolomite	53-83	112-192	110	689
	Late saddle dolomite	93-139	256-399	418-1571	3631-36294
Tunisia	Central Tunisia				
M'Rabet (1981)	(L. Cretaceous)				
	Dolomite associated				
	with quartz	30-65	390-1370		11600-68100
	Dolomite associated				
	with evaporite	56-175	440-1940		3000-11900
	Dolomite associated				
	with palae-karst	50-90	440-950		2000-22600
	Dolomite associted				
	with lacustrain	60-150	380-980		600-10800
U.S.A.	Subsurface cores				
Zenger & Dunham	(Siluro-Devonian)				
(1988)	Saddle dolomite	28	759	117	250
	Medium to coarse dol.	24	884	75	134
	Fine dolomite	38	832	74	154
	Coarse to fine dol.	34	1165	52	593
	Medium to coarse				
	dolomite	29	1053	73	314
Tunisia	Central Tunisia				
Soussi & M'Rabet	(Jurassic)				
(1994)	Burial dolomite	20-50	65-2025	38-382	255-8290
Libya (This study)	Ain Tobi Member				
	(M. Cretaceous)				
	Dolomite Type-1	110	444	241	4591
	Dolomite Type-2	122	255	312	4664
	Dolomite Type-3	77	307	592	6961
	Dolomite Type-4	87	262	193	4034
	Dolomite Type-5	81	411	221	2162

The manganese concentration in the Ain Tobi Dolostone Member is higher in the western part of Jabal Nafusah escarpment and decreases towards north-east. Mn average concentration in dolostones from western escarpment is 473 ppm, 440 ppm, 345 ppm and 298 ppm at sections #9, #8, #7 and #1 respectively. Mn average concentration in the eastern area of the Jabal Nafusah escarpment is 332 ppm, 338 ppm and 101 ppm at sections #2, #3 and #4 respectively.

Mn concentration in zoned dolomite (dedolomitization) samples is widely variable and ranges from 32 to 2064 ppm with an average of 505 ppm. Dedolomitized samples have the highest Mn concentration in the Ain Tobi dolostones. Stratigraphically, Mn concentration decreases from bottom to top (Figs. 7.14 through 7.19). In space it decreases from south-west to north-east.

Iron: Concentration of Fe may provides information on the oxidation-reduction state of the diagenetic environment. The low concentrations probably represent precipitation from oxidizing diagenetic water (Humphery, 1988 and many others). Iron concentration is widely variable and ranges from 204 to 20871 ppm in Type-1 dolomite, with an average of 4591 ppm. Type-2 dolomite has Fe concentration ranges from 707 to 10774 ppm, the average being 4373 ppm. Type-3 dolomite has high Fe concentration compared to other types. It ranges from 2989 to 24223 ppm, having an average of 6913 ppm. Fe content in Type-4 dolomite is low compared to other types (Types-1, -2 and -3), and it ranges from 181 to 13194 ppm, having an average of 4034 ppm. Fe concentration in the very coarse saddle dolomite (Type-5) is the lowest compared to other types of Ain Tobi dolomites, and it ranges from 474 to 4636 ppm, with an average of 2162 ppm.

Fe concentration in western part of Jabal Nafusah is 4971 ppm, 9034 ppm, 5851 ppm and 6111 ppm at sections #9, #8, #7 and #1 respectively and it is 3158 ppm, 2350 ppm

and 2972 ppm at sections #2, #3 and #4 located in the eastern part of the Nafusah

escarpment. It is obvious that Fe concentration in the Ain Tobi dolostones is higher in

the western part of the study area. No correlation between Fe and crystal size (Fig.

7.12c).
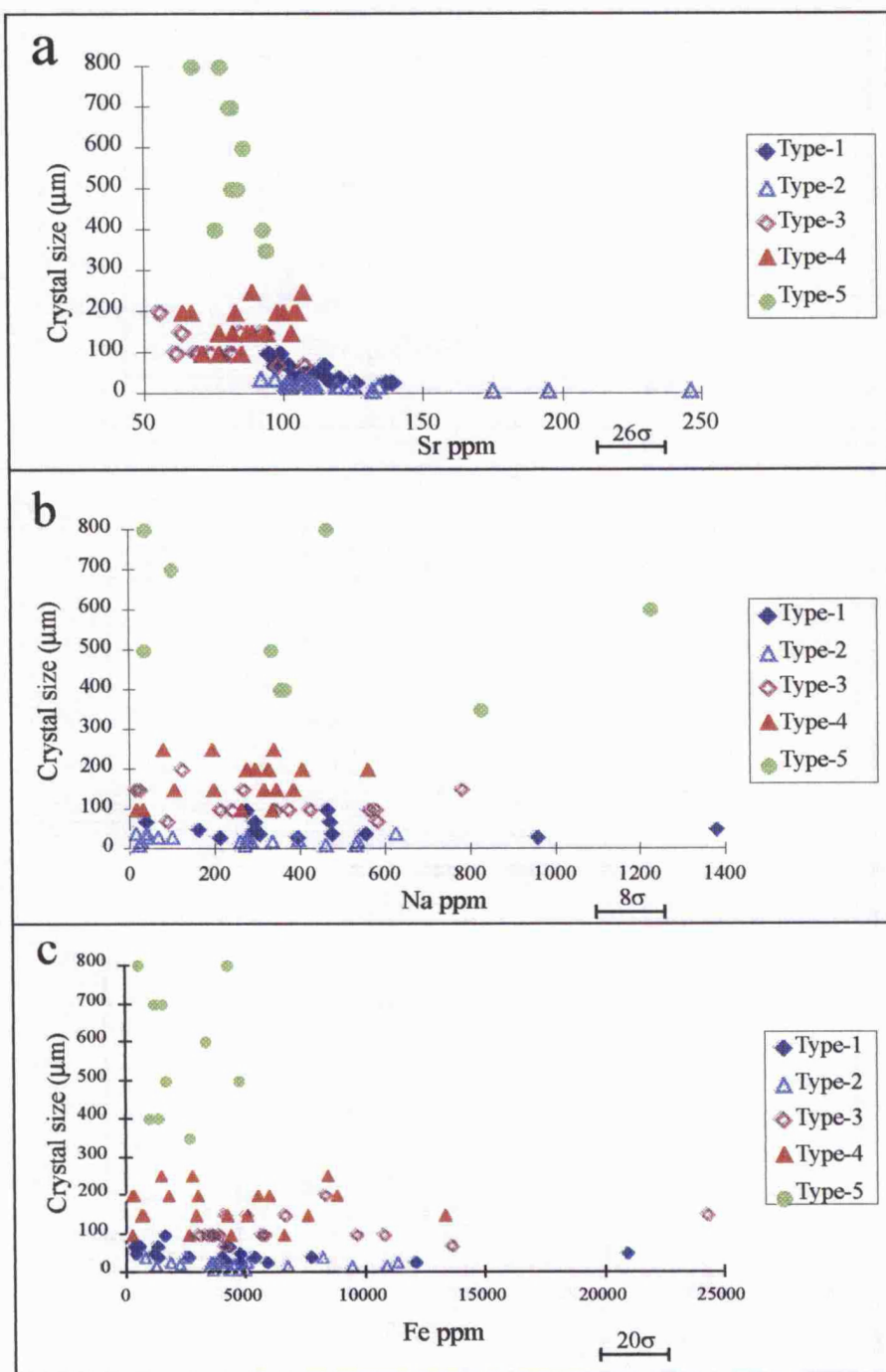
Fig. 7.12. Cross-plot showing relationship between crystal size and trace element concentrations of the Ain Tobi dolomite types. 2σ in (a) = 2.02ppm Sr, therefore scale bar represents 26σ. In (b) 2σ = 44ppm Na, so scale bar represents 8σ similarly 2σ in (c) = 330ppm Fe, therefore scale bar represents 20σ.

7.3.5. Stable isotopes

Samples for stable isotopic analysis from the Ain Tobi Dolostone Member include different dolomite whole-rock samples, calcite whole-rock samples, dedolomite samples and mixed-mineralogy dolomite-calcite whole-rock samples. Table 7.5 and Fig. 7.13 report stable isotope data for the samples from the Ain Tobi dolomites. All isotopic measurements reported here are in per mil PDB values.

Average $\delta^{18}O$ and $\delta^{13}C$ of fine crystalline dolomite Type-1 are -2.08 and +1.61‰ respectively. $\delta^{18}O$ varies from -2.73 to -1.33‰ and $\delta^{13}C$ from +0.22 to +4.84‰ (Fig. 7.13).

Type-2 is similar to Type-1 dolomite in terms of $\delta^{18}O$, but has depleted values compared to Type-3 dolomites (Table 7.5). Average $\delta^{18}O$ of this dolomite is -2.06‰ and ranges from -2.99 to -1.12‰. $\delta^{13}C$ values of Type-2 dolomite are similar to Type-1 dolomite, but it is $\delta^{13}C$-enriched compared to Type-3 dolomite. $\delta^{13}C$ values range from +0.05 to +3.25‰ (average +1.55‰).

Average $\delta^{18}O$ of dolomite Type-3 is relatively heavy compared to other types having an average of -1.67‰. $\delta^{18}O$ values range from -2.11 to -1.14‰, less variable than they are in Type-1 and Type-2 dolomites. Carbon isotope ratios have a scattered range within the Type-3 dolomite (Fig. 7.13). $\delta^{13}C$ values varies from -3.1 to +0.64‰ more variable than they are in other Ain Tobi dolomites. Two samples (S8-11 and S9-17) of Type-3 dolomite exhibit positive $\delta^{13}C$ values, 0.38 and 0.64‰ respectively.

Dolomite Type-4 is slightly depleted in $\delta^{18}O$ compared to Type-1 and -3 dolomites and enriched compared to Type-5. The average $\delta^{18}O$ value is -2.34‰. $\delta^{18}O$ varies from -2.95 to -1.32‰. $\delta^{13}C$ ranges from +0.29 to + 2.86 having an average of +1.312‰ (Fig. 7.13).
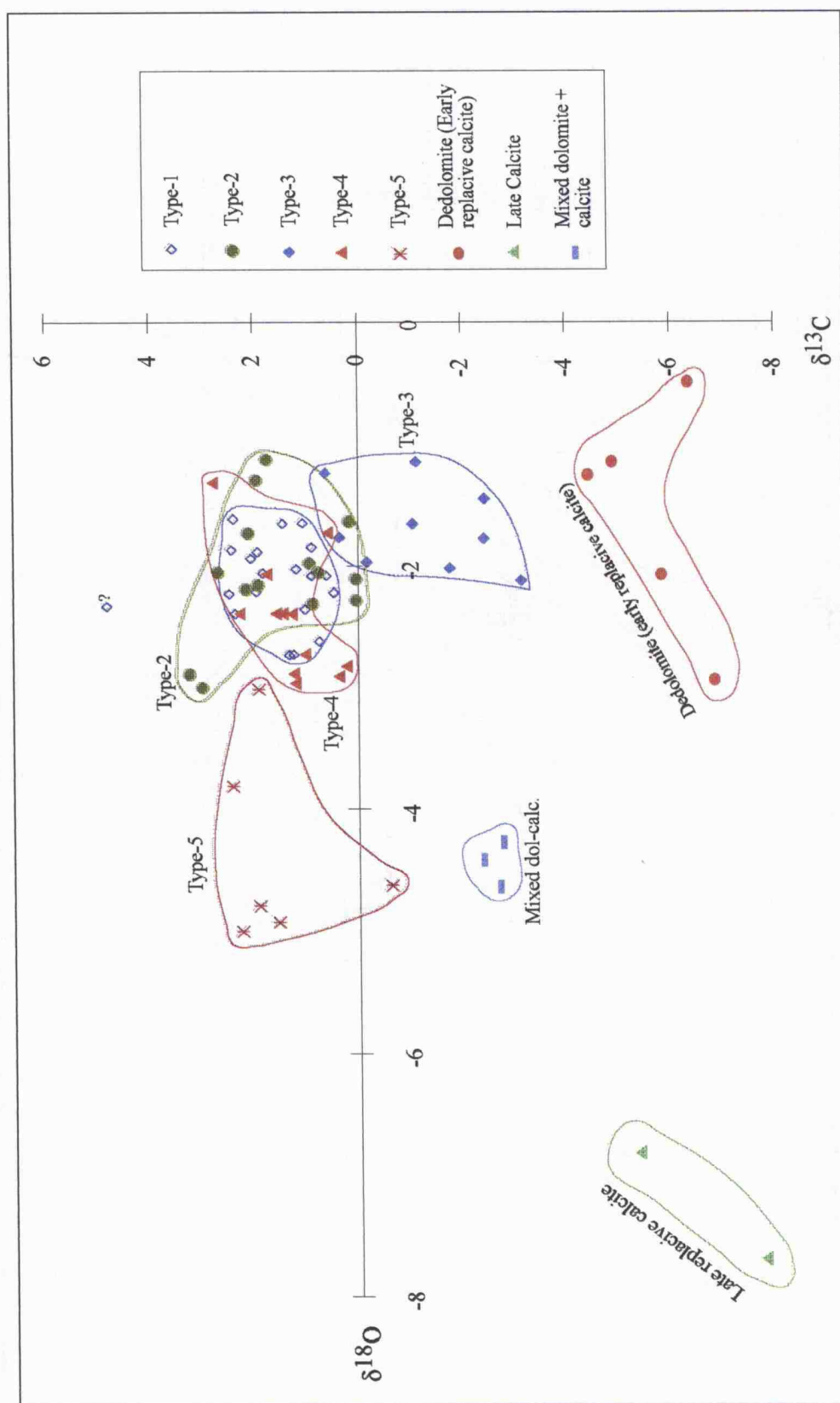
Fig. 7.13 Plots of oxygen and carbon isotope compositions of the Ain Tobi dolostone types in NW Libya.

Dolomite Type-4 is depleted in $\delta^{13}C$ compared to Types-1, -2 and -5, but enriched comparing to Type-3.

Saddle dolomite (Type-5) is light or depleted in $\delta^{18}O$ compared to all other dolomite types of the Ain Tobi dolostones (Fig. 7.13). Average $\delta^{18}O$ value is -4.36‰. Six samples analysed, have $\delta^{18}O$ ranging from -5.00 to -3.00‰. $\delta^{13}C$ in Type-5 dolomite ranges from -0.58 to +2.41‰ (average +1.58‰), similar to dolomite Types-1 and -2. Only one sample (S3-4) has negative $\delta^{13}C$ value (-0.58‰).

Five dedolomitized whole-rock samples were analysed for $\delta^{18}O$ and $\delta^{13}C$. Average $\delta^{18}O$ value is -1.572‰ and ranges from -2.93 to -0.50‰. These values are heavier than Types-1, -2, -4 and -5 dolomites but similar to dolomites Type-3. $\delta^{18}O$ value is enriched compared to calcite and mixed dolomite-calcite samples. Dedolomitized samples have carbon isotope ratios ranging from -6.80 to -4.39‰ (Fig. 7.13) having an average of -5.62‰, slightly heavier than calcite samples and lighter than mixed dolomite-calcite. $\delta^{13}C$ value of the dedolomitized samples is very light compared to all dolomite types of the Ain Tobi dolostones.

Calcite filled geodes within the Ain Tobi sediments were analysed for oxygen and carbon isotopes. These calcite samples have very negative values of both oxygen and carbon isotopes compared to dolomite and dedolomite samples from the Ain Tobi. $\delta^{18}O$ varies from -7.69 to -6.81‰ (Fig. 7.13) with an average of -7.25‰. $\delta^{13}C$ ranges -5.30 to -7.72‰, average -6.51‰.

Mixed dolomite-calcite samples have $\delta^{18}O$ values range from -4.68 to -4.32‰ with an average of -4.49‰, heavier than calcite, but lighter than dolomite (except Type-5) and dedolomite. $\delta^{13}C$ values for mixed dolomite-calcite samples range from -2.73 to -2.34‰

having an average of -2.58‰. Carbon values are light compared to all dolomite types but are enriched compared to calcite and dedolomite.

Trace element and stable isotope plots against stratigraphy show that Sr contents are high in the lower part of the succession close to the unconformity surface and in the top of the sequence (e.g. Fig. 7-14). Carbon isotope values increase towards the top of each cycle (Fig. 7-14). These relationships are not the same in other locations. Sr and carbon isotope values increase towards the top of each cycle in Yifran area (section # 7, Fig. 7-16).

In the eastern part of the study area (east of the Wadi Ghan), the Ain Tobi dolomites are coarser in the upper part of the succession and finer in the lower part of the sequence (Figs. 7-18 and 7-19). In the western part of the study area (west of the Wadi Ghan), the Ain Tobi dolomites are coarser in the lower part of the sequence and finer in the upper part (Fig. 7-14 through Fig. 7-17).

Generally, the combination of stratigraphic and geochemical data (Fig. 7-14 through 7-19) does not show an obvious relationship.

Table 7.5: Stable isotope data for the Ain Tobi dolostone types in NW Libya

Dolomite type-	Sample No.	$\delta^{18}O$ (PDB)	$\delta^{13}C$ (PDB)
Type-1	S1-3	-1.632	1.068
	S1-14	-1.863	2.452
	S2-4	-2.342	1.041
	S2-7A	-1.842	0.911
	S2-8A	-1.918	2.102
	S2-12	-1.592	2.389
	S2-13	-2.048	1.85
	S3-5	-2.216	1.993
	S7-2	-1.33	0.219
	S7-11	-2.067	0.626
	S7-15	-2.37	2.377
	S7-19	-1.654	1.46
	S8-16	-2.597	0.787
	S8-17	-2.027	1.197
	S8-18	-1.879	1.899
	S9-11	-2.204	0.481
	S9-18	-2.086	0.913
	S9-23A	-2.71	1.259
	S9-23B	-2.225	2.508
	S9-30	-2.725	1.325
	S9-37	-2.315	4.843
	Average	*-2.078*	*1.605*
Type-2	S1-8	-2.06	0.753
	S1-10	-1.285	1.943
	S1-12	-1.121	1.776
	S2-2A	-2.278	0.047
	S2-11B	-1.735	2.091
	S2-10	-2.207	2.158
	S4-A	-2.876	3.253
	S4-C	-2.993	3.006
	S4-19A	-2.072	2.706
	S7-16	-2.177	1.928
	S7-22	-1.637	0.184
	S7-24	-2.118	0.056
	S8-14	-2.308	0.893
	S8-15	-1.981	0.926
	Average	*-2.061*	*1.551*
Type-3	S1-0	-1.96	-0.137
	S2-1	-1.778	-2.406
	S2-2	-1.443	-2.457
	S7-4	-1.632	-1.033
	S7-26	-2.002	-1.737
	S8-11	-1.756	0.38
	S9-4B	-1.141	-1.115
	S9-9	-2.106	-3.098
	S9-17	-1.231	0.641
	Average	*-1.672*	*-1.218*
Type-4	S1-1	-1.728	0.669
	S1-5	-2.382	1.573
	S1-7	-2.813	0.293
	S1-15	-2.046	1.845

Dolomite type-	Sample No.	$\delta^{18}O$ (PDB)	$\delta^{13}C$ (PDB)
	S4-2	-2.893	0.447
	S4-4	-2.706	1.109
	S4-5	-2.404	1.379
	S4-20	-2.873	0.296
	S7-10	-2.875	1.29
	S7-14	-2.38	1.65
	S9-27	-1.318	2.856
	S9-34	-2.945	1.292
	Average	*-2.335*	*1.312*
Type-5	S3-1	-3.802	2.41
	S3-4	-4.631	-0.583
	S4-7	-3.002	1.96
	S4-14	-4.922	1.547
	S4-16	-4.797	1.922
	S4-18	-4.997	2.228
	Average	*-4.359*	*1.581*
Dedolomite	S8-19	-2.069	-5.794
	S9-1	-2.926	-6.801
	S9-2	-1.142	-4.846
	S9-3	-1.227	-4.391
	S9-6	-0.496	-6.262
	Average	*-1.572*	*-5.619*
Calcite	S4-12B	-7.693	-7.719
	S9-25A	-6.81	-5.302
	Average	*-7.252*	*-6.511*
Mixed dolomite+calcite	S2-6	-4.682	-2.676
	S8-5	-4.317	-2.733
	S8-13	-4.459	-2.343
	Average	*-4.486*	*-2.584*
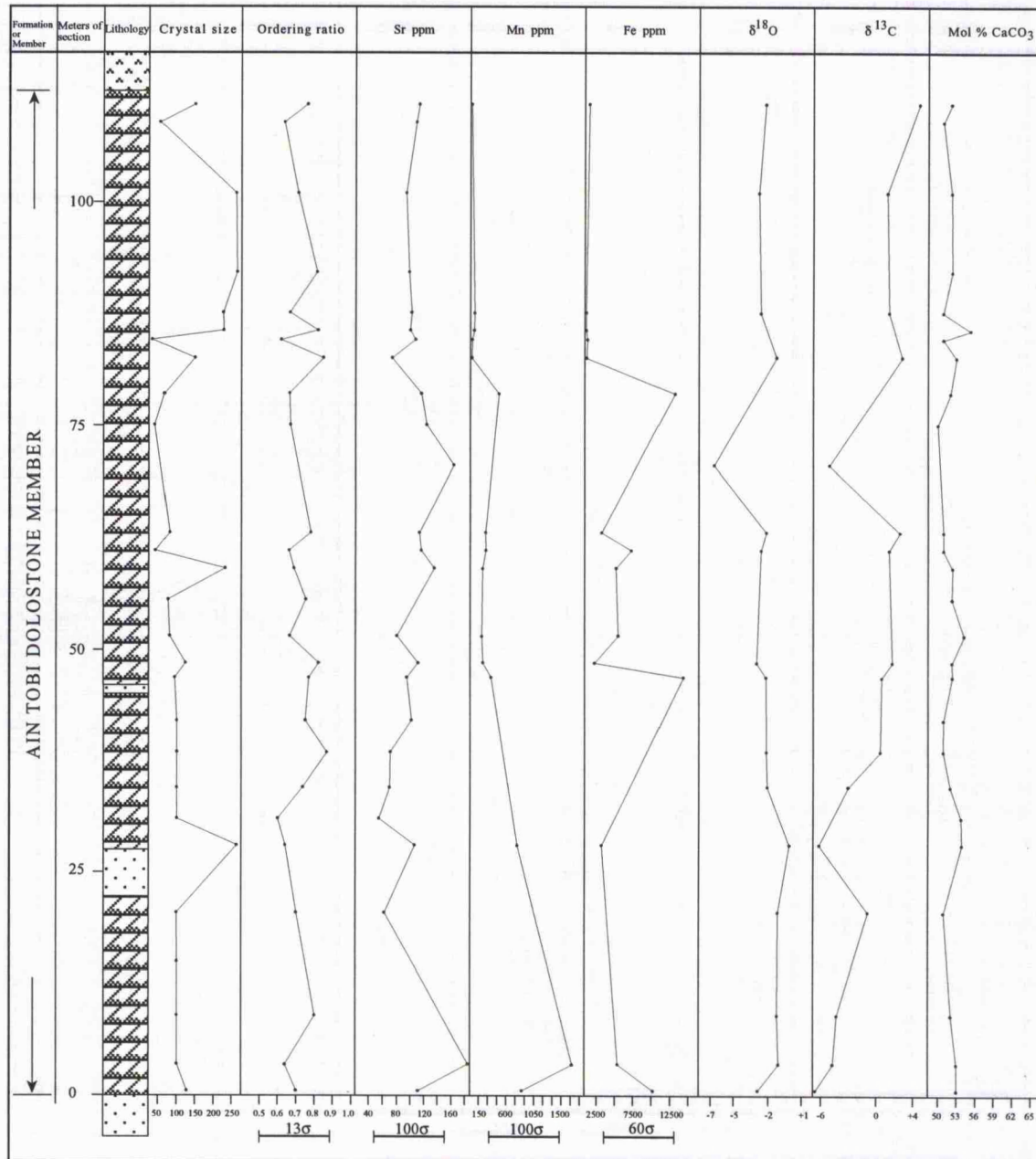
Fig.7.14 Stratigraphy, crystal size, ordering ratio, trace elements and isotopes of the dolomite of the Ain Tobi Dolostone Member at Jadu area. [0.3cm = 0.1 0rder degree which represents 4σ , therefore scale bar (1ccm) = 13σ. 0.4 cm = 40ppm Sr which represents 40σ, therefore scale bar (1cm) = 100σ. Similarly 1cm scale bar represents 100σ and 60σ for Mn and Fe respectively]. Same calculationis applicable for figures 7-15 through 7-19.
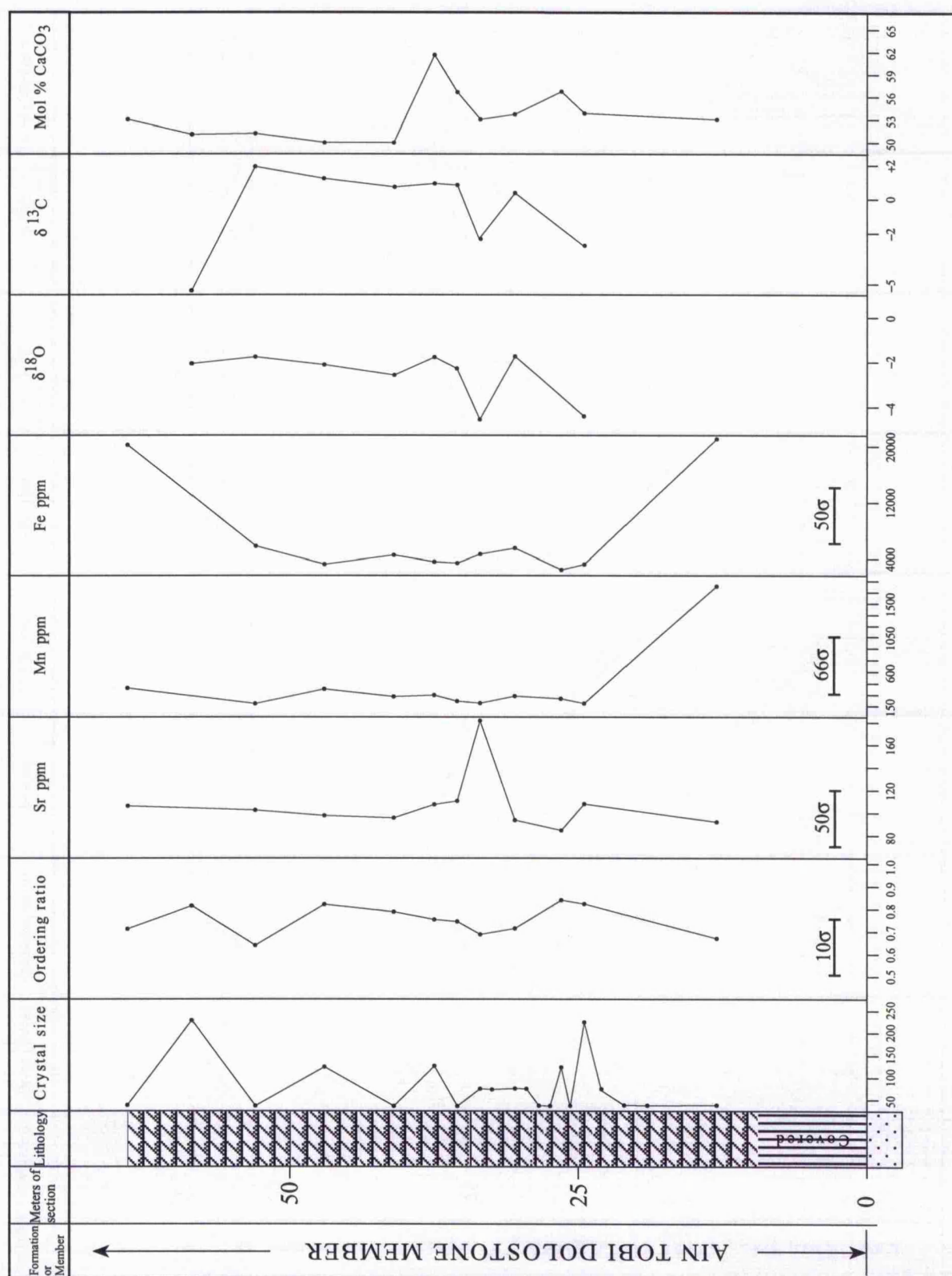
Fig. 7.15. Stratigraphy, crystal size, ordering ratio, trace elements and isotopes of the dolomite of the Ain Tobi Dolostone Member at Riaynah area
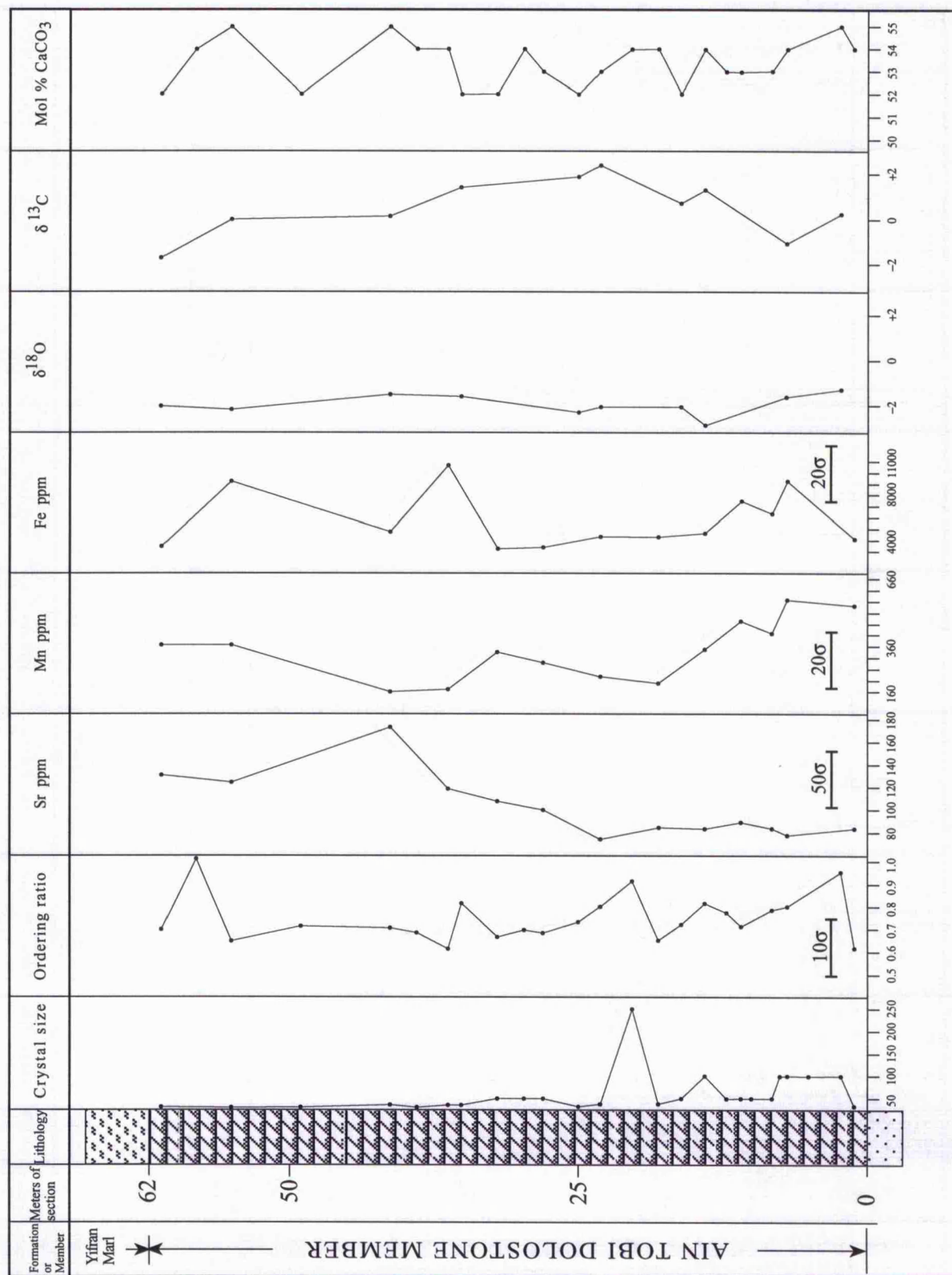
Fig. 7. 16.   Stratigraphy, crystal size, ordering ratio, trace elements and isotopes of the dolomite of the Ain Tobi Dolostone Member at Taghmah or Yifran area
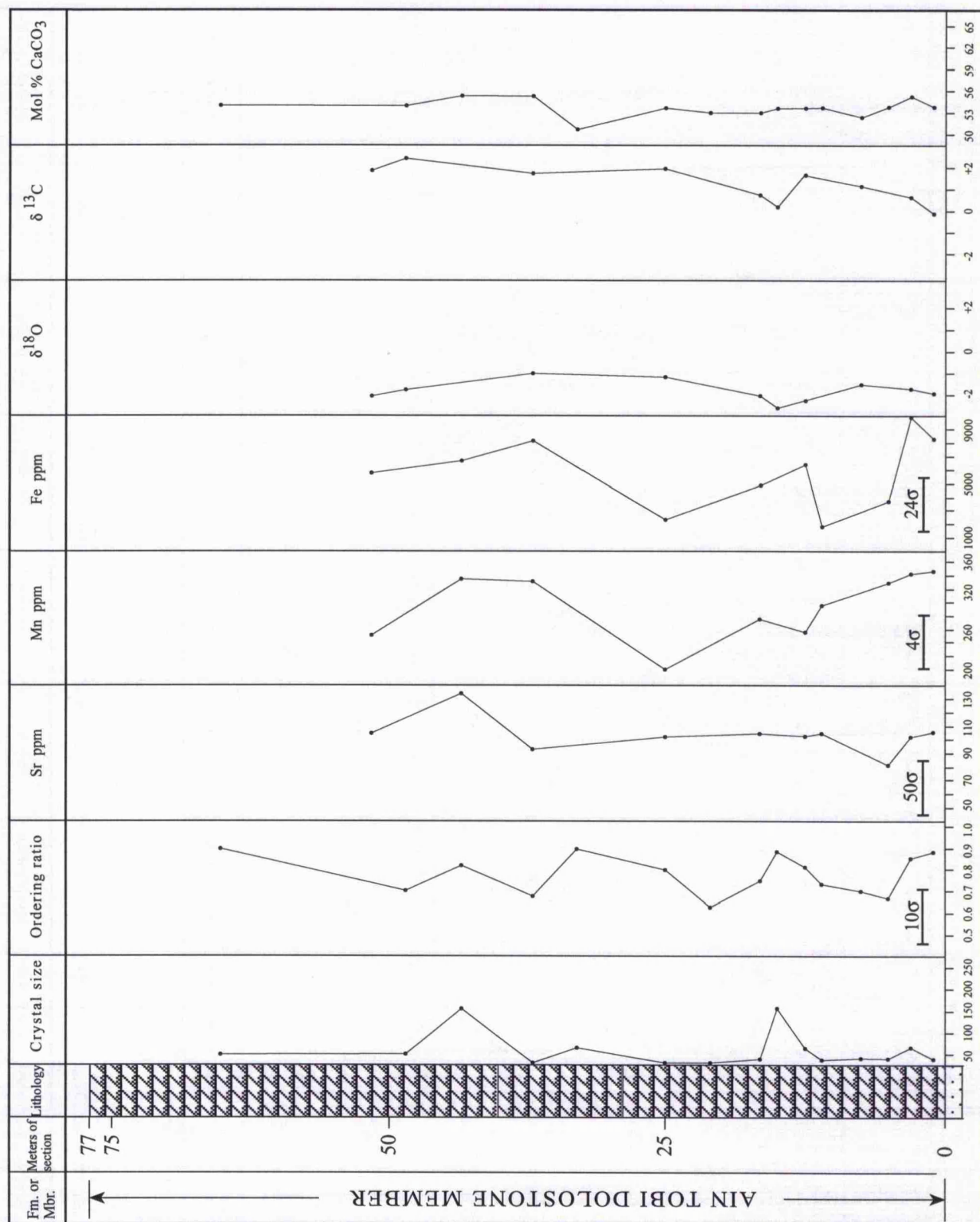
Fig. 7. 17 Stratigraphy, crystal size, ordering ratio, trace elements and isotopes of the dolomite of the Ain Tobi Dolostone Member at Abu Ghaylan area
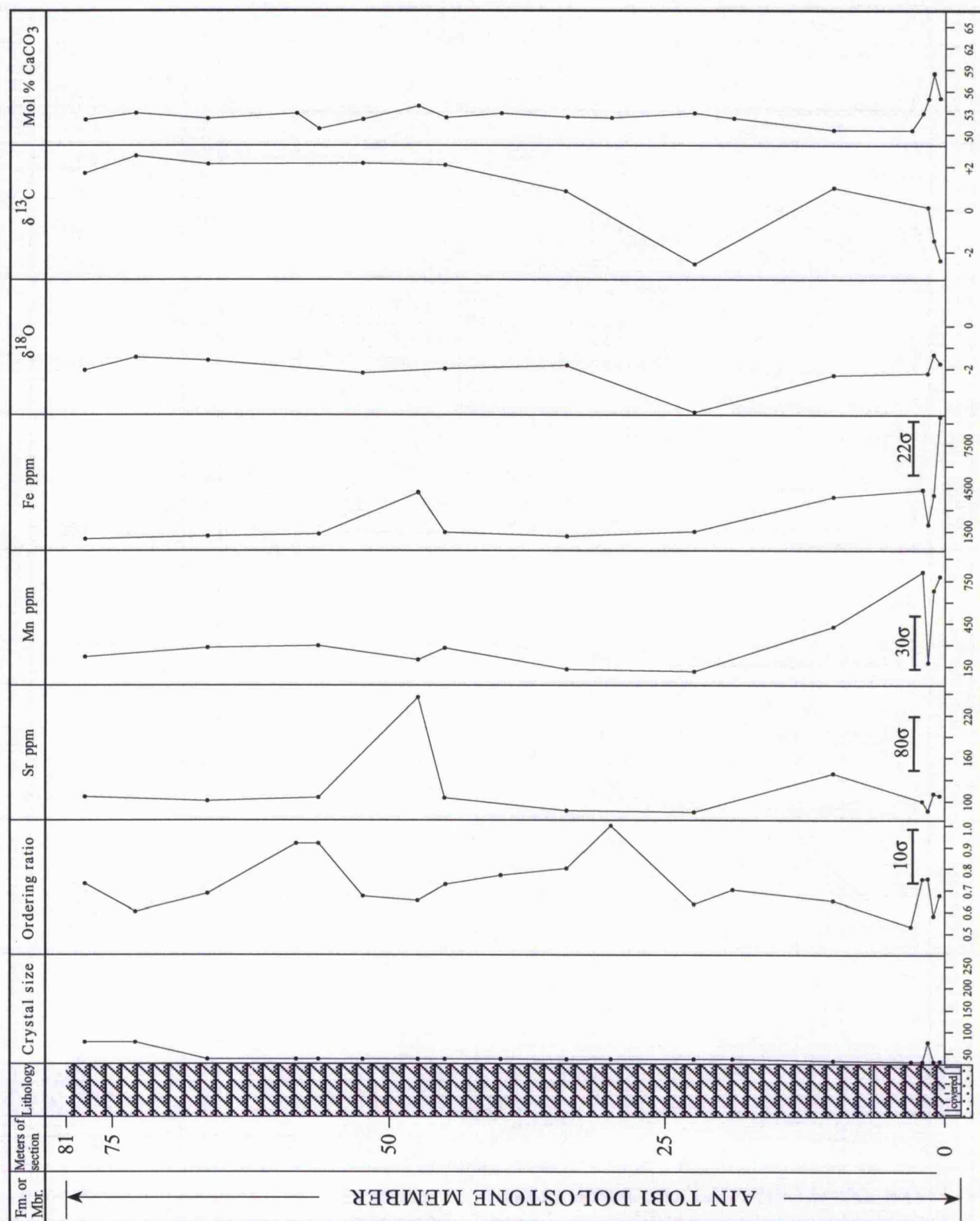
Fig. 7. 18 Stratigraphy, crystal size, ordering ratio, trace elements and isotopes of the dolomite of the Ain Tobi Dolostone Member at Fam Mulghah area
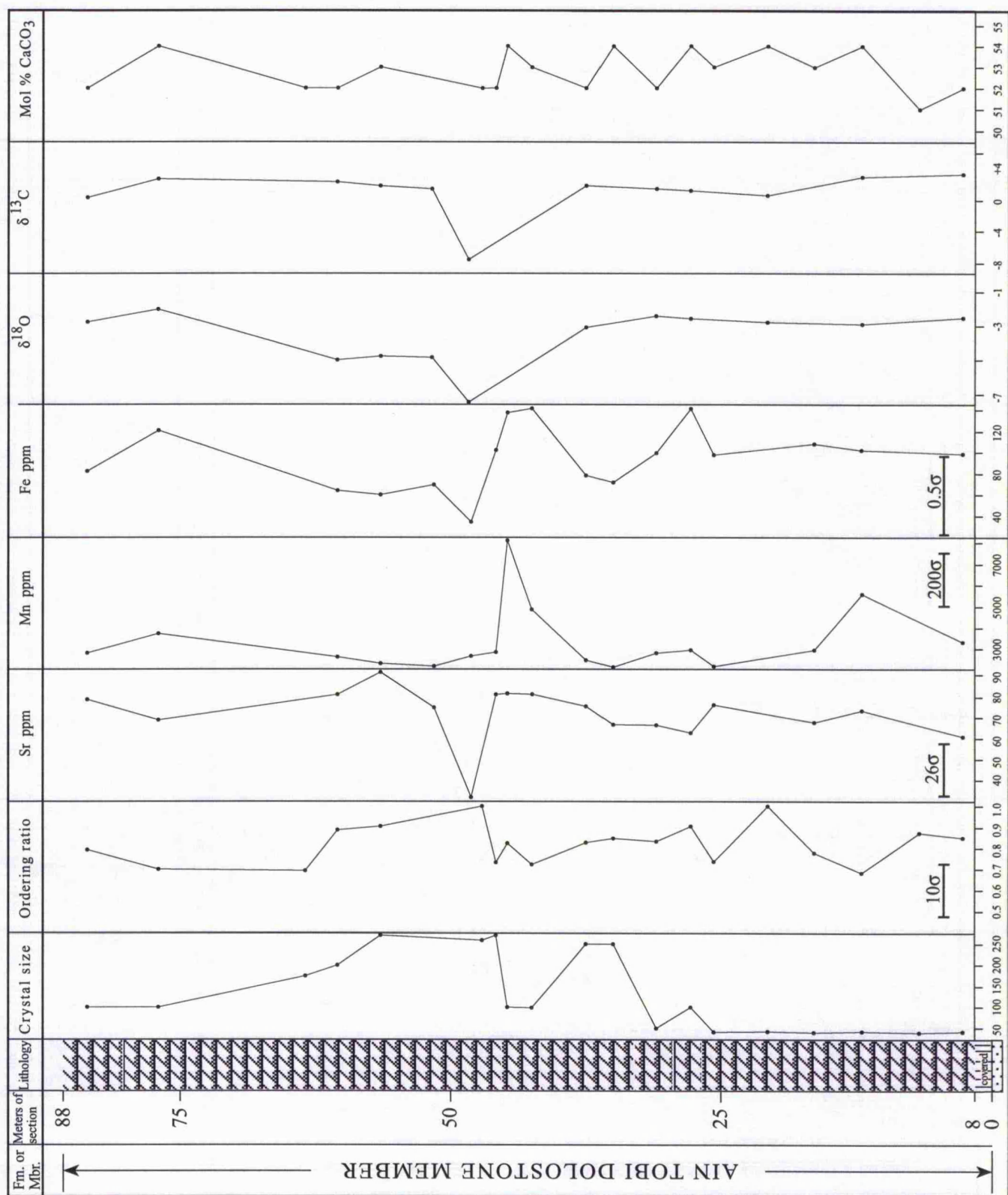
Fig. 7.19. Stratigraphy, crystal size, ordering ratio, trace elements and isotopes of the dolomite of the Ain Tobi Dolostone Member at Wadi Jabbar area

7.3.6. Conclusion

Five types of dolomite have been identified and differentiated petrographically and geochemically in the Ain Tobi Dolostone Member in NW Libya (Fig. 7.1b). They are Type-1 dolomite which is laminated, fine anhedral to subhedral, replacing mudstone and wackestone facies and shows homogeneous luminescent pattern. Type-1 crystals at the SEM scale are isolated and their cores are dissolved. These crystals are stoichiometric to nearly stoichiometric and poorly to moderately ordered. Type-1 dolomite has low Fe and Mn concentrations and relatively high Sr and Na contents. Oxygen isotope composition of this dolomite is negative (average -2.08‰) and the carbon composition is positive (average 1.61‰).

Dolomite Type-2 is very fine crystalline, closely packed and non-planar-a replacing packstone and grainstone facies. Crystals replacing concentric layers of ooids show a bright yellow luminescent pattern, whereas crystals lining ooids moulds or pores show red to dark brown luminescence. Type-2 dolomite is calcian-rich and poorly ordered. Type-2 dolomite is depleted in Fe, Mn and Na, but contains the highest Sr concentration among other types (average 123 ppm). Oxygen and carbon isotopic compositions of dolomite Type-2 are similar to Type-1 dolomite.

Type-3 dolomite is fine to medium, subhedral crystalline, and often is interbedded with quartz sandstone. At the SEM scale crystals of Type-3 dolomite are subhedral to euhedral and have irregular contacts with quartz grains. They exhibit dirty orange luminescent cores and very thin bright rims. Type-3 dolomite is calcian, moderately ordered and has the highest Fe concentration among the Ain Tobi dolomites, but has low Na and Sr concentrations. $\delta^{18}O$ within Type-3 is slightly heavier than Type-1 and Type-2

dolomites (average -1.67‰) and it is $\delta^{13}C$ -depleted compared to all other types (-1.22‰).

Dolomite Type-4 is medium to coarse, planar-s, characterized mainly by cloudy cores and clean rims, and shows little effect of dissolution as seen on SEM scale. Inclusion-rich cores show dirty orange luminescence and inclusion-free rims exhibiting a dull luminescent pattern. Common intercrystalline porosity associated with the euhedral and separated crystals of Type-4. Dolomite Type-4 is clacian, well ordered and is depleted in trace elements. Dolomite Type-4 has slightly more negative $\delta^{18}O$ values compared to dolomites Type-1, -2 and -3 and has a similar carbon isotopic composition to dolomites Type-1 and Type-2 but heavier than Type-3.

Type-5 dolomite is coarse to very coarse, subhedral crystalline with cloudy cores and clean rims. It has curved faces and exhibits undulatory extinction. Cloudy cores show dirty orange luminescence whereas clean rims show dull luminescent patterns and very thin bright luminescent cleavage lines. Type-5 dolomite is calcian-rich and well ordered. It is depleted in Fe, Mn and Sr, but relatively enriched in Na. $\delta^{18}O$ composition of dolomite Type-5 is very light compared to other types (average -4.36‰) and it has similar carbon isotopic composition to other dolomite types except Type-3.

Some dolomite crystals are replaced by calcite (calcitization). Calcitization occurs mainly close to unconformity surfaces. These dedolomitized crystals are medium in size, rounded and zoned. They show complex luminescent zonation. Dedolomitized samples have the same oxygen isotope values as dolomite Type-3, but they are $\delta^{13}C$-depleted compared to dolomite samples (average -5.62‰). Calcite samples are coarse to very coarse and are precipitated within geopetals in the upper part of the Ain Tobi sequence. They show a dull luminescence pattern. The $\delta^{18}O$ and $\delta^{13}C$ compositions of calcite

samples are very light compared to dolomite (average -7.53‰ and -6.51‰ respectively).

The mixed dolomite-calcite samples have negative oxygen and carbon isotopic

compositions but are less negative than calcite (average $\delta^{18}O$ -4.49‰ and $\delta^{13}C$ -2.58‰).

CHAPTER EIGHT

CHAPTER   EIGHT

8. DISCUSSION OF PETROGRAPHIC AND GEOCHEMICAL CONSTRAINTS ON THE ORIGIN OF AIN TOBI DOLOMITES IN NW LIBYA

8.1 Introduction

The origin of large scale ancient dolomite has been a controversial subject. Pervasively dolomitized ancient sequences such as the Ain Tobi Member contrast with Holocene dolomites, which are extremely limited in both areal extent and occurrences throughout the world. No modern analog exists for these extensive, thick, ancient dolomites.

Table 8.1. summarizes some examples of thickness and origin of Holocene dolomite occurrences. They are smaller in scale than the extensive dolomitized portions of many carbonate platforms throughout Palaeozoic and Mesozoic times. The lack of a comparable present day analogue limits the application of information to develop models for ancient dolomites. Also it has not yet proved possible to synthesise dolomite in laboratory at conditions which approximate the earth's surface (low temperature, see Usdowski, 1994).

In considering models for thick, extensive dolomites in the past, there must be a source for magnesium and a mechanism to pump the dolomitizing fluid through thick sediments. Land (1985) has pointed out that seawater is the only natural source for extensive dolomitization on the earth's surface. Seawater may be the ultimate source of Mg for many regionally extensive dolomite sequences. Dolomites are susceptible to varying source and composition, which may produce new textures and compositions on precursor phases (Banner, 1986; Gregg and Shelton, 1990; Kupez *et al*, 1993; Malone *et al*, 1994, Nielsen *et al*, 1994). Early diagenetic dolomites in many ancient carbonate platforms were formed by seawater, modified seawater and mixed meteoric-marine water (Adams and Rhodes, 1960; Mckenzie *et al*, 1980; Land, 1985; Machel and Mountjoy, 1986; Hardie, 1987; James *et al*, 1993; Sun, 1994). These early diagenetic dolomites are subsequently altered, because they are initially metastable, Ca-rich phase (Land, 1985). Many examples of alteration have been recognized in recent years (Banner *et al*, 1988; Kupecz *et al*, 1993; Smith and Dorobeck, 1993; Gao *et al*, 1995).

Locality(age)	Thickness (meter)	Origin	References
Abu Dhabi, UAE, Arabian Gulf (Recent)	0.3	Marine brines	McKenzie (1981)
Coorong, South Australia (Quaternary)	4.0	Continental brines	Von der Borch *et al* (1975)
Little Bahama Bank (Recent)	4.0	Seawater	Mullins *et al* (1985)
Sugarloaf Key, Florida (Recent)	0.1	Tidal pumping of seawater	Carballo *et al* (1987)
Northern Belize (Holocene)	0.3	Subtidal dolomitization	Mazzullo *et al* (1995)

Table 8.1. Thickness of Recent dolomite occurrences.

This study represents the first attempt of analysing trace elements and stable isotope composition of Middle Cretaceous rocks from the Nafusah escarpment in northwest

Libya and may shed light on the processes of dolomitization of the Ain Tobi Dolostone Member in this area and in the Ghadamis Basin south of Nafusah uplift.

In this Chapter the features of various models for dolomitization of ancient limestones will be discussed.

8.2. Models for Dolomitization

8.2.1. Mixing Meteoric and Marine Water Model

The area where fresh water and seawater lenses mix in coastal aquifer systems is termed the mixing zone (Fig. 8.1a). In this zone magnesium is provided by seawater and circulated by freshwater through sediment (Land, 1973; Badiozamani, 1973). The high CO_3^{-2} concentration contributed by dilute continental groundwaters favours dolomite formation of moderately to highly-ordered structure (Folk and Land, 1975). This model is an attractive hypothesis to explain large scale dolomite occurrences because the mixing zone can be extended through large masses of sediment during a sea level rise and fall. Dolomite occurrences formed by this process have been reported in north Jamaica (Land, 1973), Bonaire (Sibley, 1980) and Yucatan Peninsula (Ward and Halley, 1985) and other places. Land (1973) and Morrow (1982b) suggested that many ancient platform dolomites which lack evaporites, medium crystalline with cloudy cores and clean rims, calcian-rich and depleted in both trace elements (Sr and Na) and heavy isotopes (^{18}O and ^{13}C) may have formed in the mixing zone of fresh and marine waters.

8.2.2. Hypersaline or Seepage-Reflux Dolomitization

This model was proposed by Adams and Rhodes (1960). In this model seawater chemistry is modified by evaporation and further by $CaSO_4$ precipitation as it passes landward across a hypersaline shelf lagoon. A pumping mechanism for circulating such Mg-rich brines is provided by dense evaporation brines overlying sediments containing

normal seawater or freshwater (Fig. 8.1b). Simms (1984) proposed that Bahamian

bankwaters of slightly elevated salinity can reflux through carbonate platforms, and this

may provide a large scale dolomitization. Dolomite formed by this model is expected to

be calcian, poorly to moderately ordered, nonferroan and may be very fine laminated

(M'Rabet, 1981). Geochemically, it has low Fe content and high Sr and Na concentration

and enriched in $\delta^{18}O$ (M'Rabet, 1981; Morrow, 1982b; Tucker and Wright, 1990).

8.2.3. Normal Sea Water Dolomitization

Land (1985; 1991) and Tucker and Wright, (1990) have suggested that seawater with

little modification may be able to dolomitize limestone in the presence of a mechanism to

pump it through carbonate sediments. Surface seawater can be circulated by tidal

pumping (Fig. 8.1c) and lead to dolomitization, such as observed on Sugarloaf Key;

Florida (Carballo and Land, 1984). Circulation of seawater at the sediment-water

interface at moderate depths is also applied as a dolomite forming mechanism in the

Bahamas (Mullins *et al*, 1985). The $\delta^{18}O$ values of the dolomite formed by normal sea

water are relatively heavy which reflects precipitation from normal seawater at low

temperature (Tucker and Wright, 1990). These examples are of limited thickness and

lateral extent, which limits their applicability to ancient platform dolomite sequences.

8.2.4. Coorong Lagoon Dolomitization

The Coorong lagoon has been established as a model for early dolomitization of many

ancient dolomite that are not associated with evaporites (Von der Borch *et al*, 1975). In

this model the ephemeral lakes which extended parallel to the south coast of Australia

are filled during the humid winter by groundwater and are evaporated to partial or

complete dryness during summer (Fig. 8.1d). Dolomites formed in the landward

ephemeral lakes under the influence of continental groundwater or in the zone of mixing

between seawater and continental water (Von der Borch et al, 1975).

Magnesium necessary for dolomitization in this model is derived either from the

seawater in the case of dolomite formed close to the coast or from weathering of basic

volcanic rocks and transported by ground water in the case of dolomite formed further

inland (Von der Borch et al, 1975). Dolomite formed by this model is very fine, calcian-

rich and disordered crystalline.

Again this mechanism has limited applicability as a model for dolomitization of ancient

rock sequences.

8.2.5. Sabkha Model

The term "sabkha" is a translation of an Arabic word meaning "salt flat" (Patterson

and Kinsman, 1981). By definition it is an extensive supratidal area which occurs

landwards from the intertidal zone of the coast. In the sabkha model, storm driven flood

tides reach inland along tidal channels (Fig. 8.1e). Flooding decreases landward across

the sabkha but the Mg/Ca ratio of the floodwaters rises landward, because of gypsum

precipitation. The dense Mg^{2+} brines sink and flow seaward through the sediments.

Dolomitization of the underlying intertidal and subtidal sediments occurs beneath the

sabkha surface in regions landward of the continuous algal mat (Patterson, 1972).

McKenzie et al (1980) have developed an alternative model for sabkha dolomitization

which they term evaporative pumping. In this model a continual flow of seawater moves

landward through the sabkha sediments to replace groundwater lost by evaporation at, or

near the sabkha surface (Morrow, 1982b).

Dolomite formed by this model is mainly associated with microbial lamination,

mudcracks, evaporite nodules or solution collapse brecias. It usually exhibits rapid shifts

into undolomitized limestone, evaporite or siliciclastics laterally and vertically. Crystals of this type of dolomite are mainly very fine and metastable or calcian. Geochemically, sabkha type dolomite has low concentrations of trace elements and heavy stable isotopic ratios (Moore, 1989).

This model has a limited application in ancient sediments because thick and pervasive dolomitized sequences are not expected in the sabkha type environment.

8.2.6. Burial Dolomitization

The principal mechanism of this model is the compactional dewatering of basinal mudrocks and the expulsion of heated Mg^{2+}-rich fluids into adjacent shelf-edge and platforms carbonates (Fig. 8.1f). The magnesium source invoked is the modified seawater and clay minerals transformation with increasing depth and rising temperature (conversion of smectite to illite resulting in Mg^{2+} release) (Mattes and Mountjoy, 1980). Dolomite formed during burial and increasing temperature is usually characterized by coarse to very coarse crystalline, white or baroque (saddle) and have low concentration of Sr and Na and light $\delta^{18}O$ (M'Rabet, 1981).

8.2.7 Mechanism of Dedolomitization

The term dedolomitization is used to describe a possible mechanism by which the mineral calcite replaces the mineral dolomite. This process has often been interpreted as a near-surface diagenetic event. The mechanism of dedolomitization or calcitization has been widely discussed; e.g. recent experimental work by Kastner (1982) proved that calcitization of dolomite took place at temperatures up to 200°C. It has been suggested by Katz (1968) that dolomite is preferentially replaced by calcite under near-surface, oxidizing conditions. All occurrences of dedolomitization are indicative of either an erosional unconformity within the sequence (Scholle, 1971) or of late surface dissolution

during weathering (Chafetz, 1972). Budai *et al* (1984) pointed out that dedolomitization can occur in both outcrop and subsurface during burial at higher temperatures.

Margaritz and Kafri (1981) reported that calcitization is the product of the mixing of marine and meteoric waters, whereas Back *et al* (1983) suggested that it is the result of dolomite and gypsum dissolution during groundwater migration. Recently Theriault and Hutcheon (1987) explained that calcitization is the result of dissolution of dolomite in porous units adjacent to the unconformity or during exposure of dolostones due to sea level fluctuations (Khalifa and Abu El Hasan, 1993).
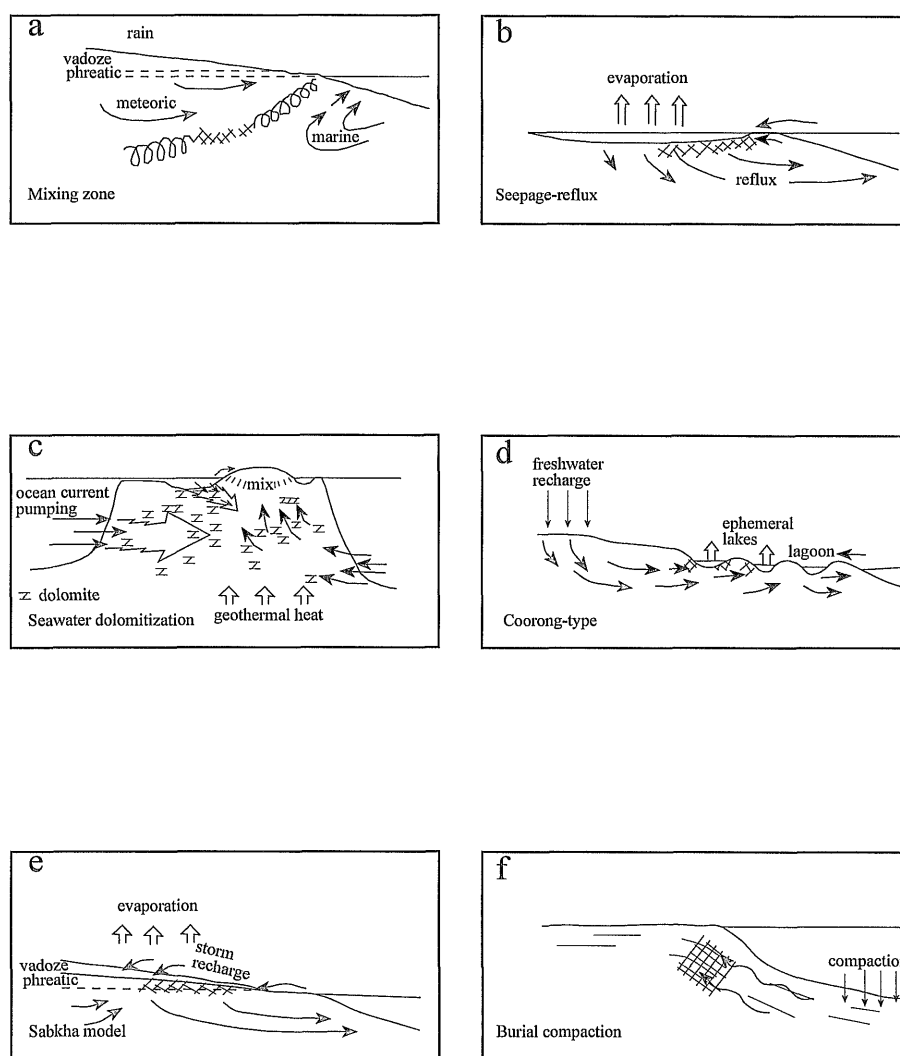
Fig. 8.1 Dolomitization models, (from Tucker and Wright, 1990).

8.3. Discussion and Interpretation of Petrography and geochemistry of Ain Tobi Dolostones

Diagenetic process by which the Ain Tobi carbonates are modified, including those that have been proposed to explain dolomitization, are influnced by depositional setting and burial (Holail *et al*, 1988). Therefore, several settings of dolomitization must be considered: 1) synsedimentary hypersaline; 2) mixed marine-meteoric; and 3) shallow and deep burial environments.

Extensive dolomites in Cretaceous subtidal ramp-facies rocks in the Nafusah uplift northwestern Libya provide a classic example of thick, widely distributed enigmatic dolomite bodies. Most subtidal carbonate ramps, such as the Ain Tobi Dolostone Member of Mid-Cretaceous, are unlikely to undergo extensive dolomitization due to refluxing hypersaline fluids or from mixed meteoric-marine waters (Burchette and Wright, 1992). Thus, dolomite in subtidal rocks is often interpreted as later dolomitization by modified seawater or other fluids (Hardie, 1987). For example, dolomite in subtidal rocks of Silurian Interlake Formation have been interpreted as early dolomitization resulting from hypersaline brines and mixed marine-meteoric or mixing marine-hypersaline fluids (Shukla, 1988). However, subtidal ramp rocks of Silurian and Devonian, Illinois Basin are pervasively dolomitized and are interpreted as dolomitization resulting from seawater or modified seawater fluids (Kruger and Simo, 1994).

In the following sections petrographic relations among varies carbonate phases in Middle Cretaceous units of the Ain Tobi Dolostone Member in conjunction with geochemical data will be combined to constrain diagenetic process relative to the origin and environment of dolomite formation and dolomite calcitization.

8.3.1. Type-1 Dolomite

Petrographically, Type-1 dolomite is fine crystalline, non-planar and shows homogeneous luminescence. The absence of vugs and moulds that formed in the subsurface environments and dissolved core of the dolomite grains is typical of dolomite formed under near-surface low temperature. The nonferroan character of dolomite Type-1 is further support for near-surface oxidizing conditions and not to the absence of iron in the dolomitizing fluids.

The sedimentary structures associated with the fine crystalline Type-1 dolomite such as microbial laminae, very thin and rare layers of gypsum and breccias, overlying supratidal deposits (Yifran Member) and the petrographic characters suggest that Type-1 is an early dolomite which has been formed in subtidal-intertidal environment under the influence of refluxing brines (Fig. 8.1b) comparable to that described from the Persian Gulf (McKenzie et al, 1980). This refluxing brine probably from the overlying restricted marine Yifran Member could be the main dolomitization agent to form early Type-1 dolomite. The sabkha and Coorong models are not important here, because the Ain Tobi rocks lack features that are typical of these models such as rapid shifts into undolomitized limestone, evaporite or siliciclastics (section 8.2.5) and absence of nearby volcanic rocks (section 8.2.4).

Growing awareness of minor and trace element distribution within dolomite is shown by the numerous recent studies that incorporate such data into various dolomitization models. The degree of Ca in dolostones reflects the Mg/Ca ratio of the precipitation solution (e.g. Füchtbauner, 1974; Lumsden and Chimahusky, 1980; Morrow, 1982b). They stress that fine crystalline dolomites that are associated with evaporites have calcium contents near 50 mole% that are lower than for finely crystalline dolomites not

associated with evaporites which are more variable and Ca-rich. If this interpretation is correct then the XRD data (Table 7.2) for the composition of Type-1 dolomite indicates that it is an early diagenetic dolomite (see also Sperber *et al*, 1984; Hardy and Tucker, 1988) precipitated from solutions with relatively high Mg/Ca ratios which were probably evaporitic (reflux model).

The proposed model is consistent with the early timing and relatively high Na content (average 444 ppm) and high Sr content (average 110 ppm) compared to other dolomite types of Ain Tobi. These concentrations may indicate the influence of hypersaline fluids. Similarly, Fe and Mn contents are uniformly low (average 4591 ppm and 241 ppm, respectively). Oxygen isotopic data (Table 7.5) for dolomite Type-1 (ranges from -2.73‰ to -1.33‰ PDB).
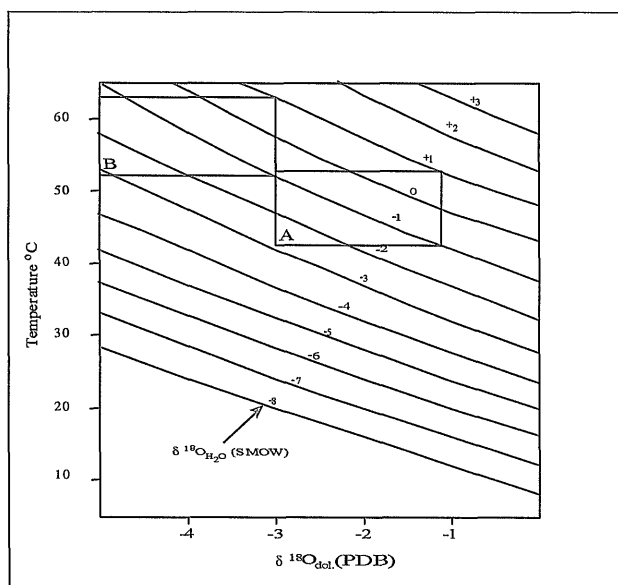
Fig. 8.2. Plotted are the curves for various values of δ $^{18}O_{water}$ as a function of both δ $^{18}O_{dol.}$ and temperature (T) of dolomite precipitation, according to the relationship (Friedman and O'Neil, 1977):
δ $^{18}O_{dol.}$ - $^{18}O_{water}$ = [3.2 * 10^6 $T(K^o)^{-2}$] - 1.5. Box A represents temp. range of Type-1 through Type-4 dolomites, Box B represents temp. range of saddle dolomite Type-5.

These negative oxygen isotope compositions are not comparable to that of any other penecontemporaneous Recent and Pleistocene dolomites whose values are more positive than seawater composition (Supko, 1977; Land *et al*, 1975; Tucker and Wright, 1990 their Fig. 8.18). The light oxygen isotope composition of this dolomite type indicates that it must have formed from: 1) fluids depleted in ^{18}O relative to seawater (less than 0); 2) high temperature of formation; 3) recrystallization either (or both) at high temperature, or in contact with water of $\delta_w < 0$, in either case with high water/rock ratio (Hudson, pers. com.). ^{18}O depletion in dolomite has been attributed to mixed seawater and meteoric water (Badiozamani, 1973; Land, 1973). However, petrographic observations such as dissolution of the crystal cores and absence of moulds and vugs formed in the subsurface environments (due to exposure and invasion of meteoric water) and geochemical observations discussed above do not favour formation of Type-1 dolomite as being of mixing-zone origin. Moreover, oxygen isotope compositions of Type-1 dolomite are lighter than the general values estimated for marine calcite (0‰ to +2‰) proposed by Hudson (1977). Therefore, Type-1 dolomite is interpreted as being formed by the hypersaline reflux model (Fig. 8.1b).

In summary, early dolomitization (Type-1) of the Middle Cretaceous Ain Tobi carbonates in northwestern Libya took place in subtidal-intertidal environment under the influence of refluxing brines of low temperature and $\delta_w < 0$ from the overlying Yifran Member of the Sidi as Sid Formation.

8.3.2. Type-2 Dolomite

Dolomite Type-2 of Ain Tobi dolostones is very fine crystalline (< 20μm). It is mimetically replaced packstone and grainstone facies with excellent fabric preservation (Fig. 7.4a). The absence of evaporites, occurrence of meteoric diagenetic fabrics such as

mouldic porosity and free of inclusions, all suggest that dolomite Type-2 is an early replacement in a mixing marine-meteoric water zones.

Dolomite Type-2 is poorly ordered and calcium-rich (Table 7.2, Fig. 7.11a). These show that this dolomite type was precipitated at an early stage from solutions of low Mg/Ca ratio probably were more humid and non-evaporitic which suggest mixed marine-meteoric fluids as the diagenetic solution for the Type-2 dolomite formation. Type-2 dolomite has high Sr content compared to other types. In fact, it has the highest Sr concentration among Ain Tobi dolostones (average 123 ppm) without any evidence of recrystallization. Dolomite which formed from aragonite, high-Mg calcite and low-Mg calcite during the early stages has a high Sr contents (500-600 ppm), this may indicate that the dolomite has been precipitated from hypersaline solution process (Tucker, 1982, 1983; Tucker and Wright, 1990). The Sr content of dolomite Type-2 does not favour hypersaline model. Instead, it favours a mixing zone situation which usually has Sr contents of 70-300 ppm (Rodgers *et al*, 1982; Tucker and Wright, 1990), or not more than 550 ppm as pointed out by Veizer (1983), and would support a high-Mg calcite precursor rather than aragonite (Veizer, 1978). Furthermore, the mimetic textures of completely dolomitized ooids (Fig. 7.3d and 7.6d) should have heavy isotopic composition if the precursor was aragonite (Zempolich and Bocker, 1993). The isotope composition of sample (S2-2, oolitic dolograinstone) for instance is light (-1.44‰ and -2.46‰ PDB, $\delta^{18}O$ and $\delta^{13}C$ respectively) and is consistent with a high-magnesian calcite precursor.

Low Fe and Mn contents noted in dolomite Type-2 (average 4373 ppm and 271 ppm respectively) clearly indicates diagenesis dominated by meteoric water under oxidizing conditions during dolomitization. On the other hand, marine and hypersaline dolomites

clearly contain high Na concentrations, as would be expected from precipitates of these diagenetic environments. Type-2 dolomite (average 254 ppm) falls within the range of other dolomites (Fig. 8.4a) whose origin is ascribed to mixed-water precipitation (Humphrey, 1988).

The wide range of isotopic compositions for Type-2 dolomite might suggest more variable fluid compositions than for Type-1 dolomite. Therefore Type-2 dolomite probably is formed in a mixing zone of $\delta^{18}O$ and $\delta^{13}C$-enriched seawater and $\delta^{18}O$ and $\delta^{13}C$-depleted freshwater at low temperature ranges from 42° to 52 ° C (average 47 ° C, Fig. 8.2 assuming $\delta_w = -1‰o$). It is worth noting that Type-2 dolomite has heavier $\delta^{13}C$ and lower Fe contents compared to Type-3 dolomite discussed below. This indicates that Type-2 dolomite precipitated in a shallower environment than dolomite Type-3 and possibly in a mixed solution of higher freshwater percentage. The positive correlation between Sr contents and oxygen isotope values for Type-2 dolomite (Fig. 8.3b) may reflect lower salinity (M'Rabet, 1981) related to meteoric influences. Furthermore oxygen isotope values of this dolomite are comparable to other values for dolomites attributed to a mixed water origin, such as Holocene dolomites from Jamaica (Land, 1973) and Upper Cretaceous dolomites from Egypt (Holail *et al*, 1988).

In summary, Type-2 dolomite from Ain Tobi dolostones is an early replacement dolomite from high-Mg calcite precursor that precipitated from mixed marine-meteoric solutions with different degrees of mixing from that of Type-3 dolomites and may be shallower.

8.3.3. Type-3 Dolomite

Type-3 dolomite is fine to medium crystalline associated with quartz grains. This type is found mainly at the base of the Ain Tobi Dolostone Member. Type-3 dolomite

postdates compaction as indicated by its association with collapse breccias in a few cases

(Morrow, 1982b) and its occurrences along fractures within coarse quartz grains (Fig.

7.2c and 7.6a). Therefore, Type-3 dolomite is relatively later than Type-1 and Type-2

dolomites and may be deeper.

One of the frequently suggested mechanisms is for dolomitization in zones of mixed

marine and meteoric water. On basis of petrography just mentioned above, geochemical

and stable isotopes data (discussed below) I suggest that mixed marine and meteoric

water (Badiozamani, 1973; Land, 1973) is the mechanism responsible for formation of at

least three dolomite types of the Ain Tobi rocks. These three types are Type-2, Type-3

and Type-4. Although they formed in the mixing zone, but on basis of major and trace

elements and stable isotopes, each one may represent different degrees of mixing due to

different depth of burial (Magaritz *et al*, 1980; Harris and Meyers, 1987, Holail *et al*,

1988) as will be discussed in the following sections.

Type-3 dolomite is relatively rich in Fe compared to other types (Table 7.4a), having

the highest $FeCO_3$ content among the Ain Tobi dolomite types (average 1.452, Table

7.3). Type-3 has higher Mn concentration than any other type (average 606 ppm). The

high Fe and Mn concentrations in Type-3 suggest that this dolomite is formed during

burial in reducing conditions and argues against precipitation from high sulphate, low Eh

brines (Harris and Meyers, 1987).

Furthermore, ferrous iron is present mainly in continental groundwater (Hem, 1970).

The high $FeCO_3$ content in Type-3 dolomite suggests that the clastics associated with it

were a source of Fe during dolomitization or reflect a groundwater origin. Moreover,

Type-3 dolomite has a low Sr content with an average of 87 ppm. According to Katz and

Mathews (1977), Sr contents in dolomite seem to be independent of temperature and

mineralogy of the precursor (aragonite, magnesian calcite). If these conclusions obtained for high-temperature dolomite can be extrapolated to low-temperature dolomite, low Sr values in Type-3 dolomite probably indicate a meteoric origin (M'Rabet, 1981).

The light oxygen of Type-3 dolomite (average -1.672‰ PDB, Table 7.5) may represent the influence of meteoric water because they are lighter than those values for pelagic carbonates proposed by Hudson (1977). Calculation of temperature of Type-3 dolomite (Fig. 8.2) shows that it has formed in a shallow-burial situation at low temperatures (ranges from 42° to 47°C, average 45°C assuming that $\delta_w = -1‰$). $\delta^{18}O$ values of Type-3 dolomite are similar to those dolomites reported from the Holocene in Jamaica (-0.9‰ to -1.6‰) (Land, 1973). They are very close to those reported from the Middle Eocene dolomite around Bahariya Oasis in Egypt (Land *et al*, 1975) and to those of the Upper Cretaceous El Heiz and El Hefhuf formations in Egypt reported by Holail *et al* (1988). They suggest that the Holocene, the Eocene and the Upper Cretaceous dolomites formed by early replacement in meteoric-marine diagenetic settings. The negative $\delta^{13}C$ values (average -1.22‰ PDB) also further support the influence of meteoric water during dolomitization and argue against depth-burial temperature. Because carbon isotopes should become heavier with increasing depth and temperature and not lighter as in the Type-3 dolomite (Fig. 7.14 and Fig. 7.18).

Two possible conditions exist whereby isotopically light carbon is produced for incorporation into carbonate minerals. First, meteoric water passing through a soil zone dissolves soil-gas CO_2, derived from decaying organic material, resulting in a ^{13}C-depleted groundwater (Humphrey, 1988 and many others). Second, isotopically light carbon can be produced by bacterial sulphate reduction of organic matter within the sediments under reducing conditions (Baker and Burns, 1985). The first scenario can

easily occur in well oxygenated or oxidizing meteoric waters. The absence of pyrite within Type-3 dolomite, its buff colour and its occurrence close to the unconformity surface indicate oxidizing conditions. On the other hand, carbon produced through sulphate reduction requires reducing conditions which is inconsistent with the petrographic observation and trace element concentration within Type-3 dolomite. It could tentatively be said that, based on the above evidence, the light carbon in Type-3 dolomite originates from waters percolating through a soil zone during exposure.

Positive correlation between $\delta^{18}O$ and $\delta^{13}C$ for dolomite Type-3 (not strong correlation) is shown in (Fig. 8.3a). Similar trends in $\delta^{18}O$ and $\delta^{13}C$ for Silurian and Devonian dolomite in Illinois Basin have been interpreted as resulting from the mixing of meteoric water containing ^{13}C-depleted from reducing conditions or soil zones during exposure, with connate fluids in phreatic zones (Allan and Matthews, 1982; Kruger and Simo, 1994). Therefore, positive correlation between oxygen and carbon isotopes in Type-3 dolomite (Fig. 8.3a) further indicate that the mixing of marine and meteoric water is the mechanism responsible for its formation.

According to Harris and Meyers (1987) the younger dolomite could be formed in more burial depth than the earlier ones during mixing zone. Therefore Type-3 dolomite probably formed later than Type-2 in slightly deeper environment and possibly in different degree of mixing between marine and meteoric fluids.

In summary, dolomite Type-3 from the Ain Tobi Member is formed earlier than Type-4 and Type-5 dolomites but later than Type-1 and Type-2 dolomites in a zone of mixed marine and meteoric water at shallow burial. The high Fe contents, probably derived from associated clastics and reset for reduction by organic matter, contributed light carbon to the dolomite.

8.3.4. Type-4 Dolomite

The medium to coarse, planar-s crystals of dolomite Type-4 commonly contain cloudy cores with a dirty orange luminescent pattern surrounded by clean rims with dirty dull luminescent patterns. The differences in cathodoluminescent appearances reflect the differences in Fe/Mn ratios between cores and rims (see section 8.3.9). Clean rims may represent dissolution of the original calcium carbonate and/or metastable fine dolomite crystals are followed by overgrowth of clean rims under the influence of meteoric water diagenesis (Sibley, 1980; Dorobek *et al*, 1993; Nielsen *et al*, 1994) and join along irregular compromise boundaries to produce tight interlocking mosaic (Morrow, 1978). Therefore, Type-4 dolomite is interpreted to represent the stablization of precursor dolomite in an intermediate to late diagenetic process (Amthor and Friedman, 1991, 1992).

Type-4 dolomite is calcian to calcian-rich and has a better ordering ratio compared to earlier dolomite types of Ain Tobi dolostones (Table 7.2, Fig. 7.11a) and Holocene dolomites. Microprobe results furthermore support the conclusion that Type-4 dolomite is the result of neomorphism, where cloudy cores are found to be more calcian, less Sr and Na and less Fe/Mn ratio than clean rims (Table 7.3). Trace element contents are generally low in Type-4 dolomite due to recrystallization. The low Sr and Na concentration (Table 7.4a, Fig. 8.4 a & b) are similar to those concentrations in dolomites interpreted as non-evaporitic or mixing zone in origin (Land *et al*, 1975; M'Rabet, 1981; Holail *et al*, 1988; Khalifa and Abu El Hasan, 1993). Plots of Sr versus crystal size (Fig. 8.3f) show negative relationships indicating that Sr contents are modified due to recrystallization. The decrease in Sr content and increase in dolomite crystal size due to recrystallization have been observed elsewhere (e.g. Dunham and Olsen, 1980; M'Rabet, 1981; Malone *et al*, 1996). Fe and Mn contents in dolomite
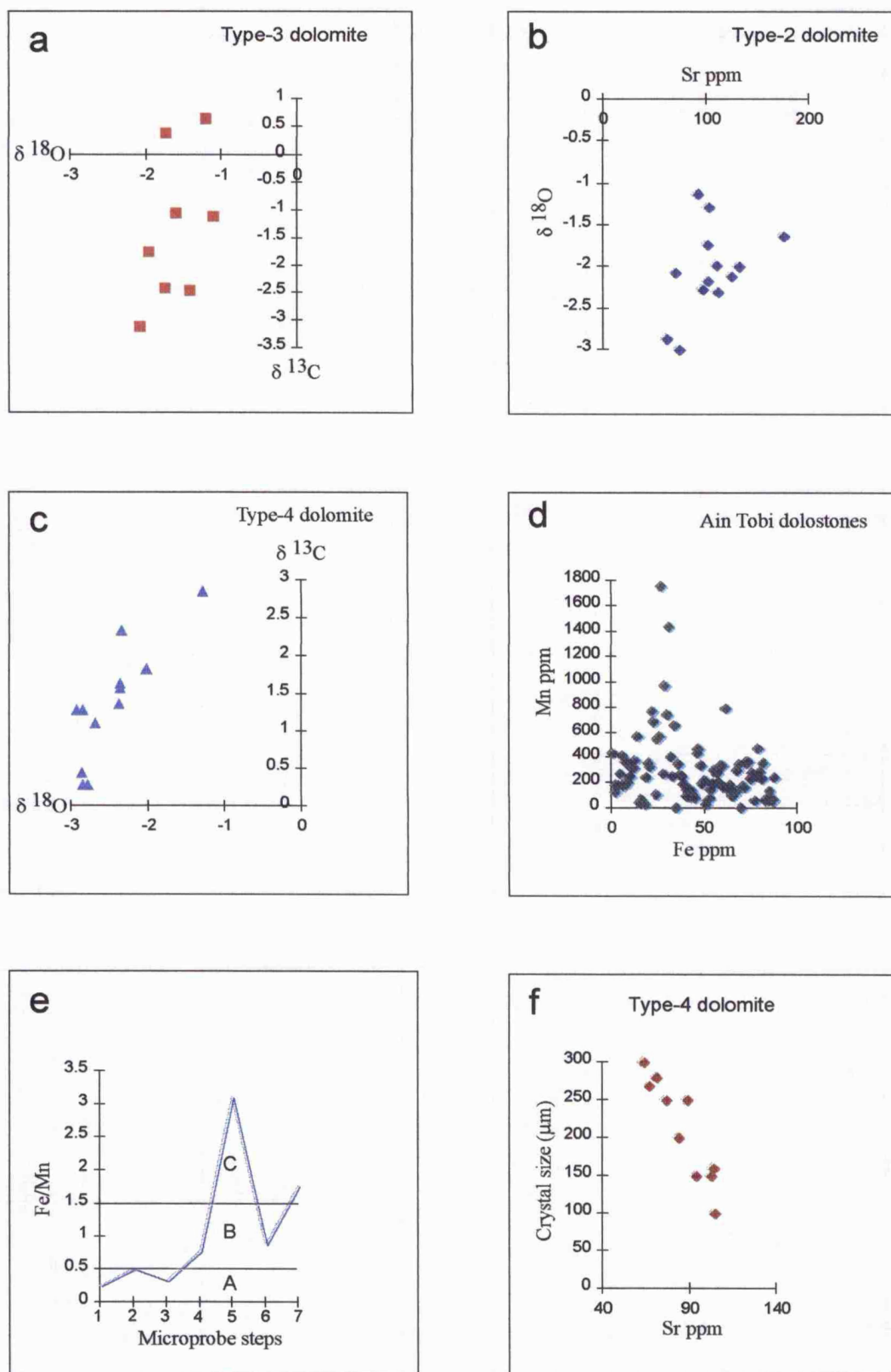
Fig. 8.3: a) Relationship between oxygen and carbon stable isotopes of dolomite Type-3. b) Oxygen and Sr content relation in dolomite Type-2. c) Isotopic composition of Type-4 dolomite. d) Relationship between Fe and Mn in the Ain Tobi dolostones. e) Role of Fe/Mn ratio in luminescence as deduced by probe (zone A bright luminescence, zone B mderate luminescence and zone c dull and/or no luminescence). f) Relationship petween Sr content and crystal size in dolomite Type-4.

Type-4 are lower than would be expected from values from dolomite formed late due to increasing depth and temperature. Thus, Type-4 dolomite formed either in the near-surface mixing zone or during shallow burial and subsequent modification by neomorphism. According to temperature of this dolomite (ranges from 43 to 52°C, average 49°C assuming that δ_w = -1‰, Fig. 8.2) calculated from $\delta^{18}O$; Type-4 dolomite possibly formed during shallow burial at medium temperature and subsequently was exposed and recrystallized under the influence of meteoric water. The temperature of Type-4 dolomite is intermediate between early dolomites and those interpreted as saddle dolomite of Ain Tobi dolostones indicating its formation to be an intermediate to late diagenetic event.

Moreover, the relatively wide range in $\delta^{18}O$ and $\delta^{13}C$ show as overlapping plots for Type-1 and Type-2 dolomites (Fig. 7.13) and allow an interpretation that dolomite Type-4 is the result of recrystallization of early dolomites in the presence of isotopically depleted freshwater (Moore *et al*, 1988). This is concordant with the positive correlation between oxygen and carbon stable isotopes (Fig. 8.3c) which is often interpreted as the result of mixing marine-meteoric fluids. If $\delta^{13}C$ values for Type-4 dolomite represent the composition of the original carbonates as suggested by Magaritz (1985), the carbon isotopes may by derived from dissolution of the precursor carbonate minerals. Concordant dolomite of the Mesozoic carbonate platform for the Tethys region shows a similar range of oxygen isotope values (e.g. Magaritz, 1985; Varol and Magaritz, 1992). They interpreted those dolomites as the result of mixing-water in origin.

In summary, dolomite Type-4 represents stabilization of precursor metasable dolomites (Type-1 and Type-2) during the intermediate to late stage. It is interpreted on

basis of petrography and geochemistry as dolomite formed under the influence of mixed

marine and meteoric fluids (Fig. 8.1a) at moderate temperatures.

8.3.5. Type-5 Dolomite

Saddle dolomite such as Type-5 of the Ain Tobi is always interpreted to have

occurred during deeper burial (Mattes and Mountjoy, 1980; Alsharhan and Williams,

1987; Qing and Mountjoy, 1989). Type-5 dolomite of Ain Tobi dolostones is

characterized by coarse to very coarse anhedral crystals up to 1500 μm in size with

compromise boundaries and undulatory extinction. It is commonly dominated by cloudy

cores and clean rims. Type-5 dolomite could be formed by non-mimetic replacement, by

recrystallization of earlier types and/or under high temperature conditions. On the basis

of petrography, non-mimetic replacement of precursor limestone is eliminated because

crystals of this dolomite type are clearly replaced or recrystallized from precursor

euhedral crystalline dolomite (Fig. 7.9c). Type-5 dolomite is nonstoichiometric and well

ordered indicating that it is formed in the late diagenetic stages (Lumsden and

Chimahusky, 1980).

Type-5 dolomite from the Ain Tobi dolostones have a low Sr content but relatively

high Na concentrations (Fig. 8.4a & b) averaging 81 and 411 ppm respectively. Because

saline solutions should precipitate dolomites that are enriched in trace elements, this low

concentration of trace elements (particularly Sr) is possibly due to recrystallization under

the influence of diluted solution. So it is likely that hydrothermal and relatively saline

solutions were involved in the precipitation of Type-5 dolomite. On the other hand, Fe

and Mn contents are very low compared to dolomites resulting from reducing conditions.

Low Fe and Mn values (average 2162 and 221 ppm respectively) can be attributed to the

recrystallization and/or to the solution that depleted in both elements rather than to oxidizing environment.

Oxygen and carbon isotope analysis of Type-5 saddle dolomite show that it is considerably ^{18}O-depleted compared to other dolomites from the Ain Tobi dolostones (Table 7.5 and Fig. 7.13). These light oxygen compositions (average -4.36‰) obviously demand either lower δ_w, or high temperature of the precipitating waters or a combination of both (Hudson, 1977, personal comm.; Friedman and O'Neil, 1977; Land, 1980). The δ^{13}C composition of Type-5 dolomite (average 1.58‰ PDB) is similar to other types from the Ain Tobi dolostones with one exception of Type-3 dolomite. The similarity in carbon isotopes of most of the Ain Tobi dolomites may reflect the original δ^{13}C composition of the precursor sediments as suggested by Magaritz (1985) and many others. The light oxygen isotope values of saddle dolomite from other localities suggest that it formed at temperatures of 50-150°C (e.g. Choquette, 1971; Beales and Hardy, 1980). Although no oxygen isotope analysis has been done directly on the formation water of the Ain Tobi Dolostone Member, I will assume as a working hypothesis that -1.00‰ PDB is a reasonable value for the Mid-Cretaceous waters in the region following suggestions made by Kolodny and Raab (1988). Allan and Wiggins (1993) and Huber et al (1995) also used the same value. Therefore, the formation temperature of saddle dolomite Type-5 from the Ain Tobi dolostones can be estimated using δ^{18}O values by first converting these dolomite values from PDB scale to SMOW scale using the following equation (Allan and Wiggins, 1993):

δ^{18}O (SMOW) = [1.03086 * δ^{18}O (PDB) + 30.86]. Then temperature can be calculated using the equation of Friedman and O'Neil (1977):

$[3.2 * 10^6 \ T(°K)^{-2}] - 1.5 = \delta^{18}O_d - \delta^{18}O_w$; where $\delta^{18}O_d$ is oxygen isotope for dolomite in SMOW scale, and $\delta^{18}O_w$ is for seawater (assumed = -1.00‰). Using the above method; temperature at which saddle dolomite from the Ain Tobi dolostones is formed ranges from 52 to 64°C (average 60°C). An alternative graphical method to estimate temperature from $\delta^{18}O_d$ is given in Figure 8.2.

Isotopic composition and estimated temperature, suggest that fluids from which late phase diagenetic Type-5 dolomite precipitated was most likely to have been either subsurface brines or mixed meteoric-sea water fluid in the subsurface environment. The subsurface component is likely to have been an evaporation-concentrated interstitial water from underlying evaporites. Movement of such fluids is likely to have taken place during burial by upward migration (Garven, 1985). I believe that the major evaporite deposits in the Nafusah escarpment which could act as the source of this brine are the Lower and Middle Jurassic Abu Ghaylan and Bi'r al Ghanam formations. These fluids probably circulated along fault systems (intersection of Al Aziziyah fault and Hun Graben). This interpretation is supported by the limited distribution of saddle dolomite Type-5 in the eastern part of the study area (i.e. close to the fault system).

The timing of Type-5 dolomitization may be evaluated as follows. $\delta^{18}O$ study reveals that the temperature of saddle Type-5 dolomite from the Ain Tobi dolostones reached 64°C. If a Cretaceous surface temperature of 20°C (Hudson and Anderson, 1989), and a regional geothermal gradient of 40°C/1000m (Ben Dhia, 1987) are assumed, a maximum depth of 1300m is required in order to attain a burial temperature of 64°C (1600m considering a normal geothermal gradient of 20°C/1000m). Such a depth corresponds to the total decompacted thickness of the Upper Cretaceous rocks and the overlying Palaeogene (assuming decompaction factors of 20% and 30% for carbonate-sands and

shales, respectively, Soussi and M'Rabet, 1994). Thus, the burial dolomitization of the

Ain Tobi facies may have begun by the end of Palaeocene if not during the Lower

Eocene.

In summary, Type-5 burial dolomitization of the Middle Cretaceous Ain Tobi

carbonates began locally as early as the Upper Palaeocene, and was completed by the

end of Eocene. It is formed by recrystallization of precursor dolomite in the subsurface

environment with a maximum burial (1600m), and temperature of approximately 60°C

possibly by evaporation-concentrated interstitial water from underlying evaporites (Fig.

8.1f).

In general, the low positive $\delta^{13}C$ values of most dolomites suggests a predominant

marine source for the carbon, as expected.

8.3.6. Dedolomitization

Some dolomites are observed to be calcitized in some places mainly in the lower part

of the Ain Tobi Member (close to unconformity surface) and less commonly in the upper

part of the member (in geopetals). The common textures related to dedolomitization are

the presence of rounded dolomite crystals with a core and/or zones replaced by calcite

(replacive calcite) and dolomite rhombs floating in very coarse clean late calcite.

Dedolomitization has been observed only in completely dolomitized levels (e.g. sample

S10-2) or associated with collapse breccias (e.g. sample S9-1).

Calcitization has mainly been ascribed to the effect of meteoric water on dolomites

(e.g. Budai *et al*, 1984; Theriult and Hutcheon, 1987; Holail *et al*, 1988; Khalifa and Abu

El Hasan, 1993). Calcitization in the Ain Tobi dolostones most probably resulted from

the reaction of meteoric water with dolomites and associated anhydrite. This may have

depended on constant stratigraphic position of the calcitization on the unconformity

surface; its association with collapse breccias and the geochemical evidence. The persistent occurrence of dedolomitization at levels close to the unconformity at the inner-ramp south-westwards, suggests that the fluctuation in sea level prevailing during deposition may be responsible for the exposure of the dolomites. During exposure, percolation of meteoric water was active and dissolving dolomites and anhydrites gave rise to the dedolomitization. The subaerial exposure is documented by the presence of some brecciation (sample S9-1). Moreover, the common occurrence of intra- and intercrystalline porosity indicates the continuous flow of meteoric water through permeable dolostones.

Furthermore, isotopic compositions of dolomite, replacive calcite and late calcite define distinct fields demonstrating that the petrographic groupings do, in fact, reflect different genetic processes (Fig. 7.13 and Table 7.5).

Early and late replacive calcites exhibit similar carbon isotope and different oxygen isotope compositions. On the basis of these data, two conclusions can be drawn concerning replacive and late calcites. First, that early calcite and late calcite are chemically different and they were precipitated under different conditions. Second, the range of oxygen isotopic compositions of replacive calcites, in conjunction with field and petrographic data indicate an early origin for replacive calcite precipitated on the unconformity surface, suggesting that this phase was precipitated in a diagenetic environment of mixed marine-meteoric water. On the other hand, field, petrographic observations and light oxygen isotopic compositions of calcite precipitated within geodes in the top of the sequence (average -7.25‰) suggest that this phase was precipitated during later stages under the influence of freshwater. Moreover, trace element composition is generally low in both phases. Fe contents in replacive calcite is lower than
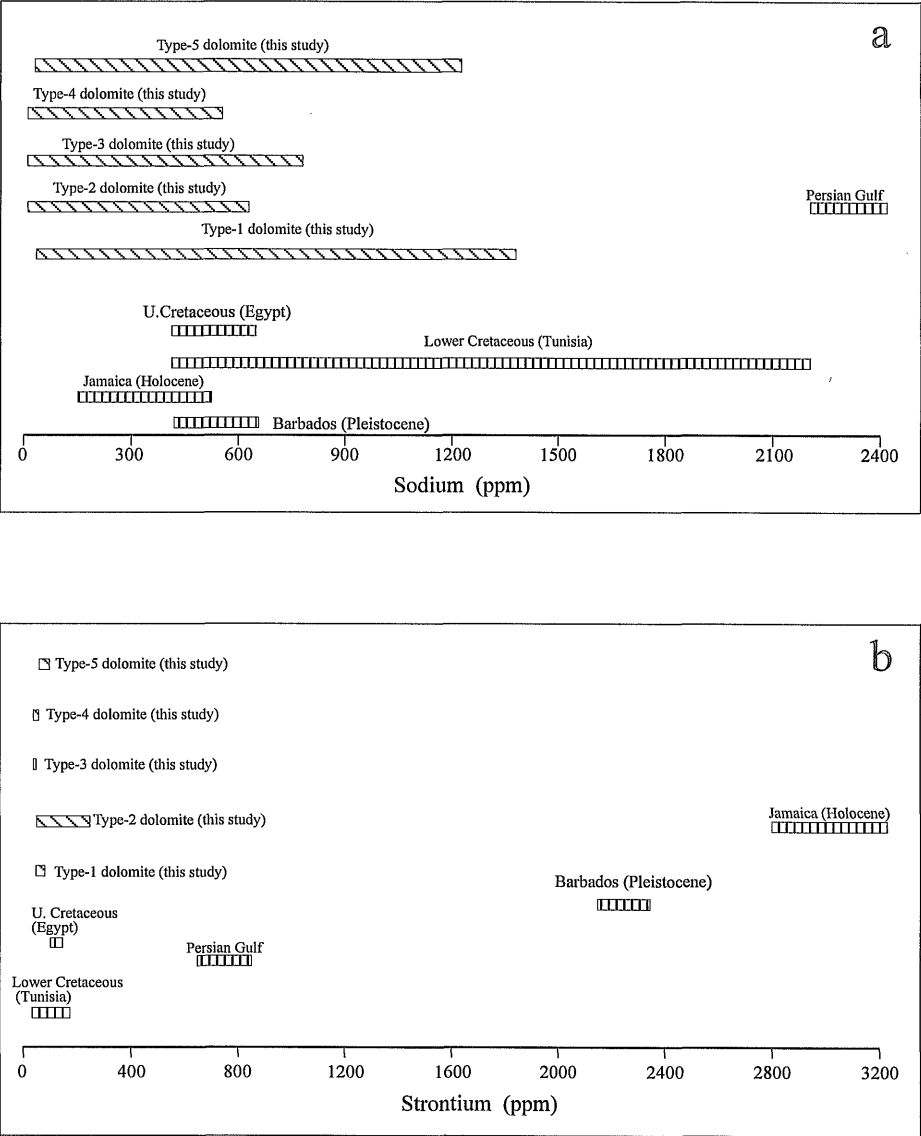
Fig. 8.4. Sodium and strontium comparision plots. a). The range of sodium concentrations of the Ain Tobi dolostones in comparision with other dolomites. b). The range of strontium compositions of the Ain Tobi dolostones in comparision with other dolomites. [Data from M'Rabet, 1981 (Tunisia); Land, 1973 (Jamaica Holocene); Land & Hoops, 1973 (Persian Gulf); Humphrey, 1988 (Barbados Dolomites); Holail et al, 1988 (Egypt)].

late calcite, whereas Mn shows reciprocal contents. These are consistent with the observation that early replacive calcites (dedolomites) display complex luminescent zonation and no luminescence in the late calcite phase. Sr concentration in the early calcite phase is high (average 162 ppm) compared to late calcite (average 98 ppm). The source of strontium in the dedolomite phase may be from nodules of anhydrite now represented by breccias that are associated with dolomites (Budai *et al*, 1984).

In summary, early replacive and late replacive calcite phases (dedolomitization) observed only in completely dolomitized intervals and/or associated with breccias. The early replacive calcite occurs close to the unconformity surface and took place early near-surface in mixed marine and meteoric water during fluctuation in sea level. The source of Ca and Sr may be dissolution of metastable dolomites and anhydrites associated with it. The other calcite phase precipitated in later stages near-surface under the influence of freshwater at low temperature, which is capable for removal of major and minor elements.

8.3.7. Magnesium source

The only major source of magnesium for early and intermediate near-surface dolomitization such as Type-1, Type-2, Type-3, and Type-4 dolomites may be seawater (Land, 1985). However, Mg absorbed on biogenic silica (Machel and Anderson, 1989) associated with Type-3 dolomite may account for an extra Mg source for this type of dolomitization.

Magnesium for deeper-burial dolomites such as Type-5 can be supplied from pressure dissolution (stylolitization), connate waters (trapped seawater), compaction of underlying shales (Mattes and Mountjoy, 1980), basinal brines or dissolution of precursor dolomites (Lee and Friedman, 1987; Land *et al*, 1987; Machel and Anderson,

1989). Pressure dissolution source is not important here because no stylolitization is observed in Type-5 dolomite. Connate water source is not possible because it can only provide a limited amount of Mg to sediments (average thickness of Type-5 dolomite is 25m) and it is possible that the composition of connate water may change or be modified as diagenesis of sediment proceeds. Land *et al* (1987) have shown that shale diagenesis can cause the precipitation of ferroan dolomite or ankerite. Shale compaction as Mg-source for Type-5 dolomite is not possible because of two reasons: 1) absence of underlying shale sequences, 2) dolomite Type-5 is non-ferroan. It therefore, seems possible that dissolution of earlier dolomite generations by reactive basin-derived fluids could provide the Mg necessary for later generation (Type-5). This is consistent with petrographic observations where crystals of dolomite Type-5 replaced earlier and euhedral dolomite. The later have been partially and/or completely dissolved (Fig. 7.9c).

8.3.8. Lateral variation in $\delta^{18}O$ and $\delta^{13}C$ of Ain Tobi dolostones

$\delta^{18}O$ values range from a maximum of -1.50‰ to a minimum of -4.43‰ PDB, and a general decrease in $\delta^{18}O$ is observed eastward. Mean values vary from -1.98‰ in the west to -3.19‰ in the east. $\delta^{13}C$ values increase eastward, ranging from a minimum of -1.39‰ to a maximum of +2.99‰ PDB. Mean values vary from 0.18‰ in the west to 1.19‰ in the east.

The variations observed in $\delta^{18}O$ are likely to represent reflection of temperature of initial formation of dolomites, reflection of temperature of dolomite recrystallization or combination of both factors. A variety of diagenetic reactions can affect the original composition of oxygen isotope in the pore water. Precipitation of dolomite could theoretically cause the pore water $\delta^{18}O$ to decrease slightly (Malone *et al*, 1994), but this process is insignificant during early diagenesis. Recrystallization of marine sedimentary

carbonates at temperature greater than 15°C could lead to a small increase $\delta^{18}O$ of the pore waters (Lawrence *et al*, 1975). However, there is a decrease in dolomite $\delta^{18}O$ eastward and, therefore, any potential variation in $\delta^{18}O$ of the pore waters as a result of carbonate diagenesis had a minimum effect on the observed variation in the $\delta^{18}O$ composition of the dolomites. The $\delta^{18}O$ variations could reflect variations in temperature of initial formation of the dolomites. This explanation would require that dolomite formation occurred deeper in the east than in the west. This is consistent with the proposal palaeoenvironment model (ramp) for the Ain Tobi which becomes deeper and thicker towards the northeast. Furthermore, dolomite formed in the eastern part of the study area has more negative $\delta^{18}O$ and subsequently higher temperature of formation than in the western part (Fig. 8.2).

I believe that the variation in the $\delta^{18}O$ compositions of the dolomites are the result of combination of both factors; temperature of initial formation of dolomite and the extensive recrystallization at the higher temperatures that are prevalent during burial diagenesis in the eastern area. The later interpretation is consistent with the high temperature formation of saddle dolomites in the eastern part of the study area and its absence in the western area. The increase of $\delta^{13}C$ values eastward may reflect that the sedimentation rates were higher (Malone *et al*, 1994) in the east towards the basin centre. I believe that the progressive recrystallization of dolomite eastward with increasing burial and higher rate of sedimentation, are the main reasons responsible for decreasing $\delta^{18}O$ and increasing $\delta^{13}C$ values in the same direction for at least most of the Ain Tobi dolostone.

In summary, recrystallization of Ain Tobi dolostones and increasing burial eastward are responsible for their present $\delta^{18}O$ and $\delta^{13}C$ signatures.

8.3.9. Role of Fe and Mn in luminescence

From the microprobe date it seems that Mn is the source for luminescence, Fe quenches luminescence. The zoned dedolomitized sample shown in (Fig. 7.7d) was analysed by microprobe. All zones in a single crystal have low Fe concentration (average 148 ppm) and ranges from 54 to 311 ppm and low Mn concentration (average 178 ppm) and ranges from 23 to 332 ppm. From the above data, the luminescence is independent of absolute concentration of Fe and Mn, but it depends on the Fe/Mn ratio (Fig. 8.3e) (Henning *et al*, 1989, Allan and Wiggins, 1993). Small changes in this ratio have been observed to produce large variations in luminescence within a single crystal (Fig. 8.3e).

At Fe/Mn ratios of above 1.5 the zone shows no luminescence or dull (zone C in Fig. 8.3e) and the zone is moderately luminescent when the ratio is between 0.5 to 1.5 (zone B in Fig. 8.3e), but if the ratio is less than 0.5 the zone shows bright luminescent (zone A in Fig. 8.3e), provided that Fe concentration does not exceed more than 3000 ppm. Because luminescence properties are lost when Fe contents are more than 3000 ppm regardless of the concentration of manganese. A similar observation was made for calcite by Henning *et al* (1989). Meyers (1974) suggest that the minimum of Mn^{+2} required in order to produce a detectable luminescence is 1000 ppm. In this study the Mn concentration required to produce luminescence is well below that. Actually, as little as 70 ppm is found to be sufficient to produce luminescence emission provided that the Fe/Mn ratio is less than 0.5. In fact, all bright luminescence zones contain between 200 to 300 ppm Mn and moderately luminescent zones contain 70 to 300 ppm Mn. A similar conclusion is suggested by Pierson (1981).

Variations in the Fe/Mn ratio are caused by changes in the supply of Fe and Mn to the pore water, in the oxidation state of pore water, and in the H_2S content of the pore

water. In the Ain Tobi dolomites, Fe/Mn ratio at rims of all dolomite types is higher than

in the cores. These rims or outer zones show no or dull luminescence and are interpreted

as products of recrystallization or cementation during later time (e.g. Type-4 dolomite).

These rims are less calcian and contain lower $MgCO_3$ than the cores. This confirms the

instability and earlier formation of the interior of most dolomite types. These

characteristics may be taken as evidence to differentiate between early replacive dolomite

(more calcian, low Fe and high Mg) and recrystallization or cementation (less calcian,

high Fe and low Mg).

8.4. Conclusions

Petrographic and geochemical data suggest that dolomitization of the Ain Tobi carbonates took place in 1) reflux, 2) near-surface mixed-water, 3) shallow burial mixed-water, and 4) deeper burial environments which overlapped in time and space to form a platform-scale dolostone body composed of complex mixture of dolomites.

Dolomite Type-1 formed in the near-surface early diagenetic stage under the influence of refluxing brines that have $\delta^{18}O$ less than zero. The overlying sabkha sediments of Yifran Member is the source of the dolomitizing brines. Type-1 dolomite is the most common type in the Ain Tobi dolostones. Type-2 dolomite is early and clearly replacement dolomite of high-magnesium packstone and grainstone facies. It precipitates near-surface from mixed marine-meteoric solution. Type-2 dolomite is not widely distributed and is limited to grain-supported facies. Type-3 dolomite is observed mainly in the lower part of the Ain Tobi Member. It is formed in the intermediate diagenetic stage after burial that post-dates Type-1 and Type-2 dolomites and predates Type-4 and Type-5 dolomites. It is suggested that dolomite Type-3 formed near-surface in the zone of mixed marine and meteoric water that has a different degree of mixing from the zone where dolomite Type-2 was formed. Its high Fe contents were probably derived from the associated clastics. Dolomite Type-4 represents recrystallization of precursor metastable dolomites (Type-1 and Type-2) in the intermediate to late diagenetic stage (long lasting dolomitization). It is interpreted that dolomite Type-4 formed under the influence of mixed marine-meteoric conditions in a shallow burial and slightly elevated temperature. Type-4 dolomite is the second most common type among the Ain Tobi dolostones. Type-5 dolomite occurs only in eastern parts of the study area. This dolomite type probably began locally as early as Upper Palaeocene, and was completed by the end of

Eocene. It is formed in the subsurface environment under the influence of evaporation-concentrated interstitial water from the underlying evaporites at deeper burial and high temperature.

The distribution of dolomite types shows that reflux and shallow burial mixed-water dolomitization formed the most regionally extensive and thickest dolostones. Near-surface mixed-water and deeper burial dolomites are more restricted in distribution.

The early and late replacive calcite phases or dedolomitization are observed only in completely dolomitized intervals. Early replacive calcite occurs close to unconformities and is associated with breccias under the influence of mixed water during fluctuations in sea level. Late replacive calcite precipitates in the upper part of the Ain Tobi carbonate sequence under the influence of freshwater.

A magnesium source for the early and intermediate Ain Tobi dolomite phases may be seawater (Land, 1985) and dissolution of precursor dolomites could provide the Mg required for the late burial phase. The lateral variation in oxygen and carbon isotopic composition of the Ain Tobi dolostones suggests increasing depth and temperature towards the northeast.

It has been found that the Fe/Mn ratio affects the degree of luminescence within dolomites. Fe/Mn ratio < 0.5 produces bright luminescent provided that the Fe content does not exceed 3000 ppm. Fe/Mn ratio between 0.5 and 1.5 produce moderate luminescent whereas, ratios above 1.5 show no luminescent. This study documents that as little as 70 ppm Mn are sufficient for luminescence; if the Fe/Mn ratio is less than 1.5.

CHAPTER NINE

CHAPTER NINE

9. DIAGENETIC HISTORY

9.1 Introduction

The petrographic relationships described in Chapter 7 can be used to interpret different paragenetic sequences that are recognized in the Ain Tobi carbonates. These sequences are shown in Table 9.1. The paragenetic sequence recorded within the Ain Tobi carbonates includes three generations of replacement dolomites and rare generations of dolomite and calcite cements, in addition to dissolution and calcitization or replacement by calcite (dedolomitization).

Early diagenetic events include the first generation of replacement dolomite (herein referred to as Type-1 and Type-2 dolomites), and nonferroan replacive calcite and early dissolution. This early dolomite is a pervasive phase which replaces all mudstone through grainstone lithologies. An early to intermediate diagenetic phase includes a second generation of replacement dolomite (herein referred to as Type-3). Late diagenetic events include a third generation of replacement dolomites (herein referred to as Type-4 and Type-5 dolomites), replacement by calcite and late dissolution.

9.2. Replacement by dolomite

The Ain Tobi Member has undergone complicated diagenesis. The major diagenetic event that occurred in the Ain Tobi rocks was dolomitization which can change the rock fabric significantly. If the rock has been dolomitized the overprint of dolomite crystals commonly obscures the grain and mud fabric. Grain and mud fabrics in very fine and fine crystalline dolostones are easily recognizable (Fig. 7.3d and 7.4a); however as the crystal size increases, the precursor fabrics become more difficult to determine (Lucia, 1995). Remnants of micrite envelopes (Fig. 9.1c) and micritized grains can be also recognized. These diagenetic phases are among the first to have occurred in the sequence (Bathurst, 1975). The dolomitization of the Ain Tobi rocks produced five diagenetic types of dolomite that are distinguished on the basis of petrography and geochemistry.

9.2.1. Early diagenetic replacement dolomites

Early dolomite makes up approximately from 70 to 95% of all matrix dolomite in the Ain Tobi carbonates, and occurs rarely as cement in primary porosity.

Early dolomites typically form non-porous, tightly interlocking mosaics of fine and very fine dolomite (Type-1 and Type-2). Type-1 dolomite crystals exhibit dark to orange luminescence with dissolved interiors and are variably overgrown by late diagenetic dolomites. Type-2 dolomite has yellow luminescence pattern. It mainly replaced packstone and grainstone facies, whereas rare dolomite crystals have red to brown luminescent appearance and occur within primary pores as cement e.g. intraparticle pores especially in the oolitic dolograinstone facies. Type-2 dolomite is very fine, poorly ordered and calcian-rich which indicates that it is formed in early stages as replacive dolomite.

9.2.2. Early to intermediate diagenetic dolomites

Type-3 shows dark luminescent cores and orange to bright orange outer zones with no porosity. Type-3 dolomite probably formed postburial as indicated by its occurrence within microfractures within the quartz grains which were created by compaction. Furthermore, dolomite Type-3 is variable in composition from near stoichiometric to calcian dolomite which suggest that it is an early to intermediate formed dolomite, but later than Type-1 and Type-2 dolomites.

9.2.3. Intermediate to late diagenetic replacement dolomites

Intermediate to late diagenetic replacement dolomite consists of recrystallized dolomite (Type-4) and saddle dolomite (Type-5).

Type-4 dolomite is medium to coarse with orange luminescent inclusion-rich cores and dull inclusion-free rims. Type-4 dolomite is replacive or overgrown from earlier types. This is indicated by relics of euhedral cores, stoichiometric to calcian and well ordered crystalline. The concentration of Sr, Mn and Fe is low within crystals of this type due to continued recrystallization processes. This may explain the relationship between crystal size and trace element concentration where the coarser the crystal the lower the concentration (Fig. 8.3f). Furthermore, inter-rhomb pores occur predominantly in Type-1 dolomite (Fig. 7.8a); they are rare or absent in Type-4 dolomite. Isolated crystals of Type-4 dolomite have also replaced matrix and allochems which survived earlier dolomitization. They occur as medium, euhedral and isolated crystals.

Because Type-4 dolomite is overgrown within intercrystalline pores it formed after all precursor calcite has been replaced by earlier dolomite (Lucia and Major, 1994). Type-4 dolomite recrystallized from earlier dolomite types and was partially replaced by late calcite and affected by late dissolution (selectively zones between cores and rims are dissolved, Fig. 7.8d). This type is believed to be formed in intermediate to late diagenetic

stages, post-dates Type-1, Type-2 and Type-3 and is condidered to pre-date calcitization and late dissolution. This interpretation is consistent with the wide range of composition from stoichiometric to Ca-rich and well ordered lattice. In cases where sample consists entirely of dolomite Type-4, it is unclear whether dolomite Type-4 was the initial dolomite phase or whether it completely replaced earlier precursor dolomites.

The late, coarse to very coarse saddle dolomite (Type-5) occurs mainly in the eastern part of the study area as a replacive crystalline variety. Elsewhere, it occurs rarely as cement filling voids and moulds. Crystals of saddle dolomite are characterized by euhedral cloudy cores and thin clean rims with irregular dissolution contact between them. Some coarse idiotopic crystals of Type-4 dolomite are partially to completely dissolved out and replaced by coarser saddle crystals (Fig. 7.9c), indicating that Type-5 dolomite post-dates Type-4 dolomite.

Saddle dolomite of the Ain Tobi dolostones has low Fe, Mn and Sr concentrations and is always calcian-rich and well ordered suggesting late stage formation. Oxygen and carbon isotopes of saddle dolomite are very light values compared to other dolomite types indicating the influence of high temperature during deep burial of the fluid involved in generation of this type of dolomite (Radke and Mathis, 1980). It was suggested previously (Chapter 8) that saddle dolomite from the Mid-Cretaceous Ain Tobi dolostones probably began as to develop early as the Upper Palaeocene, and was complete by the end of Eocene.

9.3. Dissolution

9.3.1. Early Dissolution

This regional dissolution is thought to be the event which is responsible for removing previously formed evaporite minerals and generation of mouldic and intracrystalline porosities by dissolving nonstable minerals such as high magnesium calcite allochems and

aragonite. Some intraparticle and mouldic porosity are partially filled by late nonferroan

calcite cement. This early dissolution is less effective than the late dissolution and may

serve as one of events producing the Mg necessary for intermediate types dolomitization.

9.3.2. Late Dissolution

Late dissolution of dolomite and calcite resulted in different crystals with textures

including debris of dolomite crystals, dolomite crystals with cores and Fe-rich zones

being removed. Although dissolution may have continued from the early dissolution

episodes resulting micropores were enlarged into intracrystalline voids and the whole

crystal was eventually dissolved from the inside outwards. The differences in relative

solubility within single dolomite crystals is due to the poorly ordered and calcium-rich

nature of the core and high iron content of the outer band as pointed out by James *et al*

(1993).

This late dissolution created intercrystalline, mouldic and vuggy porosities by

dissolving micrite matrix, surviving allochems and calcite cement and enlarging

intercrystalline pores respectively.

9.4. Replacement by calcite

Dolomite rhombs have undergone extensive dissolution and replaced by early calcite

or calcitization close to the unconformity beneath the Ain Tobi Member (Fig. 7.7c).

Dedolomitization is manifested by calcite cementation in dissolution pores of the Ca-rich

cores and narrow Fe-rich zones within rhombs. Dolomite crystals which are replaced by

early calcite show complex luminescent zonation.

The dissolution of the interiors of dolomite Type-1 (early) associated with unaffected

dolomite crystals of Type-4 (intermediate) suggest that dissolution of the inner parts of

the Type-1 dolomite is mainly associated with pre-existing intercrystalline pores where

dedolomitized fluids were allowed to reach non-stable cores. Type-4 dolomite also has

non-stable cores compared with its margins, but the dense impermeable nature of dolomite Type-4 prevented dedolomitized fluids having free access to the cores.

In other samples, however, dedolomitization was not zone-selective, and both entire rhomb and outer growth dolomite have been replaced by late calcite (Sibley, 1982; Holail *et al*, 1988). These dedolomite-related calcites, exhibit dull cathodoluminescence zonation, occur both as a cement in dissolved cores of rhombs and in intercrystalline pores within the dolomite (Fig. 9.1a), and as the replacive phase in optical continuity with dolomite substrates in dedolomite (Fig. 9.1a). The unreplaced dolomite zones of these rhombs show bright luminescence.

The timing of the dedolomitization process is not established exactly, but dissolution of cores of Type-1 dolomite suggests that replacement by calcite was probably early. The rare replacement of rims of Type-5 dolomite and light oxygen isotope composition of the replacive calcite suggest that calcitization may have taken place at an intermediate to late stage.

9.5. Porosity types and development

The relationship between dolomitization and microscopic porosity is such that dolomitization may decrease the porosity of precursor carbonates, because of crystal overgrowth within primary pore space. Where dolomitization occurs during burial, mechanical compaction may also reduce porosity.

Dolomitization may redistribute pre-existing pore space but not necessarily increase or decrease it (Purser *et al*, 1994). Intercrystalline porosity is the most typical porosity form in dolomite rocks and its origin has often been assumed to result from the dolomitization process (Purser *et al*, 1994). This intercrystalline porosity may also be enlarged by dissolution associated with dolomitization to create vugs.

9.5.1. Porosity Types

The most common porosity types (Choquette and Prey, 1970) are: 1. Non-fabric selective and 2. Fabric selective.

1. Non-fabric selective: This includes vuggy and channel porosity. Vuggy porosity is common in the dolowackestone through dolograinstone facies (Fig. 7.4b and d), where it occurs mainly as a result of dissolution enlargement of intercrystalline and/or micromouldic porosity. The size of the vugs varies from small (300μm) to a few millimetres. The shape is usually irregular. This porosity is locally occluded by the precipitation of late stage minerals such as dolomite and calcite.

Channel porosity in the Ain Tobi dolostones is very rare, where millimetre to centimetre wide, irregular channels are encountered (Fig. 9.1b). The channels are not occluded by any late minerals precipitation, but cut all phases of dolomitization and cementation.

2. Fabric-selective porosity: This includes intercrystalline and intracrystalline, interparticle and intraparticle and oomouldic porosities. Intercrystalline porosity is the most common type within the Ain Tobi dolostones. It occurs mainly in mosaics of planar-e and planar-s dolomites (Fig. 7.3a, b and Fig. 7.8d) and it is characteristic of the dolomudstone and dolowackestone facies. In some cases this intercrystalline porosity has been dissolution enlarged to produce vugs.

Intracrystalline porosity is common within Type-1 dolomite and less commonly occurs within Type-4 and other types. It occurs mainly as a result of dissolution of unstable or high-calcium cores and narrow zones of dolomite rhombs (Fig. 7.4d, 7.7d and 7.8a). The contact between dissolved interior and rims of the crystal is usually irregular. Some of the intracrystalline pores are occupied by late replacive calcite.

Intraparticle porosity is not common, but occurs within ooids in the oolitic dolopackstone and dolograinstone facies (Figs. 7.3c & d; 7.9a & b). It occurs mainly as a result of primary or early dissolution of parts of ooid nucleus or concentric layers.

Interparticle porosity occurs commonly between allochems of grain supported facies such as oolitic dolopackstone and dolograinstone (Figs. 7.3d and 7.4a).

The sizes and shapes of the interparticle pores are controlled by the sizes and shapes of the grains themselves and by the ways in which the grains are arranged in the mosaic. Interparticle porosity may be reduced by later diagenetic events , such as cementation and compaction. The well preserved primary interparticle or intergranular porosity is characteristic of dolomite formed in high-energy subtidal or lagoon environments (Sun, 1995; McLane, 1995).

The last type of porosity occurs within the Ain Tobi dolostones is oomouldic. It occurs commonly with oolitic dolopackstone/dolograinstone facies (Fig. 9.1c). Oomouldic secondary porosity is one of the most important pore types in the middle and lower parts of the Ain Tobi Dolostone Member. It is formed by the dissolution of high-Mg ooids. Ooid dolograinstones with some preserved primary pore space, in addition to oomouldic porosity, have high porosity and permeability (Figs. 9.1c and 7.9a & b).

9.5.2. **Porosity Developments**

Dissolution and dolomitization are cited to be most important for porosity developments in the Ain Tobi Dolostone Member. Dolomitization is associated with the development of secondary porosity because dolomitization pre- and post-dates dissolution and corrosion, and no secondary porosity generation occurred in limestone samples. The most common porosity types observed within the Ain Tobi dolostones are intercrystalline and vuggy.

Fig. 9.1. Example of late replacive calcite, dedolomitization, fabric and non-fabric selective porosity in the Ain Tobi Dolostone Member.

a. Photomicrograph showing very coarse blocky calcite cement (C) filling intercrystalline porosity (P) and replacing outer margins of the dolomite crystals (D). Sample S4-12B (Wadi Jabar Section). ppl.

b. Photomicrograph showing channel porosity (C) cross-cuting early dolomite as well as late calcite cement (white). ppl view from sample S6-16 (Ar'Rabtah Section).

c. Photomicrograph showing oomouldic porosity (O) within pellet dolopackstone/dolograinstone facies. Sample S8-9 (Riaynah Section), ppl.
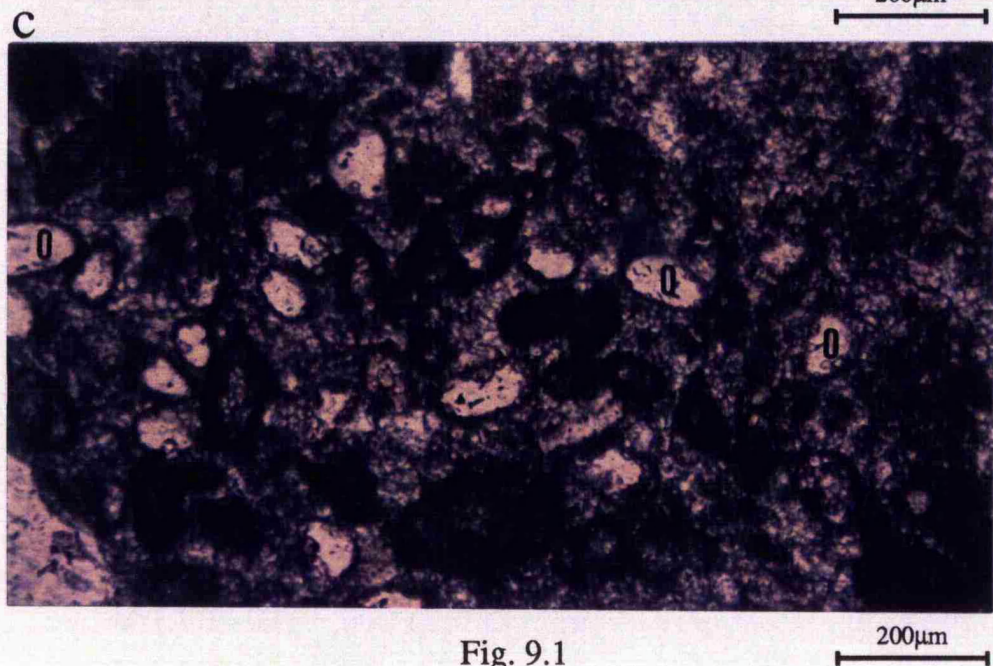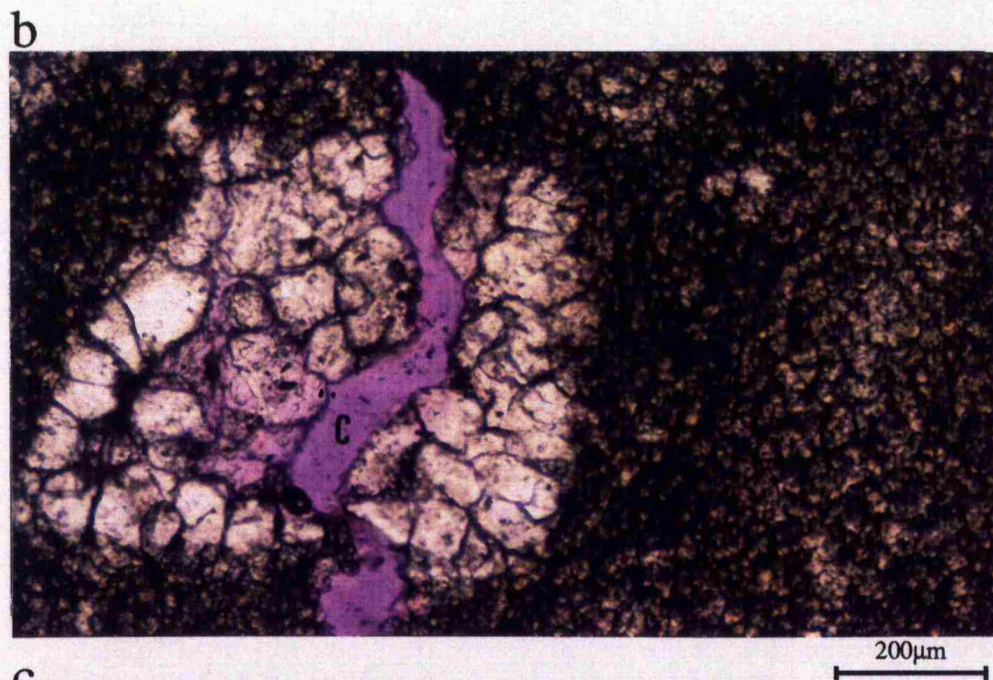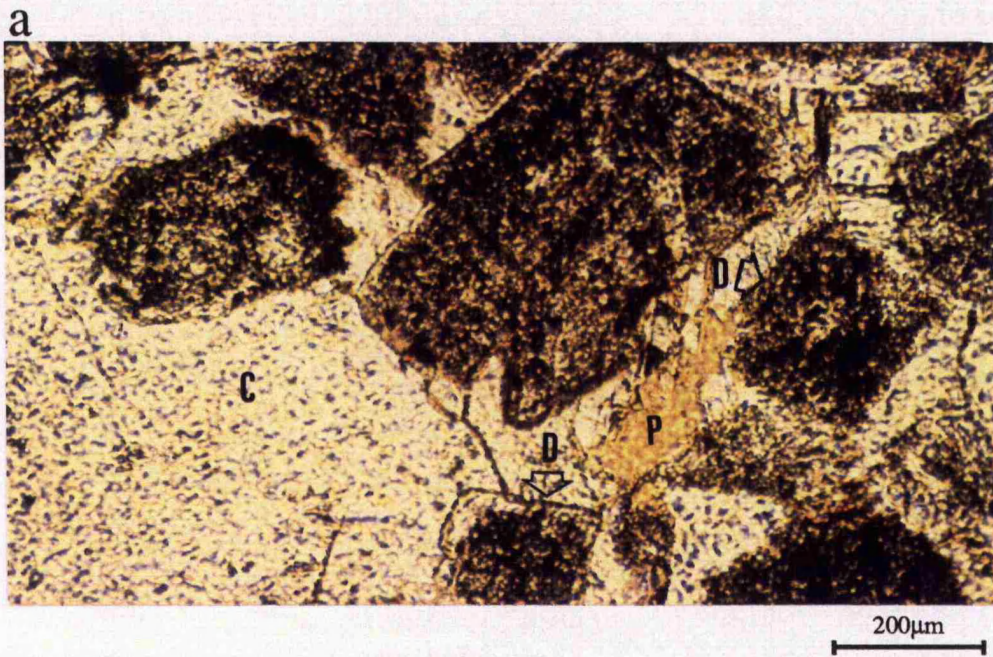
Fig. 9.1

The non-fabric selective vuggy porosity was formed by dissolution of calcite, followed by dolomitization of the precursor sediments. Dissolution and corrosion of medium and coarse dolomite crystals are observed using cathodoluminescence, indicating that in many examples dolomite has been dissolved (Figs. 7.7d; 7.8d),

Intercrystalline porosity is also of importance within Ain Tobi dolostones (Figs. 7.3a, b and 7.8d), where it occurs mainly in planar-e or euhedral crystalline fabrics and planar-s or subhedral crystalline fabrics of dolomite Type-4. This intercrystalline porosity is in many cases solution enlarged and become vuggy porosity. Both vuggy and intercrystalline porosity are partially or totally occluded by late calcite or non-planar dolomite cements.

Dissolution events can be related to invasion of freshwater resulting in undersaturated fluids with respect to dolomite. Dolomite, leaching, and secondary porosity development are associated in the Ain Tobi Dolostone Member.

9.6. Summary

Type-1 dolomite stoichiometry, crystal ordering and crystal size all suggest that Type-1 dolomite is early or penecontamporaneous with deposition. Type-1 dolomite apparently predates dissolution as indicated by leaching of cores of its crystals. Type-2 dolomite predates compaction and formed in the early stages after deposition as indicated by the preservation of primary texture. Type-2 is calcian-rich, poorly ordered and very fine crystalline. These features further support its formation in early stages. Type-1 dolomite replaces mudstone to wackestone facies whereas Type-2 dolomite replaces packstone and grainstone facies.

Type-3 dolomite post-dates mechanical compaction as indicated by its occurrences within fractures which resulted from compaction on the surface of quartz grains. Type-4 dolomite was a continuous form of dolomitization from the intermediate to late stage and was recrystallized from earlier dolomites, most probably Type-1 dolomite. Type-4 dolomite is medium to coarse with cloudy cores and clean rims, well ordered and nonstoichiometrically crystalline. It is characterized by patchy orange luminescent cores and dull rims. All these features suggest that Type-4 dolomite has been recrystallized from precursor finer dolomites. Furthermore, trace element concentrations within Type-4 are depleted relative to earlier fine grained material indicating modification during recrystallization.

Type-5 dolomite is the youngest among the Ain Tobi dolomites and formed in the late stages by the influence of high temperature in deep-burial. This is indicated by the crystal shape and size of Type-5 (subhedral and very coarse with extremely undulose extinction). The low concentrations of trace elements, the presence of well ordered and calcium-rich dolomite as well as oxygen and carbon isotopes also indicate that Type-5 dolomite formed during the later stages during deep-burial. Trace elements and

DIAGENETIC PROCESS	EARLY	LATE
Micrite envelopes	▨	
Micritization	▨	
Dolomite Type-1	▤▤▤	
Dolomite Type-2	▤▤▤	
Mechanical compaction	? ▤▤▤ ?	
Dolomite Type-3	▤▤▤▤▤	
Dissolution and early calcitization	▤▤▤▤▤	
Dolomite Type-4 (recrystallization)	▤▤▤▤▤▤▤	
Dolomite Type-5 (saddle dolomite)		▤▤▤▤▤
Late replacive calcite		▤▤▤
Channel porosity		▨
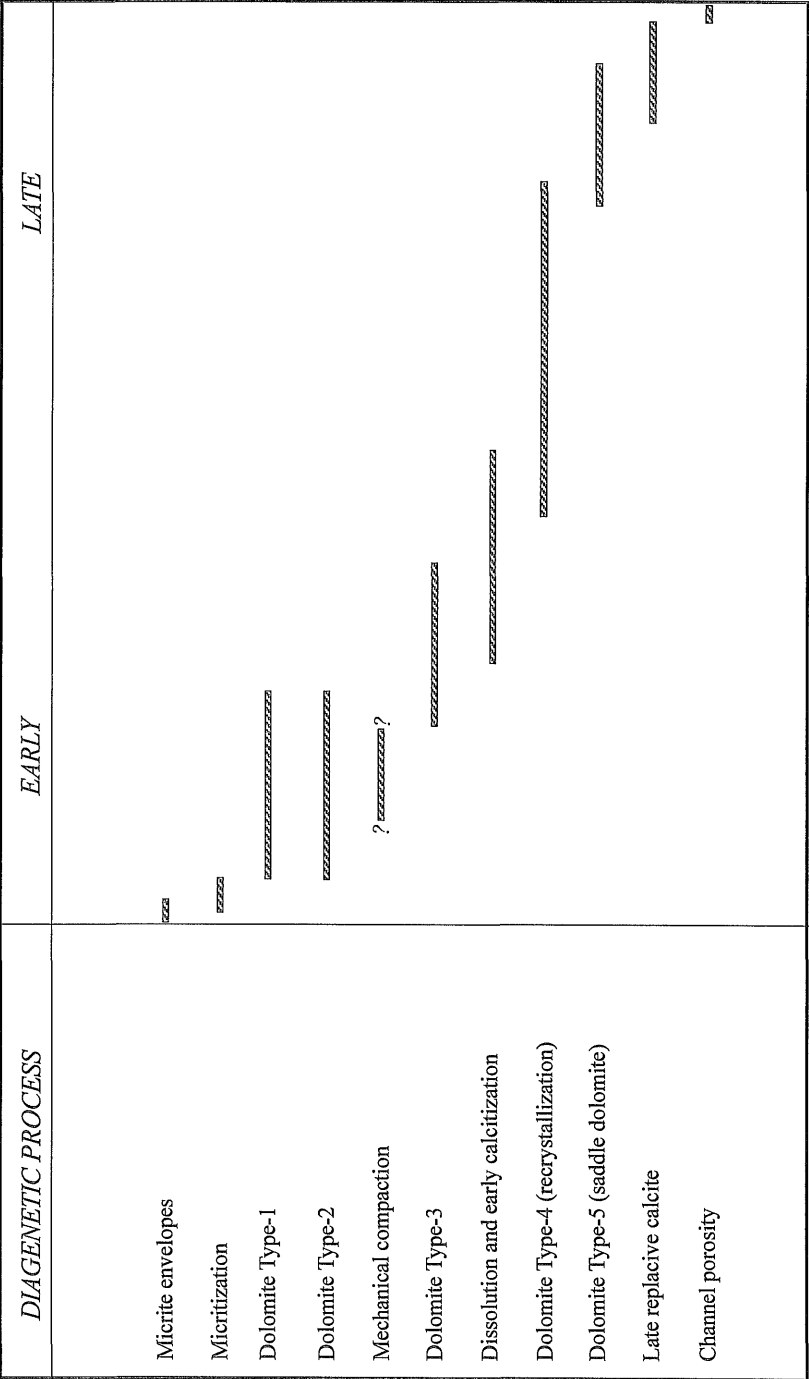
Table 9.1. Schematic sequence of the most important diagenetic events within the Ain Tobi dolostones in NW Libya

stoichiometry within a single crystal of Type-5 saddle dolomite is shown in (Fig. 7.11).

Stoichiometry and Sr concentration decrease towards the margin, whereas Mn, Fe and

Mg increase.

CHAPTER TEN

CHAPTER   TEN

10. LITHOSTRATIGRAPHIC CORRELATION OF THE SIDI AS SID FORMATION WITH THE LIDAM FORMATION AND HYDROCARBON POTENTIAL

10.1. Correlation with the Lidam Formation in Sirt Basin

The Lidam Formation of the Sirt Basin is an example of a carbonate shallowing sequence that is similar to the Sidi as Sid Formation. The Lidam Formation is considered to be part of the Upper Cretaceous system, and approximately Cenomanian in age (Barr and Weegar, 1972). The Lidam Formation is found in the subsurface and widely distributed in the Sirt Basin; the Sidi as Sid Formation is well exposed along the Jabal Nafusah escarpment and it is subsurface in the Ghadamis Basin. The Lidam Formation as characterized by El-Bakai (1989) consists of three facies that resulted from changes of sea level. The first facies is composed of laminated and bioturbated wackestones and dolowackestones commonly with an open marine fauna and is interbedded with levels of sandstone and glauconite.

A significant fall in sea level resulted in the deposition of the second facies. This consists of high-energy ooidal-peloidal slightly dolomitized grainstones. The third facies is composed of wackestone/packstone, anhydrite and fine dolomite. A large quartz and clay lenses is present in this interval.

The Sidi as Sid Formation seems to contain the same sediments, textures and structures found in the Lidam Formation. Both formations represent shallowing upward sequences. The lower member of the Sidi as Sid Formation (Ain Tobi Dolostone Member) is similar to the first and second facies of the Lidam Formation. Although the Ain Tobi has lost much of the faunal data due to extensive dolomitization. The upper member of the Sidi as Sid Formation (Yifran Member) is more restricted and of a shallower environment and is similar to the third facies of the Lidam Formation.

The depositional environment for the Lidam Formation is divided into three ramp-lithofacies (El-Bakai, 1989, 1992). Some of the rock types in the three facies exhibit many of the shallow shelf structures found in the Sidi as Sid Formation.

A limited comparison can be made between the Lidam oolitic shoal and the *Ichthyosarcolites* Band of the Ain Tobi Member. These intervals in both the Lidam Formation and Ain Tobi Member consist of small scale cross-bedded oolitic grainstones and dolograinstones respectively. Rudists observed within the Ain Tobi are not present in core samples taken from the Lidam Formation. The fauna is recognizable in the Lidam Formation, but not in the Ain Tobi Member because of the extensive dolomitization.

Dolomite types of the Ain Tobi are similar to those types found in the Lidam Formation. Two mechanisms are involved in the formation of the Lidam dolomite types; they are reflux and deep-burial models (El-Bakai, 1989). The Ain Tobi dolomite types are more extensive and complicated where more than two mechanisms were responsible

for their formation (Chapter 8). All dolomite types of the Ain Tobi Member are non-ferroan unlike dolomite types of the Lidam Formation which are ferroan and occur as a cements (deep burial dolomites) and non-ferroan dolomites (reflux dolomites).

10.2. Hydrocarbon Potential

The potential for significant hydrocarbon accumulations in the Sidi as Sid Formation is low. Porosity in the Ain Tobi Dolostone Member is of reservoir quality at the surface and whenever the member has been penetrated in the subsurface south of the Libyan-Tunisian coast. The Yifran Marl Member contains sufficient shale or evaporite material to act as an updip seal in the same area. However, the potential for hydrocarbon accumulation is low because of the following reasons: 1) no source beds are present in the onshore Cretaceous section and 2) lack of suitable structures. With respect to the absence of structures, the Ain Tobi Member has been eroded over the Jifarah Plain and the Mesozoic part of the Ghadamis Basin is a syncline.

The potential for hydrocarbon accumulations in the offshore is also low. In the offshore the Sidi as Sid's equivalent is, in general, buried too deep to be a drillable prospect. If the Sidi as Sid's equivalent can be found in shallower depths source rock becomes a problem. Again, in the offshore no source beds are known in rocks of Cretaceous age.

In contrast, the Sidi as Sid Formation's equivalent in the Sirt Basin (Lidam Formation) represents a producing zone in the central and extreme eastern parts of the basin (Dür-Mansür and Masrab Oil Fields respectively). In these parts of basin the Lidam Formation is found on depositional platforms. It is affected by late diagenesis such as dolomitization wich increases porosity. The Lidam Formation within troughs is mainly shale and along with the Sirt Shale they might act as source rock for these reservoirs.

The Lidam Formation in the western part of the Sirt Basin deposited in the deepest part of the Az Zahrah-Al Hufra Platform. It is composed of mudstones through well cemented grainstones, partially dolomitized with common occurrence of stylolites and low porosity; thus it is not prospective target.

CHAPTER ELEVN

CHAPTER ELEVEN

11. CONCLUSIONS

1. The lower member of the Sidi as Sid Formation (Ain Tobi Member) is composed entirely of dolomite and dedolomite. It has previously been described as being composed of dolomitic limestone. Therefore, this member is re-named in this study as the "Ain Tobi Dolostone Member".

2. The thickness of the Ain Tobi Member increases towards the northeast.

3. The sedimentary environment of the Ain Tobi Member is a ramp. This ramp can be divided into three depositional environments from the southwest to the northeast:

a. A restricted or lagoon ramp which represented by the Yifran Member in southern Nafusah uplift and in the Ghadamis Basin. Lithologies and textures include marl, marly limestone, dolomitic limestone, solution breccias, gypsum and rare fauna.

b. An open to semi-restricted ramp is represented by the Ain Tobi Member in Jabal Nafusah and Ghadamis Basin. It is laminated and bioturbated dolomudstones through dolograinstones.

c. A mid-ramp or ramp margin, thought to be deposited parallel to the present coast line. This part of the ramp was removed by the post-Cretaceous erosion. The outer ramp deposits are represented by the Sidi as Sid's equivalent Alalgah Formation. It includes laminated dolomitic marls and pelagic foraminifera.

4. Petrographic and geochemical data suggest that dolomitization of the Ain Tobi carbonates took place in early through late diagenetic stages as follows:

a. Type-1 dolomite formed early by reflux model and the overlying Yifran Member acted as a source for dolomitization brines.

b. Type-2 dolomite formed early or near-surface by mixed marine-meteoric pore waters.

c. Intermediate Type-3 dolomite formed after burial later than Type-1 and Type-2 but pre-dated Type-4 and Type-5 dolomites, by varying degrees of mixing between meteoric and marine waters from those involved in the formation of Type-2 dolomite.

d. Intermediate to late Type-4 dolomite formed by recrystallization or overgrowth on earlier types under the influence of mixed marine and meteoric water at shallow burial and medium temperature.

e. Type-5 dolomite (saddle dolomite) formed late and probably began in the Upper Palaeocene. It was completed by the end of Eocene. It is formed in the subsurface at elevated temperature.

5. Two phases of replacive calcite occur in the form of dedolomitization. The first phase replaced cores and zones of dolomite crystals in the early diagenetic stages. It was formed in the lower part of the member close to the unconformity under the influence of a mixed marine and meteoric water regime. The second phase replaced rims or entire dolomite crystals at a late stage. It was formed in the top of the member under the influence of freshwater as indicated by the light isotopic composition.

6. It has been found that Fe/Mn ratio of the dolomites reflects the luminescence degree and as little as 70 ppm Mn is sufficient to create luminescence.

APPENDECIES

APPENDIX 1

Details of the method used for Cathodoluminescence Microscopy and details of the XRD method and precision

1. Cathodoluminescence Microscopy (CL)

200 polished thin-sections from the Ain Tobi Dolostone Member were examined by Technosyn Cold Cathodoluminescence Model 8200 Mark II. Operating conditions were 16-20 kV gun potential, 420µA beam current, 0.05 Torr vacum and 5mm beam width.

The luminescence is produced when atoms absorb one form of energy and emit energy as visible light. Cathodoluminescence is produced from the absorbed energy produced by an electron beam. Many materials luminese when excited in this manner (Smith and Streastrom, 1965). The colour of emitted radiation tends to remain constant for the range of voltages used in cathodoluminescence (10 to 20 kV).

2. X-ray Diffractometer

153 samples from Ain Tobi Member were crushed into 5mm or less size using a fly press. These samples were ground into 50µm or less size using the Tungsten Carbide Tema Mill (T100) for 30 seconds. The samples were finally micronized or reduced in size to 5-10µm by McCrone Micronizing Mill Model Ompron H3BA for about 10 minutes and dried in a furnace at 100°C for overnight.

A Philips PW 1729 x-ray diffractometer generator attached to PW diffractometer controlled by Sieronics Sie 1710 software running on a Viglen 386 computer were used. The operating conditions were as follows:

X-ray radiation:	Cu κα
Generator voltage and current:	Kv mA 40, 30
Scanning speed:	1°/min. Time constant: 2 seconds
Start position:	2θ End position: 65θ
Count full scale	2000 counts/sec
Tube:	Copper
Filament:	Nickel

One dolomite sample from the Ain Tobi dolomites was divided into two parts; the first part was mixed with 20% wt. pure fluorite prior to analysis. All three samples (pure fluorite, dolomite + 20% wt. fluorite and dolomite) were run at the same time and each replicated three times in order to determine the error in the d-spacing values. The difference in 2θ between standard fluorite and the mixed sample was 0.02. Adding this value to the 2Φ determined by the XRD for the 104 dolomite peak which was (30.907) to become (30.927, 2θ). Using the following equation to calculate the d-spacing for dolomite ($n\lambda = 2d \sin\theta$) the result was 2.891, whereas the d-spacing of the same sample determined by XRD was 2.893. To correct the d-spacing, the difference between the two values (0.002) was subtracted from all d-spacing of the 104 peak for all dolomite samples used in this study. Mole% $CaCO_3$ for dolomite was determined by this equation: Mole% $CaCO_3$ = Md+B; where M is 333.33; B is (-911.99) and d is the d-spacing after correction. Degree of order of dolomite is calculated by dividing the intensity of the peak 015 by intensity of the peak 110 after subtracting the background hight. The accuracy of the instrument in calculation of the degree of order was determined by running the samples mentioned above three times. The minimum was 0.719; maximum was 0.768; mean was 0.748 and two standard deviation (2σ)were 0.052.

APPENDIX 2

Details of the method and precision used for Inductively Coupled Plasma Mass Spectrometry (ICP-ES)

The powdered samples were analysed for Al, Ba, Ca, Fe, Mg, Mn, Na, Sr, and Ti. This was done through the method of Inductively Coupled Plasma Emission Spectrometry (ICP-AES). The following procedure was adopted for preparing and analysing the samples: A weight of 100mg of each sample (79 samples) were used in this analysis. 1ml of concentric hydrochloric acid added to each sample and all samples were placed on hot block at $50^{\circ}C$ and left overnight. Allow the samples to cool and add 9ml of de-ionized water to each sample and mix thoroughly using a "whirly mixer". Allow the sediments (if any) to settle. Samples are now ready for analysis by the ICP.

For each sample, 9 trace elements were measured with a fully computerized ICP-ES (Optical Emission Spectrometer, Philips PV 8060) connected with PC computer and standard software for carbonates were used in this course. In order to know about the possible contamination during the sample preparation process, 4% of the total number included blank samples. The degree of precision and accuracy of the method was quantified by repeating 10% of the analysed samples and including 5% of standard.

The accuracy of the machine is fairly good on international reference materials with approximate degree of precision (as determined by multiple analysis on international reference materials) for the different elements analysed with ICP-Es are as follows:

Element	Al	Sr	Fe	Mg	Mn	Na
Number of analysis	9	9	9	9	9	9
Minimum	9183.173	40.202	7917.758	1985.303	525.978	1199.110
Maximum	9880.739	43.186	8436.546	2134.632	563.978	1255.068
Mean	9532.925	41.811	8143.687	2060.280	542.252	1225.046
Standard deviation	239.974	1.008	164.489	53.645	12.035	21.805

APPENDIX 3

Details of the method and precision used for Microprobe Analysis

Polished thin-sections were carbon coated in order to determine the major elements

using Microprobe instrument JEOL JXA-8600S, with an on-line computer for ZAF

corrections.

The running conditions were as following:

Beam conditions:
Accelerating Voltage	15kV
Probe Current	30nA
Beam Diameter	15μm

Element	X-ray line	Analysing crystal	Count time peak	Count time (-) Bg	Count time (+) Bg	Standard
Ca	Kα	PET	20	10	10	Wollastonite (natural)
Mg	Kα	TAP	20	10	10	MgO (synthetic)
Fe	Kα	LiF	20	10	10	Fe_3O_4 (synthetic)
Mn	Kα	LiF	20	10	10	Rhodonite (natural)
Sr	Lα	PET	20	10	10	Sr_2F (synthetic)
Ba	Lα	LiF	20	10	10	Barite (natural)

The carbonate was analysed for all common major oxides (i.e. CaO, MgO, FeO,

MnO, SrO and BaO) and the amount of CO_2 was calculated by difference. The accuracy

of the ZAF correction is as follow:

The minimum detection limit (MDL) and an estimation of the degree of precision (2σ)

are listed in Table A3.1.

Table A3.1: Minimum detection limit (MDL) (3σ), typical dolomite analysis (TD),
typical calcite analysis (TC) and degree of precision (2σ) for probe analysis.

Oxide	Dolomite			Calcite		
Descr.	MDL	TD	Precision	MDL	TC	Precision
CaO	0.03	31.35	0.24	0.03	56.00	0.36
MgO	0.02	20.08	0.15	0.02	0.20	0.03
FeO	0.04	0.03	0.04	0.04	0.10	0.05
MnO	0.04	0.02	0.04	0.05	0.04	0.05
SrO	0.04	0.02	0.04	0.05	0.05	0.05
BaO	0.13	0.02	0.14	0.17	0.02	0.21

A P P E N D I X 　 4

Details of the method and precision used for Stable Isotopes analysis

Powdered samples from dolomite, dedolomite and mixed dolomite-calcite were analysed at the University of East Anglia by Mass Spectrometry for oxygen and carbon isotopes.

The CO2 was liberated from the samples and analysed (for more details of the method used see Fairchild *et al*, 1988).

To check the quality of the results an internal standard was used at random in with samples. This standard is carbonate (Carrara Marble). The values are presented below:

$\delta^{18}O$	$\delta^{13}C$
-2.181	1.892
-2.078	2.007
-2.025	2.012
-2.069	1.937
-1.996	1.896
-2.004	1.943
-2.096	2.027
-2.056	2.015
-2.065	1.990
-2.023	1.990

The calibrated composition of UFA Carrara Marble is $\delta^{18}O$ = -2.044 and $\delta^{13}C$ = 1.988. The mean composition measured whilst analysing these samples is

$\delta^{18}O$ = -2.059 ± 0.054

$\delta^{13}C$ = 1.971 ± 0.050

These values are in excellent agreement with the accepted composition, so all is in good order.

REFERENCES

REFERENCES

ABATE, B., CATALANO, R., D'ARGENIO, B., DI STEFANO, E., DI STEPHANO, P., LO CICERO, G. AND RENDA, P. (1977). Facies Analyais and Tectonics of Western Sicily: *A Five Day Field Trip From Palermo to Sciacca, Palermo, 12-17 July, 1977, Institute de Geologica, Palermo, Instituto de Geologica e Geofisica, Napoli*: 38p.

ADAMS, A. E., MACKENZIE, W. S. AND GUILFORD, C. (1984). Atlas of Sedimentary Rocks Under the Microscope. *Halsted Press, John Wiley and Sons Inc., U.S.A.*: 104p.

ADAMS, J. E. AND RHODES, M. L. (1960). Dolomitization by Seepage Refluxion. *Bull. Am. Ass. Petrol. Geol., 44:* 1912-1920.

AHR, W. M. (1973). The Carbonate Ramp - An Alternative to the Shelf Model. *Trans., Gulf Coast Ass. Geol. Soc., 23:* 221-225.

ALLAN, J. R. AND MATTHEWS, R. K. (1982). Isotope Signatures Associated with Early Meteoric Diagenesis. *Sedimentology, 29:* 797-817.

ALLAN, J. R. AND WIGGINS, W. D. (1993). Dolomite Reservoirs, Geochemical Techniques for Evaluating Origin and Distribution. *Am. Ass. Petrol. Geol. Continuing Education Course, 36*: 129p.

ALMOND, D. C., BUSREWIL, M. T. AND WODSWORTH, W. J. (1974). The Ghirian Tertiary Volcanic Province of Tripolitania, Libya. *Geol. J., 9*: 17-28.

ALSHARHAN, A. S. AND WILLIAMS, D. F. (1987). Petrography and Stable Isotope Composition of Baroque Dolomite from the Shuaiba Formation (Lower Cretaceous), Abu Dhabi, United Arab Emirates. *J. African Earth Sci., 6(6):* 881-890.

AMTHOR, J. E. AND FRIEDMAN, G. M. (1991). Dolomite-Rock Textures and Secondary Porosity Development in Ellenberger Group Carbonates (Lower Ordovician), West Texas and Southeastern New Mexico. *Sedimentology, 38:* 343-362.

AMTHOR, J. E. AND FRIEDMAN, G. M. (1992). Early-to Late- Diagenetic Dolomitization of Platform Carbonates: Lower Ordovician Ellenburger Group, Permian Basin, West Texas. *J. Sed. Petr., 62(1):* 131-144.

ANKETELL, J. M. AND GHELLALI, S. M. (1991). A Palaeogeography Map of the Pre-Tertiary Surface in the Region of the Jifarah Plain and its Implication to the Structural History of Northern Libya. In: *The Geology of Libya* (ed. by: Salem, M. J., Sbeta, A. M. and Bakbak, M. R.), *VI:* 2381-2406.

ANKETELL, J. M. AND KUMATI, S. M. (1991). Structure of Al-Hofrah Region-Western Sirt Basin, G.S.P.L.A.J. In: *The Geology of Libya* (ed. by: Salem, M. J., Sbeta, A. M. and Bakbak, M. R.), *VI:* 2353-2370.

ANTONOVIC, A. (1977). Geological Map of Libya, 1: 250,000, Sheet Mozdah, NH33-1, Explanatory Booklet. *Publication of the Industrial Research Centre, Tarabulus, Libya:* 68p.

BADIOZAMANI, K. (1973). The Dorag Dolomitization - Application to the Middle Ordovician of Wisconsin. *J. Sed. Petr., 43:* 965-984.

BACK, W., HANSHAW, B. B., PLUMMER, N., RAHN, P. H., RIGHTMIRE, C. T. AND RUBIN, M. (1983). Process and Rate of Dedolomitization: Mass Transfer and 14C Dating in a Regional Carbonate Aquifer. *Geol. Soci. Am., Bull., 94:* 1415-1429.

BAKER, P. A. AND BURNS, S. J. (1985). Occurrence and Formation of Dolomite in Organic-Rich Continental Margin Sediments. *Bull. Am. Ass. Petrol. Geol., 69:* 1917-1930.

BANERJEE, S. (1980). Stratigraphic Lexicon of Libya. *Publication of the Industrial Research Centre, Bull., 13*: 300p.

BANNER, J. L. (1986). Petrologic and Geochemical Constraints on the Origin of Regionally Extensive Dolomites of the Mississippian Burligtone and Keokuk Fms., Iowa, Illinois and Missouri. *Unpublished Ph. D. Thesis*, State University of New York: 368p.

BANNER, J. L., HANSON, G. L. AND MEYERS, W. J. (1988). Water-Rock Interaction History of Regionally Extensive Dolomites of the Burligton-Keokuk Formation (Mississippian): Isotopic Evidence. In: Sedimentology and Geocemistry of Dolostones (ed. by: Shukla, V. and Baker, P. A.), *Spec. Publ., Soc. Econ. Paleont. Miner., 43:* 97-113.

BARR, F. T. AND WEEGAR, A. A. (1972). Stratigraphic Nomenclature of the Sirte Basin, Libya. *Publ. of the Petr. Expl. Soc. of Libya*: 179p.

BATHURST, R. G. C. (1975). Carbonate Sediments and Their Diagenesis. *Elsevier,* 658p.

BAUSCH, W. M. AND MEDUNA, J. V. (1991). Geochemical Position of the Jabal Nafusah Phonolites. In: *The Geology of Libya* (ed. by: Salem, M. J., Busrewil, M.T. and Ben Ashour, A. M.), *VII:* 2681-2687.

BEALS, F. W. AND HARDY, J. W. (1980). Criteria for the Recognition of Diverse Dolomite Types with an Emphasis on Studies of Host Rocks for Mississippi Valley-Type Ore Deposits. In: Concepts and Models of Dolomitization (ed. by: Zenger, D. H., Dunham, J. B. and Ethington, R. L.). *Soc. Econ. Paleont. Mineral., Spec. Publ., 28:* 197-214.

BEN DHIA, H. (1987). The Geothermal Gradient Map of Central Tunisia: Comparision with Structural, Gravimeteric and Petroleum Data. *Tectonophysics, 142:* 99-109.

BEN ISMAIL, M. H. (1991). Jurassic Evaporitic Deposits in Southern Tunisia: A Climatically and Tectonically Controlled Sedimentation. *J. African Earth Sci., 12(1/2):* 117-123.

BIJU-DUVAL, B., LETOUZEY, J., MONTADERT, L., COURRIER, P., MUNGNIOT, J. F. AND SANCHO, J. (1974). Geology of the Mediterranean Sea Basins. In: *The Geology of Continental Margins* ((ed. by: Burk, C. A. and Drake, C. L.), New York: Springer-Verlag: 695-721.

BIJU-DUVAL, B., DERCOURT, J. AND LE PICHON, X. (1977). From the Tethys Ocean to the Mediterranean Seas: A Plate Tectonic Model of the Evolution of the Western Alpine System. In: Structural History of the Mediterranean Basins (ed. by: Biju-Duval, B. and Montadert, L.), *Symposium International, XXV Congres-Assemblee Pleniere De La Commission Internationale Pour L'Exploration Scientifique De La Mediterranean, Split, Yougslavie, 25-29 October, 1976*: 143-164.

BISHOP, F. (1975). Geology of Tunisia and Adjacent Parts of Algeria and Libya. *A.A.P.G., Bull., 59(3):* 413-450.

BUDAI, J. M., LOHMANN, K. C. AND OWEN, R. M. (1984). Burial Dedolomitization in the Mississippian Madison Limestone, Wyoming and Utah Thrust Belt. *J. Sed. Petr., 54:* 276-288.

BURCHETTE, T. P AND WRIGHT, V. P. (1992). Carbonate Ramp Depositional Systems. *Sed. Geol., 79:* 3-57.

BUROLLET, P. F. (1956). Contribution a L'Etude Stratigraphique de la Tunisie Central. *Annale des Mines et de la Geologie, No. 18.*

BUROLLET, P. F. (1960). Names and Nomenclature Committee of the Petroleum Exploration Society of Libya. *Lexique Stratigraphique International. IVa Libya*: 1-62.

BUROLLET, P. F. (1963a). Le Trias en Tunisie et Libye. Relations avec le Trias Europeen et Saharrien. *86th Cong. Soc. Sav., Colloque Trias, Montpellier 1961: 1-15, Carte. Fr. Bur. Rech. Geol. Minieres, Mem., 15:* 482-494.

BUROLLET, P. F. (1963b). Discussion of Libyan Stratigraphy. *Rev. Inst. Petrole, 18:* 1323-1325.

BUROLLET, P. F. (1963c). Field Trip Guidbook of the Excursion to Jebel Nefus (Mesozoic/Tertiary Section in Tripolitania). *First Saharan Symp., Petr. Explor. Soc. Libya,* 17p.

BUROLLET, P. F. (1967). General Geology of Tunisia. In: *Guidebook to the Geology and History of Tunisia* (ed. by: Martin, L.), *Petr. Explo. Soc. of Libya, 9th Ann. Field Conference*: 51-58.

BUROLLET, P. F. (1969). Petroleum Geology of the Western Meiterranean Basin. In: The Exploration for Petroleum in Europe and North Africa: *Institute of Petroleum, Brighton Proce.,* 19-30.

BUROLLET, P. F. (1977). Morphologie et Pedelogie D'une Plaine Couverte de la Sable la Jeffara Libyenne. *Notes, Mém Comp. Fr. Pétrole, 13:* 11-30.

BUROLLET, P. F. AND MANDERSCHIED, G. (1965). Le Cretace Inferieur en Tunisie et en Libya, Colloque sur Cretace Inferieur. *Mem. B.R.G.M., Paris, 34*: 785-794.

BUROLLET, P. F. AND ROUVIER, H. (1971). La Tunisie. In: Tectonique de' L Afrique, Tectonics of Africa (ed. by: Choubert; G.), *UNESCO:* 91-100.

BUROLLET, P. F., MUGNIOT, J. M. AND SWEENEY, P. (1978). The Geology of the Pelagian Block: The Margins and Basins off Southern Tunisia and Tripolitania. In: The Ocean Basins and Margins (ed. by: Nairn, A. E. M., Kanes, W. H. and Stehli, F. G.), *4B-The Western Mediterranean*: 331-359.

BUSREWIL, M. T. AND WADSWORTH, W. J. (1980a). Preliminary Chemical Data on the Volcanic Rocks of Al Haruj Area, Central Libya. In: *The Geology of Libya* (ed. by: Salem, M. J. and Busrewil, M. T.), *III*: 1077-1080.

BUSREWIL, M. T. AND WADSWORTH, W. J. (1980b). The Basanitic Volcanoes of the Gharyan Area, NW Libya. In: *The Geology of Libya* (ed. by Salem, M. J. and Busrewil, M. T.), *III*: 1095-1105.

BUSSON, G. (1967a). Mesozoic of Southern Tunisia. In: *Martin, L. (ed.), Guidebook to the Geology and History of Tunisia, Petr. Expl. Libya, 9th Ann. Field Conf.*: 131-152.

BUSSON, G. (1967b). Le Mesozoique Saharien, Premiere Partie, Extreme-Sud Tunisien, Centre de Recherche sur les Zones Arides. *Serie: Geologie, 18:* 194p.

BUSSON, G. (1970). Le Mesozoique Saharian Essai de Syntheses des Donnes des Sondages Algero-Tunisiens. *Centre de Recherches sur les Zones Arides, Serie: Geologie, 11, Editions du Centre National de la Recherche Scientifique, Paris*: 811p.

BUTT, A. A. (1986). Upper Cretaceous Biostratigraphy of the Sirte Basin, Northern Libya. *Rev. De. Paleob., 5(2)*: 175-191.

BUXTON, M. W. N. AND PEDLEY, H. M. (1989). A Standardized Model for Tethyan Carbonate Ramps. *J. Geol. Soc. London, 146:* 746-748.

BYRAMJEE, R. S., BIJU-DUVAL, B. AND MUGNIOT, J. F. (1975). Petroleum Potential of Deep Water Areas of the Mediterranean and Caribean Seas. *9th World Petr. Cong., Tokyo, Panel 5*: 299-312.

CABLE, D. G. (1978). Paleoenvironments and Hydrocarbon Potential of the Lower Cretaceous Chicla and Cabao Formations in the Jebel Nefusa Escarpment and the Gabes-Sabratha Basin, Northwestern Libya. *Unpub. M. Sc. Thesis, Dept. of Geology, University of South Carolina*: 56p.

CAMPBELL, A. S. (1968). The Barce (Al Marj) Earthquake of 1963. In: Geology and Archaeology of Northern Cyrenaica, Libya (ed. by: Barr, F. T.). *Petr. Expl. Soc. Libya, 10th Ann. Field Conf.*: 183-196.

CARBALLO, J. D., LAND, L. S. (1984). Holocene Dolomitization of Supratidal Sediments by Active Tidal Pumping, Sugarloaf Key, Florida. *Am. Ass. Petrol. Geolo., Bull. (abs.), 68:* 459.

CARBALLO, J. D., LAND, L. S. AND MISER, D. E. (1987). Holocene Dolomitization of Supratidal Sediments by Active Tidal Pumping, Sugarloaf Key, Florida. *J. Sed. Petrol., 57(1):* 153-165.

CARTER, T. G., FLANAGAN, J. P., JONES, C. R., MARCHANT, F. L., MURCHISON, R. R., REBMAN, J. H., SYLVESTER, J. C. AND WHITNEY, J. C. (1972). A New Bathymetric Chart and Physiography of the Mediterranean Sea. In: The Mediterranean Sea: A Natural Sedimentation (ed. by: Stanley, D. J.), *Laboratory, Dowden, Huchinson and Ross, Inc., Stroudsburg, Penn.*: 1-23.

CASTANY, G. (1954). L'Accident Sud-Atlasique D'Algerie. *Acad. Sci. Comptes Rendus, 238(8)*: 916-918.

CHAFETZ, H. S. (1972). Subsurface Diagenesis of Limestone. *J. Sed. Petr., 42:* 325-329.

CHOQUETTE, P. W. (1971). Late Ferroan Dolomite Cement, Mississippian Carbonates, Illinois Basin, USA. In: Carbonate Cements (ed. by: Bricker, O. P.). *Johns Hopkins Univ. Studies in Geology, 19:* 339-348.

CHOQUETTE, P. W. AND PRAY, L. C. (1970). Nomenclature and Classification of Porosity in Sedimentary Carbonates. *Bull. Am. Ass. Petrol. Geol., 54:* 207-250.

CHRISTIE, A. M. (1955 reprinted, 1966). Geology of the Garian Area, Tripolitania, Libya. *Geol. Section, Bull., 5, Kingdom of Libya, Ministry of Industry: Willimer Bros. Ltd.. Birkenhead, UK:* 64p.

CONANT, L. C. AND GOUDARZI, G. H. (1964). Geological Map of Kingdom of Libya. *U.S. Geological Survey, Misc. Geol. Inv. Map 1-350A, Scale 1: 2,000,000, Washington.*

CONANT, L. C. AND GOUDARZI, G. H. (1967). Stratigraphic and Tectonic Framework of Libya. *AAPG, Bull., 51(5):* 719-730.

COQUE, R. AND JAUZEIN, A. (1967). The Geomorphology and Quaternary Geology of Tunisia. In: Guidebook to the Geology and History of Tunisia (ed. by: Martin, L.). *Petr. Explo. Soc. of Libya, 9th Ann. Field Conference:* 227-258.

DEPAOLO, D. J. AND INGRAM, B. L. (1985). High Resolution Stratigraphy with Strontium Isotopes. *Science, 227:* 938-941.

DESIO, A., RONCHETTI, C. R., POZZI, R., CLEICI, F., INVERNIZZI, G., PISONI, C. AND VIGANO, P. L. (1963). Stratigraphic Studies in the Tripolitanian Jebel (Libya). *Riv. Ital. Paleont., Mem., 9:* 126p.

DEWEY, J. F., PITMAN, W. C., RYAN, W. B. F. AND BONNIN, J. (1973). Plate Tectonics and the Evolution of the Alpine System. *Geol. Soc. America, Bull., 84(10):* 3137-3180.

DICKSON, J. A. D. (1965). A Modified Staining Technique for Carbonates in Thin Section. *Nature, 205*: p. 587.

DOROBEK, S. L., SMITH, T. M. AND WHITSITT, P. M. (1993). Microfabrics and Geochemistry of Meteorically Altered Dolomite in Devonian and Mississippian Carbonates, Montana and Idaho. In: Carbonate Microfabrics (ed. by: Rezak, R. and Lavoie, D. L.), *Frontiers in Sedimentary Geology*. Springer-Verlag, New York: 205-225.

DRIGGS, A. (1977). The Petrology of the Three Upper Permian Bioherms, Southern Tunisia. *Brighan Young University, Geology Studies, 24(1)*: 37-53.

DUNHAM, J. B. AND OLSON, E. R. (1980). Shallow Subsurface Dolomitization of Subtidally Deposited Carbonate Sediments in the Hanson Creek Formation (Ordovician-Silurian) of Central Nevada. In: Concepts and Models of Dolomitization (ed. by: Zenger, D. H., Dunham, J. B. and Ethington, R. L.). *Soc. Econ. Paleont. Mineral., Spec. Publ., 28:* 139-161.

DURAND-DELGA, M. (1967). Structure and Geology of the Northeast Atlas Mountains. In: Guidebook to the Geology and History of Tunisia (ed. by: Martin, L.). *Petr. Explo. Soc. of Libya, 9th Ann. Field Conference*: 59-84.

EL-BAKAI, M. T. (1989). The Sedimentology of the Lidam Formation in Northwest Sirte Basin, Libya. *Unpubl. M. Sc. Thesis, Geology Department, Hull University, England*: 172p.

EL-BAKAI, M. T. (1991). Petrography and Diagenesis of the Lidam Formation (Carbonate Units): From Selected Wells in Sirt Basin, Libya. *Petr. Resea. J., Petroleum Research Centre, Tarabulus, Libya, 3*: 35-43.

EL-BAKAI, M. T. (1992). Environment of Deposition of the Lidam Formation in NW Sirte Basin, Libya. In: Geology of the Arab World (ed. by: Sadek, A.), *Proc. of the 1st. Inter. Conf. on Geol. of the Arab World, Cairo University*. **I:** 343-352.

EL HINNAWY, M. AND CHESHITEV, G. (1975). Geological Map of Libya, 1: 250,000, Sheet Tarabulus, NI33-13, Explanatory Booklet. *Publication of the Industrial Research Centre, Tarabulus, Libya*: 75p.

ELRICK, M. AND READ, J. F. (1991). Cyclic Ramp-to-Basin Carbonate Deposits, Lower Mississippian, Wyoming and Montana: A Combined Field and Computer Modeling Study. *J. Sed. Petrol., 61(7):* 1194-1224.

EL-RWEIMI, W. S. (1991). Geology of the Aouinet Ouenine and Tahara Formations, Al Hamadah Al Hamra Area, Ghadamis Basin. In: *The Geology of Libya* (ed. by: Salem, M. J., Sbeta, A. M. and Bakbak, M. R.), *VI*: 2185-2193.

ETOURBI, I. Y. (1989). Study of the Main Facies of the Faarwah Group)Late Paleocene-Early Middle Eocene) of the Northwestern Libya Offshore. *Unpub. M. Sc. Thesis, Dept. Geol., Manchester University, England*: 166p.

EL-ZOUKI, A. Y. (1976). Sedimentological and Stratigraphical Aspects of the Chicla, Cabao, and Chameau Mort Formations (Upper Jurassic-Lower Cretaceous) of the Jebel Nefusa NW Libya. *Unpub. Ph.D Thesis, University of Brisol, U.K.*: 300p.

EVAMY, B. D. (1967). Dedolomitization and the Development of Rhombohedral Pores in Limestones. *J. Sed. Petr.*, **37:** 1204-1215.

FAIRCHILD, I., HENDRY, G. QUEST, M. AND TUCKER, M. (1988). Chemical Analysis of Sedimentary Rocks. In: Techniques in Sedimentology (ed. by: Tucker, M.). *Blackwell Scientific Publications, Ch. 7:* 274-354.

FATMI, A. N. AND SBETA, A. M. (1991). The Significance of the Occurrence of Abu Ghaylan and Kiklah Formations East of Wadi Ghan, Eastern Jabal Nafusah. In: *The Geology of Libya* (ed. by: Salem, M. J., Sbeta, A. M., and Bakbak, M. R.), *VI*: 2227-2233.

FATMI, A. N., ELIAGOUBI, B. A. AND SBETA, A. M. (1978a). Field Trip to Jabal Nefusa Itinerary for the 1978 Symposium on the Geology of Libya. *Dept. Geol., Al Fatah University*: 13p.

FATMI, A. N., SBETA, A. M. AND ELIAGOUBI, B. A. (1978b). Guide to the Mesozoic Stratigraphy of Jabal Nefusa, Libyan Jamahiriya. *Arab. Dev. Inst., Tripoli, 7*: 35p.

FATMI, A. N., ELIAGOUBI, B. A., HAMMUDA, O. S. (1980). Stratigraphy Nomenclature of the Pre-Upper Cretaceous Mesozoic Rocks of Jabal Nafusah, NW Libya. In: *The Geology of Libya* (ed. by: Salem, M. J., and Busrewil, M. T.), Academic Press, *I*: 57-65.

FINETTI, I. (1982). Structure, Stratigraphy and Evolution of the Central Mediterranean. *Boll. Geof. Teor. Appl., 24*:247-312.

FOLK, R. L. AND LAND, L. S. (1975). Mg/Ca Ratio and Salinity: Two Controls Over Crystallization of Dolomite. *Bull. Am. Ass. Petrol. Geol., 59(1):* 60-68.

FRIEDMAN, G. M. (1965). Terminology of Crystallization Textures and Fabrics in Sedimentary Rocks. *J. Sed. Petr., 35(3):* 643-655.

FRIEDMAN, G. M. (1971). Staining. In: *Procedures in Sedimentary Petrology* (ed. by Carver, R. E.), *Wiley-Interscience, New York*: 511-530.

FRIEDMAN, G. M. AND SANDERS, J. E. (1967). Origin and Occurrences of Dolostones. In: *Carbonate Rocks, Origin, Occurrence, and Classification* (ed. by: Chilingar, G. V., Bissell, H. J. and Fairbridge, R. E.), Amsterdam, Elsevier: 267-348.

FRIEDMAN, I. AND O'NEIL, J. R. (1977). Compilation of Stable Isotope Fractionation Factors of Geochemical Interest. *U.S. Geol. Surv. Profess. Paper 440kk*: 12p.

FRISIA, S. (1994). Mechanisms of Complete Dolomitization in a Carbonate Shelf: Comparison Between the Norian Dolmia Principle (Italy) and the Holocene of Abu Dhabi Sabkha. In: Dolomites A Volume in Honour of Dolomieu (ed. by: Purser, B., Tucker, M. and Zenger, D. J.), *Inter. Assoc. Sediment., Spec. Publ., 21:* 55-74.

FÜCHTBAUER, H. (1974). Sediments and Sedimentary Rocks 1. In: Sedimentary Petrology II (ed. by: Engelhardt, W., Füchtbauer, H. and Müller, G). *Schweizerbart, Stuttgart:* 464p.

GAO, G. (1990). Geochemical and Isotopic Constraints on the Diagenetic History of a Massive Stratal, Late Cambrian (Royer) Dolomite, Lower Arbuckle Group, Slick Hills, SW Oklahoma, USA. *Geochimica et Cosmochimica Acta, 54:* 1979-1989.

GAO, G., LAND, L. S. AND ELMORE, R. D. (1995). Multiple Episodes of Dolomitization in the Arbuckle Group, Arbuckle Mountains, South-Central Oklahoma: Field, Petrographic, and Geochemical Evidence. *J. Sed. Research, A65(2):* 321-331.

GARVEN, G. (1985). The Role of Regional Fluid Flow in the Genesis of the Pine Point Deposit, Western Canada Sedimentary Basin. *Econ. Geol., 80:* 307-324.

GLANGEAUD, L. (1962). Paleogeographic Dynamique De La Mediterranee Et De Ses Bordures. Le Role Des Phases Ponto-Plio-Quaternaires. In: *Oceonegraphic Geologique et Geophysique De La Mediterranee Occidental* (ed.: by Bourcart, J.): 125-165.

GORHBANDT, K. H. A. (1966). Some Cenomanian Foraminifera from Northwestern Libya. *Micropaleontology, 12:* 65-70.

GOUDARZI, G. H. (1970). Geology and Mineral Resources of Libya. A Reconnaissance. *U.S. Geol. Survey, Prof. Papers, 660*: 104p.

GOUDARZI, G. H. (1980). Structure-Libya. In: *The Geology of Libya* (ed. by: Salem, M. J., and Busrewil, M. T.), Academic Press, *III*: 879-892.

GOUDARZI, G. H. AND SMITH, J. P. (1977). Preliminary Structure-Contour Map of the Libyan Arab Republic and Adjacent Areas. *U.S.G.S. Map, 1-350-C, Misc. Invest. Series.*

GRANDJACQUET, C. AND MASCLE, G. (1978). The Structure of the Ionian Sea, Sicily and Calabria-Lucania. In: *The Ocean Basins and Margins* (ed. by: Nairn, A. E. M., Kanes, W. H., and Stehli, F. G.), *4B-The Western Mediterranean*: 257-329.

GRAY, C. (1971). Structure and Origin of the Garian Domes. In: *Symposiun on the Geology of Libya* (ed. by: Gray, C.), *Faculty of Science, University of Libya, Tripoli, Libyan Arab Republic*: 307-319.

GREGG, J. M. AND SHELTON, K. L. (1990). Dolomitization and Dolomite Neomorphism in the Back Reef Facies of the Bonneterre and Davies Formations (Cambrian), Southeastern Missouri. *J. Sed. Petr., 60:* 549-562.

GREGG, J. M. AND SIBLEY, D. F. (1984). Epigenetic Dolomitization and the Origin of Xenotopic Dolomite Textures. *J. Sed. Petr., 54:* 908-931.

GUMATI, Y. D. AND KANES, W. H. (1985). Early Tertiary Subsidence and Sedimentary Facies-Northern Sirte Basin, Libya. *Bull. Am. Ass. Petrol. Geol., 69(1)*: 39-52.

GUMATI, Y. D. AND SCHAMEL, S. (1988). Thermal Maturation History of the Sirte Basin, Libya. *J. Sed. Pet.,* **11(2)**: 205-218.

HALL, S. (1977). Gravity and Magnetic Survey of Northwestern Libya. *Unpub. Marengo, Ltd. Ann. Report*: 30p.

HAMMUDA, O. S. (1969). Jurassic and Lower Cretaceous Rocks of Central Jabal Nefusa, Northwestern Libya. *Petr. Expl. Soc. Libya*: 74p.

HAMMUDA, O. S. AND MISSALLATI, A. A. (1980). A Study of the Libyan-Tunisian Contenantal Shelf. *Unpub. Rep. Submitted by Soci. Rep. Libyan Arab Jamahiriya to the International Court of Justice*: 24p.

HAMMUDA, O. S., SBETA, A. M, MOUZUGHI, A. J. AND ELIAGOUBI, B. A. (1985). Stratigraphic Nomenclature of the Northwestern Offshore of Libya. *The Earth Sciences Soc. Libya, Tarabulus, Libya:* 166p.

HANSHAW, B. B., BACK, W. AND DIEKE, R. G. (1971). A Geochemical Hypothesis for Dolomitization by Groundwater. *Econ. Geol., 66:* 710-724.

HARDIE, L. A. (1987). Dolomitization: A Critical View of Some Current Views.*J. Sed. Petr., 57:* 166-183.

HARDY, R. AND TUCKER, M. E. (1988). X-Ray Powder Diffraction of Sediments. In: Techniques in Sedimentology (ed. by: Tucker, M. E.). Blackwell, Oxford: 191-228.

HARRIS, D. C. AND MEYERS, W. (1987). Regional Dolomitization of Subtidal Shelf Carbonates: Burlington and Keokuk Formations (Mississippian), Iowa and Illinois. In: Diagenesis of Sedimentary Sequences (ed. by: Marshal, J. D.), *Geol. Soc., Spec. Publ. 36:* 237-258.

HARRIS, P. M., FROST, S. H. AND KENDAL, C. (1980). Cretaceous Sea level and Stratigraphy, Eastern Arabian Peninsula. *Am. Ass. Petrol. Geol., Bull., 65(5):* 718-719.

HARRIS, P. M., FROST, S. H., SEIGLIE, G. A. AND SCHNEIDERMANN, N. (1984). Regional Unconformities and Depositional Cycles, Cretaceous of the Arabian

Peninsula. In: Interregional Unconformities and Hydrocarbon Accumulations (ed. by: Schlee, J.), *Am. Ass. Petrol. Geol., Mem., 36:* 67-80.

HECHT, F., FURST, M. AND KLITZSCH, E. (1964). Zur Geologie Von Libyen (Contribution a La Geologie de la Libye). *Geol. Rundschau Dtsch., 53(2):* 413-470.

HEM, J. D. (1970). Study and Interpretation of the Chemical Characteristics of Natural Water. *U. S. Geol. Surv. Water-Supp. Pap. 1473.*

HENNING, N. G., MEYERS, W. J. AND GRAINS, J. C. (1989). Cathodoluminescence in Diagenetic Calcites: the Roles of Fe and Mn as Deduced from Electron Probe and Spectrophotometric Measurements. *J. Sed. Petr.,59(3):* 404-411.

HINE, A. C. (1977). Lily Bank Bahamas: History of an Active Oolite Sand Soal. *J. Sed. Petr., 47:* 1554-1583.

HOLAIL, H., LOHMANN, K. C. AND SANDERS, I. (1988). Dolomitization and Dedolomitization of Upper Cretaceous Carbonates: Bahariya Oasis, Egypt. In: Sedimentology and Geocemistry of Dolostones (ed. by: Shukla, V. and Baker, P. A.), *Spec. Publ., Soc. Econ. Paleont. Miner., 43:* 191-207.

HUBER, B. T., HODELL, D. A. AND HAMILTON, C. P. (1995). Middle-Late Cretaceous Climate of the Southern High Latitudes: Stable Isotopic Evidence for Minimal Equator-to-Pole Thermal Gradients. *Bull. Geol. Soc. Am., 107(10):* 1164-1191.

HUDSON, J. D. (1977). Stable Isotopes and Limestone Lithification. *J. Geol. Soc. London, 133:* 637-660.

HUDSON, J. D. AND ANDERSON, T. F. (1989). Ocean Temperatures and Isotopic Compositions Through Time. *Trans. Royal Soc. Edinburgh: Earth Sci., 80:* 183-192.

HUMPHREY, J. D. (1988). Late Pleistocene Mixing Zone Dolomitization, Southeastern Barbados, West Indies. *Sedimentology, 35:* 327-348.

JAMES, N. P., BONE, Y. AND KYSER, T. K. (1993). Shallow Burial Dolomitization of Mid-Cenozoic, Cool-Water, Calcitic, Deep-Shelf Limestones, Southern Australia. *J. Sed. Petr., 63(3):* 528-538.

JORDI, H. A. AND LONFAT, F. (1963). Stratigraphic Subdivision and Problems in Upper Cretaceous-Lower Tertiary Deposits in North-Western Libya. *Rev. Inst. France Petrole, 18(10/11):* 1428-1436.

KASTNER, M. (1982). When Does Dolomitization Occur and What Controls It. *11th Int. Cong. Sed. (abs.), Hamilton, Ontario, Canada:*p. 124.

KATZ, A. (1968). Calcian Dolomites and Dedolomitization. *Nature, 217:* 439-440.

KATZ, A. AND MATTHEWS, A. (1977). The Dolomitization of $CaCO_3$: An Experimental Study at 252-295°C. *Geochim. Cosmi. Acta, 41:* 297-308.

KENNEDY, W. Q. (1965). The Influence of Basement Structure on the Evolution of the Coastal (Mesozoic and Tertiary) Basins of Africa. In: Salt Basins Around Africa, *Procedings of Meeting of the Instit. of Petroleum and the G. S., London, 3d March, 1965:* 7-16.

KHALIFA, M. A. AND ABU EL HASAN, M. M. (1993). Lithofacies, Cyclicity, Diagenesis and Depositional Environments of the Upper Cenomanian, El Heiz Formation, Bahariya Oasis, Western Desert, Egypt. *Jour. African Earth Sci., 17(4):* 555-570.

KLITZSCH, E. (1968). Outline of the Geology of Libya. *Petr. Expl. Soc. Libya, 10th Ann. Field Conf.* (ed. by: F. T. Barr): 71-78.

KLITZSCH, E. (1971). The Structural Development of Parts of North Africa Since Cambrian Time. In: *Symposiun on the Geology of Libya* (ed. by: Gray, C.), *Faculty of Science, University of Libya, Tripoli, Libyan Arab Republic:* 253-262.

KLITZSCH, E. (1981). Lower Paleozoic Rocks of Libya, Egypt and Sudan. In: *L. Paleozoic of the Middle East, Eastern and Southern Africa and Antarctica* (ed. by: Holand, C. H.): 132-163.

KOLODNY, Y. AND RAAB, M. (1988). Oxygen Isotopes in Phosphatic Fish Remains from Israel: Palaeothrmometry of Tropical Cretaceous and Tertiary Shelf Waters. *Palaeogeog. Palaeoclim. Palaeoecol., 64:* 59-67.

KRUGER, J. M. AND SIMO, J. A. (1994). Pervasive Dolomitization of a Subtidal Carbonate Ramp, Silurian and Devonian, Illinois Basin, USA. In: Dolomites A Volume in Honour of Dolomieu (ed. by: Purser, B., Tucker, M. and Zenger, D. J.), *Inter. Assoc. Sediment., Spec. Publ., 21:* 387-405.

KUPECZ, J. A., MONTANEZ, I. P. AND GAO, G. (1993). Recrystallization of Dolomite with Time. In: , Carbonate Microfabrics (ed. by: Rezak, R. and Lavoie, D. L.), *Frontiers in Sedimentary Geology. S*pringer-Verlag, New York: 187-194.

LAND, L. S. (1973). Contemporaneous Dolomitization of Middle Pleistocene Reefs by Meteoric Water, North Jamaica. *Bull. Marine Science, 23:* 64-92.

LAND, L. S. (1980). The Isotopic and Trace Element Geochemistry of Dolomite: The State of the Art. In: Concepts and Models of Dolomitization (ed. by: Zenger, D. H., Dunham, J. B. and Ethington, R. L.). *Soc. Econ. Paleont. Mineral., Spec. Publ., 28:* 87-110.

LAND, L. S. (1983). Dolomitization. *Am. Ass. Petrol. Geol., Course Note Series 24:* 20p.

LAND, L. S. (1985). The Origin of Massive Dolomite. *J. Geol. Education, 33:* 112-125.

LAND, L. S. (1986). Environments of Limestone and Dolomite Diagenesis: Some Geochemical Consideration. In: Carbonate Depositional Environments Modern and

Ancient, Part 5: Diagenesis 1 (ed. by: Warme, J. E. and Shanley, K. W.), *Colorado School of Mines Quart., 81(4):* 26-41.

LAND, L. S. (1991). Dolomitization of the Hope Gate Formation (North Jamaica) by Seawater: Reassessment of Mixing-Zone Dolomite. In: Stable Isotope Geochemistry: A Tribute to Samuel Epstein (ed. by: Taylor, H. P., O'Neil, J. R. and Kaplan, I. R.), *The Geochem. Soci., Spec. Publ., 3:* 121-133.

LAND, L. S., MILLIKEN, K. L. AND MCBRIDE, E. F. (1987). Diagenetic Evolution of Cenozoic Sandstones, Gulf of Mexico Sedimentary Basin. *Sed. Geol., 50:* 195-225.

LAND, L. S., SALEM, M. R. I. AND MORROW, D. W. (1975). Paleohydrology of Ancient Dolomites: Geochemical Evidence. *Bull. Am Ass. Petrol. Geol., 59:* 1602-1625.

LAWRENCE, J. R. GIESKES, J. M. AND BROECKER, W. S. (1975). Oxygen Isotope and Cation Composition of DSDP Pore Waters and the Alteration of Layer II Basalts. *Earth Planet. Sci. Lett., 27:* 1-10.

LEE, Y. I. AND FRIEDMAN, G. M. (1987). Deep-Burial Dolomitization in the Ordovician Ellenburger Group Carbonates, West Texas and Southeastern New Mexico. *J. Sed. Petr., 57(3):* 544-557.

LONGMAN, M. W. (1980). Carbonate Diagenetic Textures from Nearsurface Diagenetic Environments. *Bull. Am. Ass. Petrol. Geol., 64(4):* 461-487.

LUCIA, F. J. (1995). Rock-Fabric/Petrophysical Classification of Carbonate Pore Space for Reservoir Characterization. *Bull. Am. Ass. Petrol. Geol., 79(9):* 1275-1300.

LUCIA, F. J., AND MAJOR, R. P. (1994). Porosity Evolution Through Hypersaline Reflux Dolomitization. In: Dolomites A Volume in Honour of Dolomieu (ed. by: Purser, B., Tucker, M. and Zenger, D. J.), *Inter. Assoc. Sediment., Spec. Publ., 21:* 325-341.

LUMSDEN, D. N. (1979). Discrepancy Between Thin Section and X-Ray Estimates of Dolomite in Limestone. *J. Sed. Petr., 49:* 429-436.

LUMSDEN, D. N. AND CHIMAHUSKY, J. S. (1980). Relationship Between Dolomite Nonsoichiometry and Carbonate Facies Parameters. In: Concepts and Models of Dolomitization (ed. by: Zenger, D. H., Dunham, J. B. and Ethington, R. L.), *Spec. Publ., Soc. Econ. Paleont. Miner., 28:* 123-137.

MACHEL, H. G.AND ANDERSON, J. H. (1989). Pervasive Subsurface Dolomitization of the Nisku Formation in Central Alberta. *J. Sed. Petr., 59(6):* 891-911.

MACHEL, H. G. AND MOUNTJOY, E. W. (1986). Chemistry and Environments of Dolomitization - A Reapraisal. *Earth-Science Reviews, 23:* 175-222.

MACHEL, H. G. AND MOUNTJOY, E. W. (1987). General Constraints on Extensive Pervasive Dolomitization-and Their Application to the Devonian Carbonates of Western Canada. *Bull. Ca. Petr. Geol., 35(2):* 143-158.

MAGARITZ, M. (1985). The Carbon Isotope Records of Dolostones as a Stratigraphic Tool: A Case Study from the Upper Cretaceous Shelf Sequence, Israel. *Sed. Geol., 45:* 115-123.

MAGARITZ, M. AND KAFRI, U. (1981). Stable Isotope and Sr^{2+}/Ca^{2+} Evidence of Diagenetic Dedolomitization in a Schizohaline Environment: Cenomanian of Northern Israel. *Sed. Geol., 28:* 29-41.

MAGARITZ, M., GROLDENBERG, L., KAFRI, U. AND ARAD, A. (1980). Dolomite Formation in the Seawater-Freshwater Interface. *Nature, 287:* 622-624.

MAGNIER, P. (1963). Etude Stratigraphique dan le Gebel Nefousa e le Gebel Garian (Tripolitaine, Libye). *Bull. Soc. Geol. France, Ser. 7, 5(2):* 89-94.

MALONE, M. J., BAKER, P. A. AND BURNS, S. J. (1994). Recrystallization of Dolomite: Evidence from the Mounterey Formation (Miocene), California. *Sedimentology, 41*: 1223-1239.

MALONE, M. J., BAKER, P. A. AND BURNS, S. J. (1996). Recrystallization of Dolomite: An Experimental Study from 50-200°C. *Geoch. Cosmoch. Acta, 60(12):* 1989-2207.

MANN, K. (1975a). Geological Map of Libya, 1: 250,000, Sheet Al Khums, NI33-14, Explanatory Booklet. *Publication of the Industrial Research Centre, Tarabulus, Libya*: 88p.

MANN, K. (1975b). Geological Map of Libya, 1: 250,000, Sheet Misratah, NI33-15, Explanatory Booklet. *Publication of the Industrial Research Centre, Tarabulus, Libya*: 30p.

MASSA, D. AND DELORT, T. (1984). Evolution of the Sirte Basin (Libya) from Cambrian to Cretaceous. *Bull. Soc. Geol. France, XXXVI(6)*: 1087-1096.

MATTES, D.H. AND MOUNTJOY, E. W. (1980). Burial Dolomitization of the Upper Devonian Miette Buildup, Jasper National Park, Alberta. In: Concepts and Models of Dolomitization (ed. by: Zenger, D. H., Dunham, J. B. and Ethington, R. L.), *Spec. Publ., Soc. Econ. Paleont. Miner., 28:* 259-297.

MAZZULLO, S. J., BISCHOFF, W. D. AND TEAL, C. S. (1995). Holocene Shallow-Subtidal Dolomitization by Near-Normal Seawaters, Northern Belize. *Geology, 23(4):* 341-344.

McKENZIE, J. A. (1981). Holocene Dolomitization of Calcium Carbonate Sediments from the Coastal Sabkhas of Abu Dhabi, UAE: A Stable Isotope Study. *J. Geol., 89:* 185-198.

MCKENZIE, J. A., HSU, K. J. AND SCHNEIDER, J. F. (1980). Movement of Subsurface Waters Under the Sabkha, Abu Dhabi, U.A.E., and its Relationship to Evaporative Dolomite. In: Concepts and Models of Dolomitization (ed. by: Zenger, D. H., Dunham, J. B. and Ethington, R. L.), *Spec. Publ., Soc. Econ. Paleont. Miner., 28:* 11-30.

MCLANE, M. (1995). Sedimentology. Oxford University Press: 423p.

MEGERISI, M. F. AND MAMGAIN, V. D. (1980a). The Upper Cretaceous-Tertiary Formations of Northern Libya: A Synthesis. *Publ. of the Industrial Research Centre, Tarabulus, Libya, Bull. 12*: 85p.

MEGERISI, M. F. AND MAMGAIN, V. D. (1980b). The Upper Cretaceous-Tertiary Formations of Northern Libya. In: *The Geology of Libya* (ed. by: Salem, M. J., and Busrewil, M. T.), *Academic Press, I*: 67-72.

MEYERS, W. J. (1974). Carbonate Cement Stratigraphy of the Lake Valley Formation (Mississippian), Sacramento Mountains, New Mexico. *J. Sed. Petr., 44:* 837-861.

MIKBEL, S. R. (1977). Basement Configuration and Structure of West Libya. *Libyan J. of Sci., 7A*: 19-34.

MILLIMAN, J. D. (1974). Marine Carbonates. Springer-Verlag, New York, 375p.

MOORE, C. H. (1989). Cabonate Diagenesis and Porosity, Development in Sedimentology **46**. *Elsevier:* 338p.

MOORE, C. H., CHOWDHURY, A. AND CHAN, L. (1988). Upper Jurassic Platform Dolomitization, Northwestern of Mexico: A Tale of Two Waters. In: Sedimentology and Geocemistry of Dolostones (ed. by: Shukla, V. and Baker, P. A.), *Spec. Publ., Soc. Econ. Paleont. Miner., 43:* 175-190.

MORROW, D. W. (1978). The Influence of the Mg/Ca Ratio and Salinity on Dolomitization in Evaporite Basins. *Bull. Can. Petrol. Geol., 26:* 389-392.

MORROW, D. W. (1982a). Diagenesis 1. Dolomite-Part 1: The Chemistry of Dolomitization and Dolomite Precipitation. *Geoscience Canada, 9(1):* 5-13.

MORROW, D. W. (1982b). Diagenesis 2. Dolomite-Part 2: Dolomitization Models and Ancient Dolostones.*Geoscience Canada, 9(1):* 95-107.

M'RABET, A. (1981). Diffrentiation of Environments of Dolomite Formation, Lower Cretaceous of Central Tunisia. *Sedimentology, 28:* 331-352.

MUCHEZ, P. AND VIAENE W. (1994). Dolomitization Caused by Water Circulation Near the Mixing Zone: An Example from the Lower Viséan of the Campine Basin (Northern Belgium). In: Dolomites A Volume in Honour of Dolomieu (ed. by: Purser, B., Tucker, M. and Zenger, D. J.), *Inter. Assoc. Sediment., Spec. Publ., 21: 1*55-166.

MULLINS, H. T., LAND, L. S., WISE, S. W., JR., SLEGAL, D. I. MASTERS, P. M., HINCHEY, E. J. AND PRICE, K. R. (1985). Authigenic Dolomite in Bahamian Slope Sediment. *Geology, 13:* 292-295.

NAIRN, A. E. M. AND SALAJ, J. (1991). Al Gharbiyah Formation, Upper Campanian-Upper Maastrichtian (North-west Libya). In: *The Geology of Libya* (ed. by: Salem, M. J., Hammuda, O. S. and Eliagoubi, B. A.), *IV:* 1621-1635.

NEWELL, N. D., RIGBY, J. K., DRIGGS, A., BOYD, D. W., AND STEHLI, F. G. (1976). Permian Reef Complex, Tunisia. *Brighan Young University, Geology Studies, 23(1):* 75-112.

NIELSEN, P., SWENEN, R. AND KEPPENS, E. (1994). Multiple-Step Recrystallization within Massive Ancient Dolomite Units: An Example from the Dinantian Of Belgium. *Sedimentology, 41:* 567-584.

NOVOVIC, T. (1977a). Geological Map of Libya, 1: 250,000, Sheet Djeneien, NH32-3, Explanatory Booklet. *Publication of the Industrial Research Centre, Tarabulus, Libya*: 34p.

NOVOVIC, T. (1977b). Geological Map of Libya, 1: 250,000, Sheet Nalut, NH32-4, Explanatory Booklet. *Publication of the Industrial Research Centre, Tarabulus, Libya*: 74p.

PATTERSON, R. J. (1972). Hydrology and Carbonate Diagenesis of a Coastal Sabkha in the Persian Gulf. *Unpub. Ph.D Dissertation, Princeton Univ., Princeton, New Jersey:* 498P.

PATTERSON, R. J. AND KINSMAN, D. J. J. (1981). Hydrologic Framework of a Sabkha Along Arabian Gulf. *Bull. Am. Ass. Petrol. Geol., 65:* 1457-1475.

PATTERSON, R. J. AND KINSMAN, D. J. J. (1982). Formation of Diagenetic Dolomite in Coastal Sabkha Along Arabian (Persian) Gulf. *Amer. Assoc. Petrol. Geol., Bull., 66:* 28-43.

PEDLEY, H. M. AND GRASSO, M. (1991). Sea-Level Change Around the Margins of the Catania-Gela Trough and Hyblean Plateau, Southeast Sicily (African-European Plate Convergence Zone): A Problem of Plio-Quaternary Plate Buoyancy? In: Sedimentation, Tectonics and Eustasy Sea-Level Changes at Active Margins (ed by: Macdonald, D. I. M.), *Int. Ass. Sed., Spec. Publ., 12:* 451-464.

PEDLEY, H. M., BELL, B. S., THUNELL, R. AND ARTHUR, M. A. (1982). The Zebbag Formation in Central Tunisia. *Earth Science and Resources Institute, University of South Carolina, Unpub. Report:* 53p.

PICCOLI, G. (1971). Outlines of Volcanism in Northen Tripolitania. In: *Symposiun on the Geology of Libya* (ed. by: Gray, C.), *Faculty of Science, University of Libya, Tripoli, Libyan Arab Republic*: 323-331.

PIERSON, B. J. (1981). The Control of Cathodoluminescence in Dolomite by Iron and Manganese. *Sedimentology, 28:* 601-610.

PITMAN, W. C. AND TALWANI, M. (1972). Seafloor Spreading in the North Atlantic. *Bull., Geol. Soc. Am., 83*: 619-646.

PITMAN, W. C., COCHRAN, J. R., RYAN, W. B. F. AND LADD, J. W. (1981). Evolution of the Libyan Margin. *Technical Report Submitted to the International Court of Justice, Annex-6*: 12p.

PURSER, B. H., TUCKER, M. E. AND ZENGER, D. H. (1994). Problems, Progress and Future Research Concerning Dolomites and Dolomitization. In: Dolomites A Volume in Honour of Dolomieu (ed. by: Purser, B., Tucker, M. and Zenger, D. J.), *Inter. Assoc. Sediment., Spec. Publ., 21:* 3-20.

QING, H. AND MOUNTJOY, E. W. (1989). Multistage Dolomitization in Rainbow Buildups, Middle Devonian Keg River Formation, Alberta, Canada. *J. Sed. Petr., 59:* 114-126.

RADKE, B. H. AND MATHIS, R. L. (1980). On the Formation and Occurrence of Saddle Dolomite. *J. Sed. Petr., 50:* 1149-1168.

REEDER, R. J. (1983). Crystal Chemistry of the Rhombohedral Carbonates. In: Minerology and Chemistry: Reviews in Minerology (ed. by: Reeder, R.). *Minerol. Soc. Amer., 11:* 1-48.

REYRE, D. (1966). Particularities Geologiques des Bassins Cotiers de L'Ouest African. In: Bassins Sedimentaires du Littoral African, Symposium, 1st. Re Partie, Littoral Atlantique, *Union Int. Sci. Geol. Assoc. Serv. Geol. African*: 253-301.

RODGERS, K. A., EASTON, A. J. AND DOWNES, C. J. (1982). The Chemistry of Carbonate Rocks of Niue Island, South Pacific. *J. Geol., 90:* 645-662.

ROSSI-RONCHETTI, C. AND ALBANESI, C. (1961). Fossili Cenomaniani Del Gebel Tripolitano. *Riv. Ital., Paleont., LX VII(3)*: 251-318.

RUPPEL, S. C. AND CANDER, H. S. (1988). Dolomitization of Shallow-Water Carbonates by Seawater and Seawater-Derived Brines: San Anders Formation (Guadalupian), West Texas. In: Sedimentology and Geocemistry of Dolostones (ed. by: Shukla, V. and Baker, P. A.), *Spec. Publ., Soc. Econ. Paleont. Miner., 43:* 245-262.

RYAN, W. B. F., STANLEY, D. J., HERSEY, J. P., FAHLQUIST, D. A. AND ALLAN, J. D. (1970). The Tectonics and Geology of the Mediterranean Sea. In: *The Sea* (ed. by: Maxwell. A. E.), Wiley-Interscience, *4(2)*: 387-492.

SALAJ, J. (1978). The Geology of the Pelagian Block: The Eastern Tunisian Platform. In: *The Ocean Basins and Margins* (ed. by: Nairn, A. E. M., Kanes, W. H. and Stehli, F. G.), *4B- The Western Mediterranean*: 361-416.

SANDERS, N. J. (1970). Structural Evolution of the Mediterranean Region During the Mesozoic Era. In: Geology and History of Sicily (ed. by: Alvarez, W., and Gohrbandt, K. H. A.), *Pet. Expl. Soc. of Libya*: 43-132.

SAVIN, S. M. (1977). The History of the Earth's Surface Temperature During the Past 100 Million Years. *Ann Rev. Earth and Planetary Sci., 5*: 319-356.

SBETA, ABDUL. M. (1979). Stratigraphy of the Upper Cretaceous and Pre Upper Cretaceous Rocks, East of Tarhuna Between Suq El-Ahad and Ras Zerzer (Gezzar), Jebel Nefusa. *Unpub. Report*: 35p.

SCHOLLE, P. A. (1971). Diagenesis of Deep-Water Carbonate Turbidites, Upper Cretaceous Monte Antola, Flysch, Northern Apennines, Italy. *Jour, Sed. Petrol., 41*: 233-250.

SGHAIR, A. M. (1990). Stratigraphy, Lithofacies and Environmental Analysis of the Bahi Formation (Late Cretaceous) in the North-Western Sirte Basin, Libya. *Unpubl. M.Sc. Thesis, Department of Applied Geology, University of Glasgow, Scotland*: 171.

SGHAIR, A. M. (1993). Depositional Environment of the Bahi Formation Deduced by Textural Analysis, NW Sirt Basin, Libya. *Petr. Resea. J., Petroleum Research Centre, Tarabulus, Libya, 3*: 35-43.

SHINN, E. A. (1973). Sedimentary Accretion Along the Leeward, SE Coast of Qatar Peninsula Persian Gulf. In: The Persian Gulf-Holocene Carbonate Sedimentation and Diagenesis in Shallow Epicontinental Sea (ed. by: Purser, B. H.), Springer-Verlag: 199-209.

SHUKLA, V. (1988). Sedimentology and Geochemistry of a Regional Dolostone: Correlation of Trace Elements with Dolomite Fabrics. In: Sedimentology and Geochemistry of Dolostones (ed. by: Shukla, V. and Baker, P. A.), *Spec. Publ., Soc. Econ. Paleont. Miner., 43*: 145-157.

SHUKLA, V. AND FRIEDMAN, G. M. (1983). Dolomitization and Diagenesis in Shallowing-Upward Sequence: The Lockport Formation (Middle Silurian), New York State. *J. Sed. Petr., 53(3)*: 703-717.

SIBLEY, D. F. (1980). Climatic Control of Dolomitization, Seroe Domi Formation (Pliocene), Bonaire, N. A. In: Concepts and Models of Dolomitization (ed. by: Zenger, D. H., Dunham, J. B. and Ethington, R. L.). *Soc. Econ. Paleont. Mineral., Spec. Publ., 28:* 247-258.

SIBLEY, D. F. (1982). The Origin of Common Dolomite Fabrics. *J. Sed. Petr., 52:* 1087-1100.

SIBLEY, D. F. AND GREGG, J. M. (1987). Classification of Dolomite Rock Textures. *J. Sed. Petr., 57:* 967-975.

SIBLEY, D. F., DEDOES, R. E. AND BARTLETT, T. R. (1987). Kinetics of Dolomitization. *Geology, 15:* 1112-1114.

SIMMS, M. (1984). Dolomitization by Groundwater-Flow Systems in Carbonate Platforms. *Trans.-Gulf Coast Assoc. Geol. soci., XXXIV:* 411-420.

SINHA, R. N. (1992). Antiquity of Sirt Basin, Libya - A Discussion. *Unpub. Internal Report, Petroleum Research Centre, Tripoli, Libya*: 18p.

SMITH, A. G. AND BIDEN, J. C. (1977). Mesozoic and Cenozoic Paleocontinental Maps, Cambridge Univ. Press, New York, 63.

SMITH, T. M. AND DOROBEK, S. L. (1993). Alteration of Early-Formed Dolomite During Shallow to Deep Burial: Mississippian Mission Canyon Formation, Central to Southwestern Montana. *Geol. Soc. Am., Bull., 105:* 1389-1399.

SMITH, J. V. AND STREASTROM, R. C. (1965). Electron-Excited Luminecence as Petrologic Tool. *Geology, 73:* 627-635.

SOUSSI, M. AND M'RABET, A. (1994). Burial Dolomitization of Organic-Rich and Organic-Poor Carbonates, Jurassic of Central Tunisis. In: Dolomites A Volume in

Honour of Dolomieu (ed. by: Purser, B., Tucker, M. and Zenger, D. J.), *Inter. Assoc. Sediment., Spec. Publ., 21:* 429-445.

SPERBER, C. M., WILKINSON, B. H. AND PEACOR, D. R. (1984). Rock Composition, Dolomite Stoichiometry and Rock/Water Reactions in Dolomitic Carbonate Rocks. *J. Geol., 92:* 609-622.

STEPHENS, D. (1977a). Marengo Ltd., *Unpubl. Ann. Report (1977), Section on Western Tripolitania, Subsurface Report:* A1-A6.

STEPHENS, D. (1977b). Le Golfe de Gabes. In: *Rapport sur les Trauaux Effectuees en Tunisie Par L'Equipe de Caroline du Sud, Symposium December 5-6, 1977, N.S.F.* International Programs: 11p.

SUN, S. Q. (1994). A Reappraisal of Dolomite Abundance and Occurrence in the Phanerozoic. *J. Sed. Research, A64:* 396-404.

SUN, S. Q. (1995). Dolomite Reservoirs: Porosity Evolution and Reservoir Characteristics. *Bull. Am. Ass. Petrol. Geol., 79(2):* 186-204.

SUPKO, P. R. (1977). Subsurface Dolomites, San Salvador, Bahamas. *J. Sed. Petr., 47:* 1063-1077.

SYLVESTER-BRADLY, P. C. (1968). Tethys: The Lost Ocean. *Sci. J., 4:* 47-53.

THERIAULT, F. AND HUTCHEON, I. (1987). Dolomitization and Calcitization of the Devonian Grosmont Formation, Northern Alberta. *Jour. Sed. Petrol., 57(6):* 955-966.

TUCKER, M.E. (1982). Precambrian Dolomites: Petrographic and Isotopic Evidence that they Differ from Phanerozoic Dolomites. *Geology, 10:* 7-12.

TUCKER, M. E. (1983). Diagenesis, Geochemistry, and Origin of a Precambrian Dolomite: The Beck Spring Dolomite of Eastern California. *J. Sed. Petr., 53(4):* 1097-1119.

TUCKER, M. E. AND WRIGHT, V. P. (1990). Carbonate Sedimentology. Blackell, Oxford: 482p.

USDOWSKI, E. (1994). Synthesis of Dolomite and Geochemical Inplications. In: Dolomites A Volume in Honour of Dolomieu (ed. by: Purser, B., Tucker, M. and Zenger, D. J.), *Inter. Assoc. Sediment., Spec. Publ., 21:* 345-360.

VAIL, J. R. (1971). Dike Swarms and Volcanic Activity in Northeastern Africa. In: Symposium on the Geology of Libya (ed by: Gray, C.), *Faculty of Sci., Geol. Dept., University of Libya, Tripoli*: 341-347.

VAIL, J. R. (1991). The Precambrian Tectonic Structure of North Africa. In: *The Geology of Libya* (ed. by Salem, M. J., Sbeta, A. M., and Bakbak, M. R.), *VI*: 2259-2268.

VAN HOUTEN, F. B. (1980). Latest Jurassic-Cretaceous Regressive Facies, Northeast African Craton. *Am. Ass. Petrol. Geol., Bull., 64(6)*: 857-867.

VAN HOUTEN, F. B. (1983). Sirte Basin, North-Central Libya: Cretaceous Rifting Over a Fixed Mantle Hotspot? *Geology, 11*: 115-118.

VAROL, B. AND MAGARITZ, M. (1992). Dolomitization, Time Boundaries and Unconformities: Examples from the Dolostone of the Taurus Mesozoic Sequence, South-Central Turkey. *Sed. Geol., 76:* 117-133.

VEIZER, J. (1978). Simulation of Diagenesis- A Model Based on Strontium Depletion: Discussion, *Can. J. Earth Sci., 15:* 1683-1685.

VEIZER, J. (1983). Chemical Diagenesis of Carbonates: Theory and Application of Trace Element Technique. *Soc. Eco. Paleont. Mineral., Short Course, 10:* 30-1 to 3-100.

VON DER BORCH, C. C., LOCK, D. E. AND SCHWEBEL, D. (1975). Groundwater Formation of Dolomite in the Coorong Region of South Australia. *Geology, 3:* 283-285.

VON MORLOT, A. V. (1848). Sur L'Origine de la Dolomite. *Acad. Sci.* (Paris), *Comptes Rendus, 26:* 311-316.

WADE, H. K.(1989). Geochemistry, Mineralogical Associations and Origin of Near-Surface Dolomite from Salt Basin West Texas. *Unpubl. MS.C Thesis, University of Texas at El Paso, U.S.A.:* 168p.

WARD, W. C AND HALLEY, R. B. (1985). Dolomitization in a Mixing Zone of Near-Seawater Composition, Late Pleistocene, Northeastern Yucatan Peninsula. *Jour. Sed. Petr., 55:* 407-420.

WILSON, J. L. (1975). Carbonate Facies in Geologic History. *Springer-Verlag, New York*: 471p.

WILSON, J. L. (1985). Tectonic Controls of Carbonate Platforms. In: Carbonate Depositional Environments, Modern and Ancien, Part 2: Carbonate Platforms (ed. by: Harris, P. M., Moore, C. H., and Wilson, J. L.). *Colorado School of Mines, Quarterly, 80(4):* 9-29.

WOLLER, F. AND FEDIUK, F.(1980). Volcanic Rocks of Jabal as Sawda. In: *The Geology of Libya* (ed. by: Salem, M. J., and Busrewil, M. T.), *III:* 1081-1093.

ZACAGNA, D. (1919). Itinerari Geologici/Della Tripolitania Occidental Con Appendice Paleontologica. *Mem., Descr. Carta. Geol. Italia, XVIII:* 126p.

ZEMPOLICH, W. G. AND BOCKER, P. A. (1993). Experimental and Natural Mimetic Dolomitization of Aragonite Ooids. *J. Sed. Petr., 63(4):* 596-606.

ZENGER, D. H. AND DUNHAM, J. B. (1980). Concepts and Models of Dolomitization -

An Introduction.In: Concepts and Models of Dolomitization (ed. by: Zenger, D. H.,

Dunham, J. B. and Ethington, R. L.), *Spec. Publ., Soc. Econ. Paleont. Miner., 28:* 1-

9.

ZENGER, D. H. AND DUNHAM, J. B. (1988). Dolomitization of Siluro-Devonian

Limestones in a Deep Core (3,350m), Southeastern New Mexico. In: Sedimentology

and Geocemistry of Dolostones (ed. by: Shukla, V. and Baker, P. A.), *Spec. Publ.,*

Soc. Econ. Paleont. Miner., 43: 161-173.

ZIEGLER, A. W. (1975). Outline of the Geological History of the North Sea. In:

Petroleum and Continental Shelf of North-West Europe (Ed. by: Woodland, A. W.).,

*Appl. Sci. Pub., London, 1***:** 163-190.

ZIVANOVIC, M. (1977). Geological Map of Libya, 1: 250,000, Sheet Beni Walid, NH32-

2, Explanatory Booklet. *Publication of the Industrial Research Centre, Tarabulus,*

Libya: 71p.